W-Pos230

PLANCK-BENZINGER THERMAL WORK FUNCTION: DEFINITION OF TEMPERATURE-INVARIANT ENTHALPY IN BIOLOGICAL SYSTEMS.
((Paul W. Chun)) Department of Biochemistry and Molecular Biology, University of Florida, Gainesville, Florida 32610.

In reexamining the thermodynamic parameters of a number of self-associating protein systems in the standard state near 300 degrees Kelvin, we found that at the stable temperature $\langle T_s \rangle$, the thermodynamic quantities $\Delta G^0(T_s)$ and $\Delta W^0(T_s)$ reach a minimum and maximum, respectively, while $T\Delta S^0(T_s)$ approaches zero. Based on the Planck-Benzinger thermal work function, (Chun, 1988), $\Delta W^0(T) = \Delta H^0(T_0) - \Delta G^0(T)$. Therefore $\Delta H^0(T_0) = \Delta W^0(T_s) + \Delta G^0(T_s)$ at $\langle T_s \rangle$. Values for $\Delta H^0(T_0)$ at $\langle T_s \rangle$ for four self-associating protein systems were found to deviate by less than 0.05% from values for $\Delta H^0(T_0)$ at zero degrees Kelvin. Benzinger's definition (1971) is applied in measuring $\Delta H(T_0)$ for DNA unwinding and protein unfolding in the non-standard state near 340°K. $\Delta H(T) = \Delta H(T_0) + \int \Delta Cp(T)dT$ at the melting temperature, $\langle T_m \rangle$, where $\Delta H(T)$ and $T\Delta S(T)$ are of the same magnitude, $\Delta W(T) = \Delta H(T_0)$ and $\Delta G(T)$ approaches zero. Values for $\Delta H(T_0)$ at $\langle T_m \rangle$ for the proteins we examined deviated by less than 0.04% from values for $\Delta H(T_0)$ at zero degrees Kelvin. The heat of reaction of any biological system consists of two terms, the heat capacity integral between product and reactant, and the temperature-invariant chemical bond energy, $\Delta H(T_0)$, which is a primary, indispensable source of the energy which allows life processes to proceed with quantitative precision. Failure to evaluate $\Delta H^0(T_0)$ or $\Delta H(T_0)$ in assessing any biological system will thus give only a partial picture of the processes taking place within that system.

†This work was supported by a faculty development award, Division of Sponsored Research, University of Florida.

W-Pos231

PROBABILITY DISTRIBUTION FOR SYSTEMS WITH MULTIPLE STATIONARY STATES.
((M. Samoilov)) Biophysics Program, Chemistry Department, Stanford University, Stanford, CA 94305 (Spon. by O. Jardetzky)

Autocatalytic reactions arise frequently in biological processes. A general form for the system with two intermediates could be written as:

$$A + (m-1)X \underset{k2}{\overset{k1}{\rightleftharpoons}} mX$$

$$sX + (r-1)Y \underset{k4}{\overset{k3}{\rightleftharpoons}} (s-1)X + rY$$

$$nY \underset{k6}{\overset{k5}{\rightleftharpoons}} (n-1)Y + B$$

where the chemical potentials of A and B are held constant. If at least one of the coefficients is greater then one, chemical kinetics of these reactions allows for the existence of multiple stationary state solutions. The question of relative likelihood of these states and fluctuations around them could be answered if we consider the system to be stochastic. Stochastic analysis requires finding a stationary probability distribution. A thermodynamic and stochastic theory based on the concept of work was proposed by Ross, Hunt and Hunt (RHH) [J. Chem. Phys. 88, 2719 (1988) and 92, 5272 (1990) and 96, 618 (1992)]. The authors suggest a form for the probability distribution, which makes it proportional to the exponent of the sum of integrals of chemical potential differences (between the actual and the reference system) over the respective concentrations. This formulation depends on the integration path in the concentration space. The extremal action principle applied to RHH formalism gives a way for the numerical evaluation of the probability distribution. The results yield relative probabilities of the various stationary states, as well as predict the likelihood of possible fluctuations away from them.

W-Pos232

DIVALENT EFFECTS ON MONO-VALENT CATION CHANNELS, AN EXTENSION OF POISSON-NERNST-PLANCK THEORY

Duan P. Chen and Robert S. Eisenberg, Department of Physiology, Rush Medical College, Chicago, Illinois 60612, U. S. A.

The Poisson-Nernst-Planck theory of open ionic channels is extended to account for the divalent effects on the mono-valent cation ion channels. We have proved that there is a unique Donnan's potential created by the surface charge on the two sides of the membrane when divalent ions are present. Our numerical results have shown: (1) Micromolar to millimolar divalent cation concentration in the cytoplasmic side will rectify the IV curve from strictly linear to the shape of an inward rectified channel, while the inwardly rectified single channel conductance is slightly increased; (2) Divalent ions do not contribute appreciably to the net current. That is to say that the reversal is mainly determined by the monovalent ion concentrations; (3) More than one steady state solutions to the above set of coupled non-linear equations are found even for uniform permanent charge distribution when divalent ions are present. These results agree well with the experimental facts known about the inwardly rectified potassium channels.

W-Pos233

POLYELECTROLYTE MEDIATED INTERACTIONS BETWEEN OPPOSITELY CHARGED PLANAR SURFACES AND MICELLAR AGGREGATES.
((R. Podgornik and B. Jönsson)) LSB / DCRT, NIH, Bethesda, MD 20892 and Physical Chemistry 2, Chemical Center, POB 124, Lund, SWEDEN (Spon. by D.Juretić)

Using mean - field theory, Monte Carlo simulations and scaling arguments we investigated forces between apposed charged planar surfaces and spherical aggregates, conferred by oppositely charged polymeric chains. In the planar case the most important characteristics of the forces is a region of intersurface separations characterised by net attractive roughly exponentially decaying forces between bounding surfaces, stemming from the bridging of polyelectrolyte chains between the two charged surfaces. The forces conferred by confined polyelectrolyte chains depend in an essential way on the conformation of the chains between the surfaces as can be ascertained from comparison between the monomer intersurface density profile and the concurrent forces. In the case of polyelectrolyte mediated forces between charged spherical aggregates the situation is quite similar. At interaggregate separations comparable to the length of the chain the force is attractive and linear in the interaggregate separation due to a special type of long range bridging attraction mediated by the polyelectrolyte chain, adsorbed to both aggregates. Beyond a certain separation (*capture separation*) there is a symmetry breaking transition in the monomer density distribution, resulting in a preferential adsorption of the chain to one of the aggregates. In both cases the attractive forces can be orders of magnitude stronger than the standard van der Waals attractions.

FOLDING AND SELF-ASSEMBLY II: STRUCTURE OF PROTEINS AND COMPLEXES

W-Pos234

MECHANISMS BASED ON X-RAY STRUCTURES OF TWO $(\beta/\alpha)_8$ BARREL ENZYMES: ADENOSINE DEAMINASE AND ALDOSE REDUCTASE
((David K. Wilson[1] & Florante A. Quiocho[1,2])) Baylor College of Medicine[1] and Howard Hughes Medical Institute[2], Houston, TX 77030.

We have determined the crystal structures of two different enzymes — adenosine deaminase (ADA) and aldose reductase (ALR2)*. Based upon these structures, the mechanism for each has been determined. ALR2 is currently the target of drug design efforts to reduce diabetic complications assocated with a number of tissue types. Aside from the implications for rational drug design, our structure has also shed light on the catalytic mechanism for the enzyme. It catalyzes a simple reaction in which a hydride is donated from an NADPH cofactor to the substrate. Subsequently a proton is abstracted from a general acid on the enzyme. The structure has allowed us to identify the residue most likely to be responsible for this and provided the basis for site directed mutants to test this theory. ADA is an enzyme which functions in the purine salvage pathway and is a critical component in the development and competence of the immune system. The initial structure revealed not only a previously unknown yet necessary Zn^{2+} cofactor but also that the inhibitor which was assumed to be a ground state analog had been converted into a transition-like state which is stable in the enzyme-bound form. Structures of the enzyme bound with a series of inhibitors were then determined. These inhibitors were carefully chosen such that the reaction "stalled" at different points along its course. This has painted a very clear picture of all of the detailed steps in the reaction pathway.

*In collaboration with J.M. Petrash, University of Washington Medical School.

W-Pos235

CRYSTAL STRUCTURE OF PORCINE RIBONUCLEASE INHIBITOR, A PROTEIN WITH LEUCINE-RICH REPEATS: A NOVEL CLASS OF ALFA/BETA STRUCTURE.
((Bostjan Kobe and Johann Deisenhofer)) Department of Biochemistry and Howard Hughes Medical Institute, University of Texas Southwestern Medical Center, Dallas, TX 75235. (Spon. by J. Deisenhofer)

Ribonuclease inhibitor (RI) is a 49-kDa protein that inhibits neutral and alkaline ribonucleases and angiogenin by very tight binding. The primary structure of RI consists of 15 leucine-rich repeats (LRR), alternately 28 and 29 residues long. RI belongs to a large family of proteins that all seem to be involved in protein-protein or protein-membrane interactions. The crystal structure of porcine RI was solved by multiple isomorphous replacement using ten heavy atom derivatives. The model has been refined to 2.5 Å resolution with an R-factor of 18.2% and contains all 456 residues. RI is a horseshoe-shaped protein with dimensions 70 x 62 x 32 Å. Individual LRR correspond to right-handed β–α structural units, similar to those found in many α/β proteins. The β–α units are, however, arranged in a way different from other known α/β structures. β-strands form a parallel β-sheet on the inner circumference of the horseshoe, while helices align on the outer circumference. The structure of RI and the available biochemical data suggest a possible ribonuclease binding region incorporating the surface formed by the parallel β-sheet and the neighboring loops. The crystal structure of RI represents the first three-dimensional structure of any protein containing LRR.

W-Pos236

USING CRYO-CRYSTALLOGRAPHY AT A SYNCHROTRON SOURCE TO SOLVE THE CATALYTIC MECHANISM OF AN ALTERED ACTIVE SITE OF ISOCITRATE DEHYDROGENASE. ((D. B. Cherbavaz, M. E. Lee, D. E. Koshland, Jr., and R. M. Stroud)) Dept. of Biochemistry & Biophysics, U.C. San Francisco and Dept. of Molecular and Cellular Biology, U.C. Berkeley

NADP+-dependent isocitrate dehydrogenase (IDH), catalyses the oxidative decarboxylation of D-isocitrate (IC) to α-ketoglutarate (αKg). Previous structures implicate the involvement of specific residues in the acid-base mechanism. An alteration at the 230 position (K230M) has been shown to decrease enzyme activity a thousand-fold. Kinetic analysis indicates that Lys-230 is intimately involved in both the substrate binding and turnover and data suggest that the residue is the primary proton donor.

Data, previously collected on area detectors, has not proven useful in determining the subtle changes in ligand binding in the active site. To overcome those problems, data were collected, for K230M crystallized with both reactant and product, at liquid N_2 temperatures at the Stanford Synchrotron (SLAC/SSRL) facility. The change in procedure resulted in greater than a half Angstrom increase in resolution to 2.09 Å and yielded excellent statistics. The overall R_{sym} for K230M*IC is 5.6% for 198,600 observations of which 40,300 are unique, resulting in five-fold redundancy. The average $I/\sigma(I)$ is 8.8 and the completeness to 2.12 Å is 89.6%. Similar statistics were obtained for K230M*αKg.

The low temperature (LT) cell decreased relative to the room temperature (RT) cell by -2% in a and remained unchanged in c; a = b = 102.8 Å c = 150.1 Å. The space group, $P4_32_12$, did not change. LT data is related to the RT model by a relatively small rotation/translation. These data are promising as features that were unplaced in the RT model, such as some side chains, are now clearly visible. Implications of these structures as they relate to the catalytic mechanism as well as improvements due to cryocrystallography at a Synchrotron source will be discussed.

W-Pos237

STRUCTURAL STUDIES ON CHEMICALLY MODIFIED HEMOGLOBINS.

((Fernandez, E. J.))., Department of Chemistry, Loyola University, 6525 N. Sheridan Road, Chicago, IL 60626.

The potential use of cross-linked hemoglobins as blood substitutes has generated significant research into the properties of these modified proteins. Of the most interesting ones in terms of oxygen binding and stability properties one has a fumarate cross-link between the two α99 lysine residues (α99XLHbA) and the other is cross-linked between the two β82 lysines (β82XLHbA). We will present X-ray diffraction results on the 1.9Å structure of deoxy α99XLHbA and on the 2.2Å structure of deoxy β82XLHbA. The α99XLHbA crystals were grown by the standard method (Perutz, M. F. (1968) J. Crystal Growth 2:54) and were $P2_1$ with a = 63.2Å, b = 84.0Å, c = 53.8Å and β = 99.95°. These unit cell parameters are almost identical to those for deoxy HbA and those reported for a low resolution structure of α99XLHbA (Chatterjee, et al. (1986) J. Biol. Chem. 261:9929). A difference electron density map has been calculated using the PROTEIN program. The β82XLHbA crystals were grown from solutions of PEG-6000 by the method of Ward et al. (Ward, K. B. et al. (1975) J. Mol. Biol. 98:161) and were also $P2_1$ with a = 65.3Å, b = 96.2Å, c = 101.5Å and β = 101.5° with two tetramers in the asymmetric unit. The structure was examined by Molecular Replacement with the program MERLOT. Model building and refinement are currently being done using the graphics program CHAIN. (Supported in part by a grant from the Research Corporation.)

W-Pos238

STRUCTURAL ANALYSIS OF BULLFROG RED CELL FERRITINS. ((J.Trikha[1], G. S. Waldo[2], Y. Ha[1], E. C. Theil[2], P. C.Weber[3]and N. M.Allewell[1])) [1]Department of Biochemistry, University of Minnesota, St. Paul MN 55108, [2]Department of Biochemistry, North Carolina State University, Box 7622, Raleigh NC 27695, [3]The DuPont Merck Pharmaceutical Company, P. O. Box 80228, Wilmington DE 19880.

Ferritin is a 24 subunit protein that stores cellular iron in animals, bacteria and plants. Ferritin is differentially expressed as particular combinations and abundancies of two subunit classes, H and L, with the H subunit having more rapid rates of mineralization. To examine ferritin from a highly differentiated cell type and to clarify the relationship between ferritin structure and function, bullfrog red cell L and H ferritins have been cloned and overexpressed in *E. coli* [Dickey *et al.*, J. Biol. Chem. 262:7901 (1987)]. Crystals of both H and L subunits and two single site mutants with altered rates of iron transport have been obtained under two sets of conditions and high resolution structures of the L-subunit and a mutant in which four Glu residues were replaced with Ala have been solved by molecular replacement. These structures provide new insights into the structural requirements for rapid and slow mineralization and the extent to which structural changes can be accommodated in four helix bundles.

Supported by the University of Minnesota, and NIH grants DK-30351 (ECT) and F32DK-08793 (GSW)

W-Pos239

THE STRUCTURE OF ADENOVIRUS BY ELECTRON MICROSCOPY AND X-RAY CRYSTALLOGRAPHY.

((P.L. Stewart[1], S.D. Fuller[2] and R.M. Burnett[1]))
[1]The Wistar Institute, Philadelphia, PA 19104 and
[2]European Molecular Biology Laboratory, Heidelberg, Germany.

A novel combination of electron microscopy and X-ray crystallography has revealed the various structural components forming the capsid of human type 2 adenovirus. An image reconstruction of the intact virus, derived from cryo-electron micrographs, was deconvolved with an approximate contrast transfer function to mitigate microscope distortions. A model capsid was calculated from 240 copies of the crystallographic structure of the major capsid protein and filtered to the correct resolution. Subtraction of the calculated capsid from the corrected reconstruction gave a three-dimensional difference map revealing the minor proteins that stabilize the virion. Elongated density penetrating the hexon capsid at the facet edges was ascribed to polypeptide IIIa, a component required for virion assembly. Density on the inner surface of the capsid, connecting the ring of peripentonal hexons, was assigned as polypeptide VI, a component that binds DNA. Identification of the regions of hexon that contact the penton base suggests a structural mechanism for previously proposed events during cell entry.

W-Pos240

TOWARDS THE STRUCTURAL BASIS OF ROTAVIRUS INFECTIVITY

((Shaw, A.L., Rothnagel, R., *Chen, D., *Ramig, R.F., Chiu, W., Prasad, B.V.V.))
Department of Biochemistry and Keck Center for Computational Biology, *Division of Molecular Virology, Baylor College of Medicine, Houston, TX

We have recently determined the three-dimensional structures of a simian rotavirus, SA11-4F, and an SA11-4F reassortant, R-004, to 28 Å resolution by electron cryomicroscopy and computer image processing techniques. The infectivity of the reassortant is markedly reduced compared to the simian parent due to loss of the VP4 spikes. Difference calculations between parent and reassortant structures reveal a domain of VP4 buried beneath the VP7 shell. This finding implies that the stability of the VP4 spike is due largely to the VP4-VP6 interaction. Our results provide new insight into the rotavirus assembly process.

We have also investigated the structural basis of trypsin-enhanced infectivity. We have determined the three-dimensional structures of non-trypsinized and trypsinized SA11-4F to 28 Å resolution. Trypsinization causes noticeable structural changes in the structure of the VP4 spike. A clear separation of the two VP4 molecules is observed in the body of the non-trypsinized spike, which appears to close after trypsinization. We hypothesize that a functional domain necessary for cell entry is exposed following proteolysis. Future structural studies, with gold-labeled modifiers and monoclonal antibodies, will aid in identifying the location of functional domains within the three-dimensional structure.

This research is supported by the W. M. Keck Center and NIH grants.

W-Pos241

Modeling Pf1 Virus with Everted DNA

((D.J. Liu and L.A. Day)) The Public Health Research Institute, New York, NY 10016, and the Dept. of Biochemistry, New York University School of Medicine, New York, NY 10016

Filamentous virus Pf1 has the highest length/diameter ratio (2040 nm/7 nm) among all known viruses. It contains a highly extended and twisted circular ssDNA structure in a helical shell of coat protein subunits, one for each base. Based on available results in the literature from UV absorbance, CD, Raman scattering, electron microscopy (STEM), X-ray fiber diffraction, neutron diffraction and solid-state NMR, models for Pf1 virus have been built with everted DNA and helical coat protein. The DNA models have backbones near the structural axis ($R_{Phosphorus}$≅2Å), bases are not stacked, the phosphate groups of both up- and down- strands are highly symmetric and the sugar has C2'-endo configuration, e.g. {q,P,S,Γ}={0.42Å,173°,0.29Å,77°}. Strong electrostatic interactions between DNA and protein are allowed through the side-chains of R_{44} and/or K_{45}.

The radial positions of protein side-chains given from various data sets are satisfied with curved helical subunit models which contain two major segments at the inner and outer layers of the protein shell, forming coiled coils.

A top view of one such Pf1 virus model (right) shows a 67 Å section of 11 structural units each consisting of two nucleotides and their associated protein subunits. Nearly 50% of total volume is occupied by solvent.

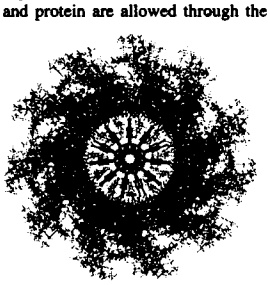

W-Pos242

SELF-ORGANIZATION OF FIBROIN IN SILK FIBERS
((K.A.Trabbic, B.L. Thiel*, D.B. Gillespie, C. Viney, P. Yager))
Molecular Bioengineering Program, Center for Bioengineering, WD-12, *Department of Materials Science and Engineering, FB-10, University of Washington, Seattle, WA 98195. (Sponsored by James Bassingthwaighte)

Silks are natural protein fibers that have mechanical properties comparable to high-performance synthetic fibers, yet are processed under environmentally benign conditions. Silk from the silkworm *Bombyx mori* and dragline from the spider *Nephila clavipes* have been studied using a variety of complementary techniques to investigate the hierarchical molecular order. Quantitative Raman spectroscopy, using a non-negative least squares algorithm to fit the amide I band, showed these silk fibers to consist primarily of β-sheet and β-turn, with the peptide backbones aligned predominantly along the fiber axis. These data were complemented by birefringence measurements. Analytical transmission electron microscopy showed the existence of crystalline regions within an amorphous matrix in *N. clavipes* fibers. Electron energy loss spectroscopy indicated 0.2 weight percent calcium exclusively within the crystallites. As the next step towards producing a synthetic analog of this system, fibers have been spun from reconstituted *B. mori* fibroin. By gaining a better understanding of the way in which nature engineers fibers, we hope to simulate natural processing routes for spinning high-performance polymer fibers.

W-Pos243

DIFFUSION OF GLOBULAR PROTEINS AMONG CYTOSKELETAL FIBERS.
((Jining Han and Judith Herzfeld))
Department of Chemistry, Brandeis University, Waltham, MA, 02254-9110.

The effect of excluded volume on the self or tracer diffusion of macromolecules in a crowded solution is an important but difficult problem, for which there has, so far, been no rigorous treatment. Muramatsu and Minton[1] suggested a simple model to calculate the diffusion coefficient of a hard sphere among other hard spheres. In this treatment, scaled particle theory is used to evaluate the probability that the target volume for a step in a random walk is free of any macromolecules. We have improved this approach by using a more appropriate target volume which allows the calculation to be extended to the diffusion of a hard sphere among hard spherocylinders. Using the tracer specific parameter obtained by fitting diffusion data for solutions of globular proteins we can predict the anisotropy of the diffusion coefficient of the same globular protein among rod-like proteins with arbitrary length and orientation distributions. We conclude that, to the extent that proteins can be approximated as hard particles, the hindrance of globular proteins by other proteins is reduced when the background proteins aggregate (the more so the greater the decrease in particle surface area), the hindrance due to rod-shaped background particles is reduced slightly if the rod-like particles are aligned, and the anisotropy of the diffusion of soluble proteins among cytoskeletal proteins will normally be small.

[1]N. Muramatsu and A. P. Minton, Proc. Natl. Acad. Sci. USA. 85, 2984 (1988).

W-Pos244

SPONTANEOUS SORTING OF TWO TYPES OF MODEL CYTOSKELETAL ELEMENTS: EXCLUDED VOLUME-DRIVEN SEPARATION OF SELF-ASSEMBLED FILAMENTS WITH DIFFERENT FLEXIBILITIES.
((Daniel T. Kulp and Judith Herzfeld))
Department of Chemistry, Brandeis University, Waltham, MA, 02254-9110.

Macromolecular crowding in the cytoplasm leads to highly-non-ideal behavior, including the spontaneous alignment of self-assembled filaments and the spontaneous coalescence of these filaments into bundles. Here we extend the statistical thermodynamic description of these phenomena to consider the behavior of two different types of filaments under crowded conditions. The theory combines a phenomenological description of reversible filament self-assembly and a scaled particle treatment of excluded volume. Filament flexibility is treated according to Khokhlov and Semenov. When filaments are rigid, they form a single nematic phase, even if their widths and/or lengths are different. However, flexible filaments sort into two distinct nematic phases. The degree of demixing of the filaments depends on the difference in their flexibilities and geometries. The demixing is dramatic when the more flexible filaments are also the narrower ones. In addition, the solvent partitions preferentially with the more flexible and narrower filaments, forming looser bundles for these than for the stiffer, wider filaments. Filament sorting is found at filament concentrations well within the range of those that have previously been predicted to be induced by the excluded volume of the non-polymerizing cytosolic proteins.

W-Pos245

CYTOSKELETON IN INTACT CELLS IMAGED BY DIRECT-VIEW 3-D TEM.
((A. Cole)) 2707 Westgrove, Houston, TX 77027.(Spon. by A. Ansevin)

A modified electron microscope provided simultaneous multiple views, for 3-D analysis, of total cytoskeletal structures either in mammalian cells grown on EM membranes or in whole-mount extracts. In round cells a network of 6 nm diameter actin fibers reflected cell shape. In round or flat cells four-stranded actin ribbons, 80 nm wide with transverse rib-pairs at 40 nm intervals, lay along and normal to plasma membranes to form "buttressed" surfaces. Trypsin Sensitivity of one rib of each rib-pair implied ribbon polarity. Some thin areas had planar arrays of actin fibers that may act in cell or metabolite transport. At cell division radial arrays of 180 nm long actin fibers at the cleavage zone may act as a contractile ring but the function of similar arrays that radiate from the nuclear surface is unknown. Single microtubules (22 nm diam.) were seen in non-overlap segments of pole-to-pole (polar) spindles of early mitosis. In overlap regions two microtubules of opposite polarity were linked every 30 nm by offset transverse ribs that may be bipolar complexes that "walk" to the positive end of both microtubules to extend the polar spindle while shortening the overlap. Four-stranded 90 nm wide microtubular ribbons with transverse densities (ribs) at 50 nm intervals provided stiff connections from centrioles to each kinetochore and, after anaphase, also to the overlap region. At telophase polar spindles condensed radially. Planar arrays, with extendible links between parallel microtubules, are made in manchettes that girdle developing sperm nuclei. Flexible intermediate filaments (10 nm diam.) formed global networks that attached to membranes of nuclei, mitochondria, and other organelles to fix cell organization. Global organization of the genome was maintained at interphase by attachments of chromatid backbones (Lange et al. Adv.in Rad.Biol.17:Ch 6, J.Lett, ed. Academic Press,1993) to the nuclear lamina, a thin rigid lattice of intermediate filaments. At mitosis, genome organization is conserved, in part, by transitory attachments of chromatid backbones to the surrounding network of flexible intermediate filaments.

W-Pos246

ASSEMBLY OF TUBULIN DIMERS INTO POLYMERS WITH THE OPTIMA XL–A ANALYTICAL ULTRACENTRIFUGE.
((J.J. Correia)) Dept. of Biochemistry, Univ. of Mississippi Medical Center, 2500 North State St., Jackson, MS. 39216.

The majority of the hydrodynamic studies on tubulin have been performed in low ionic strength phosphate buffer (10 mM, pH 7.0 at 20°C). In contrast, the formation of microtubules in vitro is often performed in 0.1 M Pipes or Mes buffer. At low ionic strength tubulin assembles into a Mg–dependent double walled ring (42s). At high ionic strength tubulin will readily form extensive divalent cation dependent sheets of rings, especially after limited subtilisin digestion (Lobert, et al., Cell Motil. Cytoskel. 25:282–297, 1993). These ring polymers are not microtubule nuclei and may affect the kinetics of microtubule polymerization. In addition, the nature of the microtubule nucleation structure in vitro is unknown. We have found that the GTP analog GMPCPP readily nucleates microtubule and ribbon formation under a wide range of temperatures and ionic strengths. A study of the assembly properties of tubulin as a function of solution conditions may reveal important relevant properties. The new Beckman Optima XL–A analytical ultracentrifuge utilizes absorption optics, a Xenon flash lamp, a direct drive motor and a computer interface for rapid data collection and analysis. A study of the hydrodynamic properties of tubulin as a function of temperature, ionic strength, divalent cation concentrations and guanine nucleotides present (GDP, GTP and GMPCPP) has been initiated on the XL–A to investigate the assembly of tubulin into ring and nucleation polymers. [Supported by NIH grant GM41117 and NSF grant BIR–9216150.]

W-Pos247

MELITTIN TETRAMERIZATION DEPENDENCE ON TEMPERATURE, AMINO ACID REPLACEMENT, IONIC STRENGTH AND PH.
((S.Yu.Venyaminov, D.M. Dousa and F.G.Prendergast)) Department of Biochemistry and Molecular Biology, Mayo Clinic, Rochester, MN 55905.

The physical properties of wild type melittin and of five mutants (G1A, G3A, T11G, K21H and K23H) have been studied by circular dichroism. Measurements of ellipticity at 222nm were conducted under conditions of continuously varied temperature. The results were interpreted in terms of conformational transitions and monomer/tetramer interconversions caused by cold and heat-induced association-dissociation. We assumed that the tetramer is folded as described by the crystal structure and that the monomer is largely unfolded. The monomer-tetramer equilibrium at peptide concentration of 50μM was changed by temperature (3-93°C), ionic strength(0-0.92M) and pH(7-9). Phase diagrams of this conversion were constructed in coordinates of temperature and ionic strength at different pH for all six peptides.

We demonstrated that the phase diagrams were very sensitive to pH change and amino acid replacement. For example, replacement of Lys at positions 21 and 23 for His, in the first case shifts equilibrium towards tetramer and in the second case towards monomer in comparison with wild type melittin. According to X-ray data the side chains of Lys21 are oriented on the outer surface while that of Lys23 is directed toward the interface of the melittin tetramer. The results will be discussed with respect to the balance of electrostatic and hydrophobic interactions between amino acid side groups of melittin in the tetramer state and the dependence of this balance on the changes in pH and the nature of amino acid replacements. (Supported by GM34847.)

W-Pos248

BAND 3, THE ERYTHROCYTE ANION TRANSPORT PROTEIN, EXPRESSED *IN VITRO* CONTAINS MORE THAN ONE SIGNAL SEQUENCE. ((L. Tam, D.M. Clarke, R.A.F. Reithmeier)) MRC Group in Membrane Biology, Departments of Medicine and Biochemistry, University of Toronto, Ont. Canada.M5S 1A8. (Spon. by R.A.F. Reithmeier)

Multi-spanning membrane proteins often contain multiple signal sequences to insert transmembrane (TM) segments into the ER membrane. Band 3, the erythrocyte anion transporter, is a multi-spanning membrane protein with a N-terminal cytosolic domain of 43 kDa and a C-terminal TM domain of 52 kDa. The protein contains a single extracellular N-glycosylation site at Asn 642. A cell-free translation system was used to study the integration and topology of the protein in membranes. Full-length Band 3 and deletion mutant mRNAs were translated in a rabbit reticulocyte lysate system supplemented with canine pancreatic microsomes. Correct integration of Band 3 and the mutant polypeptides into microsomes was assessed by alkaline extraction, deglycosylation and proteolysis. C-terminal truncation showed that the first four TM segments were sufficient for integration into the membrane with the first TM segment likely acting as the signal sequence. N-terminal truncations beginning with the 7th TM segment were also properly inserted into the membrane. Furthermore, the 7th TM segment can translocate the extracellular sequence distal to the 7th TM with the glycosylation site into the lumen of the ER without TM 8 to 14. This suggests that the 7th TM segment can acts as a signal sequence to translocate the TM domain that follows.
(Supported by Medical Research Council of Canada)

W-Pos249

VALIDATION OF ENERGY MINIMIZED PREDICTED MODELS FOR CASEIN SUBMICELLES WITH ELECTRON MICROSCOPY, FTIR AND SMALL ANGLE X-RAY SCATTERING. ((T.F. Kumosinski, P.H. Cooke, G. King, and H.M. Farrell)) ERRC, USDA, PHILADELPHIA, PA 19118.

An energy minimixed three dimensional (3D) model of a putative casein submicelle was constructed using monomeric κ-, α_{s1}- and β-casein 3D energy minimized predicted models. Docking of one κ- and four α_{s1}-casein molecules produced a framework structure whose external portion is composed of the hydrophilic domains of α_{s1}- and κ- and whose central portion contains two large hydrophobic cavities. Symmetric and asymmetric dimers (formed by docking the hydrophic C terminal regions of two β-casein molecular models) could easily be placed into the two central cavities on the κ-, α_{s1}- framework yielding two plausable energy minimized 3D structures for submicellar casein. To test these two refined, 3D structures, theoretical computer generated topographical models were compared to experimental electron microscopic data. Good comarisions of the 3D models with electron microscopy were achieved for both the symmetric and asymmetric submicelle models. Comparisons of these models with FTIR, small-angle X-ray scattering and biochemical data will also be given.

W-Pos250

DETERMINATION OF SOLUTION STRUCTURES OF PHOSPHOLIPASE A_2 BY MULTI-DIMENSIONAL ^1H AND ^{15}N NMR
((G. Rule, Q. Ye, B. Lathrop, and R. L. Biltonen)) University of Virginia Depts. of Biochemistry and Pharmacology, Charlottesville, VA 22908

Multi-dimensional NMR is being used to determine the three-dimensional structure of recombinant phospholipase A_2 (PLA_2) in aqueous solutions. A synthetic gene has been constructed to express the *Akistrodon piscivorous piscivorous* venom PLA_2 in *E. Coli*. The N terminal Asn residue penultimate to the initiator was replaced with Ser to permit quantitative removal of the initiator Met by the endogenous methionine aminopeptidase. The N-Ser PLA_2 was purified from intracellular inclusion bodies and refolded after sulfonation of the SH groups. The renatured enzyme has been found to have the same specific activity toward its lipid substrate as the wild-type venom PLA_2 (N-Asn). One-dimensional ^1H NMR spectra of N-Ser and N-Asn in solution were found to be very similar, indicating a similar solution structure of these two proteins. On the other hand, a different form of N-Ser PLA_2 (N-Ser-X) produced according to an incorrect protein sequence published in the literature shows distinct differences in its ^1H NMR spectrum from those of N-Ser and N-Asn, indicating a different solution structure. However, the enzymatic turnover of N-Ser-X was found to be identical to those of N-Ser and N-Asn, suggesting that all three enzyme forms adopt a similar structure when interacting with the lipid substrate. Labeling of N-Ser PLA_2 with ^{15}N has allowed us to obtain 2D and 3D ^1H-^{15}N correlated spectra to facilitate a complete assignment of the spin systems in the protein. The structural features will be discussed in the light of their importance in the understanding of the activation of PLA_2. (Supported by NSF and NIH)

W-Pos251

STRUCTURE STUDIES OF THE MYTILUS EDULIS FOOT PROTEIN MEFP-2 ((Mark W. Trumbore, Howard S. Young. and Victor Skita)) Biomolecular Structure Analysis Center, Univ. of Conn. Health Ctr., Farmington, CT 06030-2017

The marine mussel *Mytilus edulis* inhabits the intertidal regions of the North Atlantic and Pacific Oceans. This environment is characterized by large variations in temperature and salinity as well as periodic high mechanical stress caused by wave action. *M. edulis* has evolved a holdfast mechanism known as the bysuss which enables it to maintain a stable position in the intertidal zone. The byssus consists of a system of proteinaceous threads each of which terminate in an adhesive plaque. Two of the major proteins associated with the adhesive plaque are Mefp-1 and 2. Because of the ability of the plaque to form a stable adhesive bond in this harsh environment, we have been studying the structure of proteins associated with the plaque to gain insights into the structure-function relationships involved in adhesion. Mefp-2 is an ~ 50kd protein isolated from the foot of the *M. edulis*. It is highly resistant to proteolysis, contains 2-3 mol% dihydroxyphenylalanine and 7-8 mol% cystine and appears to be extensively intramolecularly crosslinked. Fourier transform infrared spectroscopic studies of Mefp-2 in D_2O indicates that the protein exists in a primarily alpha-helical conformation. X-ray solution scattering studies of Mefp-2 show that the protein adopts a spherical conformation in solution with an Rg of 19.2A. These results indicate that Mefp-2 has a compact highly ordered structure in solution and may be amenable to x-ray crystallographic analysis. M. Trumbore is supported by NIH postdoctoral fellowship #1 F32 DE05612-01A1. The solution scattering studies were carried out at beamline X9B at NSLS. X9B is funded by NIH research resource grant #RR01633

W-Pos252

STRUCTURAL STUDIES OF AN *E. COLI* GLUTAREDOXIN VARIANT. ((N.A. Wilson, J.A. Fuchs, C.K. Woodward)) University of Minnesota, Dept of Biochemistry, 1479 Gortner Ave, St. Paul, MN 55108

E. coli glutaredoxin is an oxidoreductase which uses glutathione as its reductant. It has the same protein fold as *E. coli* thioredoxin, although the first α-helix and β-sheet in thioredoxin are absent in glutaredoxin. The two proteins have little sequence homology. Glutaredoxin is present naturally in two forms, glutaredoxinA, which has 85 residues, and glutaredoxinN which has an extra 5 residues at the N terminus. The less abundant glutaredoxinN is a product of the *grx* gene, but uses an upstream ribosome binding and start site. By mutating the ribosome binding site for glutaredoxinA to non-concensus sequences, we are able to produce large amounts of pure glutaredoxinN. We are examining the three dimensional structure of glutaredoxinN by NMR and circular dichroism to determine what local changes occur in the N-terminal region relative to glutaredoxinA. In glutaredoxinA, the N-terminus has a perturbed pKa and changes in the structure in that region are expected when it is blocked by addition of these extra residues.

W-Pos253

LOCALIZATION, DYNAMICS AND DISTRIBUTION OF AN UNFOLDED PROTEIN ON A PUTATIVE CHAPERON: THE CASE OF INSULIN B-CHAIN BOUND TO α-CRYSTALLIN.
((Zohreh T. Farahbakhsh, Qing-L. Huang, Lin-L. Ding, Heinz-J. Steinhoff, Wayne L. Hubbell and Joseph Horwitz)) Jules Stein Eye Institute and Department of Chemistry and Biochemistry, UCLA, Los Angeles, CA 90024-7008

α-Crystalline is the major protein of the vertebrate lens, but it may act as a molecular chaperon in a variety of tissues. It has been previously shown to associate with denatured or unfolded proteins, and to suppress non-specific aggregation (Horwitz (1992) PNAS 89:10449-10453). In these experiments, the target protein as well as the chaperon were exposed to denaturing agent (guanidine HCl, urea, pH or temperature), raising the possibility that the chaperon structure may have been changed by the denaturing agent. In recent work, we have used insulin as the target protein and initiated denaturation by disulfide reduction with DTT, a treatment which does not effect α-crystallin. Reduction of insulin results in precipitation of the B-chain. However, in the presence of α-crystallin, the aggregation is suppressed and the B-chain associates with the crystallin in a stoichiometry of one mole of insulin B-chain per mole of α-crystallin monomer. Experiments with spin-labeled insulin reveal that the B-chains are tightly adsorbed in an extended conformation to a solvent-exposed surface of the α-crystallin, with an inter-chain distance of 25 Å or greater.

W-Pos254

DETECTING CONFORMATIONAL CHANGES IN GROEL INDUCED BY THERMAL SWITCHING OR ATP BINDING

((John E. Hansen and Ari Gafni)) Department of Biological Chemistry and Institute of Gerontology, University of Michigan, Ann Arbor, MI 48109

GroEL assists other proteins to fold *in vivo*, usually requiring Mg^{+2} and ATP to function. Electron micrographs reveal that ATP binding induces a conformational change in this chaperonin. Previously we have suggested (J. Biol. Chem. (1993) 268, 21632-21636) that a thermally-induced conformational change in GroEL results in the switching between enhanced and arrested reactivation of bacterial glucose-6-phosphate dehydrogenase. This thermal switching occurs over a narrow temperature range (25° and 30°). Recently it has also been reported that the binding affinity of the P22 tail spike polypeptide to GroEL changes abruptly over this same temperature range. To detect these conformational changes in solution we have stoichiometrically labeled GroEL with N-(acetylaminoethyl)-5-naphthamine-1-sulfonic acid, a fluorescence label whose emission is environment-sensitive. By measuring changes in the fluorescence Stokes' shift we have detected two thermally induced conformational changes between 25° and 30°. One of these changes occurs between 25° and 26° C resulting in a 1 nm shift in the fluorescence. The second conformational change occurs between 27° and 30° C resulting in a 3 nm fluorescence shift. The conformational change induced by ATP binding also results in a 3 nm shift in the fluorescence. Our data provides a correlation between functional change and structural change in GroEL. This work was supported by NIA grant AG097GI and ONR contract N00014-91-J-1938

FOLDING AND SELF-ASSEMBLY III: NUCLEIC ACIDS; PEPTIDES; MEMBRANES

W-Pos255

PRESSURE, CHAIN LENGTH, AND THE THERMAL TRANSITIONS OF DNA

((RB Macgregor* & JQ Wu†)) *Faculty of Pharmacy, University of Toronto, Toronto, ON M5S 1A1; †NIDDK, NIH, Bethesda, MD 20892

We have reported the pressure dependence of the helix-coil transition for several polymeric forms of DNA. Of the double stranded polymers studied to date, poly[d(G-C)] exhibits the largest pressure induced change in the helix-coil transition temperature (dT_m/dP) and poly[d(I-C)] the smallest. The simple, repetitive dA·dT polymers fall between these extremes. To explain these results we have proposed that the molar volume change of the transition (ΔV) derived from the experimental dT_m/dP values are a consequence of a balance between the effect of pressure on the electrostatic and hydrophobic (stacking) forces responsible for double strand stability.

In an effort to further elucidate the relative contributions of these two factors to the ΔV, we are studying the dependence of ΔV on chain length. In 0.05 M NaCl, the value of dT_m/dP for poly(dA)·poly(dT) is 3.15 °C/kbar and that for $dA_{19}\cdot dT_{19}$ is equal to 1.8 °C/kbar. We attribute this difference to the greater importance of end effects in the oligomer. Frayed ends effectively increase the molar volume of the helix form of the oligomer relative to that of the polymer, thus decreasing the ΔV. We are extending these measurements to other oligomers in order to quantify the volume increment arising from end fraying.

W-Pos256

AN INTERMOLECULAR DUPLEX OF POLY(U) WITH AN ASYMMETRIC H-BONDING PATTERN. EXPERIMENTAL AND SIMULATION VCD RESULTS

((L. Wang, V.Baumruk, and Timothy A. Keiderling)) Department of Chemistry, University of Illinois at Chicago, m/c 111, Chicago, IL 60607-7061

The ordered structure of poly(U) that is present at low temperature (~4 °C) has been studied with vibrational circular dichroism (VCD) and the spectra were simulated with a nondegenerate extended coupled oscillator (NECO) model. Upon formation of the ordered poly(U) structure, both of the C2=O and C4=O absorption bands are shifted to higher energy, giving rise to two biased positive couplets. A concentration dependence study indicated that this ordered poly(U) structure was found to be primarily an intermolecular double stranded helix under our sampling conditions. Addition of Mg^{2+} stabilized this ordered structure, raising its transition temperature. The VCD features of poly(U)•poly(U) were qualitatively explained with an asymmetric base pairing structure based on our NECO calculations which were carried out using structural models derived from duplex poly(s^2U) for asym and sym H-bonding patterns.

W-Pos257

STRUCTURE, INTERACTIONS AND THERMOSTABILITY OF THE MEMBRANE-PACKAGED dsDNA GENOME OF BACTERIOPHAGE PRD1.

((R. Tuma, D.H. Bamford and G.J. Thomas, Jr.)) Division of Cell Biology and Biophysics, School of Biological Sciences, University of Missouri, Kansas City, MO 64110.

PRD1 is a dsDNA bacteriophage infecting *E. coli* and *S. typhimurium*. The viral genome is packaged within a lipid vesicle inside an icosahedral capsid. We have developed a novel protocol for purification of PRD1 and subviral particles for Raman spectroscopic analysis. Application to the following will be described: (i) Wild type PRD1 virions; (ii) packaging-defective mutant (*sus1*) particles lacking DNA; and (iii) icosahedral shells devoid of DNA and lipid. Structure markers in Raman spectra of PRD1 and its extracted DNA indicate a *B* form structure in both packaged and unpackaged states. Small hyperchromic effects suggest only minor disruptions of *B* DNA base stacking in native virions. The spectra also indicate that the stabilizing effect of Mg^{2+} on PRD1 is due to strong cation binding to phosphate groups of the packaged dsDNA. Temperature dependence of the Raman spectra of wild type PRD1 and *sus1* particles show further that the membrane is strongly coupled to the packaged DNA. A model which accounts for coupling of the lipid assembly with DNA and which explains observed differences in thermostability of packaged and unpackaged DNA will be described.
[Supported by NIH Grant GM50776.]

W-Pos258

DETERMINATION OF LOCAL RAMAN TENSORS OF B-DNA AND A-DNA BY POLARIZED RAMAN MICROSPECTROSCOPY.

((J.M. Benevides, S.A. Overman, M. Tsuboi and G.J. Thomas, Jr.)) Division of Cell Biology and Biophysics, School of Biological Sciences, University of Missouri, Kansas City, MO 64110, USA.

The polarized Raman spectra of oriented fibers of B-DNA and A-DNA in the region 200-1800 cm^{-1} have been obtained by use of a Raman microscope. Raman intensities were measured for the following sample orientations: (i) I_{cc}, in which the incident and scattered light are polarized parallel to the axis (*c*) of the DNA helix; (ii) I_{bb}, in which the incident and scattered light are polarized perpendicular to *c*; and (iii) I_{bc} and I_{cb}, in which the incident and scattered light are polarized in mutually perpendicular directions. Structural homogeneity and unidirectional orientation of DNA were evaluated by comparison of the measured Raman anisotropies with those reported previously for oligonucleotide single crystals [Benevides et al. (1993) *J. Am. Chem. Soc.* 155:5351-5359]. The fiber Raman anisotropies and solution depolarization ratios were combined to determine local Raman tensors of key conformation-sensitive Raman bands of the DNA bases and sugar-phosphate backbone. Significant findings include the demonstration of complex patterns of A form and B form indicator bands in the regions 750-900 and 1050-1100 cm^{-1}, and the identification of highly anisotropic bands assignable to deoxyribose and phosphate moieties. The present results provide a basis for future exploitation of polarized Raman microspectroscopy as a probe of DNA orientation in complex biological assemblies.
[Supported by NIH AI18758.]

W-Pos259

MELTING STUDIES OF DNA DUMBBELLS WITH A SIXTEEN BASE PAIR STEM SEQUENCE AND X_n END-LOOPS (X = A,T,C; n = 2,3,4,6,8,10,14). (T.M. Paner, P.V. Riccelli and F.J. Gallo) Dept. of Chemistry, Univ. of Illinois, Chicago, IL 60607.

Melting curves were measured for DNA dumbbells with the duplex stem sequence 5'-G-C-A-T-C-A-T-C-G-A-T-G-A-T-G-C-3' as a function of [Na^+] from 30 to 120 mM. In all salt environments dumbbells with T_n end-loops were the most stable while stabilities of the dumbbells with A_n and C_n end-loops were equivalent. For dumbbells with loops comprised of at least three nucleotides stability is inversely proportional to loop size. Dumbbells with loops comprised of only two nucleotide residues have stabilities intermediate between those with three and four nucleotide loops. Thermodynamic parameters of dumbbell melting transitions were evaluated by analysis with the numerically exact (multistate) statistical thermodynamic model of dumbbell melting and the van't Hoff (two-state) model. Comparisons of the results revealed dumbbells with nucleotide loops comprised of six or less residues melt in an essentially two-state manner while the melting process for dumbbells with larger end-loops deviates from two-state behavior. Analysis also revealed how free-energies of loop and circle formation depend on end-loop size, sequence and [Na^+]. Dependence of the transition temperatures of the dumbbells on [Na^+] as a function of loop size indicated greater counterion release per phosphate upon melting for dumbbells with larger end-loops independent of end-loop sequence.

W-Pos260

FLUORESCENCE, CIRCULAR DICHROISM, AND THERMAL STABILITIES OF SITE-SPECIFIC BPDE-OLIGONUCLEOTIDE DUPLEXES.

((Nai-qi Ya, Sergei Smirnov, Scott Courtney, Tongming Liu, Victor Ibanez, and Nicholas E. Geacintov)) Chemistry Department, New York University, New York, NY 10003

We have synthesized covalent adducts in which 7β,8α-dihydroxy-9α,10α-epoxy-tetrahydrobenzo[*a*]pyrene (*anti*-BPDE, or BPDE) is linked via its 10-position to N^2-dG in an oligonucleotide 11 bases long [5'-d(CCATCG^{BPDE}CTACC)]. Using (±)-BPDE enantiomers, four stereochemically different adducts can be obtained [(+)-*trans*-, (-)-*trans*-, (+)-*cis*-, and (-)-*cis*-N^2-dG-modified oligonucleotides]. The fluorescence, circular dichroism, and UV absorbance of BPDE-modified oligonucleotide adducts are distinctly different from one another in the single-stranded and double-stranded forms. Upon duplex formation, the two *trans*-adducts exhibit blue shifts from 351 nm to 347 nm, consistent with their known minor groove conformations (de los Santos et al., *Biochemistry* 31,5245, 1992); in contrast, both *cis*-adducts exhibit red-shifts from 352 nm to 353 nm. In all cases, the presence of the lesion destabilizes the duplexes thermodynamically. Using a time correlated single photon counting system (a synchronous pump dye laser and a microchannel plate PMT), the fluorescence decay profiles were measured. Upon duplex formation, the mean fluorescence decay times of the *trans*-adducts decreases from ≈ 6 ns to 2 ns, while in the case of the *cis*-adducts, the lifetimes remain virtually unchanged (≈ 4 ns). These observations are related to the increased solvent-exposure of the *trans*-adducts in double-stranded DNA.

Supported by DOE Grant DE-FGO2-86ER60645 and NSF Instrumentation Grant 9011268.

W-Pos261

PARAMETRIZATION OF DIRECT AND SOFT STERIC - UNDULATORY FORCES BETWEEN DNA DOUBLE HELICAL POLYELECTROLYTES IN SOLUTIONS OF SEVERAL DIFFERENT ANIONS AND CATIONS. ((R. Podgornik, D.C. Rau and V.A. Parsegian)) LSB / DCRT, NIH, Bethesda, MD 20892

Directly measured forces between DNA helices in ordered arrays have been reduced to simple force coefficients and mathematical expressions for the interactions between pairs of molecules. These force parameters can be applied to parallel molecules or, by a suitable transformation, to skewed molecules of variable separation and mutual angle. This 'tool-box' of intermolecular forces is intended for use in modelling molecular interactions, assembly and conformations. The coefficients characterizing both hydration and electrostatic interactions depend strongly on the univalent counterion species in solution, but are only weakly sensitive to anion type and temperature (from 5 to 50 °C). Interaction coefficients for the exponentially varying hydration force seen at spacings less than 10 to 15 Å between molecular surfaces are extracted directly from pressure vs. interaxial distance curves. Electrostatic interactions are only observed at larger spacings and are always coupled with configurational fluctuation forces that result in observed exponential decay lengths that are twice the expected Debye - Hückel length. The extraction of electrostatic force parameters relies on a theoretical expression describing steric forces of molecules 'colliding' through soft exponentially varying direct interactions and connecting the experimentally determined width of the X-ray diffraction peaks with the magnitude of the forces acting in the macromolecular array.

W-Pos262

HIGHLY REPETITIVE AMPHIPHILIC PEPTIDES DESIGNED WITH TWO DISTINCT LEUCINE ZIPPER BINDING DOMAINS. ((S.M. Cowell, J.C. Hogan, C.L. Becker, M.L. McLaughlin, M.M. Juban*)) Department of Chemistry and *Department of Biochemistry, Louisiana State University, Baton Rouge, Louisiana 70803.

Natural leucine zipper binding domains have been recognized in several protein-DNA complexes in both homo- and heterodimeric peptide coiled-coil structures. Leucine zippers are formed by highly cooperative hydrophobic interactions between α-helical peptides. The individual leucine zipper binding domains must be α-helical, be at least four heptad units in length, and have heptad units with 3,4 hydrophobic repeat residues. These hydrophobic sites are usually leucines. A generic leucine zipper peptide monomer could have for example the sequence, $(XXLXXXL)_4$. We have synthesized a series of peptides designed to have two leucine zipper binding domains within a highly repetitive amphiphilic α-helical peptide. One of these peptides, $(L^XKL^YAL^XKL^Y)_4$, has two distinct leucine 3,4 repeats. Leucine residues labelled L^X repeat every three and four residues as do leucine residues labelled L^Y. The alanine residues separate the two distinct leucine X and Y faces forming the remainder of the nonpolar face of the amphiphilic peptide. The lysine residues also separate the two distinct leucine faces X and Y and form the polar face of the amphiphilic peptide. The unique purification problems and aggregation behavior of this and related peptides in this series will be presented.

W-Pos263

SOLUTION NONIDEALITY RELATED TO SOLUTE MOLECULAR CHARACTERISTICS IN AMINO ACIDS

((C. Keener, G. Fullerton, I. Cameron, and J. Xiong)) UTHSCSA, San Antonio, TX 78284-7800. (Sponsored by B. Goins)

It is hypothesized that nonideality in aqueous solutions is due to solute-induced water structuring near hydrophobic surfaces and solute-induced water destructuring in the electric fields generated by dipolar molecules.

This hypothesis is tested by measuring the freezing point depression for dilute, aqueous solutions of all water-soluble amino acids. Nonideality is expressed with a single solute/solvent interaction parameter I, calculated from experimental measure of ΔT. This gives a method of directly relating solute characteristics to solute-induced water structuring or destructuring. I-values correlate directly with hydrophobic surface area and inversely with dipolar strength. By comparing the nonideality of amino acids with progressively larger hydrophobic side chains, structuring is shown to increase with hydrophobic surface area at a rate of one perturbed water molecule per 9.1 square angstroms, implying monolayer coverage. Destructuring is attributed to dielectric realignment as described by the Debye-Hückel theory, but with a constant separation of charges in the amino-carboxyl dipole. By using dimers and trimers of glycine and alanine, this destructuring is shown to increase with the separation of dipolar charge.

The capacity to predict nonideal solution behavior on the basis of amino acid characteristics will permit prediction of free energy of transfer to water, which may help predict the energetics of folding and unfolding of proteins based on the characteristics of constituent amino acids.

W-Pos264

PROTEIN ENGINEERING WITH THE ISOMORPHOUS TRP ANALOGS 7-AZATRYPTOPHAN AND 4-FLUOROTRYPTOPHAN ((C.W.V. Hogue)) Dept. of Biochemistry, University of Ottawa, 451 Smyth Rd., K1H 8M5.

The amino acids that can be chosen for recombinant protein engineering studies are not limited to 20 common amino acids, but rather by the amino acid specificity of aminoacyl-tRNA synthetases. Here 7-azatryptophan (7AW), and 4-fluorotryptophan (4FW) have been biosynthetically incorporated into *B. subtilis* tryptophanyl-tRNA synthetase (TrpRS) in place of the single Trp-92. This was achieved using an expression system in a tryptophan auxotroph of *E. coli* and a "bait and switch" approach (Hogue *et al.*, 1992. *FEBS Lett.* 310:269-72). The yield of the incorporated TrpRS, irrespective of analog, was half that of the wild-type enzyme. The kinetics of $tRNA^{Trp}$ aminoacylation show little effect from 4FW substitution, but a significant decrease in k_{cat}/K_m with 7AW substitution. Notably, both substituted enzymes are active, unlike previous mutations of position 92. Nonfluorescent 4-fluorotryptophan was incorporated to avoid native Trp-92 fluorescence, in order to study the interactions of the natural Trp substrate. It was found that the substitution of 4FW for Trp resulted in a 5°C increase in the melting temperature of TrpRS, while 7AW resulted in a 2°C decrease. The melting temperatures are consistent with the hydrophobic properties of these isomorphous analogs: 7AW < Trp < 4FW. The substitution of hydrophobic amino acids with *more hydrophobic* isomorphous fluoroanalog amino acids may be a general strategy for increasing the thermal stability of enzymes - *without prior knowledge of tertiary structure*. The fluorescence of 7AW-92 exhibited triple-exponential decay kinetics, with a long average decay time, a 360 nm maximum and a high quantum yield. The unique photophysical properties of 7AW make its fluorescence much more sensitive to changes in solvent exposure compared to Trp (Hogue and Szabo, 1993. *Biophys Chem.* 48:in press). Evidence for its utility in detecting denaturation events is shown using W92(7AW) TrpRS. 7AW has *significant potential for studies of protein folding events*, since it is capable of exclusive fluorescence excitation above 310 nm.

W-Pos265

EFFECTS OF Cα-METHYL SUBSTITUTION ON THE CONFORMATION OF LINEAR GNRH ANTAGONIST ANALOGS.

((Mark I. Liff*, Kenneth D. Kopple**, Zhenping Tian*** and Roger Roeske***)) *Philadelphia College of Textiles and Science, Philadelphia, PA 19144, **SmithKline Beecham Pharmaceuticals, King of Prussia, PA 19406, ***Indiana University School of Medicine, Indianapolis, IN 46292. (Spons. by L. Mayne)

We have examined the effect of alpha-methyl groups on the conformational ensemble of GnRH analog peptides by comparing ^{1}H 2D NMR data from two analogs, Ac-D-Nal^1-D-4-Cl-Cα-Me-Phe^2-D-Pal^3-Ser^4-Tyr^5-D-Arg^6-Leu^7-Arg^8-Pro^9-D-Ala^{10}-NH$_2$ (1) and Ac-D-Nal^1-D-4-Cl-Cα-Me-Phe^2-D-Pal^3-Ser^4-Cα-Me-Tyr^5-D-Arg^6-Leu^7-Cα-Me-Arg^8-Pro^9-D-Ala^{10}-NH$_2$ (2). Although the Cα-Methyl groups eliminated some of the connectivity information normally available, complete and inambiguous assignments were obtained from TOCSY and NOESY data. The two additional Cα-methyl groups in residues 5 and 8 of 2 do not influence significantly the pattern of the observable main chain NOE intensities, which indicates that they do not produce global changes in the conformational ensemble of the peptide. A local change induced by the substitution was observed in the conformartion at Arg^8-Pro^9.

W-Pos266

SELECTIVE DISULFIDE FORMATION IN HYBRIDS OF APAMIN AND SARAFOTOXIN.

((G.H. Snyder, K. Sitwala and K. Ramalingam)) Biological Sciences, State Univ. of NY, Buffalo, NY 14260.

Apamin (apmn) and sarafotoxin (srtx) have 18 and 21 residues respectively. They both have four cysteines at locations 1,3,11 and 15, but their disulfides and other residues differ. The naturally occurring disulfides are globule (1..11, 3..15) in apmn and ribbon (1..15, 3..11) in srtx. Truncated hybrids (15 residues long) were constructed from four segments, which are residues 1-4, 5-7, 8-11, and 12-15. Equilibrium constants for formation of disulfide arrangements from fully reduced peptides and glutathione in 0 and 5 M GdmCl are listed below. "A" (apmn) and "S" (srtx) denote the origin of each segment. Hybrid SASS inserts residues 5-7 of apmn into the srtx host. This inverts the topology specificity of srtx from ribbon to globule. Changing ASSA->SSSS decreases the absolute value of K for ribbon but increases the specificity ratio for ribbon. The ASAA hybrid in 5 M GdmCl exhibits the lowest values for K's and topological specificity.

K (M^2) in:	0 M Guanidine HCl(GdmCl)			5 M Gdm Cl		
Protein	Globule	Ribbon	Ratio	Glob	Ribb	Ratio
Apmn AAAA	0.25	-0-	>10:1	0.09	-0-	>10:1
Hybrid SASS	0.097	0.040	2.4:1	n.d.	n.d.	
Hybrid ASAA	0.087	0.10	1:1.2	0.010	0.013	1:1.2
Hybrid ASSA	0.018	0.68	1:3.7	0.063	0.43	1:6.8
Srtx SSSS	0.021	0.15	1:7.2	0.009	0.09	1:9.5

Truncated:apmn= CNCKAPETALCARRC;srtx= CSCKDMTDKECLYFC

W-Pos267

NMR SOLUTION STRUCTURE OF NEUTROPHIL ACTIVATING PEPTIDE-2.

((Yingqing Yang, Vikram Roongta, Robert Milius, K.H. Mayo)) University of Minnesota, UMHC, Box 609, Minneapolis, MN 55455.

Neutrophil Activating Peptide-2 (NAP-2) is a 72 residue protein demonstrating a range of proinflammatory activities. The solution structure of NAP-2 has been investigated by two- and three-dimensional ^{1}H/^{13}C/^{15}N-NMR spectroscopy. Sequence specific resonance assignments have been made, and structural elements have been identified on the basis of nuclear Overhauser data, coupling constants and amide hydrogen/deuteron exchange. Distance geometry, restrained molecular dynamics and simulated annealing calculations show that NAP-2 consists of a triple stranded anti-parallel β-sheet arranged in a "Greek key" and a C-terminal helix (residues 59-72) folded onto that β-sheet scaffold. The structure of NAP-2 is very similar to that found in the NMR solution conformation of interleukin-8 and the crystal structures of bovine and human platelet factor-4, all of which are homologs of NAP-2. Structural results are discussed in terms of NAP-2 heparin binding and neutrophil activation.

This project has been supported by NIH Research Grant HL43194.

W-Pos268

CORRELATING TRYPTOPHAN TIME-RESOLVED FLUORESCENCE DECAY PARAMETERS WITH SECONDARY STRUCTURE.

A STUDY OF SYNTHETIC α-HELICAL PEPTIDES WITH A CENTRAL TRYPTOPHAN RESIDUE. ((K. J. Willis[1,2], W. Neugebauer[1], M. Sikorska[1], & A. G. Szabo[1])). [1]Institute for Biological Sciences, National Research Council, M54 Montreal Rd., Ottawa Canada, K1A 0R6. [2]Allelix Biopharmaceuticals Inc., 6850 Goreway Dr., Mississauga, Canada, L4V 1P1.

The relationship between α-helical secondary structure and the fluorescence properties of an intrinsic tryptophan residue were investigated. A monomeric α-helix forming peptide and a dimeric coiled-coil forming peptide containing a central tryptophan residue were synthesized. The fluorescence parameters of the tryptophan residue were determined for these model systems at a range of fractional α-helical contents. The steady-state emission maximum was independent of the fractional α-helical content. A minimum of three exponential decay times was required to fully describe the time-resolved fluorescence data. Changes were observed in the decay times and more significantly, in their relative contributions that could be correlated with α-helix content. The results were also shown to be consistent with a model in which the decay times were independent of both α-helix content and emission wavelength. In this model the relative contributions of the decay time components were directly proportional to the α-helix content. Data were also analyzed according to a continuous distribution of exponential decay time model, employing global analysis techniques. The recovered distributions had "widths" that were both poorly defined and independent of peptide conformation. We propose that the three decay times are associated with the three ground-state χ_1 rotamers of the tryptophan residue and that the changes in the relative contributions of the decay times are the result of conformational constraints, imposed by the α-helical main-chain, on the χ_1 rotamer populations.

W-Pos269

TIME RESOLVED FLUORESCENCE OF ENANTIOMERS OF MODEL PEPTIDES CONTAINING 7-AZATRYPTOPHAN.

((A. Ito[1], J.D. Brennan[2], L. Juliano[1], J.S. Mort[3], A. Paiva[4], and A.G. Szabo[2,5*])) [1]Department of Biophysics, Escole Paulista de Medicina, Sao Paulo, Brazil, [2]Department of Biochemistry, University of Ottawa, Ottawa, Ontario, Canada, [3]Department of Surgery, McGill University, Montreal, PQ, Canada, [4]Inst. Fisica, Universidad de Sao Paulo, Brazil, [5]Institute for Biological Sciences, National Research Council of Canada, Ottawa, Ontario, Canada.

Two small peptides, each containing a single 7-azatryptophan (7AW) residue were synthesized and purified by HPLC. One peptide, T(7AW)QAG emulates the N-terminal end of the cathepsin pro-fragment. The other, K(7AW)K-OMe is analogous to the peptide KWK whose interactions with acidic lipids are well characterized. It has not been possible to achieve the separation of (7AW) D and L enantiomers using HPLC conditions that normally are used to separate enantiomers of amino acids. HPLC of the peptides, however, indicated that there were two main components of nearly equal concentration in the partially purified synthetic peptides. Mass spectra and steady state absorption and fluorescence spectra showed that for both of the peptides the two peaks corresponded to species with the same chemical composition. The difference in retention time was attributed to the presence of different enantiomers of the peptide in a racemic mixture. Time-resolved fluorescence measurements of the purified enantiomers of the two peptides both in H_2O and D_2O indicated that there were differences in the excited sate decay parameters. Interestingly, the decay kinetics showed the signature of the presence of an excited state reaction of the 7AW residue. The nature of the interaction of the different enantiomers of the peptides with acidic lipids can be followed using time resolved and steady state fluorescence measurements.

W-Pos270

A PEPTIDE WITH A PHOTOISOMERIZABLE AMINO ACID CHANGES CONFORMATION AFTER IRRADIATING OR CHANGING SOLUTION CONDITIONS

((R. Cerpa, F.E. Cohen and I.D. Kuntz)) Graduate Group in Biophysics, Univ. of California at San Francisco, San Francisco, CA 94143.

A peptide containing the photoisomerizable artificial amino acid p-phenylazo-L-phenylalanine has been synthesized. The sequence was derived by mutating a single tyrosine in a de novo designed peptide that was strongly helical (Bradley et al., J. Mol. Biol. (1990) 215:607). Circular dichroism spectra of the phenylazoPhe-containing mutant peptide strongly suggest that the mutant now adopts a beta-sheet conformation. After various perturbations to the peptide solution, including irradiation (which isomerizes the side chain of phenylazoPhe), or heating, the spectra of the peptide indicate an alpha-helical conformation. NMR characterization of the peptide under conditions giving rise to the beta-sheet and alpha-helix conformations is in progress. One objective of the study is to create a system with which to measure rapid folding events in simple peptide models.

W-Pos271

ANALYSIS OF MODEL HELICAL PEPTIDE THERMAL TRANSITIONS USING ^{13}C NMR. ((W. Shalongo, L. Dugad, and E. Stellwagen)) Department of Biochemistry, University of Iowa, Iowa City, IA 52242.

The correlation of the effects of temperature, pH and salt concentration on ^{13}C NMR and circular dichroic measurements of the model peptide, acetylW(EAAAR)$_3$Aamide, suggest that both measurements observe a common two-state helix/coil transition. The thermodynamic parameters characterizing each residue thermal transition suggest that the peptide helical conformation is stabilized by hydrogen bonds and by burial of apolar surfaces and that the helical conformation melts as a largely cooperative unit. The terminal regions of the helix appear less frayed than expected from the Lifson-Roig statistical mechanical model for a peptide helix/coil transition, indicating contributions from stabilizing noncovalent interactions in addition to backbone hydrogen bonds. Preliminary amide proton exchange equilibrium measurements at low temperature indicate that the proton on the peptide bond amide adjacent to each alanine residue is significantly protected from exchange with the solvent. This enhanced protection is consistent with a high helical content of the central residues and also suggests a higher than expected helical content in the carboxy terminal frayed end.

W-Pos272

CONFORMATION OF LIPID-BOUND AND FREE APOLIPOPROTEIN A-I PROBED BY CHYMOTRYPSIN PROTEOLYSIS ((Linda M. Roberts, Marjorie Ray, Tzu-Wen Shih, and Christie G. Brouillette)) Center College, Danville, KY40422 and Southern Research Institute, Birmingham, AL 35205

Apolipoprotein A-I is the major protein component of high density lipoprotein (HDL). Human apo A-I was reconstituted with palmitoyl-oleoyl phosphatidylcholine at a starting molar ratio of 1:100 and the reconstituted lipoprotein (rLp) products were purified based on size using native gradient gel electrophoresis (GGE). Three major rLp resulted with Stoke's radii of 89Å, 115Å, and 148Å. Chemical crosslinking with BS^3 indicates the presence of three apo A-I molecules on each of the particles. Chymotrypsin, which cleaves primarily at hydrophobic aromatic amino acids, was used to probe the differences in apo A-I conformation on the different rLp as well as to determine the change in conformation when apo A-I binds to lipid. Proteolysis products were separated by sds page and N-terminal sequences were determined. Free apo A-I is most susceptible to chymotrypsin at the C-terminus of the protein. On the other hand, lipid-bound A-I is less susceptible to C-terminal cleavage and is susceptible to N-terminal cleavage as well. Chymotrypsin does not distinguish differences in apo A-I conformation between the different rLp particles.
Supported by NIH P01 HL34343.

W-Pos273

ASPARAGINE-LINKED OLIGOSACCHARIDES ARE RESTRICTED TO SINGLE EXTRACELLULAR SEGMENTS IN MULTI-SPAN MEMBRANE GLYCOPROTEINS. ((Carolina Landolt and Reinhart A.F. Reithmeier)) MRC Group in Membrane Biology, Departments of Medicine and Biochemistry, University of Toronto, Toronto, Ontario, Canada, M5S 1A8.

A survey of mammalian multi-span membrane proteins demonstrated that utilized sites for asparagine-linked glycosylation (Asn-X-Ser/Thr, X ≠ Pro) are localized to the first protein loops of a minimum size exposed to the glycosylation machinery in the endoplasmic reticulum lumen. The incidence of potential glycosylation sites on alternative loops are rare although multiple glycosylation sites may occur on a single polypeptide loop. In situations where consensus glycosylation sites are contained within more than one extracellular domains only sites on the first acceptable loop are utilized. The α subunit of the Na^+ - channel, which consists of a duplicated structure is an exception to this glycosylation pattern. The average size of utilized glycosylated loops connecting two transmembrane segments was 61 residues with the smallest glycosylated loop being 33 residues in size. Glycosylation sites were more common toward the amino-terminus of the membrane domain of the surveyed polytopic proteins. The restriction of utilized carbohydrate sites to a single protein loop suggests that only a single polypeptide domain can be glycosylated during biosynthesis or that glycosylation of multiple loops may compromise protein folding or function. This survey serves to refine the requirements guiding the glycosylation of multi-span membrane proteins by determining that utilized sites for N-linked glycosylation are restricted to a single extracellular loop of a minimum size.
(Supported by the Medical Research Council of Canada).

W-Pos274

ENERGETICS OF THE REENTRANT HEXAGONAL - LAMELLAR PHASE TRANSITION IN PHOSPHOLIPIDS. ((M. Kozlov (a), S. Leikin (b), R.P. Rand (c))) (a) Frei Universitat, Berlin, (b) NIH, Washington, (c) Brock University, Canada. (Spon. P. Nicholls)

We have re-examined the energetics of the hexagonal-lamellar -hexagonal reentrant transition sequence of phases that dioleoylphosphatidylethanolamine (DOPE) undergoes as water is osmotically removed from the lipid (Biochemistry 31:2856). The variation in chemical potential of the lipid molecules in each phase is described as a function of osmotic pressure. The change in chemical potential is defined in the hexagonal phase only by a curvature energy of the lipid monolayer, in the lamellar phase only by the energy of interbilayer hydration repulsion. Examination of these two energies defines curvatures and osmotic pressures where the phase transition can be found. On the basis of this simple model, conditions are defined where the reentrant transition can occur. On the basis of this simple model, conditions are defined where the reentrant transition can occur. Using measured hydration energy parameters and monolayer bending elasticities, these conditions for the rentrant transition are satisfied. Consistent with the observation that the osmotic pressure range of the lamellar phase is extremely narrow, those conditions are also very limited in range. In addition, this model predicts the measured relation between the interbilayer distance and the radius of the hexagonal water cylinder at the transition.

W-Pos275

CONFORMATION, HYDROPHOBICITY AND MODEL MEMBRANE INTERACTION OF DIPHTHERIA TOXIN AND TOXOID ((R. Paliwal and E. London)) Department of Biochemistry and Cell Biology, SUNY, Stony Brook, NY 11794.

The conformations of diphtheria toxin and diphtheria toxoid prepared by formaldehyde crosslinking were compared in order to understand the nature of the changes that occur upon toxoid preparation. We found that the conformations of the toxoid and toxin were very similar as judged by fluorescence and hydrophobicity properties. However, the toxoid only underwent thermal, low pH and guanidinium chloride induced changes at more extreme conditions than needed for the toxin. Therefore, the toxoid appears to be significantly stabilized towards conformation changes that involve partial unfolding to a molten globule-like state as well as to complete unfolding. In addition, the toxoid only became hydrophobic and gained the ability to interact with model membrane vesicles at significantly lower pH than the toxin. Because low pH unfolding and membrane penetration are critical steps in the entry of diphtheria toxin into cells, their inhibition in the toxoid may be linked to its lack of toxicity. These results may have important implications for the design of clinically valuable toxoids.

W-Pos276

STUDY OF THE ROLE OF CHARGED SPECIES AND FATTY ACIDS ON THE LYTIC ACTIVITY OF MELITTIN BY SOLID-STATE NMR SPECTROSCOPY. ((Martine Monette and Michel Lafleur)) Université de Montréal, Montréal, Québec, Canada, H3C 3J7.

Phosphorus NMR spectroscopy was used to characterize the interaction between phospholipid bilayers and melittin, an amphiphilic peptide that causes disruption of lipid membranes through an unknown mechanism. This technique is very powerful since the resulting lineshape depends on the size of the assemblies under study. Large lipid bilayers give rise to powder pattern. Conversely, small particles resulting from the lysis induced by melittin lead to an averaged chemical shift: an isotropic signal is observed in that case. Therefore ^{31}P NMR spectroscopy provides a straightforward way to obtain an estimation of the amount of lysed vesicles. To get insights into the lysis mechanism, we have studied the effect of charged species on the lytic power of melittin. Our results show that an increase in the surface charge density caused by the presence of negatively charged species severely inhibits the lysis. On the other hand, introduction of positively charged lipids into the bilayer leads to an increase in the lysed vesicles proportion. We suggest that the modulation of the lytic effect originates from electrostatic interactions between the peptide and the bilayer surface: attractive interactions anchor the peptide at the surface, therefore inhibiting the lysis while repulsive interactions favor the peptide insertion in the bilayer, causing the lysis. We have also studied the effect of unsaturated and saturated fatty acids on the lysis. The presence of small amount (10(mol)%) of protonated palmitic acid promotes the lysis. Conversely, the same amount of unsaturated fatty acids (oleic or linoleic acid) has a protective effect on the lytic activity of melittin. We propose that this modulation is related to the changes in chain packing of the gel-phase bilayer.

W-Pos277

CHARACTERIZATION OF TWO MEMBRANE-BOUND FORMS OF OMPA IN LIPID BILAYERS. ((N. A. Rodionova, S. A. Tatulian, T. Surrey[1)], F. Jähnig[1)] and L. K.Tamm)) Dept. of Molecular Physiology and Biological Physics, University of Virginia, School of Medicine, Charlottesville, VA 22908, and Dept. of Membrane Biochemistry, Max Planck Institute for Biology, Tübingen, Germany[1)]

The insertion of the outer membrane protein A (ompA) into lipid bilayers was studied by limited proteolysis, fluorescence spectroscopy and polarized Fourier transform infrared (FTIR) spectroscopy. In the native state, ompA forms a barrel of antiparallel β-strands. For the present study, it was isolated in an unfolded form, purified and exposed to preformed vesicles of POPC, DMPC, DPPC and three phospholipids that were brominated in different positions of their *sn*-2 chains (4,5-BrPC, 9,10-BrPC, 11,12-BrPC). Limited proteolysis revealed two membrane-bound forms of ompA ("adsorbed" and "inserted", Surrey and Jähnig, PNAS 89:7457). In each lipid the predominant form was the adsorbed form below and the inserted form above the chain melting phase transition of the lipid, respectively. The proteolytic fragments that accumulated during trypsin digestion of the adsorbed form were different from the ones of the inserted form. Fluorescence spectroscopy in the presence of the soluble quencher acrylamide showed that the five tryptophan residues of ompA are protected from the aqueous environment to the same extent in both forms. The extent of quenching of the tryptophan fluorescence in the presence of brominated lipids depended on the position of the bromines in the fatty acyl chain. 4,5-BrPC quenched the fluorescence most efficiently, which indicated an average location of the tryptophan residues closer to the bilayer surface. The binding kinetics were much faster for the adsorbed than for the inserted form. Polarized ATR-FTIR spectra were recorded with ompA inserted or bound to germanium-supported bilayers of POPC, DMPC and DPPC at room temperature. The position of the amide I' band indicated a large fraction of β-strand conformation of ompA in DMPC and a mixture of β-strand and random coil in DPPC. The average orientation of the β-strands was found to be approximately parallel to the plane of membrane when ompA was adsorbed to bilayers of DPPC and close to perpendicular when it was inserted into bilayers of DMPC.

W-Pos278

PHASE BEHAVIOR OF LIPIDS CONTAINING POLYENOIC ACYL CHAINS IN THE PRESENCE OF CHOLESTEROL.((Beth A. Cunningham, D.H. Wolfe, and J.M. Collins)) Bucknell University, Physics Department, Lewisburg, PA 17837, Lycoming College, Physics Department, Williamsport, PA 17701, Marquette University, Physics Dept., Milwaukee, WI 53233.

The low temperature thermal character of both Phosphatidylethanolamine (PE) and Phosphatidylcholines (PC) containing polyenoic acyl chains exhibit broad, low enthalpy transitions. Real time X-Ray diffraction (XRD) measurements indicate the low enthalpy and the reduced cooperativity of the gel to the liquid crystalline phase transition may be attributed to the decreased inter-acyl chain van der Waals interactions. Thus, polyenoic lipid acyl chains are able to form well ordered lattices, but only with the additional energy constraints of the establishment of a hydrogen bond network in the polar headgroup region of the bilayer. If so, then the addition of cholesterol to these polyenoic lipids should disrupt the hydrogen bond network in the intra-headgroup realm along with the known disruption of the acyl chain lattice. We report the calorimetric analysis and the real time XRD analysis of polenoic lipid systems in the presence of cholesterol.

W-Pos279

THE VESICLE-MICELLE TRANSITION IN DMPC-CHOLATE MIXTURES. ((A. Walter[1], L. Iverson[2], A. Kaplun[3], M. He[4] and T. Wiedmann[5])) [1]Dept. Physiol. & Biophys. Wright State Univ., Dayton, OH; Depts. [2]Chemistry, [4]Chem. Engin. & Mat. Sci., [5]Pharmaceutics, Univ. Minn., Minneapolis, MN; [3]Dept. Chem. Engin., Technion-Israel Institute of Technology, Haifa, Israel.

Although the interaction of bile salts and phosphatidylcholine (PC) has been studied extensively, the intermediates between the vesicular and small micellar structures are still controversial. We examined this transition using the bile salt sodium cholate and dimyristoyl-PC (DMPC) expecting this lipid with only one type of acyl chain to form more discrete transition boundaries than the commonly examined egg PC. Visual inspection and absorption spectroscopy indicated that as cholate was added to DMPC vesicles the bluish dispersions became less turbid until at a specific ratio of cholate:PC in the structures, the sample fully clarified. Near this boundary, the samples were viscous. At 22°C, below but near the DMPC main transition, T_m, the mixtures were fairly clear and flow birefringent. Rheological analysis confirmed these samples were viscoelastic and at low to moderate shear, the data were fit with a single Maxwell element. At 30° the samples were turbid, not flow birefringent and viscous but with very different rheological properties. The viscosity dropped dramatically but the solutions remained clear as the temperature approached 4°C. ^{31}P-NMR and small angle X-ray analysis detected no major changes with temperature. DPPC-cholate mixtures in the same transition region had similar behavior near the T_m for DPPC. The data are consistent with presence of long entangled worm-like mixed micelles. This was confirmed by cryo-TEM. The rheological properties just below T_m are very similar to those observed with mixtures of cetyltrimethylammonium-salicylate mixtures. The temperature dependence may be reflective of a change in the rate at which the micelles can undergo molecular rearrangement. The narrow composition region expressing these properties probably is the only region in the vesicle-micelle structural transition comprised solely of worm-like micelles.

W-Pos280

FILAMIN-LIPID BINDING STUDIED BY DIFFERENTIAL SCANNING CALORIMETRY, FILM BALANCE AND HYDROPHOBIC LIPID LABELING TECHNIQUE. (W.H. Goldmann, M. Tempel, C. Dietrich, V. Niggli* and G. Isenberg) TU Munich, Biophysics E22, D-85747 Garching; *Uni Bern, Pathol. Inst., CH-3010 Bern. Switzerland.

The interaction of native filamin with mixtures of DMPC and/or DMPG is studied in reconstituted lipid bilayers. Protein incorporation as a function of lipid composition is determined by measuring the protein/lipid ratio, using protein and phosphate assays in parallel with gel electrophoresis. Protein-lipid interactions are monitored by (hs)-differential scanning calorimetry. The width at half height $T_{1/2}$ of the phase transition, which is a measure of the relative cooperativity, is gradually reduced with increasing filamin concentration. This decrease in cooperativity observed for charged DMPG and for pure DMPC systems is indicative of hydrophobic binding. Further, native filamin also interacts hydrophobically with negatively or weakly negatively charged lipid monolayers. This is observed in time/area diagrams of film balance studies. Using the lipid analogue [^{125}I] TID-PC, which selectively labels membrane-embedded hydrophobic domains of proteins, we show that filamin partially inserts into the hydrophobic bilayer of liposomes. These results are intriguing and suggest that filamin may be a possible candidate for linking the cytoskeleton to the lipid membrane.

W-Pos281

CONSTANT VOLUME MOLECULAR DYNAMICS STUDIES OF HYDRATED LIPID BILAYERS. ((M. M. Clark[†], H. L. Scott[†], S. W. Chiu[‡], E. Jakobsson[‡], and S. Subramaniam[‡])), [†]Department of Physics, Oklahoma State U., Stillwater, Ok. 74078, [‡] Department of Biophysics, U. of Illinois, Urbana, Ill., 61801.

In order to better understand the structure and dynamics of lipid membranes we have carried out Molecular Dynamics (MD) simulations of hydrated lipid bilayers at constant pressure and at constant volume, utilizing different starting configurations. In this poster we present the results of the constant volume (NVT ensemble) simulations. We have used the GROMOS modeling programs to run MD simulations for at least 200 ps on bilayers consisting of 200 molecules of dimyristoylphosphatidylcholine (DMPC), 100 in each monolayer, and at least 6000 water molecules. Simulations were run at gel phase densities (46 Å^2 / mol) and fluid phase densities (62 Å^2 / mol) with periodic boundary conditions imposed. In the latter case two trajectories were run using different starting configurations. We have calculated a number of properties of the lipid chains from the trajectories, including order parameter profiles, average chain tilt, average number of *gauche* isomers per chain, electron density, average dipole potential, and reorientational autocorrelation functions. Results are compared with experimental data, with data generated from NPT simulations run by our group, and with data from other recent simulations run by Heller et. al. (J. Phys. Chem 97, 8343, 1993) and Venable, et. al. (Science 262, 223, 1993) using different simulation cells, boundary conditions, and starting configurations.

W-Pos282

CONSTANT PRESSURE MOLECULAR DYNAMICS STUDIES OF HYDRATED LIPID BILAYERS. ((S. W. Chiu[‡], E. Jakobsson[‡], S. Subramaniam[‡], M. M. Clark[†], and H. L. Scott[†])) [‡] Department of Biophysics, U. of Illinois, Urbana, Ill. 61801, [†]Department of Physics, Oklahoma State U., Stillwater, Ok. 74078.

In order to better understand the structure and dynamics of lipid membranes we have done molecular dynamics simulations using the GROMOS modeling programs of hydrated DMPC bilayers at constant pressure and at constant volume, utilizing different starting configurations. In this poster we present the results of the constant pressure (NPT ensemble) simulations. Two simulations were done with 1 atm pressure and periodic boundary conditions, one starting at fluid phase density and the other at gel phase configuration . In heating the gel phase we saw a collective change in the tilt of the hydrocarbon chains at a lower temperature than the fluid phase transition. This may have been the system's attempt to go into a ripple phase, frustrated by the periodic box being smaller than the periodicity of the ripple. We have calculated a number of properties of the lipid chains from the trajectories, including order parameter profiles, average chain tilt, average number of *gauche* isomers per chain, electron density, average dipole potential, and reorientational autocorrelation functions. Results are compared with experimental data, with data generated from NVT simulations and with data from other recent simulations run by Heller et. al. (J. Phys. Chem 97, 8343, 1993) and Venable, et. al. (Science 262, 223, 1993) using different simulation cells, boundary conditions, and starting configurations.

W-Pos283

THE ANTI-VIRAL PEPTIDE CARBOBENZOXY-D-PHE-L-PHE-GLY CHANGES THE AVERAGE CONFORMATION OF PHOSPHOLIPIDS IN MEMBRANES. ((P. L. Yeagle, A. R. Dentino, T. F. Smith, P. Spooner and A. Watts)) Department of Biochemistry, School of Medicine and Biomedical Sciences, University at Buffalo, 140 Farber Hall, Buffalo, New York 14214; Department of Biochemistry, University of Oxford, South Parks Road, Oxford OX1 3QU

The influence of the anti-viral, carbobenzoxy-D-phe-L-phe-gly (ZfFG), on the average conformation of phosphatidylcholine (PC) in hydrated bilayers was investigated with multinuclear solid state magnetic resonance (NMR). ^2H NMR of the PC perdeuterated in the acyl chains showed a loss of intensity from the deuteriums with the largest quadrupole splitting in the presence of ZfFG. The remainder of the powder pattern was largely unaffected. The PC specifically deuterated at the C_2 carbon showed the same loss of intensity suggesting changes in the phospholipid conformation and conformational dynamics near the glycerol. Powder patterns from PC labeled with ^{13}C in the carbonyl carbons revealed a significant change in the average orientation of the *sn-1* carbonyl due to the presence of the ZfFG, and no change in the *sn-2* carbonyl orientation. Changes in the headgroup conformation, as detected by ^2H NMR of the deuteriums in the α and β methylenes of the choline headgroup, and ^{31}P NMR of the phosphate segment, reflected the electrostatic nature of the interaction of the carboxyl of ZfFG with PC bilayers. From these data it was concluded that in the absence of ZfFG, the two carbonyls are inequivalent in their orientation. ZfFG favored a conformation in which the average orientations of the two ester carbonyls were approximately equivalent.

W-Pos284

STRUCTURE OF THE SUB-GEL AND GEL PHASES IN ORIENTED PHOSPHATIDYLCHOLINE MULTILAYERS. ((J. Katsaras, E.J. Dufourc and J. Dufourcq))CRPP-CNRS, Bordeaux, France. (Spon. by J. Dufourcq)

We report small- and wide-angle x-ray diffraction measurements on highly oriented films of dipalmitoyl phosphatidylcholine (DPPC) under various humidities and temperatures. The data describe the physical characteristics of the hydrocarbon chains in the $L_{c'}$ phase and show that the $L_{c'} \rightarrow L_{\beta'}$ phase transition is characterised by a change in hydrocarbon chain packing, tilt angle and direction. In addition, 1D electron density profiles of the $L_{c'}$ and $L_{\beta'}$ phases indicate that the accessibility of water to the bilayer is significantly reduced when the DPPC molecules are in the $L_{c'}$ phase.

STRIATED MUSCLE PHYSIOLOGY AND ULTRASTRUCTURE II

W-Pos285

THE EARLY PHASE OF THE DECLINE OF THE INTRACELLULAR CA^{2+} TRANSIENT IN FROG SKELETAL MUSCLE IS NOT AFFECTED BY THAPSIGARGIN. ((DR Claflin, DG Stephenson*, DL Morgan** & FJ Julian)) Dept. of Anesthesia, Brigham & Women's Hospital, Boston, MA 02115; *La Trobe University and **Monash University, Australia.

Shortly after depolarization of an intact frog skeletal muscle fiber with a single electrical stimulus, intracellular Ca^{2+} rises abruptly to a peak that occurs before the onset of positive tension generation, and then falls to a level near that in the resting fiber by the time of peak twitch tension (Claflin et al. Biophys. J. 61:A293, 1992). It is well established that the source of the Ca^{2+} that gives rise to this intracellular calcium transient (ICT) is the sarcoplasmic reticulum (SR). Several intracellular Ca^{2+} sinks exist that could be contributing to the decline in the ICT including troponin C, parvalbumin, and the SR Ca^{2+} pump. However, the relative contributions of these removal processes are not known. The aim of the experiments described here was to test the hypothesis that the early phase of the decline of the ICT is caused predominantly by the SR pump. Thapsigargin, a naturally occurring sesquiterpene lactone, has been shown by Kijimi et al. (JBC 266:22912-22918, 1991) to be a potent inhibitor of skeletal muscle SR pump proteins. To test the hypothesis, we recorded, simultaneously, twitch tension and the ICT as reported by the fluorescent dye Mag-Fura-2 (MF2) under control conditions and after treatment with 1μM thapsigargin. MF2 was chosen because its low affinity for Ca^{2+} ($Kd \approx 50\mu M$) reduces the chance of dye saturation during the peak of the ICT. MF2 is not, however, well suited to detect small elevations above resting level. Experiments were performed at 3°C using intact single fibers from the tibialis anterior muscle of the frog (*R. temporaria*) at an average sarcomere length of 2.5μm. After treatment with thapsigargin, twitch tension half-relaxation time increased from 266±54ms to 383±86ms (mean±SEM, n=3). The rise and early fall of the MF2 fluorescence signal from the thapsigargin-treated fibers was, however, virtually indistinguishable from control. These findings suggest that a process other than SR pumping dominates the early phase of the removal of Ca^{2+} from the myoplasm during a twitch contraction. Supported by: NIH HL35032 (FJJ), ARC (DGS).

W-Pos286

AFFINITY OF GTP FOR MYOSIN HEADS IN MUSCLE IS CALCIUM SENSITIVE. ((S.M. Frisbie and L.C. Yu)) NIAMS, NIH, Bethesda, MD.

In a previous publication (Kraft et al., PNAS, 1992), we have shown that the affinity of ATPγS to attached cross-bridges is highly Ca^{++} sensitive, and full saturation with ATPγS is reached only at high concentrations of nucleotide. To investigate if this Ca^{++} sensitivity is a general property of nucleotide binding to weakly attached cross-bridges, we applied 0.01 μM to 10 mM of purified GTP to skinned rabbit psoas fibers in rigor. Binding was monitored by the X-ray equatorial intensity ratio $[I_{11}]/[I_{10}]$. In the absence of Ca^{++}, saturation was reached by 10 mM. In the presence of Ca^{++}, saturation of cross-bridges with GTP varied over approximately six decades of concentration. Even at 10 mM, full saturation was not reached. Lattice spacing of the [1,0] reflections also showed a large difference in the presence and absence of calcium. The difference in titration behavior in the presence of Ca^{++} is not due to GTP turnover, since GTPase activity was found to be low. Measurement of nucleotide turnover for a single fiber showed that the GTPase rate was at least 1000 fold less than the ATPase rate (both with Ca^{++}). These results suggest that similar to ATPγS, the previously observed Ca^{++} effect on actin affinity of weakly attached cross-bridges (Dantzig et al., PNAS, 1988; Pate et al., JBC, 1993) could be due to incomplete nucleotide saturation at high Ca^{++} concentration.

W-Pos287

KINETICS OF CALCIUM BINDING TO MYOSIN LIGHT CHAIN 2 IN RABBIT PSOAS FIBERS FOLLOWING FLASH PHOTOLYSIS OF CAGED CALCIUM. ((J.R. Patel, G. Diffee, F. Reinach* and R.L. Moss)) Department of Physiology, University of Wisconsin, Madison, WI 53706, *Institute of Chemistry, University of Sao Paulo, Brazil

The kinetics of Ca^{2+} binding to myosin light chain 2 (LC2) were studied in small bundles of troponin C depleted skinned psoas muscle fibers. Fluo-3 was used to monitor changes in $[Ca^{2+}]$ after flash photolysis of DM-nitrophen, a photolabile Ca^{2+} chelator. Just subsequent to photolysis (F), $[Ca^{2+}]$ increased from pCa ~7.1 to ~6.1, and this was followed by a biphasic decline in fluorescence (trace A). There was an initial rapid decline due to Ca^{2+} binding to unphotolysed DM-nitrophen, followed by a slow decay ($0.62+0.1\ s^{-1}$, n=8) which we attribute to Ca^{2+} binding to LC2. Both the extent and the rate of Ca^{2+} binding decreased when endogenous LC2 was partially replaced with a mutant LC2 (trace B) having much lower affinity for Ca^{2+} (Reinach *et al.*, Nature 322:80-83,1986). The data suggest that the rate and the extent of Ca^{2+} binding to LC2 depend on the concentration of LC2 in the fibers.

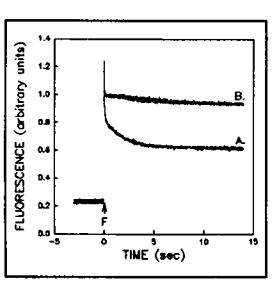

W-Pos288

RATE OF MAXIMUM FORCE DEVELOPMENT DUE TO PHOTOLYSIS OF CAGED CA^{2+} IS NOT AFFECTED BY PRESENCE OF SUBMAXIMUM FORCE IN FROG SKELETAL MUSCLE FIBERS. ((Philip A. Wahr and Jack A. Rall)) Dept. of Physiology, The Ohio State University, Columbus, OH 43210.

Mechanically skinned fibers of the tibialis anterior muscle of the frog R. temporaria were soaked at 10 °C in solutions containing 2mM DM-nitrophen, 100 mM TES, 3 mM ATP, 20 mM creatine phosphate, 25 mM HDTA, 10 mM glutathione, 36 μM Mg^{2+}, and varying amounts of Ca^{2+}, at pH 7. Force was allowed to develop to a plateau and the fibers were then maximally activated in air by flash photolysis of the DM-nitrophen. The subsequent time to half maximum force ($t_{1/2}$) was then measured and compared to the $t_{1/2}$ in the same fiber activated from zero force. Fibers exhibited a $t_{1/2}$ from zero force of 37.0 ± 11.1 ms (mean ± S.D.), n = 12. When the initial submaximum force was less than 30% of peak force, the ratio of $t_{1/2}$ to the $t_{1/2}$ from zero force was 1.02 ± 0.19, n = 2. For fibers with an initial force greater than 70% the ratio was 0.95 ± 0.19, n = 4. Thus, the initial force level, and therefore the number of force generating cross bridges, has no effect on the rate of subsequent maximum force production. Supported by: AHA, Ohio Affiliate.

W-Pos289

FORCE DEPENDENCE OF PHASE 2 TENSION RECOVERY WITH ALTERED CALCIUM OR PHOSPHATE ANALOG INHIBITORS OF SKINNED SKELETAL MUSCLE. ((D.A. Martyn, P.B. Chase, T.W. Beck, M.J. Kushmerick and A.M. Gordon)) Center for Bioengineering, Dept. of Radiology, and Dept. of Physiology & Biophysics, University of Washington, Seattle, WA 98195

The early, rapid phase of tension recovery following a step change in sarcomere length (phase 2) is thought to reflect the force generating transition of myosin bound to actin. We have measured the relation between the kinetics of phase 2, estimated from the half-time ($r = 0.79 \cdot t_{1/2}^{-1}$), during steady-state activation at varying [Ca^{2+}] and during inhibition of maximum Ca^{2+}-activated force by the tightly-binding Pi analog aluminofluoride in glycerinated, single fibers from rabbit psoas. Sarcomere length was monitored continuously by laser diffraction of fiber segments (~1.5 mm long) and sarcomere homogeneity was maintained using periodic length release/restretch cycles at 12°C. At lower [Ca^{2+}] and forces, r was elevated relative to that at pCa 4.0 for both releases and stretches (between $\pm$ 8 nm·h.s.$^{-1}$). At -4 nm·h.s.$^{-1}$, r was 3.3 $\pm$ 1.0 ms^{-1} at pCa 6.6 (10 - 20% of maximum force at pCa 4.0) while the corresponding value at pCa 4.0 was 1.0 $\pm$ 0.2 ms^{-1} (mean $\pm$ S.D.; N = 5). For stretches of 2 nm·h.s.$^{-1}$, r was 1.0 $\pm$ 0.3 ms^{-1} (N = 9) at pCa 6.6 and 0.4 $\pm$ 0.1 ms^{-1} at pCa 4.0 (mean $\pm$ S.D.; N = 14). When maximum force was decreased with AlF, r was elevated for both stretches and releases. Our results obtained during steady state activation of skinned fibers are qualitatively similar to the increase in r observed during the rise of force in a tetanus (Ford *et al.*, 1986, *J. Physiol.* 372:595) and are consistent with the model of Bagni *et al.* (1988, *Biophys. J.* 54:1105), although a possible direct effect of Ca^{2+} on phase 2 kinetics needs to be tested further. Supported by NIH HL31962.

W-Pos290

FORCE INHIBITION BY ALUMINOFLUORIDE IN SKINNED FIBERS FROM RABBIT SOLEUS MUSCLE. ((P.B. Chase and T.W. Beck)) Dept. of Radiology, University of Washington, Seattle, WA 98195. (Spon. by R.W. Wiseman)

Aluminofluoride (AlF) acts as a slowly dissociating analog of inorganic phosphate (Pi) in fast-twitch, skeletal muscle fibers (Chase *et al.*, 1993, *J. Physiol.* 460:231). For comparison with cells containing cardiac β myosin heavy chain, we have examined the effects of AlF on maximum Ca^{2+}-activated force of skinned fibers from rabbit soleus, a slow-twitch muscle. Under conditions similar to experiments on psoas fibers, AlF also inhibited force of soleus fibers. Both the onset of and recovery from inhibition by AlF were several-fold slower in soleus fibers, as expected for an inhibitor which acts at the active site of myosin; recovery from inhibition was incomplete after > 1.5 hr following removal of the inhibitor from the bathing solution (12°C). Experiments at reduced concentrations of total fluoride (0.1 - 3 mM), with either Al^{3+} or deferoxamine added, showed that inhibition was not due to effects of F^- alone. However, at 10 mM total fluoride with deferoxamine, soleus fibers were inhibited to a greater extent by fluoride alone than were psoas fibers. As found with psoas fibers, AlF appeared to be trapped in the fiber in the absence of active crossbridge cycling. These experiments demonstrate the utility of AlF for examining intermediate states occurring early in the crossbridge cycle of slow-twitch muscle. Supported by AHA WA Affiliate.

W-Pos291

INHIBITION OF FIBER SHORTENING VELOCITY BY CAGED ATP COMPOUNDS.

((Hilary Thirlwell, John A. Sleep*, John E.T. Corrie, David R. Trentham and Michael A. Ferenczi)) *National Institute for Medical Research., Mill Hill, London NW7 1AA, U.K.. *The Randall Institute, King's College London, 26-29 Drury lane, London WC2B 5RL, U.K.*

The K_m for ATP of the shortening velocity in glycerinated rabbit psoas muscle (I=0.15 M, pH 7.1, [Ca^{2+}]=32μM, 20°C) was 150 μM as reported previously for measurements at 10°C (Cooke and Pate, 1986). Both conventional caged ATP (P^3-1-(2-nitrophenyl)ethyl ATP) and the new DMB-caged ATP (the P^3-3',5'-dimethoxybenzoin ester of ATP, Corrie *et al.*, 1992) were found to inhibit the shortening velocity in a competitive manner. The inhibition constants were in the range of 1 - 2 mM. These results affect the choice of experimental conditions for caged ATP experiments, since they indicate that addition of 10 mM caged ATP will reduce the rate of ATP binding 5 to 10 fold. Doubling the caged ATP concentration from 5 to 10 mM, which approximately doubles the concentration of ATP released by photolysis also almost doubles the degree of inhibition of ATP binding, thus cancelling the concentration gain. These results may contribute to the lower rates of ATP binding to fibres in caged ATP experiments (0.5 - 1 x 10^6 $M^{-1}s^{-1}$) relative to that reported for acto-subfragment 1 (3.5 x 10^6 $M^{-1}s^{-1}$, Goldman *et al.*, 1984).

Cooke, R. and Pate, E.. (1986) *Biophys. J.* **48**: 789-798

Corrie J.E.T., Katayama Y., Reid, G.P., Anson, M. and Trentham, D.R. (1992) *Phil. Trans. R. Soc. Lond. A* **340:** 233-244.

Goldman, Y.E., Hibberd, M.G. and Trentham, D.R. (1984) *J. Physiol.* **354**: 577-604, 605-624.

W-Pos292

TRIMETHYLAMINE N-OXIDE (TMAO), BETAINE AND GLYCINE DO NOT ALTER THE CALCIUM-SENSITIVITY OF SKINNED SKELETAL AND CARDIAC MUSCLE FIBERS. ((V.S. Tivakaran, M.A. Derosa and M.A. Andrews)) Division of Physiology, NY College Osteopathic Medicine, Old Westbury, NY 11568.

Previous results have shown that the protein stabilizer TMAO significantly increases maximal calcium-activated force generation (Fmax) of skeletal (Fogaca et al. 1990. Biophys. J. 57:546) and cardiac muscle (Nosek et al. 1991. Biophys. J. 62:A18), and ameliorates the decrease of Fmax caused by inorganic orthophosphate (Andrews 1993. Biophys. J. 64:A361). The present experiments were run to determine whether or not TMAO, betaine and/or glycine (two other protein stabilizer) alter the calcium-sensitivity of muscle fibers. Such compounds have been proposed to work via a passive stabilization mechanism. If such is the case, it is proposed that specific functional alteration of the contractile proteins such as altered calcium-sensitivity should not occur. Single fibers of fast-twitch extensor digitorum longus muscle, slow-twitch soleus muscle and thin strips of rat cardiac papillary muscle were used. Muscle fibers were activated in a step-wise manner through a series of solutions of pCa 8.5 to 4.0 containing 100 mM or 300 mM TMAO, betaine, or glycine. All experiments were run at pH = 7, and 22° C. Solutions were formulated according to microcomputer programs (Turbo Pascal) which solve the set of simultaneous equations describing the multiple equilibria of ions in the solutions. All solutions contained (mM): 5 EGTA, 20 imidazole, 2 Mg^{2+}, 5 MgATP, 15 phosphocreatine, with 100 u/ml CPK at a total ionic strength of 200 mM ($KMeSO_3$ added). Results indicate that while all compounds significantly increased Fmax at pCa = 4, they only mimimally altered calcium-sensitivity of the contractile apparatus. These findings provide further evidence that the effect of protein stabilizers are via a passive thermodynamic mechanism to increase force generation, and not by any specific alteration of the contractile proteins.

W-Pos293

THE EFFECT OF EMD 57033 ON MUSCLE ACTIVATION AND RELAXATION; A STUDY USING DIAZO-2 AND NITR-5.

((S.J.Simnett, S.Lipscomb, C.C.Ashley and I.P.Mulligan*)) Uni.Lab.Physiol. Parks Rd. Oxford and *Dept. Cardiovascular Med., J.R.Hospital, Oxford. U.K.

EMD 57033 (EMD) increases the apparent calcium sensitivity of myofibrils and possibly slows the rate of Ca^{2+} dissociation from TnC. We have investigated the effect of 10 μM EMD on the speed of isometric relaxation induced by flash photolysis of 2mM diazo-2 in skinned skeletal frog muscle fibres and guinea-pig trabeculae in the presence and absence of 1mM ADP. Maximal Ca^{2+} activated force is increased by 10 μM EMD to 129.7$\pm$5.5% and 138$\pm$4.23% of control in skeletal and cardiac muscle respectively. 10 μM EMD has no effect on the speed of relaxation of skinned skeletal frog muscle fibres. In guinea pig trabeculae, EMD increases the speed of relaxation slightly (10 μM EMD: $t_{\frac{1}{2}}$ = 45.8$\pm$2.5ms, Control: $t_{\frac{1}{2}}$ = 59.2$\pm$5.5 ms), in contrast to the effect of ADP which produces a marked slowing ($t_{\frac{1}{2}}$ = 160$\pm$6.8ms). When 10 μM EMD is added to 1mM ADP solution the slowing of relaxation is not as great as that seen with 1mM ADP alone ($t_{\frac{1}{2}}$ = 140$\pm$5.2ms). In contrast EMD produces a marked acceleration of the trabecular activation rate following the photolysis of 2mM nitr-5 (Control: $t_{\frac{1}{2}}$ = 238.6$\pm$18.55msec, 10μEMD: $t_{\frac{1}{2}}$ =132.1$\pm$32.99). This suggests that the effect of EMD is mediated by an increase in the rate at which crossbridges reach the force-generating state. In contrast ADP decreases the rate of transition out of the force-generating state. EMD kindly supplied by E.Merck Pharmaceuticals, Germany.

W-Pos294

INCREASED MYOFIBRILLAR CALCIUM SENSITIVITY INDUCED BY PERCHLORATE IONS IN SKINNED FAST AND SLOW SKELETAL MUSCLE FIBERS FROM THE RAT.

((A. Khammari, S. Baudet and J. Noireaud)) UA 1340, Labo.Cardio. Exp., Nantes, France

Triton X-100-skinned muscle fibers from rat soleus (SOL) and EDL muscles were used to assess whether perchlorate (ClO_4^-)-induced twitch force potentiation[1] could relie on increased myofilament calcium (Ca^{2+}) responsiveness. ClO_4^- (1-20 mM) rapidly increased steady tension at constant [Ca^{2+}], although the effects were more marked at low than high [Ca^{2+}]: 20 mM ClO_4^- increased tension by 150% in EDL and 250% in SOL at 0.1 μM Ca^{2+} and by 25% in EDL and 10% in SOL at 3.16 μM Ca^{2+}. pCa/tension curves in the presence of 12 mM ClO_4^- were shifted leftward compared to control (Figure). For EDL, pCa_{50} increased from 5.88±0.04 to 6.08±0.02 (n=9; P<0.001) and the Hill coefficient (n_H) increased from 2.72±0.10 to 2.77±0.09 (n.s.). In SOL muscle, pCa_{50} increased from 6.13±0.04 to 6.33±0.04 (n=11; P<0.001) and n_H decreased from 1.93±0.07 to 1.76±0.07 (n.s.). Return to ClO_4^--free conditions shifted slightly, but non significantly, the pCa/tension curve rightward in both types of fibers (Figure). For EDL, "return" pCa_{50} was 5.77±0.02 and for SOL, 6.05±0.04 (n.s.).

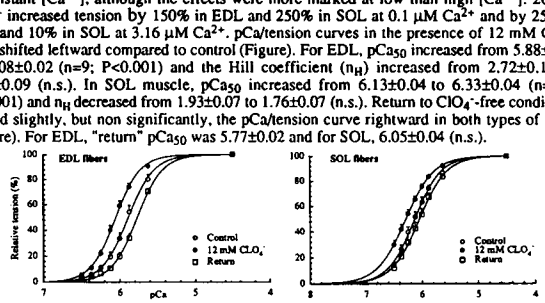

Thus, an increased myofilament Ca sensitivity may account for a fraction of the ClO_4^--induced twitch potentiation. Moreover, considering the large effect of ClO_4^- at resting [Ca^{2+}], it may explain the increase in resting tension observed with ClO_4^- application[2]. Therefore, this newly described effect of ClO_4^- should be considered in future investigations.

1 Rios, Ma & Gonzalez. 1991 *J. Muscle Res. Cell. Motil.* **12**, 127-135

2 Dulhunty, Zhu, Patterson & Ahern. 1992 *J. Physiol.* **448**, 99-119.

W-Pos295

EFFECT OF ACIDOSIS ON FORCE AND [Ca^{2+}] IN SKELETAL MUSCLE.
((AJ Baker, R Brandes*, MW Weiner)) Univ. Calif. San Francisco CA 94121 & *Loyola Univ. Chicago IL 60153.

The goal was to investigate the effects of severe acidosis (pH 6.3) on cytosolic [Ca^{2+}] and force during contractions of intact frog muscle. Studies using intracellular Ca^{2+} indicators suggest that with a moderate drop in pH (≈pH 6.8) changes in contraction occur which may be related to altered Ca^{2+}-handling. In this study, quantitation of [Ca^{2+}] was obtained using the indicator indo-1, accounting for the presence of protein and lowered pH on indicator properties. **Results:** The figure shows the effect of acidosis on tetanic force and calculated [Ca^{2+}]. Acidosis caused a small decrease in force, however, [Ca^{2+}] increased. Acidosis also considerably slowed relaxation which was parallelled by a slowed decline of [Ca^{2+}]. [Ca^{2+}] decline was biexponential: the time constant of the rapid initial phase of [Ca^{2+}] decline increased with acidosis (magnitude was unchanged), however, the time constant of the slower phase was unchanged (but the magnitude increased). **Conclusions:** 1) severe acidosis caused a small (≈10%) decrease in force which was not due to decreased tetanic [Ca^{2+}]; 2) acidosis considerably slowed relaxation which may be partially mediated by a slowed [Ca^{2+}] decline; 3) at least two processes may contribute to [Ca^{2+}] decline.

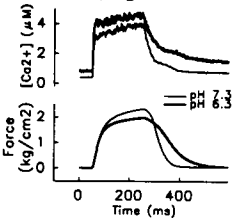

W-Pos296

EFFECT OF RAISING [ADP] OR LOWERING [ATP] ON THE TENSION TRANSIENTS OF MUSCLE
((C. Y. Seow and L. E. Ford)) Dept. of Medicine, Univ. of Chicago, Chicago, IL 60637

To learn more about the relationship between chemical and mechanical transitions of the crossbridge cycle, skinned rabbit psoas fibers were studied at 1-2°C and pH 7.0 in varying concentrations of ATP and ADP. Raising [ADP] from 0 to 5 mM (at 5 mM [ATP]) had similar effects on the steady-state force-velocity properties as lowering [ATP] from 10 to 2 mM (at 0 mM [ADP]). The two interventions increased isometric force by 25% and 23%, respectively, while decreasing maximum velocity by 36% and 31%. The effects of the two interventions on the early, rapid (Phase 2) force recovery following a step change of sarcomere length were defined by fitting the force records with three exponential processes whose time constants all varied in the same proportion with step size (J. Physiol. 269: 441, 1977). The procedure used to fit the experimental records allowed the relative amplitudes and time constants of the three processes to vary. Good descriptions were obtained when the major effect of decreased [ATP] was to slow the slowest process by 41% and the major effect of increased [ADP] was to slow the middle process by 36%, with no change in the relative amplitudes of the three processes. Thus, ADP release from the crossbridge appears to hasten a faster component of the early, rapid force recovery than ATP binding, perhaps because the responsible transition is closer in the cycle to the force producing power stroke.

W-Pos297

EFFECTS OF MgATP, MgADP AND PHOSPHATE ON COMPLEX STIFFNESS MODULI OF SKINNED FLIGHT MUSCLE FIBERS OF *DROSOPHILA*.
((D. Maughan, H. Yamashita, C. Hyatt)) Dept. Molecular Physiology & Biophysics, U. Vermont, Burlington, VT 05405.

We investigated the effect of varying MgATP, MgADP and phosphate (Pi) concentrations on the tension responses to small (0.25%) sinusoidal length perturbations (1-1000 Hz) in saponin-skinned flight muscle at 12°C (pH 7, pCa 4.5, 14 mM MgATP, 0-8 mM MgADP, 0-16 mM Pi and 15 mM creatine phosphate, 80 u/ml CPK, omitted in MgADP solutions). Nyquist plots of complex stiffness were fitted by 3 exponential processes, *A, B and C* (*B* showing a phase lag), characterized by amplitudes A, B and C and rate constants a, b and c, respectively. *A* is slow, small and variable; *B* and *C* are the basis for oscillatory work in flight muscle. At 8 mM Pi (no MgADP), parameters B, C, b and c increase as curvilinear functions of [MgATP]. At 5 mM MgATP, B and C increase but b and c decrease as functions of [MgADP] and [Pi]. The combination of 5 mM MgATP, 4-8 mM Pi and ~0 mM MgADP yields parameter estimates that are consistent with an optimum power output near 145 Hz, i.e., the wing beat frequency of the fly at 12°C. The results are consistent with a scheme in which the release of the products of MgATP hydrolysis (Pi and MgADP) follows a rate limiting, force producing isomerization of actomyosin-MgADP-Pi. **Supported by NIH AR40234.**

W-Pos298

EFFECT OF INORGANIC PHOSPHATE ON THE STRETCH-INDUCED TENSION ENHANCEMENT IN SKINNED RABBIT SKELETAL MUSCLE FIBERS
((H. Iwamoto and H. Sugi)) Dept. of Physiol., Sch. of Med., Teikyo University, Tokyo 173 Japan

To investigate the mechanical characteristics of the myosin cross-bridges in the presence of inorganic phosphate (P_i), we recorded the tension response to stretch of skinned rabbit psoas muscle fibers. The addition of 20mM P_i reduced the calcium-activated isometric tension (P_0) to ca. 30% of control (0mM added P_i, pCa=4.3) and increased the stiffness/P_0 ratio to ca. 150%. This result is in accord with the equilibrium of the attached cross-bridges shifting toward a low-force, presumably A•M•ADP•P_i state. The amplitude of tension enhancement induced by a ramp stretch (1.2% fiber length, 10ms duration) increased from 150 to 270% of P_0 as [P_i] was raised from 0 to 20mM. This effect of Pi was not apparent until the amplitude of the ramp stretch exceeded 0.3~0.6%, suggesting the presence of a critical cross-bridge extension of 4~8 nm for the P_i effect to appear. Although the P_i effect diminished as the speed of stretch was reduced, it was still apparent with a 160ms stretch. These results suggest that the low-force cross-bridges have much slower kinetics than the rapid-equlibrium relaxed cross-bridges at low ionic strength. When the isometric tension was reduced to a comparable extent by reducing free calcium concentration, no extra enhancement of tension was observed upon stretch. This raises the possibility that the point of calcium regulation is the entrance to mechanical cycles rather than the step of P_i release from the A•M•ADP•P_i state.

W-Pos299

THE IMPACT OF N-TERMINAL α-HELIX OF RABBIT SKELETAL MUSCLE TnC ON UNLOADED SHORTENING
((A. Babu, X.-L. Ding, E.H. Sonnenblick, Hong Su and J. Gulati))
Albert Einstein College of Medicine, Bronx, NY 10461 (Spon.: S. Seifter)

The crystal structure of skeletal TnC as of calmodulin is a dumbbell. But, unlike calmodulin, TnC contains an extra N-terminal α-helix (N-helix) preceding the first EF-hand Ca-binding site, as well as a KGK triplex within the stem joining the lobes. In a recent study (Gulati et al, 1993, JBC, 268, 11685) we found that deletion of the N-helix (ΔNt-TnC) diminished the Ca-induced maximal tension in the fiber. Remarkably, following concomitant deletion of the KGK triplex from central helical stem (ΔNt·ΔKGK-TnC) the tension development was well restored. To elucidate the effect of the N-helix on cross-bridge mechanism, with each mutant (1) we measured pCa-tension relations on the fiber, to estimate the pK. (2) We also measured the speed of unloaded shortening (Vmax). With ΔNt-TnC, the maximal tension level (P_o), pCa_{50} of the pCa-tension curve, and Vmax were all diminished compared with control — P_o: 45±2%; ΔpCa_{50} representing diminished Ca-sensitivity in the fiber: 0.58±.05 unit; Vmax: 55±4%. With the binary ΔNt·ΔKGK-TnC variant, the corresponding values were — P_o: 91±4%; ΔpCa_{50}: 0.48±.04 unit; Vmax: 70±4% of control. Thus with the binary mutant, despite the restored maximal tension development, fiber Ca-sensitivity and Vmax both remained abnormal. The stiffness/tension ratios were similar with both mutants. The findings suggest that communication between regulatory strands on the thin filaments is enhanced by TnC N-helix. *Supported by NIH & NY Heart*

W-Pos300

EFFECT OF PARTIAL EXTRACTION OF TROPONIN C ON ELEMENTARY STEPS OF THE CROSS-BRIDGE CYCLE IN SKINNED RABBIT PSOAS MUSCLE FIBERS.
((Y. Zhao, P.M.G. Swamy, and M. Kawai)) Department of Anatomy, University of Iowa, Iowa City, IA 52242.

Troponin C (TnC) was partially extracted in skinned rabbit psoas muscle fibers, and elementary steps of the cross-bridge cycle were investigated by sinusoidal analysis under full Ca^{2+} activation (pCa 4.82). When about 60% of the TnC was extracted as judged by SDS polyacrylamide gel electrophoresis, the remaining tension was 7-14%, indicating the presence of cooperative interaction between the thin filament regulatory units. The TnC extraction caused a 3.5 fold increase in the association constant (K_1) of the substrate (MgATP) to the myosin cross-bridge, presumably because the condition of the regulatory unit (troponin-tropomyosin-actin system) modified the shape of the substrate binding site on the myosin head. The equilibrium constant of the cross-bridge detachment step (K_2) decreased by 2.5 fold. The equilibrium constant of the cross-bridge attachment step (K_4) (force generation step) decreased by 2 fold. Our results of a large decrease in isometric tension (10X) and a small decrease in K_4 (2X) with TnC extraction are consistent with the all-or-none hypothesis of cross-bridge activation by thin filament. Our result of a small decrease in K_4 with TnC extraction is consistent with the cooperativity hypothesis of the thin filament regulatory units. The association constant of Pi (K_5) to myosin cross-bridges changed little with the TnC extraction. Our results demonstrate that the cross-bridge kinetics are under the influence of thin filament regulatory proteins.

W-Pos301

ELEMENTARY STEPS OF THE CROSS-BRIDGE CYCLE IN RABBIT SOLEUS MUSCLE FIBERS. ((G. Wang, Y. Zhao, and M. Kawai)) Dept. of Anatomy, Univ. of Iowa, Iowa City, IA 52242

Elementary steps of the cross-bridge cycle were investigated with sinusoidal analysis in skinned rabbit soleus slow-twitch fibers. The muscle preparations were activated at pCa 4.82, ionic strenghth 200 mM, 20°C, and the effects of MgATP (S), MgADP (D), and phosphate (Pi) concentrations on three exponential processes (B,C,D) were studied. Results are consistent with the following cross-bridge scheme:

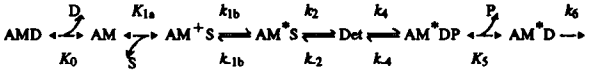

Where A=actin, M=myosin, D=MgADP, S=MgATP, P=phosphate, and Det includes all detached states (MS, MDP) and weakly attached states (AMS, AMDP). We obtained K_0=1.48 mM^{-1} (MgADP association), K_{1a}=0.56 mM^{-1} (MgATP association), k_{1b}=321 s^{-1} (ATP isomerization), k_{-1b}=307 s^{-1} (reverse isomerization), k_2=80 s^{-1} (cross-bridge detachment), k_{-2}=24 s^{-1} (reverse detachment), k_4=4.2 s^{-1} (cross-bridge attachment), k_{-4}=9.8 s^{-1} (reverse attachment), and K_5=0.10 mM^{-1} (Pi association). k_6 is the rate constant of the rate-limiting step. K_0 (MgADP binding) and K_{1a} (MgATP binding) are 2.5X of rabbit psoas, and K_5 (Pi binding) is 0.5X of psoas, indicating that the soleus muscle is more resistant to ATP depletion and Pi accumulation. The rate constants of ATP isomerization (k_{1b}, k_{-1b}) and cross-bridge detachment (k_2, k_{-2}) steps are 6 times slower than psoas. Cross-bridge attachment (k_4) step is 25 times slower, and its reverse (k_{-4}) step is 10 times slower than psoas.

W-Pos302

COMPARISON OF WEAKLY-COUPLED AND STRONGLY-COUPLED CROSS-BRIDGE MODELS BY STOCHASTIC SIMULATIONS. ((Charles J. Brokaw)) Division of Biology, Caltech, Pasadena CA 91125

In strongly-coupled cross-bridge models for motor enzyme function, ATP binding and hydrolysis are required for detachment and reattachment of every force-producing cross-bridge. In weakly-coupled models, cross-bridges that have moved far beyond their free energy minimum can detach without ATP binding when they have accumulated so much strain that the attached state is less stable than the detached state. They can then reattach to different sites as force-producing cross-bridges. In these weakly-coupled models, many cycles of cross-bridge attachment and detachment can occur without ATP binding and hydrolysis. However, all of these cycles absorb work by "protein friction". All of the work production occurs in cycles that involve attachment followed by ATP-induced detachment. A stochastic computational method was used to compare the properties of these two types of models. The model contains a four-state cross-bridge cycle, but is computationally a nine-state model, with three adjacent sites considered as possible attachment sites for each of two attached states.

Results demonstrate that the basic assumptions of the weakly-coupled model are thermodynamically valid when a rigorously defined model is used. Weakly-coupled models can have high "translocation efficiency" (translocation velocity divided by the average ATP turnover rate for each motor enzyme molecule). However, a high translocation efficiency can be obtained with strongly-coupled models by maintaining a low attachment rate, so that many attachment sites are passed without cross-bridge formation; the original Huxley (1957) model is an example. Increased translocation efficiency does not imply increased energy efficiency.

W-Pos303

MODELLING CALCIUM AND CONTRACTION COUPLING PROCESSES IN INTACT FROG MUSCLE FIBERS. ((FJ Julian & DG Stephenson*)), Dept. of Anesthesia, Brigham & Women's Hsp., Boston, MA & *LaTrobe Univ., Australia.

Most of the work done to explain the time course of the intracellular Ca^{2+} transient (ICT) in muscle fibers was based on experiments in which the coupling to contraction was avoided or suppressed. New observations made with high temporal resolution (Claflin et al., Biophys. J., 61, A293, 1992) in which force generation remained coupled to the ICT indicate that the ICT rises rapidly to a peak before the onset of positive force generation. In an attempt to explain these new results we have followed the model diagram and the values for concentrations and rate constants given by Brum et al. (J. Physiol., 398, p441, 1988). Our primary equation is: input Ca flux (from the SR) = Ca removal flux (by various binding and pumping processes) + d/dt(ICT). We have made the input Ca flux a known function of time to relate Ca removal fluxes and the ICT to a given input Ca flux. Our chosen release rate is currently near 5μM/ms. Several conclusions can be drawn from these computations. (1) The termination of the rising phase of the ICT is associated with the end of the rapid input Ca flux phase. (2) An ICT of near correct magnitude can be generated, but it is difficult to simulate our experimental findings using fluorescent dyes of very rapid upstroke followed by a relatively slow quasi-exponential decline. (3) A Ca pump (as modelled by Brum et al.) is required as a return path to the SR for "relaxation." (4) Parvalbumin can complex Ca^{2+} rapidly when it exists in the free form or when the off rate constant for Mg^{2+} is Ca-dependent. (5) The rate constants (on ≈ $0.5x10^8$ $M^{-1}s^{-1}$, off ≈ 10^2 s^{-1}) for Ca^{2+} binding to the two Ca-specific sites on troponin may be erroneous. (6) The two Ca-Mg sites on troponin may also be involved in force generation, e.g., via a Ca-dependence of the off rate constant for Mg^{2+}. (7) The molecular mechanism(s) for the coupling process between Ca^{2+} binding to troponin and force generation remains largely unknown. Supported by: NIH #HL35032 (FJJ) & ARC (DGS).

W-Pos304

CROSS-BRIDGE STIFFNESS AND FREE ENERGY FUNCTIONS DERIVED FROM NUCLEOTIDE TITRATION IN SKINNED MUSCLE FIBERS. ((H.J.Kuhn#, T. Kraft*, L.C. Yu+, B. Brenner*)) #University of Ulm, FRG; *Medical School Hannover, FRG; +NIH, USA.

Binding of ATP-γS to cross-bridges was monitored by equatorial intensity ratio I_{11}/I_{10}. At high Ca^{++}(i.e., thin filaments activated) nucleotide saturation occurs over ≈ 4 orders of [ATP-γS] (Kraft et al., PNAS, 1992), a range much wider than found in solution.

To quantitatively account for this observation we defined free energy functions (T. L. Hill, Prog. Biophys. Mol. Biol., 1974) for the attached and detached cross-bridges, both with and without nucleotide. As constraints we assumed that (i) actin affinities of unstrained cross-bridges with and without ATP-γS equal to those in solution (Marston & Weber, Biochem., 1975; Greene et al., Biochem., 1983), and (ii) without nucleotide, >85% of cross-bridges are bound to actin. On this basis, the broad titration can only be accounted for with the following features of the free energy functions:

(i) multiple (>1 per 360Å) binding sites on actin filament that are non-equivalent due to their helical arrangement, (ii) a cross-bridge stiffness somewhat larger than that of Ford et al. (J. Physiol., 1977), (iii) within a group of actin sites, minimum free energy of attached cross-bridges increases by 6-8kT from the site nearest to a cross-bridge to the next actin site 55Å away. (Supported by DFG Br849/1-4; NATO 930448.)

W-Pos305

A CELLULAR AUTOMATA MODEL FOR THE REGULATORY BEHAVIOR OF MUSCLE THIN FILAMENTS. ((G. Zou and G.N. Phillips, Jr.)) Rice University, Houston, TX 77251.

A simple cellular automaton is introduced to show how the interactions among constituent molecules give rise to the overall regulatory behavior of muscle thin filaments as observed *in vitro* and is expandable to *in vivo* measurements. The model is applied to the experimental data of the binding of myosin subfragment-1 to actin with both low and high calcium concentrations, and the binding of calcium to thin filaments in both the presence and absence of myosin. The simulations of the model are also compared with data on ATPase activity in different cases. Two important aspects of regulations are verified by the model: (1) There are strong interactions between bound myosin heads; (2) The cooperative binding of calcium to the thin filament can be attributed to the interaction between neighboring troponin–tropomyosin units. The model is qualitatively expanded to the case of muscle fibers to discuss the relationship between tension and calcium concentration, and the dynamics of muscle contraction as exhibited in X-ray diffraction data. This alternative to analytical calculations demonstrates the potential of cellular automata models in investigating very complex systems. A user-friendly interface has also been developed that allows the user to simulate the overall dynamics of muscle filament by specifying the rate constants of biochemical processes of constituent proteins.

Supported by NIH AR32764, NLM training grant LM07093, and W. M. Keck Foundation

W-Pos306

MODEL OF MUSCLE CONTRACTION BASED ON DIAGONAL MOVEMENT OF MYOSIN ON THIN FILAMENT ((Toshikazu Majima)) Electrotechnical Laboratory, Tsukuba, Ibaraki 305, JAPAN

A model of muscle contraction based on a loose coupling mechanism between power strokes of a cross-bridge and a ATP hydrolysis cycle of actomyosin ATPase is proposed. Assumptions are 1) Load dependent change of sliding direction of the myosin head on actin molecules in the actin filament; 2) Constant working time (power stroking time) of actomyosin ATPase except at slow and isometric shortening conditions; and 3) Long myosin step size; i.e., Many power strokes per single ATP hydrolysis cycle.

This model explains many experimental results: 1) Twist of F-actin in an in vitro motile system (Tanaka et al., Biochim. Biophys. Acta 1159:94-98 (1992); Nishizaka et al., Nature 361:269-271 (1993)); 2) Load-velocity relationship in muscle fibers (Edman et al., J. Physiol. 269:255-272 (1977)); and 3) Enthalpy production from shortening muscle and unexplained enthalpy production during rapid shortening (Homsher et al., J. Gen. Physiol. 84:347-359 (1984); Homsher et al., J. Physiol. 321:423-436 (1981)).

W-Pos307

A CROSS-BRIDGE MODEL TO SIMULATE MECHANICAL AND ENERGETIC PROPERTIES OF SHORTENING MUSCLE

((G. Piazzesi and V. Lombardi)). Dipartimento di Scienze Fisiologiche, Università di Firenze, I-50134 Firenze, Italy. (Spon. by Y.E. Goldman)

During stepwise shortening both the mechanical (Lombardi et al., *Nature* **355**, 638-641, 1992) and the structural manifestations (Irving et al., *Nature* **357**, 156-158, 1992) of the working stroke of the actin-myosin cross-bridges are regenerated within 15 ms, a time much shorter than the ATPase cycle time (Kushmerick & Davies, *Proc. Roy. Soc.* **B174**, 315-353, 1969). A mechanical kinetic model (Lombardi & Piazzesi, *J. Physiol.* **431**, 141-171, 1990) is able to explain these results. The model assumes loose coupling between the biochemical and the mechanical steps allowing for strain dependent detachment of cross-bridges before the completion of the working stroke followed by rapid reattachment further along the actin filament in a configuration similar to that at the beginning of the working stroke. We have now developed a thermodynamically consistent version of the model in which cross-bridge cycle through two different pathways characterized by a different efficiency in the conversion of chemical free energy into mechanical energy. The fraction of cross-bridges involved in each pathway depends on mechanical conditions. The model accurately describes mechanical and energetic properties of contracting muscle such as the dependence of power and efficiency on shortening speed (A.V. Hill, *Proc. Roy. Soc.* **B151**, 169-193, 1938) and the rate of regeneration of the ability to perform the working stroke.

W-Pos308

IMPROVED DETERMINATION OF THE CROSS-SECTIONAL AREA OF SINGLE ISOLATED MUSCLE FIBERS

((Peter J. Reiser)) Oral Biology, The Ohio State University, Columbus, OH 43210 (Sponsored by D. L. Fry).

Accurate determination of the cross-sectional area (CSA) of muscle fibers is necessary for normalizing tension production in individual fibers. This normalization permits a comparison of the tension generating ability of differently sized fibers. The circumference of most muscle fibers approximates an ellipse more closely than a circle. Therefore, accurate measurements of the width and the depth of a fiber improve the reliability of the normalization of tension. A method for photographing the side of a single isolated muscle fiber mounted in an experimental chamber to measure fiber depth has been designed and implemented. Fiber depth and width (the latter obtained as previously illustrated by Moss, J. Physiol. 292:177-192, 1979) are measured from instant photographs obtained with a microscope-mounted camera and utilized to calculate the area of what is assumed to be an ellipse. Briefly, the mounted fiber is transilluminated from the side utilizing a miniature fiber optic light source. A front-surface mirror is positioned in the chamber so that the surface forms a 45° angle with an imaginary vertical axis passing through the fiber. The side-view image of the fiber on the mirror is photographed to measure fiber depth. The standard deviation of normalized tension, based on fiber width and depth measurements obtained from photographs, is about 25% of that reported in an earlier study (Reiser et al., J. Physiol. 449:573-588, 1992) on the same number of fibers where a less direct measure of fiber depth was employed. Details of the arrangement of the light source, muscle fiber, mirror and microscope objective will be provided. Supported by NIH grant AR39652.

W-Pos309

SARCOMERE HOMOGENEITY IN SHORT MUSCLE FIBER SEGMENTS

((M.P. Slawnych, L. Morishita and B.H. Bressler)) Department of Anatomy, University of British Columbia, Vancouver, B.C., Canada.

The role of sarcomere homogeneity in active tension generation was examined in short segments of skinned rabbit psoas muscle fibers. Tension was recorded using an Akers strain gauge (AE801) and sarcomere length was obtained by off-line Fourier analysis of video images of the fiber. Fiber lengths were typically below 200 μm., thus allowing all of the sarcomeres to be visualized in the field of view (200X and 400X magnification). Contractions in pCa 4.5 were preceded by a 20 second pre-soak in HDTA which increased the activation rate and helped to maintain the striation pattern during contraction (Moss et al., *J Physiol* 440:273-289 1991).

We found that fibers could be classified into two groups - those that exhibited little sarcomere inhomogeneity, and those that exhibited a large degree of sarcomere inhomogeneity. In fibers exhibiting little inhomogeneity, we found that force levels declined to zero by 3.7μm, as predicted by models suggesting that cross-bridges act as independent force generators. Conversely, in fibers exhibiting a large degree of inhomogeneity, the length-tension relation was generally flat for sarcomere lengths up to 3.0μm before declining. In plotting these latter relations, the sarcomere length was specified in terms of the most prominent population as determined by the Fourier analysis. For both fiber groups, we found that the inhomogeneity observed during contraction increased as compared to the pre- and post-contraction inhomogeneities. However, this increase was greater for the fibers exhibiting larger initial inhomogeneity.

The use of short fiber segments offers an alternative to segment-clamping methods and allows one to monitor the behaviour of all of the sarcomeres during contraction. (Supported by the MRC).

W-Pos310

RIGOR-STRETCHED AND ACTIVATED INSECT FLIGHT MUSCLE: AN ALTERNATIVE MODEL FOR THE *IN VITRO* MOTILITY ASSAY.

((K. Trombitás and G.H. Pollack)) Center for Bioengineering, University of Washington, Seattle, WA 98195.

When insect flight muscle is stretched in rigor, thin filaments remain tightly bound to thick filaments, but break loose from the Z-line. Sarcomere integrity is maintained by the connecting filaments. Upon activation by MgATP and calcium, the freed thin filaments begin to slide along the thick filaments in the usual manner (Trombitás and Tigyi-Sebes, *Nature* 309 168-170, 1984). This unique protocol is analogous to the *in vitro* motility assay in that "pure" unloaded sliding can be followed, but here the thin filaments slide through the true muscle matrix.

In this model, thin filament translation was studied in the electron microscope. Although the extent of translation was generally consistent from sarcomere to sarcomere, in about 15% of sarcomeres the extent was variable. Within any given sarcomere, however, all thin filaments translated by the same amount. This uniformity was not restricted to the half sarcomere: the extent of translation of the sets of thin filaments in both half-sarcomeres was exactly the same. This localized consistency within the sarcomere implies that adjacent and opposite filaments translate in concert. These data affirm strict cooperativity among filaments of the same sarcomere.

Furthermore, although in the *in vitro* motility assay actin filaments can slide over the entire thick filament length, this does not occur in the present model. Broken thin filaments never enter the opposite I-band. Thus, cross-bridges may not be able to move thin filaments in both directions in the intact sarcomere.

W-Pos311

INJURY AFTER SINGLE STRETCHES OF PERMEABILIZED SLOW AND FAST MUSCLE FIBERS OF RATS.

((P.C.D. Macpherson and J.A. Faulkner)) Dept. of Physiology, and Inst. of Gerontology, Univ. of Michigan, Ann Arbor, MI 48109.

Indirect evidence suggests that fast muscle fibers are more susceptible to injury than slow muscle fibers. Our purpose was to compare the magnitude of injury caused by single stretches of maximally activated single permeabilized muscle fibers obtained from fast and slow muscles. Experiments were performed on single permeabilized fiber segments of fast extensor digitorum longus (EDL) and slow soleus muscles of rats. Measures of maximum velocity of unloaded shortening (V_o) and myosin heavy chain composition were used to confirm the types of fibers sampled. A representative sample of EDL fibers (n=6) and soleus fibers (n=6), that were subsequently injured, had V_o's of 6.8±0.2 L_f/s and 1.9±0.3 L_f/s respectively and expressed correspondingly fast and slow myosin heavy chains. Since the injury is focal, the magnitude of the injury is best evaluated by the deficit in the force developed immediately after a given stretch expressed as percentage of the maximum isometric force (P_o) prior to the stretch. We tested the hypothesis that following a single stretch, the force deficit is greater for fast fibers than for slow fibers. Fiber segment length was adjusted to the optimum length for force development (L_o). P_o was achieved by immersing fibers in a solution with a pCa of 4.5 at 15°C. With a fiber at P_o, a ramp stretch of between 5% and 40% strain was imposed at a velocity of 0.5 L_f/s. After single stretches, fibers were returned to initial length and subsequently redeveloped isometric force. Since the P_o's for fast and slow fibers were not different, the data were pooled (x= 119±1.4 kN/m^2; n=34). Stretches of EDL fibers of 5%, 10% or 20% strains resulted in force deficits of 6%±1%,* 11%±3% & 17±1%,* respectively. For soleus fibers, a strain of 10% produced no force deficit, whereas a strain of 40% resulted in a deficit of 11±1%. We conclude that fast muscle fibers are more susceptible to contraction-induced injury than slow muscle fibers. * Data presented at Exp.Biol.'93. (Supported by NIH grant AG06157)

W-Pos312

CONTRACTION-INDUCED INJURY TO SINGLE PERMEABILIZED FIBERS FROM MUSCLES OF OLD RATS.

((S.V. Brooks, P.C.D. Macpherson, and J.A. Faulkner)) The Inst. of Gerontology, Univ. of Michigan, Ann Arbor, MI 48109-2007.

After repeated lengthening contractions, delayed-onset muscle injury peaks at ~3 days. Following identical protocols, injury is more severe in muscles of old than young or adult animals. After 3 days, factors that contributed initially to injury are impossible to assess and with repeated contractions, loss of force is due to both fatigue and injury. Consequently, the susceptibility of muscle fibers in old animals to injury has not been tested rigorously. Our purpose was to examine the inherent susceptibility of fibers from muscles of old rats to contraction-induced injury. We tested the hypothesis that following single stretches of a given displacement, the magnitude of the injury is greater for passive and maximally activated fibers from muscles of old compared with adult rats. At 15°C, single permeabilized muscle fiber segments from extensor digitorum longus muscles of adult and old rats were exposed to single stretches in the absence of fatigue. Single stretches were initiated at optimal length for force (L_o) and were of 10%-70% strain for passive fibers and 5%-20% strain for maximally activated fibers. All stretches were at a velocity of 0.5 L_f/s. Injury was evaluated by the isometric force deficit immediately after a stretch expressed as a percentage of the maximum isometric force prior to stretch. For both age groups, force deficits were observed for all stretches of maximally activated fibers and stretches of passive fibers of >40% strain. Stretches of 70% strain of passive fibers resulted in greater force deficits for fibers from adult (~14%) than old (~6%) rats. In contrast, for 5% stretches of maximally activated fibers, force deficits were not different for the two age groups, while stretches of 20% strain resulted in greater force deficits for fibers from old (~27%) than adult (~17%) rats. We conclude that differences intrinsic to single fibers of old rats result in some protection from injury following large stretches of passive fibers and small stretches of maximally activated fibers. Supported by NIH grant AG-06157.

W-Pos313

RAPID RECOVERY OF MOUSE EXTENSOR DIGITORUM LONGUS MUSCLES FROM INJURY INDUCED BY SINGLE LENGTHENING CONTRACTIONS. ((KD Hunter and JA Faulkner)) Dept. of Physiology, Univ. of Michigan, Ann Arbor, MI 48109. (Spon. by JA Jacquez)

Repeated lengthening contractions injure muscle fibers mechanically. The result is an immediate disruption in the ultrastructure and decreased force development. An activation of autodegradative processes within fibers during subsequent hours has been proposed, which would increase the severity of the injury. Single lengthening contractions do not produce fatigue, but with sufficiently large displacements do produce ultrastructural damage and a significant deficit in isometric force production. We tested the hypothesis that during the hour immediately after a single lengthening contraction, the magnitude of the force deficit would increase. Mice were anesthetized and secured to a platform maintained at 37° C. The extensor digitorum longus muscle was attached to a servomotor. With the muscle fibers at optimal length for force development (L_o), maximally-activated muscles were exposed to a single stretch at a velocity of 2 L_o/s and a displacement designed to expose fibers to strains of 20%, 50%, or 70% (n = 7 muscles per group). For each muscle, isometric force production was measured prior to and at 2, 15, 30, and 60 minutes after the lengthening contraction. At any time point measured, forces produced by muscles exposed to a strain of 20% were not significantly different from those prior to the lengthening. The muscles undergoing a strain of 50% showed an average force deficit of 13% ± 3% (1 S.E.M.) 2 minutes after the lengthening contraction, with no significant change during the following hour. The muscles exposed to a strain of 70% exhibited a partial recovery in force production with deficits of 45% ± 8% at two minutes, 21% ± 3% at 30 minutes, and 17% ± 4% at 60 minutes. These results do not support the hypothesis that damage increases during the one hour period following contraction-induced injury, and consequently the activation of intracellular autodegradative mechanisms is unlikely. Supported by AG-06157.

W-Pos314

EFFECTS OF INORGANIC PHOSPHATE ON SHORT-RANGE STIFFNESS AND YIELDING OF SKINNED MUSCLE FIBERS OF THE CAT. ((C.M.J.I. Price and T.R. Nichols)) Department of Physiology, Emory University, Atlanta, GA 30322.

Chemically skinned, slow twitch fibers from the cat exhibit a larger yield and short-range stiffness (SRS) in response to ramp stretch compared to fast-twitch fibers (Malamud and Nichols (1992) Biophys. J. 61:A294). In submaximally activated fast fibers, SRS and extent of yield increase over the same range of stretch velocities (Malamud and Nichols, unpublished).

The relationship between yield and SRS was explored further by adding inorganic phosphate (Pi, 15 mM) to the activating medium. We found reductions in background force, SRS and extent of yield in slow and fast fibers as shown by Versteeg et al. (1990, Muscle & Mot. 2:253-256). However, the reduction in SRS was proportionately greater than the decrease in background force. As stretch velocity was increased, SRS of slow fibers increased over the same range of velocities (0.5 - 5 muscle lengths/s) as the SRS of fast fibers in control (no Pi) solutions.

These results support the hypothesis that the properties of SRS and yielding are linked by a common molecular mechanism. During fatigue, an increase in Pi leads to a concurrent decrease in yielding and SRS. This allows the fiber to continue to resist stretch while avoiding higher forces which could result in damage. (Supported by NS20855)

SMOOTH MUSCLE AND NONMUSCLE MYOSINS

W-Pos315

FUNCTIONAL EXPRESSION OF SMOOTH MUSCLE MYOSIN HEAVY CHAIN.
((M.Matsuura and M. Ikebe))Department of Physiology and Biophysics, Case Western Reserve University School of Medicine, Cleveland OH 44106

It is well known that smooth muscle myosin Mg^{2+}-ATPase activity is activated by actin only when the 20kDa light chain of myosin is phosphorylated by myosin light chain kinase and, thus the phosphorylation of the 20kDa light chain is necessary to initiate contraction. However, little is understood how the phophorylation activates actomyosin ATPase activity. It has been known that actin activated ATPase activity of HMM is regulated by phosphorylation while that of S-1 is not, suggesting that the S-2 portion of heavy chain of myosin plays an important role for the regulation. To define the role of heavy chain on regulation, we attempted to functionally express recombinant smooth muscle myosin heavy chain. A full length cDNA of myosin heavy chain was inframe ligated with pT7-7 expression vector. A stop codon was introduced so as to express the heavy chain containing 1110 amino acid residues, i.e., longer than S-1 but shorter than HMM. The constructed expression vector was introduced to BL21 cell and the recombinant protein expression was induced by IPTG. The myosin heavy chain apparent molecular weight of 120kDa estimated by SDS-PAGE was expressed and this was purified by F-actin affinity column. Molecular weight estimated by gel filtration was 128kDa suggesting that the expressed heavy chain is monomeric form i,e., long S-1. The recombinant myosin heavy chain showed ATPase activity which was significantly activated by actin. The actin activated ATPase activity was further increased by light chains. Phosphorylation of the 20kDa light chain, however, did not alter the actin activated ATPase activity. Therefore, the obtained results may suggested that the two headed structure is required for phosphorylation mediated regulation. The expression and characterization of the two headed recombinant HMM is progressing. (Supported by NIH and AHA)

W-Pos316

ROLE OF N-TERMINAL AND C-TERMINAL STRUCTURES OF THE REGULATORY LIGHT CHAIN ON THE REGULATION OF SMOOTH MUSCLE ACTOMYOSIN FUNCTION.
((M. Ikebe, H. Kamisoyama, S. Reardon, M. Matsuura, and R. Ikebe)), Department of Physiology and Biophysics, Case Western Reserve University, Cleveland, OH 44106.

It is obscure how 20kDa light chain (RLC) phosphorylation can activate actomyosin ATPase activity so as to initiate contraction. We have addressed this problem by analyzing the structure-function relationship of RLC. It is known that striated muscle RLCs are distinct from smooth muscle RLC in terms of their regulatory function. The two RLCs are highly homologous to each other, however, the N-terminal and C-terminal sequences are distinct from each other. We hypothesized that the functional difference between the two RLCs is due to the difference in these regions. We therefore produced various truncated/substituted mutant RLCs and introduced these mutant RLCs into myosin to investigate the structure important for regulation. The phosphorylation of the RLC by myosin LC kinase affects several properties of smooth muscle myosin; i.e., activation of actomyosin ATPase activity, myosin filament formation, and 10S-6S conformational transition. The change in these properties of the myosin containing mutant RLC was examined. The following conclusions were obtained: 1) Lys 11-Arg16 is required to stabilize the 10S form of myosin. 2) Destabilization of 10S conformation induces thick filament formation, but does not activate actin activated ATPase activity. This suggests that the formation of the 6S conformation does not necessarily activate actomyosin ATPase activity, although the common components can affect both actin activation and the stabilization of the 6S conformation. For example, phosphorylation at Ser 19/Thr 18 and substitution of Arg 16/Gln 15 for Gly/Glu affect both of them simultaneously. 3) Deletion of Glu 157-Leu 162 abolished the phosphorylation induced activation of actomyosin ATPase activity. 4) Deletion of Lys 149-Leu 162 abolished the binding of RLC and heavy chain. These suggest that the above region is the anchoring site of RLC for binding to the heavy chain and that the phosphorylation induced change in RLC conformation may be transmitted to heavy chain via this part of RLC. (Supported by NIH and AHA).

W-Pos317

CONFORMATION DEPENDENT PHOTO-CROSSLINKING IN GIZZARD MYOSIN WITH SPECIFICALLY LABELED LIGHT CHAINS. ((Jennifer Olney, and Christine Cremo)) Dept. of Biochemistry and Biophysics, Washington State University, Pullman, WA. 99164

Conformation dependent photo-crosslinking of chicken gizzard myosin subunits was examined using a photoreactive probe covalently attached to the regulatory light chain . Purified light chains were labeled on Cys-108 with benzophenone-4-iodoacetamide. The labeled light chains were exchanged onto myosin using the method of Trybus and Chatman (1993) *J. Biol. Chem.* 268, 4412-4419. We typically achieve 50-90% exchange using this method. Exchange does not alter the ability of myosin to undergo the 6S-10S transition. Polyacrylamide gel electrophoresis was used to compare the crosslinking after irradiation of thio-phosphorylated and non thio-phosphorylated myosin in various conformations. Light chain to heavy chain crosslinking was observed under both filamentous and 10S conditions but not under high salt conditions which favor the 6S monomer. We have examined the abilities of the various crosslinked species to undergo transitions between filamentous, 6S and 10S conformations. Myosin crosslinked under 10S conditions could not form filaments and did not co-migrate with 6S or 10S monomers in high salt conditions upon gel filtration. This species was shown by gel analysis to have only one of its heavy chains crosslinked to a light chain. Inter-light chain photo-crosslinking was observed in both thio-phosphorylated and non thio-phosphorylated myosin.
Supported by N.I.H. and the American Heart Association

W-Pos318

STRUCTURAL AND KINETIC STUDIES OF FLUORESCENTLY-LABELLED SMOOTH MUSCLE MYOSIN ((S.S. Rosenfeld, J. Xing, and H.C. Cheung)) Depts. of Neurology, Cell Biology and Biochemistry, Univ. Alabama at Birmingham, Birmingham, AL 35294

The conformational transitions which smooth muscle myosin undergoes after nucleotide binding have been examined using fluorescently-labelled nucleotides and regulatory light chain (RLC). 1 N6 etheno ADP (eADP)+BeF, 2'(3')-O-(N-methylanthraniloyl)ADP (mant ADP)+BeF, and mant AMPPNP induce formation of the 10S configuration of myosin in 150 mM KCl. Fluorescence lifetime studies using eADP+BeF reveal two components for both 10S and 6S myosins, with little difference in the values of these lifetimes or in their fractional emissions. A plot of 1/lifetime *versus* acrylamide concentration reveals essentially no difference in the solvent accessibilities between 10S and 6S myosin: nucleotide. Anisotropy decay studies of myosin:mant ADP + BeF complexes demonstrate that the rotational correlation time for mant ADP-labelled 10S myosin (778ns) is 3.8 times longer than for 6S myosin (204ns). A similar difference in correlation times was seen for 10S myosin:AEDANS RLC (233ns) *versus* 6S myosin:AEDANS RLC (113). mant AMPPNP can be trapped by 10S myosin, and is released at a rate of 0.00005/sec. Actin accelerates this release rate by over 100-fold. These studies reveal:1) reduction in nucleotide release rate by converting 6S to 10S myosin is not due to a reduction in solvent accessibility of nucleotide 2) the catalytic site of 10S myosin is rigidly attached to the rest of the molecule, while in 6S myosin, it has segmental flexibility 3) the RLC is more constrained in 10S than in 6S myosin, but still has more mobility than the catalytic site and 4) actin can induce the unfolding of 10S myosin in the absence of RLC phosphorylation.

W-Pos319

ANALYSIS OF REGULATORY ELEMENTS IN 5'-FLANKING SEQUENCE OF THE MOUSE SMOOTH MUSCLE 17,000 DALTON MYOSIN LIGHT CHAIN GENE. ((Qimin Wu and D.R. Hathaway)) Krannert Institute of Cardiology, Indiana University School of Medicine, Indianapolis, IN 46202

The 17,000 dalton light chain (LC_{17}) subunits of smooth muscle myosin are essential for actomyosin ATPase activity. Two isoforms have been identified and these arise by alternative mRNA splicing from a single gene. Cloning and sequencing of the mouse LC_{17} gene revealed 7 exons and 6 introns corresponding to a total length of 2.7 kb. We have now analyzed 1.5 kb of 5'-flanking sequence for promotor activity. The 1.5 kb of 5'-flanking sequence was subcloned into a pGL2 plasmid vector which contains firefly luciferase as a reporter. A total of 12 mutants (deletion or nucleotide substitution) were prepared and subcloned into the same vector for analysis of potential regulatory elements. Smooth muscle (A_{10}) and fibroblast (3T3) cell lines were transfected using the Lipofectamine reagent. Deletion of more than 1/2 of the DNA (from -1460 to -650) had no effect on promoter activity although two potential regulatory elements (i.e. both MEF-1) were removed. Deletion of an additional 130 bp fragment (-650 to -420) removed a third MEF-1 site and resulted in a 50% reduction in promotor activity. Deletion of an SP1 site (-420 to -165) caused no further reduction in activity. However, mutation of a fourth MEF-1 site contained in the 165 bp segment by nucleotide substitution, resulted in more than a 90% reduction in promotor activity. Parallel changes in promotor activity were observed in both A_{10} and 3T3 cells suggesting that with regard to LC_{17} gene expression, A_{10} cells may be more like non-muscle cells. Our results indicate that the 1.5 kb 5'-flanking sequence of the mouse LC_{17} gene contains strong promoter activity with more than 50% of the activity residing in a 165 bp sequence.

W-Pos320

MYOSIN FILAMENTS IN DIVERSE VERTEBRATE SMOOTH MUSCLES HAVE A SIDE-POLAR STRUCTURE. ((J.-Q. Xu[1], B. Harder[1,2], and R. Craig[1])) [1]Dept. of Cell Biology, U. Mass. Medical School, Worcester, MA, 01655, [2]Pharmacology Inst., University of Zürich, Zürich, Switzerland.

The *in vivo* structure of the myosin filaments in vertebrate smooth muscles is unknown. Evidence from *in vitro* studies and from observations of filaments isolated directly from smooth muscle suggests that they are side-polar. However, it remains possible that filaments in some types of smooth muscle (e.g. fast contracting) have a bipolar, helical structure as in striated muscle. We have used electron microscopy to investigate this question in a diverse group of smooth muscles (vascular, gastrointestinal, reproductive and visual) from a variety of species (mammalian and amphibian). Rapid freezing, followed by freeze-substitution, of intact muscle under physiological conditions reveals that most filaments have a square backbone in transverse section. In some cases, longitudinal sections have shown projections pointing in opposite directions on opposite sides of the filament, but these are not yet clear enough to be identified as crossbridges. Transverse sections of fixed, chemically skinned muscles also show square backbones and in addition projections (crossbridges) on only two opposite sides of the square. Filaments gently isolated from skinned smooth muscles show crossbridges with a 14.5 nm repeat projecting in opposite directions on opposite sides of the filament. Such filaments subjected to low ionic strength show bare filament ends and an antiparallel arrangement of myosin tails along the length of the filament. Taken together, these observations suggest that myosin filaments are side-polar in all smooth muscles, regardless of function. Supported by NIH (AR34711 and HL47530).

W-Pos321

CLONING AND EXPRESSION OF A NON-CONVENTIONAL MYOSIN OF BOVINE ADRENAL GLAND.
((T. Zhu and M. Ikebe)) Department of Physiology and Biophysics, Case Western Reserve University, Cleveland, OH 44106

Myosin I, one of the non-conventional myosins, is an actin based motor different from conventional myosins in that it is single headed and unable to form filament. It has been found widely distributed in low eukaryotic cells and suggested to play an important role in cell motility. Here we report that a 3.5kb cDNA clone was isolated from bovine adrenal gland by screening a λgt11 cDNA library, using a PCR-amplified fragment of chicken brush border myosin I as a probe. This chicken brush border myosin I fragment is conserved in known myosin Is and less conserved in myosin IIs. The clone contained a full-length 3-kb open reading frame, encoding a novel non-conventional myosin. The deduced amino acid sequence was highly homologous to other known myosin Is in the N-terminal 2-kb region which corresponds to myosin head domain, although no strong homology was detected in the tail region, compared with the chicken brush border myosin I. There were consensus sequences of ATP-binding site and actin-binding site in this head domain. At the head-tail junction, there were at least two putative IQ motifs, implying this molecule is capable of calmodulin binding. From above we conclude that our clone encodes a myosin I like protein. It was previously reported a mammalian myosin I was purified from bovine adrenal gland (Barylko,B. etc. 1992, P.N.A.S. 89, 490-494.), however, its peptide sequences were not found in our myosin I clone. To further study the biochemical characteristics of this novel myosin I, we expressed it in pET and pT7-E.coli bacterial expression systems. A protein with an estimated molecular weight of 105 kDa was expressed. These results suggest that there exists a novel myosin I-type molecule in bovine adrenal gland. We are currently further purifying this recombinant myosin I and testing its ability to bind actin and calmodulin (supported by NIH).

W-Pos322

Phosphorylation of nonmuscle myosins II by PK C in their heavy chains is highly correlated with their binding to phospholipid vesicles. ((Noriko Murakami, Marshall Elzinga, and Ved Chauhan)) Institute for Basic Research in Developmental Disabilities, Staten Island, NY 10314

Recent cloning and sequencing studies have shown that heavy chains of nonmuscle myosins II have phosphorylation sites within their tail end regions. To study the effect of the heavy chain phosphorylation by PK C on filament formation, we have expressed two heavy chain fragments of MIIB and MIIA (rabbit brain type and human macrophage type, respectively) coding the COOH-terminal 47 kDa regions. Using these fragments, phosphorylation efficiencies by PK C were studied in the presence of various phospholipid vesicles and micelles. PK C catalyzed phosphorylation of these heavy chains in a phosphatidylserine (PS)-concentration dependent manner in the liposomal assay. The PS liposomes mixed with phosphatidylcholine (PC) significantly reduced the phosphorylation efficiencies. The reaction did not require the presence of PK C activators such as DG or PIP_2. Mixed micelles of PS/DG did not stimulate the reaction at all. The same results were obtained by using the native myosins II purified from bovine brain and chicken intestine brush border. The phosphorylation efficiencies in the presence of various phospholipids were: PS > PS/DG >> PS/DG/PC > PS/PC.

Addition of the liposomes of PS and PS/DG significantly increased the turbidities of the heavy chain fragments and myosins at various salt concentrations, while the increases with PS/DG/PC and PS/PC liposomes occured to a significantly reduced extent. Incubation with liposomes of PS and PS/DG shifted the elution positions of the heavy chain fragments and myosins II toward the void volume by gel filtration column chromatography. These results suggest that myosins II bind directly to acidic phospholipids via the COOH terminal regions of their heavy chains, that PK C phosphorylates heavy chains when direct heavy chain-PS binding occurs, and that the phosphorylation reaction is independent of DG or PIP_2.

W-Pos323

ACTIN FILAMENTS ARE NOT MOVED BY BRUSH BORDER MYOSIN-I BOUND TO PHOSPHOLIPID MEMBRANES. ((Henry G. Zot)) Dept of Physiology, U T Southwestern Medical Center, Dallas, TX 75235

Chicken brush border myosin-I (BBMI) does not move actin filaments on planar membranes of 20% and 40% phosphatidylserine (PS) at various Ca^{2+}'s using an in vitro motility assay (Zot et al., JCB 116:367, 1992). The relative density of myosin bound to the surface was estimated from the number of actin filaments attached at various concentrations of BBMI, holding the size of the field and the amount of actin constant. Experiments at 10^{-7} M and 10^{-6} M Ca^{2+} with BSA coated glass showed that the number of actin filaments attached varies hyperbolically with the amount of BBMI and nearly all attached filaments are moved when sufficient BBMI is added. Below a critical amount of BBMI filaments attach but do not move, giving a minimal number for motility. At Ca^{2+}'s above 10^{-6} M, the number of attached filaments are below the minimum and gliding is not observed, indicating that BBMI associates poorly with BSA coated glass at elevated Ca^{2+}'s. Applying these conditions to planar membranes of 40% PS, the number of filaments attached exceed the minimum required for motility at all Ca^{2+}'s and increasing Ca^{2+} causes an increase in the number of filaments attached. Thus the absence of gliding filaments on planar membranes is probably due to the inactivity of bound BBMI, suggesting that BBMI would be incapable of movements mediated by a direct association with cell membranes. Supported by AHA 92-1571; NSF MCB-9205344.

W-Pos324

CHARACTERIZATION OF A BLOCKED-STATE OF MUSCLE THIN FILAMENTS ((M.A. Geeves, J.D.Head, M.D.Ritchie & D.A.Smith)) MPI fur molekulare Physiolgie, Dortmund, Germany & Department of Physics, Monash University, Australia.

We recently presented evidence for three states of the thin filament (McKillop & Geeves Biophys. J. **65** 693-701): The *blocked-state*, which does not significantly interact with myosin subfragment 1 (S1); the *closed-state*, which can only bind S1 in the weakly bound A-state; and the *open-state*, which can bind S1 in the strongly bound R-state and is required for both accelerated product release and tension generation. The fraction of actin monomers in the *blocked-state* can be estimated from analysis of the kinetics of excess actin binding to S1. We report here a detailed characterization of the equilibrium constant (K_B) between the *blocked* and *closed-states* of the thin filament. K_B is calcium dependent and a plot of K_B vs. pCa is a classical Hill curve with a mid point at pCa 5.6, a Hill coefficient of 1.8. and limiting values of K_B of 0.4 and >>1 at high & low pCa respectively. The high pCa value of K_B is increased by both high temperature and low ionic strength and little *blocked-state* can be identified at 35 C or ionic strengths below 0.05M
The kinetics of excess S1 binding to thin filaments in the absence of Ca is complex but modelling the complete 45-state reaction scheme show it to be consistent with the values of K_B described above.

W-Pos325

PHOSPHORYLATION DIFFERENTIATES BINDING OF HUMAN BRAIN TAU PROTEINS TO CALMODULIN, TROPONIN C, AND TROPONIN C MUTANT. ((H. Ksiezak-Reding, A. Babu and J. Gulati)) Albert Einstein College of Medicine, Bronx, NY 10461.

The microtubule-associated proteins including tau proteins play an important role in microtubule assembly and also bind to Ca^{2+}/calmodulin (CAM), a negative effector of microtubule polymerization. The phosphorylation diminishes the ability of tau to promote microtubule assembly; however, the effect on the CAM binding is not known. By affinity chromatography, we investigated the binding of tau to 3 ligands: (i) CAM, (ii) troponin C (TnC), a skeletal muscle relative of CAM and (iii) a TnC-mutant with CAM-like structure (Gulati et al., JBC 268:11685, 1993). Tau proteins with high and low phosphate contents were obtained from normal (i) fetal and (ii) adult human brains, respectively. Additionally, (iii) from Alzheimer brain, hyperphosphorylated tau, a major component of paired helical filaments (PHF-tau), was isolated. We found that in the presence of Ca^{2+}, tau from fetal and adult brains bound to all three ligands. In contrast, PHF-tau bound weakly suggesting that in Alzheimer filaments the binding sites are inaccessible. Furthermore, whereas fetal tau was effectively eluted from each of the ligands with 5 mM EGTA, adult tau was significantly eluted only from TnC and not from CAM or CAM-like TnC mutant. The results suggest that a higher degree of phosphorylation in fetal tau, compared with the adult form, is responsible for the improved Ca^{2+}-specific binding to CAM and TnC-mutant. In normal tau, phosphorylation was less critical for the Ca^{2+}-specific binding to TnC. The differences between TnC and the mutant provide an insight into structural requirements for interaction of tau with c_a^{2+}-regulated effectors of microtubule assembly.

W-Pos326

Sr^{2+}-SENSITIVITY VARIATIONS BETWEEN CARDIAC AND SKELETAL Ca^{2+}-SPECIFIC AND Ca^{2+}-Mg^{2+}-SITES
((A. Babu, V.G. Rao, Hong Su and J. Gulati)) Albert Einstein College of Medicine, Bronx, NY 10461

Although the Ca^{2+}-sensitivities for tension developments in cardiac and skeletal fibers are similar, for Sr^{2+} cardiac muscle is much more sensitive than fast-twitch skeletal fiber (Babu et al, 1987, JBC, 262, 5815-22). To test this on isolated TnC, we have now utilized mutants of sTnC to measure the Sr^{2+}-sensitivity in solution. We also questioned whether discrimination between Sr^{2+} and Ca^{2+} was evident only in the so-called Ca^{2+}-specific sites or whether Ca^{2+}-Mg^{2+} sites in the C-terminus possessed comparable capability. To probe the C-terminal sites, the fluorescence probes were endogenous tyrosines (Y-109 in sTnC and Y-110 in cTnC). To probe the Ca^{2+}-specific sites, a tryptophan replaced F26 in sTnC or in cardiac-skeletal chimera combining cardiac site 1 with skeletal TnC (Gulati et al, 1992, JBC, 267, 25073; also Rao et al, this vol). We find that pSr_{50} for site 1 were 3.98±.07 and 4.49±.05(4) for sTnC and the chimera, respectively. Thus, the cardiac N-terminal site was more sensitive by 0.51 pSr unit as in the fiber. Contrastingly, the pSr affinities of the C-terminal sites were 6.06±.12(6) and 5.12±.07(4) in sTnC and cTnC, respectively. We conclude that structural differences between the C-terminal halves of cTnC and sTnC are important in the performance of these isoforms. Furthermore, we show that putative Ca^{2+}-specific sites in isolated TnC can nearly fully account for the differences between cardiac and skeletal fiber results on Sr^{2+}-sensitivity.
Supported by NIH and NY Heart

W-Pos327

TROPOMYOSIN TRANSITIONS IN SKELETAL MUSCLE ACTIN-TROPONIN-TROPOMYOSIN ((A.M. Resetar & J.M. Chalovich)) Department of Biochemistry; East Carolina University School of Medicine, Greenville, NC 27858-4354, USA.

The regulation of striated muscle contraction is mediated by the thin filament proteins troponin and tropomyosin which interact with actin differently in the active and relaxed states. Ishii and Lehrer have shown that the fluorescence of a pyrene probe on tropomyosin is proportional to the fraction of tropomyosin molecules in the active state (Biochemistry **29**: 1160-1166, 1990). We have initiated studies to use this probe (denoted by Tm*) to monitor the rates of the transitions between the inactive and active states of the thin filaments under various conditions. In the present study, we used high concentrations of S1 to shift tropomyosin to the active conformation. In the case of actin-troponin-Tm* at 170 mM ionic strength and 20°C, the binding of an excess of S1-ADP to thin filaments resulted in an increase in fluorescence and the transient was adequately fitted to a single exponential with a rate of 0.5/sec. The rate of the transition increases with decreasing ionic strength, and the rates obtained are comparable to the rates measured for S1-ADP binding as assessed by light scattering.

W-Pos328

A CARDIAC TROPONIN C MUTANT WITH NOVEL REGULATORY PROPERTIES. ((B.-S. Pan, P.B. Chase, D.A. Martyn, R.G. Johnson, Jr., C.-K. Wang, T.W. Beck and A.M. Gordon)) Merck Research Laboratories, West Point, PA 19486, and Dept. of Radiology, Center for Bioengineering, and Dept. of Physiology & Biophysics, University of Washington, Seattle, WA 98195. (Spon. by L.L. Huntsman)

A cDNA for Human cardiac troponin C (cTnC) was isolated by PCR and used to create a mutant (cTnCF77W) in which Trp replaced Phe 77 at the NH_2-terminal end of the D helix. Wild type (WT) and mutant cTnC's were over-expressed in *E. coli* and purified. Unlike WT, cTnCF77W remained bound to Phenyl-Sepharose in the presence of 1 M KCl and 5 mM EDTA, suggesting that part of the hydrophobic patch is exposed in the mutant even in the absence of divalent cations. Ca^{2+}-affinity of the Ca^{2+}-specific site in cTnCF77W, estimated by Ca^{2+}-titration of Trp fluorescence, was 2.3×10^7 M^{-1}, which is 10- to 100-fold higher than in any other known TnC or TnC mutant. When cTnCF77W was substituted for endogenous sTnC in single skinned fibers from rabbit psoas (skeletal) muscle, force-[Ca^{2+}] relations were shifted towards lower [Ca^{2+}] by ~0.3 - 0.5 pCa units relative to those obtained either with endogenous sTnC or with fibers reconstituted with WT cTnC. Additionally, at pCa 9.2 there was significant force, equivalent to 10 - 20% of maximum Ca^{2+}-activated force obtained with sTnC, which was not due to intramolecular disulfide bond formation (Hannon *et al.*, 1993, *Biophys. J.* 64:1632). The rate of isometric force redevelopment (k_{TR}) was elevated at low forces for fibers containing cTnCF77W compared with either endogenous sTnC or with fibers reconstituted with WT cTnC, supporting our previous observation that the force-k_{TR} relationship is affected by the properties of TnC (Chase *et al.*, 1993, *Biophys. J.* 64:A345). Supported in part by Merck Res. Labs. and NIH HL31962.

W-Pos329

CONSERVATION AMONG DEVELOPING MAMMALS OF A POTENTIAL FUNCTIONALLY IMPORTANT CARDIAC TROPONIN T EPITOPE. ((P.A.W. Anderson, A. Greig, P.D. Allen, A.E. Oakeley, R. Nassar, B. Kay)) Duke University Medical Center, Durham, NC 27710; UNC-Chapel Hill, Chapel Hill, NC 27564; Brigham & Women's Hosp., Boston, MA 02115.

Multiple cardiac troponin T (TnT) isoforms are expressed in the hearts of rabbit, human, rat, and dog, while two are expressed in the chicken heart. The developmentally regulated expression of these isoforms results in a decrease in isoform size with maturation. In rabbit, rat, and chicken, a molecular basis for this decrease in size is alternative splicing of a 30 nt exon encoding a 10 residue amino terminal peptide. An antigenic peptide whose sequence was derived from the rabbit 10 residue peptide was used to raise antisera in mice. Western blots of cardiac preparations from immature and adult hearts probed with a cardiac TnT specific monoclonal antibody (MAB 13-11) demonstrated 4 or more isoforms in the mammalian preparations and two in the chicken. The antisera, raised against the 10 residue peptide, recognized the two largest isoforms in rabbit, human, and rat, multiple isoforms in the dog, and neither chicken TnT isoform. The affinity of the antisera to rabbit, human, and dog TnT was much greater than that to rat TnT. The sequence differences among the rabbit (EEDWREDEDE), rat (EDWSEEEEDE), and chicken (EEEWLEEDDG) peptides provide the basis for the differences in affinity. These results suggest the rabbit TnT 10 residue sequence is present in human and dog TnT. In the light of our previous finding that rabbit myofibrils containing more of the isoform with this peptide were more sensitive to calcium, the high expression in the immature human and dog heart of isoforms containing this rabbit sequence will confer on their myofibrils a greater sensitivity to calcium.

W-Pos330

LINKED EQUILIBRIUM ANALYSIS OF THIN FILAMENT ASSEMBLY USING ALTERED FORMS OF TROPONIN T AND ACTIN. ((D. Fisher, R. Dahiya, M. Cassell, C.A. Butters, and L.S. Tobacman)) University of Iowa, Iowa City, IA 52242

Troponin, tropomyosin, and F-actin assemble to form thin filaments in a complex process with implications for the regulation of muscle contraction. (1) Tropomyosin labeled on cys-190 with pyrenyl-iodoacetic acid was used to measure the affinity of troponin (or troponin with truncated TnT) for tropomyosin under conditions also used to assess binding of tropomyosin or troponin-tropomyosin to actin by linear lattice analysis. Troponin's affinity for actin-tropomyosin, which is too tight to measure directly, was calculated by detailed balance. Troponin affinity for actin-tropomyosin is 5 x 10^8 M^{-1}. Deletion of TnT residues 1-69 or addition of Ca^{2+} weakens this binding 2-fold by altering troponin binding to tropomyosin and not by altering troponin binding to actin. Further deletion of TnT residues 70-150 weakens troponin binding to tropomyosin another 60-fold, but leaves troponin-tropomyosin binding to actin still tight and Ca^{2+}-insensitive. Further removal of TnT residues 151-158 makes troponin-tropomyosin binding to actin dependent upon the absence of Ca^{2+}. (2) We recently proposed that cooperative binding of tropomyosin or troponin-tropomyosin to actin is primarily caused by a conformational change in the actin monomers. To test this proposal, we used actin binding isotherms to measure the strength of tropomyosin-tropomyosin interactions after altering actin-actin interactions by addition of phalloidin or by proteolytic removal of actin residues 374 and 375. Phalloidin weakened tropomyosin-tropomyosin interactions while actin C-terminal truncation strenghthened these interactions. This supports the idea that actin-actin contacts within the thin filament are critical for cooperative binding of tropomyosin to actin.

W-Pos331

TROPONIN INCREASES THE SIZE OF THE TROPOMYOSIN-ACTIN COOPERATIVE UNIT OF THE REGULATORY SWITCH OF THE MUSCLE THIN FILAMENT. ((M.A.Geeves & S.S.Lehrer)). Max Planck Institut fur Molekulare Physiologie, Dortmund, Germany & Boston Biomedical Research Institute, Boston MA, USA.

The minimal structural unit of the muscle thin filament is 7 actin monomers bridged by a single troponin/tropomyosin complex (Tn.Tm). The excimer fluorescence of a pyrene label covalently attached to Cys 190 of Tm provides a convenient probe of the state change of the thin filament associated with the cooperative binding of myosin heads (S1) to actin (Ishii & Lehrer, Biochemistry, 29, 1160, 1990). S1 binding can be monitored independently by the associated increase in light scattering. We have used these signals to study the kinetics of the thin filament state change associated both with S1 binding to, and ATP-induced dissociation of S1 from, actin subunits. For the binding experiment with excess S1, the apparent cooperative unit size, n, is given by the ratio of the fluorescence to the light scattering first order rate constants, n = kFl/kLS. For the dissociation experiment, a delay in the fluorescence signal behind the light scattering is expected, the size of which depends on n. Both sets of data show that for Tm.actin n = 5-6 actin subunits and is increased to 10-12 units for Tm.Tn.actin, independent of the presence of Ca2+. This indicates that Tm is somewhat flexible, because n < 7 and Tn increases communication between neighboring structural units because n > 7. Supported by a NATO grant and by NIH AM-22461 (SSL) and The Wellcome Trust (MAG).

W-Pos332

REQUIREMENTS OF TROPOMYOSIN'S PERIODIC SITES FOR ACTIN BINDING. ((Y.M. An and S.E. Hitchcock-DeGregori)) Dept. of Neuroscience and Cell Biology, Robert Wood Johnson Med. Sch., Piscataway, NJ 08854.

We have been investigating the requirements of TM's periodic actin binding sites. The F-actin affinity of unacetylated chicken striated muscle α-TM expressed in *E. coli* was measured by cosedimentation with Tn (+Ca^{2+}) since unacetylated TM alone binds poorly to actin. Previous work showed that deletion of site 2 (res. 47-88) reduces actin affinity about 2-fold while deletion of site 3 (res. 86-127) further reduces affinity. Interestingly, TM in which both sites 2 and 3 have been deleted (77 residues, res. 47-123) bound to actin with an affinity at least as high as that of full-length TM. A possible explanation is that the 77-residue deletion is closer to one turn of the supercoil, or the sum of two periodic sites (2 x 39.3 res., McLachlan and Stewart, 1976; or 42 + 35 res., Phillips et al., 1986), than a 42 residue deletion is to one period or a half-turn of the supercoil. If true, this implies that an *integral* number of turns (or half-turns) is more important than the *total* number for actin affinity.
To learn the importance of sequence and coiled coil structure for actin affinity, we have substituted 14 residues of site 2 or 3 with 14 residues of the leucine zipper, GCN4, or 14 residues of random coil sequence (6/14 res. are Gly). The GCN4 mutants bound well to actin, slightly weaker than wildtype. The binding of the random coil mutant was too weak to measure, even though it formed a coiled coil. The results show that a continuous coiled coil is important for actin binding. Supported by NIH.

W-Pos333

SIGNIFICANCE OF THE LENGTH OF THE TROPONIN C CENTRAL HELIX. ((S. Ramakrishnan and S.E. Hitchcock-DeGregori)) Dept. Neuroscience and Cell Biology, UMDNJ-Robert Wood Johnson Medical School, Piscataway, NJ 08854. (Spon.by H.M.Geller)

To investigate the significance of length and structure of the troponin C central helix three insertion mutants having oligomers of different predicted conformations and length were constructed. These include, 7 residues (2 turns) of an α-helix (TnCinαh) resulting in an increase in length of 10.5 Å, 9 residues of random coil (TnCinrc), and a rigid spacer of 9 prolines (TnCinpp) resulting in an increase in length of 28 Å. We previously reported that TnCinrc and Tncinαh were defective in relieving the TnIT inhibition of the actomyosin ATPase in the presence of Ca^{2+}, 50-60% and 70-80% of wild type respectively. TnCinpp was even less effective, 35-50%. These results were surprising to us because we expected TnCinrc and TnCinpp to have opposite phenotypes. Further analysis of these mutants showed that they were not significantly different from the wild type in the relief of TnI inhibition of the actomyosin ATPase activity, Ca^{2+}-dependence of the actomyosin ATPase activity, metal ion-dependent conformational changes or Ca^{2+}-binding. These results suggest that the native inter-domain distance of TnC in complex with TnI and TnT is crucial for the activation of the thin filament in the presence of Ca^{2+} and changes in the central helix can affect TnC function without affecting its Ca^{2+}-binding properties. Supported by NIH and AHA.

W-Pos334

EFFECT OF DELETION OF THE N-TERMINAL HELIX ON TROPONIN C FUNCTION. ((L. Smith, N. Greenfield, and S.E. Hitchcock-DeGregori)) Department of Neuroscience and Cell Biology, Robert Wood Johnson Medical School, Piscataway, NJ 08854 (Spon. by J. Lenard)

Troponin C (TnC) has a 14-residue helix at the extreme N-terminus (N-helix) that is absent in calmodulin. To learn the significance of this region in TnC, residues 1-14 were deleted using site-directed mutagenesis. We previously reported that the mutant TnC (Δ14-TnC) folded properly, was less stable, and, like CaM, only partially relieved TnIT inhibition of the actomyosin ATPase in the presence of Ca^{2+} (Smith et al., 1993). To determine if the impaired function of Δ14-TnC was due to altered binding to TnI, we assayed its ability to relieve TnI inhibition of the actomyosin ATPase in the absence of Ca^{2+}. The results show that Δ14-TnC could maximally relieve TnI inhibition and suggest that the deletion has no effect on the binding of TnC to TnI. Δ14-TnC also forms a stable complex with TnT in nondenaturing polyacrylamide gels. The Ca^{2+} affinity of Δ14-TnC is reduced as evidenced by the 2.4-2.8 fold increase in the Ca^{2+} concentration required to achieve half-maximal activation of the MgATPase. Ca^{2+} binding monitored by CD also showed that binding to the high affinity sites results in half the increase in α-helix compared to wildtype. This was rather surprising as the Mg^{2+} titration for Δ14-TnC was indistinguishable from wildtype. The results show that the N-helix is important for full TnC function. Supported by NIH and MDA.

W-Pos335

STABILITY AND INTERACTION OF RECOMBINANT FRAGMENTS OF THE N-TERMINAL DOMAIN OF TROPONIN C((R. S. Fredricksen AND C. A. Swenson)) Department of Biochemistry, University of Iowa, Iowa City, IA 52242.

Four recombinant protein fragments of chicken skeletal troponin C, PCR1-85, PCR1-105, PCR12-85, and PCR12-105, have been characterized with respect to folding stability, calcium binding, their interactions with troponin I (TnI) and the TnI inhibitory peptide, and dimerization (the ranges refer to particular amino acid sequences within holo-troponin C). All of the fragments include the N-terminal regulatory calcium-binding sites. The effects of the N-helix, the D/E linker helix, and calcium on protein-protein interactions and protein stability have been examined. Circular dichroism was used to study temperature and guanidine-HCl (GuHCl) induced protein denaturation. In all cases, protein stability was increased in the presence of calcium. Results indicate that PCR1-105 is the most stable protein of the series and is more stable than holo-TnC. Based on values of ΔG_u° obtained using the linear extrapolation method and on the melting temperatures, T_m, the rank order of stability is PCR1-105>TnC>PCR12-105>PCR1-85>PCR12-85. The effects of NaCl and GuHCl on the thermal transition of apoPCR1-85 were also studied. NaCl generally stabilizes the protein. GuHCl produces a variable amount of stabilization at concentrations below 1.5M and then destabilizes at higher concentrations. Fluorescence studies indicate that each fragment binds TnI and the TnI inhibitory peptide in a calcium-dependent manner that is affected by the presence of the N-helix and/or the D/E linker helix. Overall our results suggest that the N-helix and the D/E linker helix, while not participating directly in calcium ion binding, have an effect on the stability and interactions of this domain with troponin I. Supported by the Muscular Dystrophy Association.

W-Pos336

ANALYSIS OF THE DIFFERENTIAL CONTRIBUTIONS FROM TYR-10 AND TYR-109 OF SKELETAL TnC TO FLUORESCENCE INTENSITY

((D. Keleti, V.G. Rao, A. Babu, H. Su, and J. Gulati)) Albert Einstein College of Medicine, Bronx, NY 10461 (Spon.: S. Takahashi)

Intrinsic tyrosines monitored by fluorescence are sensitive reporters of local, Ca^{2+}-induced conformational changes in rabbit skeletal troponin C (sTnC). The two major contributors to the fluorescence emission spectrum of sTnC are a tyrosine (Y-10) in the N-helix and another (Y-109) in Ca^{2+}/Mg^{2+} site III. The location of the latter in a high affinity site and its proximity to a TnI binding position is of special interest in elucidating the mechanism of the contractile Ca^{2+} switch. Our goal here is to separate the individual contributions of Y-10 and Y-109 to fluorescence intensity by using sTnC mutants ΔNt [deleting the entire N-helix that includes Y-10 (Gulati et al, 1993: JBC, 258,11685)] and 109YF (substituting F for Y-109.) The fluorescence intensities of 75ug/ml protein in the presence of buffered-1mM EGTA solution (F_{EGTA} in a.u.) are: ΔNt 18.0±0.9, 109YF 50.4±2.1,sTnC 68.7±1.1. The intensities in buffered-Ca^{2+} (pCa4) solution (F_{Ca}) are: ΔNt 45.3±2.9, 109YF 52.9±3.0, sTnC 100.6±1.3. The Ca^{2+}-induced $\Delta F(= F_{Ca}-F_{EGTA})$ of the 109YF mutant was negligible, suggesting that Y-109 contributes the majority (84%) of ΔF to sTnC. In comparing F_{EGTA} of 109YF and sTnC, we conclude that Y-10 contributes 74% of the sTnC intensity. Interestingly, in comparing the F_{EGTA} of ΔNt and sTnC, we found that Y-109 contributes only 26% of the sTnC intensity. We conclude that quenching of the tyrosine in site III may be caused by the nearby carboxylates or from the differences in intrinsic flexibilities of the two tyrosines.

W-Pos337

MUTATION OF THE HIGH AFFINITY CALCIUM BINDING SITE OF SKELETAL MUSCLE TROPONIN C

((B.H. Bressler, L. Morishita, L. Gauthier, and T. Borgford)) Depts. of Anatomy, and Chemistry University of British Columbia and Simon Fraser University, Vancouver, B.C.

Chemically skinned skeletal and cardiac muscle fibers, when passively stretched or shortened, exhibit an increase or a decrease respectively in calcium sensitivity. Force-pCa curves were measured from isolated segments of skinned rabbit psoas fibers at sarcomere spacing of 2.2μm or 2.4μm (resting length) and at longer or shorter sarcomere lengths. Subsequently, troponin C was removed with 20mm imidazole and 5 mm EDTA at pH 7.8 and replaced with mutant troponin C in which the amino acid at position 130 was replaced with either glycine or serine. Replacement of amino acid at position 130 has been shown to cause the affinity of the Ca^{2+}/Mg^{2+} sites to be attenuated (G. Trigio-Gonzalez et al, Biochemistry(1993) 32:9826). Following reconstitution of the fiber with the mutant protein, force-pCa curves were measured once again at the rest length and at long or short sarcomere lengths. Video image analysis of the fibers confirmed that they exhibited a homogenous distribution of sarcomere spacing at the various lengths. Irrespective of the mutation introduced into the fiber, there were no changes in the observed shift in calcium sensitivity of the myofilaments at different sarcomere lengths. It would appear that changes in the ion affinity of the Ca^{2+}/Mg^{2+} sites of troponin C do not alter the observed change in calcium sensitivity of skinned muscle fiber segments at different sarcomere lengths.. (Supported by the MRC, NSERC, and BCHRF).

W-Pos338

FUNCTIONAL SIGNIFICANCE OF THE N-TERMINAL PEPTIDE OF CARDIAC TROPONIN I IN REGULATION OF MYOFILAMENT Ca^{2+}-SIGNALLING.

((Jonggonnee Wattanapermpool)) Dept. Physiology & Biophysics, College of Medicine, University of Illinois, Chicago, IL 60612. .

Developmental isoform switching of troponin I (TnI) was proposed to be related to the insensitivity of the neonatal heart to acidic pH (Solaro et al. Circ. Res. 58:721, 1986). A unique extension of 32 amino acids at the N-terminus, in which serines have been shown to be phosphorylated *in vivo*, is an important feature of the cardiac (c) TnI isoform. The functional significance of this N-terminal domain was studied here using bacterially expressed aminoterminal-truncated cTnI (cTnI/NH_2). The cTnI/NH_2 was no longer phosphorylated by protein kinase A, but could be phosphorylated by protein kinase C. It still formed a complex with cTnC in the presence of Ca^{2+}. The effect of pH on Ca^{2+}-dependent myofibrillar ATPase was studied using reconstituted rat heart myofibrils in which the endogenous cTnI was extracted by excess cTnT and reconstituted with the mutant protein. cTnI/NH_2 retained the ability to inhibit myofibrillar activities at low Ca^{2+} concentration. Interestingly, when pH was changed from 7.0 to 6.5, the same magnitude of rightward shift in pCa_{50} was detected in myofibrils reconstituted with either cTnI or cTnI/NH_2. Tn subunit interactions were also investigated using fluorescence-labelled cTnC. Under acidic conditions, cTnC alone demonstrated a decrease in Ca^{2+}-affinity, however, this decrease was greater in the cTnI-cTnC complex as well as in cTnI/NH_2-cTnC. Addition of cTnT and tropomyosin (Tm) in the cTnI-cTnC complex did not further change the effect. In contrast, this greater depression of cTnC Ca^{2+}-binding with acidosis did not occur either in the slow skeletal (ss)TnI-cTnC or ssTnI-cTnC-cTnT-Tm complex. These results support our hypothesis that the relatively big effect of acidic pH on Ca^{2+}-activation of cardiac myofibrils is associated with the presence of the cTnI isoform, and that this effect must reside in a domain outside the N-terminal extension.

W-Pos339

COMPARISON OF THE INTERACTION AND FUNCTIONAL PROPERTIES OF DEPHOSPHORYLATED HETERO- AND HOMO-DIMERS OF RABBIT STRIATED MUSCLE TROPOMYOSINS

((L. Thomas and L. B. Smillie)) M.R.C. of Canada Group in Protein Structure and Function, Department of Biochemistry, University of Alberta, Edmonton, Alberta T6G 2H7. (Spon. L. B. Smillie)

In rabbit striated muscle genetic variant chains of tropomyosin (TM) have led to native populations that are a mixture of homo αα- and ββ- or hetero αβ-dimer species. The functional significance of these TM isoforms is unknown. The interaction and functional properties of dephosphorylated homo- and heterodimers of TM from rabbit striated muscle have been investigated. Dephosphorylated rabbit cardiac αα-TM and rabbit skeletal αβ- and ββ-TMs were prepared by phosphatase-treatment (Heeley, D. *et al.* (1989) *J. Biol. Chem.* 264, 2424-2430). The relative viscosities of solutions of dephosphorylated TM hetero- and homo-dimers measured as a function of ionic strength and protein concentration at constant ionic strength indicate that the propensity for head-to-tail interaction is greatest for ββ-TM, intermediate for αβ-TM, and least for αα-TM. Affinity chromatography demonstrates that the strengths of binding of αα- and αβ-TMs to the TM-binding component of troponin (TnT) and the NH_2-terminal chymotryptic fragment T1 of troponin T (TnT1) are equivalent and that the strength of binding of ββ-TM to these ligands is weaker. The functional effects of the hetero- and homodimers were examined on the reconstituted Ca^{2+} regulated troponin-tropomyosin-actomyosin subfragment 1 (S1) ATPase system. Significantly higher activities are observed in tropomyosin-actin-S1 ATPase assays with αα-TM than with ββ- or αβ-TMs. In a fully reconstituted system with troponin, slightly better inhibition of ATPase activity in the absence of Ca^{2+} is observed with αα- and αβ-TMs. The homodimer αα-TM exhibits the greatest Ca^{2+}-sensitive release of troponin (TN) inhibition, while the release observed with αβ- or ββ-TMs is significantly lower. A further increase in TM potentiation and Ca^{2+}-sensitive release of TN inhibition of acto-S1 ATPase activity is observed when the penultimate serine of αα-TM is phosphorylated (supported by M. R. C. of Canada and the Alberta Heritage Foundation for Medical Research).

W-Pos340

NMR STUDIES OF CALCIUM BINDING TO N-DOMAIN OF CHICKEN TROPONIN C.

((Monica X. Li, Stephane M. Gagne, Sakae Tsuda, Lawrence B. Smillie and Brian D. Sykes)) MRC Group in Protein Structure and Function, Department of Biochemistry, Univ. of Alberta, Edmonton, Canada T6G 2H7. (Spon. by B.D. Sykes)

Binding of Ca^{2+} to sites I/II of N-domain of troponin C (TnC) is thought to be the regulatory event responsible for the triggering of muscle contraction. So far the binding mechanism is poorly understood. In this work, Ca^{2+} binding to recombinant N domain (residues 1-90) of chicken TnC has been investigated with the use of heteronuclear multidimensional NMR spectroscopy. The protein has been cloned in pET3a vector and expressed in minimal media to allow uniform ^{15}N and ^{13}C labeling. The NMR spectra have been resolved and assigned. Ca^{2+} titration monitored by ^{1}H, ^{15}N HMQC spectral changes revealed that the Ca^{2+} binding to sites I and II of TnC is a stepwise process and that chemical shift changes occurred throughout the N-domain for each Ca^{2+} bound. The Ca^{2+} dissociation constants for the binding of the first and second Ca^{2+} were determined and found to be 2.4 μM and 14 μM, respectively. The rationalization of these data together with those obtained from Ca^{2+}-induced fluorescence and far UV CD ellipticity changes (Li *et al.*, Biochemistry, in press (1993)) in terms of binding constants and cooperativity between sites I/II will be discussed. (Supported by MRC of Canada and the Alberta Heritage Foundation for Medical Research.)

W-Pos341

A SIMPLE SOLID PHASE ASSAY FOR TROPONIN SUBUNIT INTERACTIONS.

((D.R. Swartz[1], M.L. Greaser[2] and R.L. Moss[2])) [1]IU Medical Center, Indianapolis, IN 46202. [2]University of Wisconsin, Madison, WI 53706.

The subunits of troponin interact in a concerted fashion with calcium and tropomyosin to activate contraction. We have developed a simple solid-phase assay which demonstrates subunit interactions specifically between TnI and TnC as well as TnT and Tropomyosin. The assay is similar to a direct ELISA: one subunit is coated on the ELISA plate, and the second biotinylated subunit is then bound to the coated subunit. The quantity of biotinylated subunit is determined by incubation with streptavidin horseradish peroxidase with subsequent color development. Using this approach, the binding of biotinyl-TnC to TnI was demonstrated at high calcium, and this binding was substantially weakened at low calcium. The binding of biotinyl-tropomyosin to TnT was also demonstrated. Both assays showed sensitivity in the nM range for the biotinylated probes. Competition assays showed that the biotinylated proteins were displaced by their respective unlabeled proteins. The major advantage of this solid-phase approach is that competition assays can be developed to compare the binding of native protein to that of either a mutant or a protein labeled with a probe other than biotin.

W-Pos342

ARE THE 5' AND 3' ALTERNATIVE SPLICING EVENTS IN TROPONIN T mRNAs COORDINATED DURING DEVELOPMENT? ((M.M. Briggs and F. Schachat)) Department of Cell Biology, Duke University Medical Center, Durham NC 27710.

Three isoforms of troponin T are expressed specifically during early muscle development of the rabbit and rat. At their 5'-ends, all include a newly-identified cassette exon, the fetal exon, that is absent from adult fast TnTs mRNAs. We have used RNA-PCR to determine if splicing of the fetal exon is coordinated with the mutually exclusive splicing of either exon 16 or 17 that occurs at the 3'-end of the mRNA. We find that before birth nearly all TnT mRNAs include both the fetal exon and exon 16. However, this linked expression terminates early in postnatal development when expression of the fetal exon ceases, but exon 16 continues to be incorporated into approximately half of the TnT. Using an antibody directed against a synthetic peptide encoded by exon 17, we find that expression of the amino acid sequences encoded by exons 16 and 17 changes in parallel with their mRNA levels. Both exons 16 and 17 continue to be expressed in Erector spinae for at least the first month; after that time exon 16 comes to predominate. These studies demonstrate that exon 16 and the fetal exon are expressed in fetal development, but differences in their subsequent patterns of expression suggest that the 3' and 5'-splicing events in TnT are independently regulated.

W-Pos343

THE STRUCTURE OF $4Ca^{2+}$•TROPONIN C COMPLEXED WITH TROPONIN I BY SMALL-ANGLE SCATTERING ((Glenn A. Olah and Jill Trewhella)) Isotope and Nuclear Chemistry Division, Los Alamos National Laboratory, Los Alamos NM 87545.

Small-angle X-ray scattering has yielded structural information on skeletal muscle troponin C (TnC) complexed with troponin I (TnI) in the presence of Ca^{2+}. Information on the structures of the individual components of the complex and their relative dispositions has been derived from a neutron scattering and contrast variation study of deuterated $4Ca^{2+}$•TnC complexed with non-deuterated TnI. The X-ray scattering data show the complex is elongated, with a maximum linear dimension (d_{max}) of approx. 100 Å, and a radius of gyration (R_g) of 31.8 ± 0.5 Å. The neutron data show TnC is in a partially extended conformation in the complex with its two globular lobes separated giving values for d_{max} and R_g of approx. 70 Å and 23.2 ± 0.5 Å, respectively. These values, as well as the pair distribution function, are very similar to those obtained for uncomplexed TnC in solution (Heidorn and Trewhella [1988] *Biochemistry 27*, 909). The TnI component in the complex is even more elongated than the TnC (d_{max} approx. 100 Å, R_g 38 ± 1 Å) and wraps around the TnC component. The center of masses of the two components are close to coincident (<15 Å separation). A Monte Carlo modeling method has been developed to model the complex in more detail.

W-Pos344

MOLECULAR MOBILITY OF A GENETICALLY INSERTED TRYPTOPHAN IN THE Ca-DEFICIENT CARDIAC EF-HAND ((V.G. Rao, A. Babu, H. Su and J. Gulati)) Albert Einstein College of Medicine, Bronx, NY 10461 (Spon.: J. Condeelis)

The N-terminal site 1 in cardiac TnC lacks an essential Ca-coordinating residue but nonetheless is functionally active in myocardium (Gulati et al, JBC, 1992, 267, 25073). We now report the fluorescence changes in the site-1 vicinity of a genetically engineered cardiac-skeletal chimera, to draw mechanistic insights into the cardiac phenotypic determinants. Three new constructs were generated — (1) sTnC-1(F26W), with two replacements: D29→A to block Ca-binding in site 1 of rabbit sTnC, and F26→W to facilitate the measurement of structural change by fluorescence. (2) C1S(F26W), the chimera combining (bovine) cardiac residues 1-40 with (rabbit) skeletal residues 41-160. (3) sTnC4(F26W), wild type sk-TnC. In EGTA solution, the fluorescence spectrum (λ_{ex}=280nm) was similar for all three constructs (peak F_{EGTA}=100%). In pCa4, the peak emission for C1S(F26W) was enhanced by 34% (F_{Ca}= 1.34±.1F_{EGTA}, n=4), but there was zero change with STnC-1(F26W). For wildtype sTnC, F_{Ca} was nearly 3-fold higher than F_{EGTA} (F_{Ca}= 2.76±.11F_{EGTA}). The apparent Ca-affinity of site 1 in the C1S(F26W) chimera was found as 6.08±.04, and that of of the wildtype sTnC(F26W) as 6.1±.03(4). The structural modifications causing the fluorescence emission in maximal Ca indicate different molecular mobilities between card site 1 and sk site 1, which may also underlie the phenotypic determinants. Strikingly, cardiac site 1 indicates high mobility despite its Ca-deficiency. *Supported by NIH & NY Heart*

W-Pos345

MOLECULAR CONFIGURATION OF THE ACTIVE SITE OF cTnC-Ca^{+2} COMPLEX. ((R. Salcedo, L.F. del Castillo, M. García, J.A. Cogordan, J. Muñiz* and J.L. Marin*)) Instituto de Investigaciones en Materiales, UNAM. A.P. 70-360, 04510, México D.F. and *Centro Universitario de Investigaciones Biomédicas, U. de Colima. A.P. 199, 28000 Colima, Col. México.

The aim of this report is to explore through a molecular simulation some of the properties of slow skeletal or cardiac troponin C (cTnC) bounded to Ca^{+2}. The simulations were made using the MMX method that carry out a geometry optimization for classical simulation of a force field. The work is based on the sequences of bacterially sinthesized cTnC (CBMIIA and CBMIIA2) proposed by Putkey et al. (J. Biol. Chem., 1989, 264:12370) . The molecules without Ca^{+2} have a money bag shape. When the ion is coordinated it take advantage of this shape and is included into the cavity formed in the protein, this effect produce relevant geometrical and energetic changes. Thermodynamic results:

Specie	ΔU(kcal/mol)	ΔH_f(kcla/mol)	μ(Debye)
CBMIIA	41.02	-1233.68	5.16
CBMIIACa+2	31.68	-1303.46	5.49
CBMIIA2	-40.63	-1135.41	10.86
CBMIIA2Ca+2	-33.03	-1127.81	12.18

The change of the dipole moment supports the idea that Ca^{+2} bound to cTnC could act as a trigger for the contraction process in striated muscle.

MICROTUBULES AND MOTORS

W-Pos346

ALTERNATING HEAD CATALYSIS BY KINESIN DURING MICROTUBULE-STIMULATED ATP HYDROLYSIS. ((D.D. Hackney)) Depart. Biological Sci., Carnegie Mellon Univ., Pittsburgh, PA 15213.

The mechanism of the MT-stimulated hydrolysis of ATP has been determined for constructs of the cloned α subunit from *Drosophila* which consist either of monomeric head domains or a longer construct which spontaneously dimerizes. The ATPase activity of the dimeric construct is activated 10,000 fold by MTs with a maximum rate of 47 sec^{-1} (per head domain) at saturating levels of MTs. Only ~30 nM MTs are required for 50% activation and physical binding of the dimer to the MT parallels stimulation of the ATPase rate. Analysis of the occupancy of the active site by [α-^{32}P]ADP indicates that the dimer binds to the MT in the presence of low ATP levels through one head domain which is attached to the MT in a rigor-like manner without bound nucleotide. The the other head domain of the attached dimer contains one bound ADP and is likely tethered to the MT through the rigor head, but cannot itself productively interact with the MT to effect ADP release. The turnover rate of the ADP on the tethered head is sufficiently rapid for it to be an intermediate in the catalytic cycle. These and other results are consistent with the rate limiting step of the dimer being due to ATP binding to the rigor head causing its release from the MT coupled to the attachment of the tethered head to a different position on the MT and subsequent release of its bound ADP. Such a model can produce directed motility along the MT if sequential reattachment of the tethered head is biased to occur preferentially in one direction with respect to the polarity of the MT.

W-Pos347

Mechanism of Microtubule-Kinesin ATPase ((Y. Z. Ma and E. W. Taylor)) Dept. of Mol. Gen.,Univ. of Chicago,Chicago,Il,60637.

The mechanism of microtubule-kinesin ATPase was fitted to

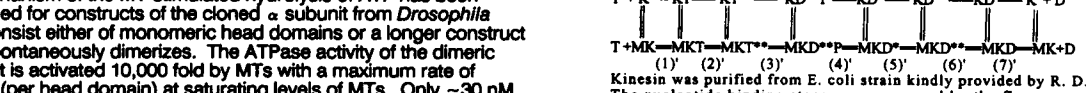

Kinesin was purified from E. coli strain kindly provided by R. D. Vale
The nucleotide binding steps were measured by the fluorescence enhancement of methyl anthranyloyl ATP (mant-ATP) and mant-ADP. An isomerization with rate constant of 200 s^{-1} at 20^0 C occurred (** states) following by a decrease of fluorescence (* states) with rate constants of 10 s^{-1} and 30s^{-1} for mant-ATP and mant-ADP respectively for kinesin and 30s^{-1} for both nucleotides with microtubule-kinesin. The rates of the phosphate burst, ADP dissociation,steady state ATPase, binding in presence of ADP and ATP were measured versus microtubule concentration for a range of ionic strength. In 150 mM NaCl, system is largely dissociated up to 35 μM tubulin but phosphate burst rate increased from 10 s^{-1} for kinesin to a maximum rate of 30 s^{-1} with dissociation constant of 4μM. In 50 mM NaCl, V_{max} was 15-20 s^{-1} and dissociation constants for ATPase, KD* and states formed in presence of ATP and ADP were in the 3 to 9 μM range while burst rate was 80-100 s^{-1} and gave only a small incease in this range of concentrations. It is concluded (1) the KT** state is more strongly bound than other intermediates except possibly KD**; (2) fluorescence decrease measures k_4, k'_4 (3) k'_4 and k'_5 are similar and determine the steady state rate. Results are consistent with detachment occuring at the MKD* state.

W-Pos348

THE FORCE-VELOCITY RELATIONSHIP IN KINESIN-DRIVEN MOTILITY
((K. Hall, D. Cole, Y. Yeh, J. Scholey, and R. Baskin)) University of California, Davis CA 95616.

How much force can kinesin generate? What is the combined force of many kinesin molecules working together? Exactly how does the velocity of kinesin-driven movement change with applied force against its movement? These are all questions fundamental to the complete understanding of kinesin and we are trying to answer them using a centrifuge microscope. Since the publication of our initial study (Hall et al. (1993) Nature 364:457-459) we have redesigned the microscope system to allow for greater measurement accuracy through the use of differential interference contrast microscopy, increased real-time magnification (40X), as well as an additional 4-fold magnification when measuring positional changes during motor protein-driven velocity measurements. In addition to the greater measurement accuracy, we are now also able to follow the changes in velocity of the same demembranated sperm through changing applied centrifugal forces. Using this new and much improved system, we are investigating the differences between our kinesin force measurements and those of others (Hunt, A. and Howard, J. (1993) J. Biophys. 64:A263; Kuo, S. C. and Sheetz, M. P. (1993) Science 260:232-234; Takagi, I. et al. (1993) J. Musc. Res. Cell Mot. 14:366.). We are also investigating the effect of various substrate and nucleotide conditions on the force-velocity curve.

W-Pos349

MICROTUBULE MOVEMENT BY A BIOTINATED KINESIN BOUND TO A STREPTAVIDIN COATED SURFACE ((E.Berliner*, H.K. Mahtani‡, S. Karki‡, L.F. Chu‡, J.E. Cronan, Jr.†, and J. Gelles‡§)) *Biophysics Program, ‡Graduate Department of Biochemistry, and §Center for Complex Systems, Brandeis University, Waltham, MA 02254 and †Departments of Microbiology and Biochemistry, University of Illinois at Urbana-Champaign, Urbana, IL 61801

Kinesin, an ATP-dependent microtubule motor, can be studied *in vitro* in motility assays where the kinesin is non-specifically adsorbed to a surface. However, adsorption can inactivate kinesin and may alter its reaction kinetics. We therefore prepared a biotinated kinesin derivative, K612-BIO, and characterized its activity in solution and when bound to streptavidin-coated surfaces. K612-BIO consists of the N-terminal 612 amino acids of *Drosophila* kinesin heavy chain linked to the 87 amino acid C-terminal domain of the biotin carboxyl carrier protein subunit of *E. coli* acetyl-CoA carboxylase. This C-terminal domain directs the efficient post-translational biotination of the protein. We expressed K612-BIO at high levels using the baculovirus expression vector system and purified it to near-homogeneity. The expressed protein is completely soluble and >90% is bound by streptavidin. K612-BIO steady-state ATPase kinetics ($K_{M,ATP}$ = 24 μM, $K_{0.5,microtubule}$ = 0.61 mg ml^{-1}, V_{max} = ~15 μmoles min^{-1} mg^{-1}, 25°) are similar to those reported for intact kinesin and are not affected by the addition of streptavidin. Enzyme bound to a surface coated with streptavidin drove microtubule gliding in the presence of 2 mM ATP at 750 ± 130 nm s^{-1} (26°). Activity was abolished by pre-treatment of the surface with biotin, indicating that the microtubule movements are due to specifically bound enzyme. Specific attachment of biotinated enzyme will be useful for quantitative analysis of kinesin motility and may provide a way to detect activity in kinesin derivatives or kinesin-like proteins that have not yet been shown to move microtubules.

W-Pos350

KINESIN DOES NOT MOVE ALONG ZINC-MACROTUBES. ((S. Ray*, S. G. Wolf^, J. Howard*, K. H. Downing^)) *Dept. of Physiology and Biophysics, Univ. of Washington, Seattle, WA 98195. ^Life Science Div., Lawrence Berkeley Laboratory. Berkeley, CA 94720. (Spon. by S. Ray)

The cylindrical wall of a microtubule typically has 13 parallel protofilaments (pfs). As kinesin moves along a microtubule, it follows the course of the pfs. It is not known whether the binding sites for kinesin lie on a single pf or in the groove between adjacent pfs. This question could be addressed by studying the movement of kinesin along zinc-induced tubulin sheets, where adjacent pfs are antiparallel and present an entirely different groove structure.

Kamimura and Mandelkow (*J. Cell Biol.* 18, 865-75, 1992) reported that kinesin moves along zinc-sheets. This result suggests that kinesin interacts with only a single pf. We found that zinc-sheets grown under their conditions often had a microtubule-like structure along one edge. Using DIC microscopy, we also observed limited kinesin-based motility of these sheets.

To resolve the question of whether this motility could be a result of the microtubule-like structure along the edge, we used zinc-macrotubes. Macrotubes have a similar pf structure to zinc sheets but are rolled up into tubes, and thus are free of edges. The macrotubes were stable in the presence of 10 μM taxol, 100 nM free Zn^{2+} at pH 6.8, and electron microscopy confirmed that samples contained only macrotubes. Under these buffer conditions, kinesin could bind strongly to axonemal doublets in the presence of AMP-PNP, and generate motility in the presence of ATP. But kinesin did not bind to or move the macrotubes. Thus, it is possible that the groove between two parallel pfs is required for kinesin's motility.

Supported by NIH grants AR40593 to JH, 5T32NS07097 to SR and GM40633 to KHD and Hollaender Postdoctoral Fellowship (DOE) to SGW.

W-Pos351

LOW-ANGLE NEUTRON SCATTERING BY THE MOTOR DOMAIN OF THE KINESIN-RELATED PROTEIN *NCD*. ((R. Mendelson†§, S. Fujiwara†§, E. Sablin§, D. Stone†§, R. Vale §‡and R. Fletterick§)) †Cardiovascular Research Institute, §Dept. off Biochem. & Biophys. and ‡Dept. of Pharmacology, Univ. of Calif., San Francisco, CA 94143.

We have investigated the shape of the motor-domain of kinesin-related non-claret disjunctional (ncd) protein from *Drosophila* by low-angle neutron scattering. This domain, consisting of residues R335-K700, was was cloned in a pHB40P vector under control of a T7 promoter and expressed in the BL21(DE3) *E. coli* strain. When purified to homogeneity R335-K700 was found to be quite suitable for scattering studies in a buffer consisting of 50 mM PIPES (pD7.4), 0.13 M NaCl, 1 mM EGTA, 1mM DTT, 2 mM $MgCl_2$, 99% D_2O at T = 6 °C. Preliminary studies using the 30 m camera at NIST showed that highly linear Guinier plots could be obtained to better than s_{min}=1/36 nm^{-1}. These Guinier plots yielded a radius-of-gyration (R_g) near 2.3 nm. Fits of the scattering intensity at large s-values showed that the ellipsoid of revolution which best fits the data was unambiguously prolate and had an axial ratio near 2.8. Thus the approximate dimensions of such an object are 3.2 x 9 nm. Because of the low ATPase rate of ncd (in the absence of microtubules) and low radiation-damage induced by cold neutrons, we are investigating changes in ncd shape which occur during ATP hydrolysis.

W-Pos352

A SIMPLE PICONEWTON-SCALE IN VITRO FORCE ASSAY FOR KINESIN.
((F. Gittes, E. Meyhöfer, S. Baek and J. Howard)) Dept. of Physiology and Biophysics and Center for Bioengineering, University of Washington, Seattle, WA 98195.

We have developed a modification of a standard *in vitro* motility assay to challenge one or few kinesin motor molecules with piconewton-scale forces, without any special apparatus, by arranging for particular microtubule-bending events to occur. In the Euler theory of elastic stability, a thin rod clamped at one end and subjected to a compressive force F at the other will buckle if its length exceeds a critical value $L_B = \gamma(EI/F)^{1/2}$, where $\gamma \cong 4.49$ and EI is the flexural rigidity of the rod. Having measured EI for microtubules in earlier work, we can apply the buckling formula to the situation where a rhodamine-labeled microtubule, "clamped" to a glass surface near its minus end, is subjected to a compressive force by a plus-end-directed kinesin motor. The clamped portion is a biotin-labeled seed that binds to streptavidin on the surface. We avoid steric problems by attaching the streptavidin to the glass indirectly via biotin-labeled BSA. After introducing kinesin onto a surface already populated by clamped microtubules, buckling events are readily observed in the presence of ATP, using fluorescence microscopy. As the concentration of kinesin is lowered, we observe events in which a microtubule is buckled through one point, consistent with buckling by a single motor. The frequency of events declines when L_B is roughly 10 μm, corresponding to a force F of about 4 pN; however, some events occur at significantly shorter buckling lengths. A possible interpretation is that some events are caused by two or three closely situated motors. This assay is feasible specifically for microtubules, where pN-scale motor forces, the flexural rigidity EI, and typical *in vitro* microtubule lengths are all consistent with the buckling formula.

W-Pos353

KINESIN SWIVELS TO PERMIT MICROTUBULE MOVEMENT IN ANY DIRECTION
((A.J. Hunt and J. Howard)) University of Washington, Seattle, WA 98195.

The motor protein kinesin is about 75 nm long and has two head domains at one end and a tail domain at the other. The heads bind to a microtubule and the tail is thought to bind to an organelle. We have asked the question: how does motility depend on the relative angle between the microtubule and the organelle?

Using the single-motor motility assay in which microtubules are observed by fluorescence microscopy to move across a glass surface sparsely coated with kinesin, we have shown that the speed a single kinesin molecule translates a microtubule is independent of the direction that the microtubule points.

What is the structural basis for this lack of angular dependence? By analyzing the thermally-induced rotation of microtubules tethered to the surface via single kinesin molecules, we discovered that kinesin has extremely high torsional flexibility: one kT of energy is sufficient to twist a kinesin molecule through more than 360 degrees.

Kinesin's high flexibility confers upon the protein two adaptations for organelle motility. First, the motor's head can rapidly bind to a microtubule irrespective of the orientation of the organelle to which the tail is attached. Second, the flexibility ensures that several motors can efficiently work together even though they are randomly oriented on the organelle's surface rather than being in precise arrays like the motors of muscle and cilia.

Supported by NIH AR40593.

W-Pos354

ELECTRON PARAMAGNETIC RESONANCE SPECTRA OF SPIN-LABELED ADP BOUND TO THE MICROTUBULE MOTORS, KINESIN AND NCD. ((Nariman Naber and Roger Cooke)) Dept. of Biochem. and CVRI, University of California, San Francisco.

We have used spin-labeled ATP analogs to study the ATP binding site of the microtubule motors, kinesin and ncd. These two proteins have similar amino acid sequences, however, they move towards different ends of the microtubules. A number of analogs with the spin label attached to the 2'- or the 3'-position of the ribose ring of ADP were found to bind to both kinesin and ncd. All probes exibited some degree of mobility relative to the protein. The mobility depended on both the number of spacer atoms between the spin label and the ribose ring and on the protein. The mobility can be determined from the splitting, $2T'_{\parallel}$, between high and low field peaks. The maximum splitting obtained for kinesin was $2T'_{\parallel}$ = 6.0 and 6.1 mTesla with the spin probe attached to the 2' or 3' positions of the ribose through a one atom link, either amide or amine. Probes on analogs bound to ncd were more mobile than those bound to kinesin, with the most immobilized probe attached to the 2'-position of 3'-dATP through an ester linkage, $2T'_{\parallel}$ = 5.3 mTesla. When the spin label was attached to the 6-position of the adenine ring, no binding was obtained with either kinesin or ncd. This observation is similar to that for myosin. These results indicate that the structures of the nucleotide sites on kinesin and ncd are different. In addition they show these spin probes can be used to study the orientation of the nucleotide site of these motors when bound to flow-oriented microtubule gels. Supported by AR30868.

W-Pos355

SPECIFIC ASSOCIATION OF PARAMECIUM 29KD DYNEIN LIGHT CHAIN TO PARAMECIUM AND TETRAHYMENA DYNEIN HEAVY CHAINS. **((K. Barkalow, T. Hamasaki and P. Satir)) Department of Anatomy and Structural Biology, Albert Einstein College of Medicine, Bronx, NY 10461.**

We have previously reported that a 29kDa polypeptide (p29) which copurifies with *Paramecium* 22S dynein (outer arm dynein) activates *in vitro* microtubule translocation activity via its cAMP-dependent, Ca^{2+}-sensitive phosphorylation (PNAS 1991, 88:7918), and isolated p29 not only rebinds to *Paramecium* 22S dynein but also increases the microtubule translocation velocity *in vitro* (Biophys. J. 1993, 62(2 pt2,264(Abst)). Isolated cAMP-dependent protein kinase (PKA) from *Paramecium* (kindly provided by Drs. Walczak and Nelson, Univ. Wisconsin) phosphorylates p29 as well as dynein heavy(H)-chain(s) *in vitro* and increases dynein-mediated microtubule translocation speed when 22S dynein is incubated with PKA. p29, therefore, should be considered a regulatory light chain of *Paramecium* 22S dynein.

This p29 rebinds not only to *Paramecium* but also to *Tetrahymena* 22S dynein. Isolated p29 rebinds to *Tetrahymena* 22S dynein but not to 14S dynein. When *Tetrahymena* or *Paramecium* 22S dynein, both of which have a three-headed bouquet structure, is subjected to mild chymotryptic digestion, they break down to yield one-headed and two-headed fragments. This one-headed fragment uniquely originates from α-H-chain in *Tetrahymena* (Toyoshima 1987, JCB 105:887). Isolated p29 rebinds, preferentially, to the one-headed fragment of either *Paramecium* or *Tetrahymena* 22S dynein. This result suggests that the activity of a particular head, of the three-headed bouquet, (α-H-chain) is regulated by cAMP-dependent phosphorylation of p29.

W-Pos356

PH-DEPENDENCE OF BRAIN MAP1C. ((A.M. Bates, J.A. Evans)) Department of Surgery, School of Medicine, University of Maryland at Baltimore, Baltimore, MD 21201.

Cytoplasmic dynein, MAP1C, is partially responsible for retrograde organelle transport and has a broad, bell-shaped ATPase dependence on pH implying multiple titrable protons are important for activity. The apparent pH-activity curve represents the sum of mechanistic and structural factors. Rat and beef brain MAP1C (25μl) in a total 200μl 150mM Na acetate; 2mM Mg acetate was reacted with 1mM ATP[γ-^{32}P] in 50mM pH buffer (pH 4.5 - 6.0: MES; pH 6.0 - 9.5: bistrispropane) for 6 hrs 37°C. We observed a broad, bell-shaped curve with a plateau from pH 7.5 to 8.5. To determine whether loss of activity results from irreversible changes in protein structure we dialyzed MAP1C versus the above pH series using 2.5mM buffer and then determined ATPase activity at pH 8.0. The apparent optimum in both curves was 7.5. Incubation at more alkaline pH resulted in a time-dependent, irreversible loss of activity. Following incubation at more acidic pH (6.0-7.5) activity is recovered by transition to pH 7.5. Therefore the descending limb of the activity curve represents protonation of a mechanistically-required group. Acidic MES incubation resulted in irreversible loss of activity. (Supported in part by USPHS training grant HL07716-02.)

W-Pos357

SIMPLE KINETIC ANALYSIS REVEALS FUNCTIONAL MULTIPLICITY OF MOTOR MOLECULES. ((C.K. Omoto*, E. Lark* and M.F. Schumaker#)) *Dept. of Genetics & Cell Biol. and #Dept. of Pure & Applied Math., Wash. State Univ., Pullman, WA 99164-4234.

We present a simple analytical solution for a kinetic model of velocity produced by motor molecules. This model has a velocity proportional to the probability that all arms in a molecule are detached from the cytoskeleton, and therefore we refer to it as obligate cooperativity. Our model is expressed as: $\omega = \frac{\omega_{max}}{\left(1+\frac{q}{S}\right)^n}$ where ω is the velocity, ω_{max} the maximum velocity, S the substrate conc., n the number of arms, and the product nq, the effective Michaelis constant at high substrate conc. A value of $n = 2$ gives the best fit to the heavy meromyosin sliding velocity data. Inspite of the complexity the axoneme, the model fits the behavior of wild-type Chlamydomonas axonemes with 3 outer arm dyneins and mutant axonemes with only the inner arm dyneins using n of 3 and 2, respectively.

W-Pos358

EVIDENCE SUGGESTS THAT AT LEAST ONE OF THE 13 PROTOFILAMENTS OF THE A-TUBULE FROM DOUBLET MICROTUBULES IS NOT COMPOSED OF TUBULIN **((D. Nojima, R.W. Linck, and E.H. Egelman)) Dept Cell Biology & Neuroanatomy, Univ Minnesota, 321 Church St, Minneapolis, MN 55455.**

Recent data suggest that not all 13 protofilaments from the A tubule are composed of tubulin. The structure of doublet microtubules have been studied by their fractionation into smaller stable components. Ciliary and flagellar axonemes can be fractionated by Sarkosyl detergent into stable ribbons of 3-4 protofilaments from the A tubule. These protofilament ribbons are composed primarily of tubulin, tektins A, B, and C, and proteins with molecular weights of 77 and 83kDa. Equatorial projections from computed Fourier transforms of ribbons imaged by cryoelectron microscopy show 1 of the 4 protofilaments of a residual ribbon with a lower density; similar data are obtained from STEM and negative stain images. The protofilament with lower density is collinear with a residual fibril which is strongly decorated by antibodies to tektin A. Decoration of the ribbons with the kinesin head fragment K401 (Harrison, B. C., *et al.* (1993) Nature 362:73-75), which has been shown to bind to β tubulin, decorate the ribbons, but with 1 of the 4 protofilaments not binding kinesin. Monoclonal antibodies against the 77kDa polypeptide do not decorate the fibril. These data suggest that one of the protofilaments, the residual fibril, is composed of tektins, resulting in the formation of a "seam" or discontinuity in the helical arrangement of tubulin subunits. **Supported by USPHS grant GM35648, and NSF grant DIR-9113444.**

W-Pos359

THE TEMPERATURE-CONCENTRATION PHASE DIAGRAM OF MICROTUBULES

((D.K. Fygenson, E. Braun & A. Libchaber)) Physics Dept., Princeton University, Princeton, NJ, USA

Microtubules are known to assemble at high temperatures (37°C) and disassemble at low temperatures (4°C). However, the detailed nature of this temperature dependence has not been studied. We investigate the T-C phase diagram for heterogeneous and homogeneous nucleation of individual microtubules. We explore a temperature range from 4°C-38°C at several different concentrations of tubulin using video-enhanced DIC microscopy. The phase-space of microtubule dynamics is bounded at high temperatures by the appearance of bulk nucleated microtubules. At low temperatures we observe an onset in the number of microtubules growing from axonemal nucleation sites. In between these two bounds we observe a gradual transition from "bounded" growth (in which shortening events often consume the entire microtubule) to "runaway" growth (in which shortening events are rare and consume a negligible portion of the microtubule). We measure the individual dynamical parameters throughout. The microtubule growth velocity increases linearly in temperature, with a concentration dependent slope. This result suggests that the strength of the tubulin-water interaction decreases at lower temperatures. Microtubules with the same growth velocities have a lower frequency of catastrophe at lower temperatures. In the context of the GTP-cap model, this result implies a temperature dependence in the rate of GTP hydrolysis.

W-Pos360

IMMUNOLOCALIZATION OF DHP RECEPTORS, RYANODINE RECEPTORS AND TRIADIN IN ADULT RABBIT ATRIUM AND VENTRICLE.

((S. Lewis Carl[§], K. Felix[§], A.H. Caswell*, N.R. Brandt*, W.J. Ball Jr.[¶], P.L. Vaghy*[¶], G. Meissner[#], and D.G. Ferguson[§])) Depts. of Physiology and Biophysics[§], Pharmacology and Cell Biophysics[¶], Univ. of Cincinnati, Univ. of Miami*, Ohio State University+, Univ. of North Carolina[#]. (Spon. by J.A. Heiny)

The dyadic couplings of cardiac muscle cells have generally been considered to be equivalent to the triad junctions of skeletal muscle. However, this question has yet to clarified using immunoprobes to co-localize the cardiac isoforms of the triadic proteins. We have used indirect immunofluorescence and laser scanning confocal microscopy to co-localize the dihydropyridine receptors (DHPR) and ryanodine receptors (RyR) in adult rabbit atrium and ventricle. We have observed that all of the DHPR are co-distributed with the RyR. This is particularly apparent in atrial cells in which labeling is observed as discrete punctate spots along the sarcolemma. On the other hand, not all RyR are associated with DHPR. Again, this is best observed in atrial cells in which RyR-specific staining forms transverse bands that mimic the sarcomeric spacing. To further characterize the molecular structure of the dyads we have co-localized triadin and the RyR in adult rabbit atrium and ventricle. The skeletal muscle triadin-specific monoclonal antibody we use here detects a 95 kDa protein in rat ventricle (Brandt et al.; J. Membr. Biol., 131:219) which is presumably an isoform of triadin. In indirect immunofluorescence studies, we have observed that triadin and the RyR are always co-distributed, even in the extended junctional SR of the atrial cells.

W-Pos361

DIHYDROPYRIDINE RECEPTORS ARE GROUPED IN THE SURFACE MEMBRANE OF AVIAN CARDIAC CELLS.

((X-H Sun*, F. Protasi*, H. Takekura*, H. Takeshima*, M. Takahashi[$], D.G. Ferguson+; C. Franzini-Armstrong*)) *Un. Pennsylvania ; [#]IIAS, Tokyo; [$] MKILS, Tokyo; +Un. Cincinnati.

In the junctional domains of surface membrane/T tubules of skeletal muscle fibers, dihydropyridine receptors (DHPRs) form tetrads which are located in arrays corresponding to the location of the underlying feet or ryanodine receptors (RyRs) of the sarcoplasmic reticulum (SR). In cardiac muscle, on the other hand, feet are known to form ordered clusters in junctional and corbular SR, but the disposition of DHPRs is yet unknown. Chick myocardium has no transverse tubules and numerous peripheral couplings. We have used a polyclonal antibody (CR2) raised against fragments at the C terminus of the α_1 subunit of rabbit cardiac DHPR (Yoshida, et al., FEBS Lett. 309:343, 1992) and a monoclonal antibody (34C) against α, β and cardiac avian RyRs (Airey, et al., J. Biol. Chem. 265: 14187, 1990) for immunofluorescent localization of DHPRs and RyRs in myocardium of chicken at hatching. In cross sections, both DHPRs are RyRs are located in hot spots around the perimeter of the muscle fibers. In longitudinal sections the hot spots for both molecules are often located in linear arrangements parallel to the fibers' long axis. Freeze-fracture of the surface membrane reveals domains containing groups of large particles which are not arranged in tetrads. The domains occupy areas of membrane comparable in size to the junctional, feet-bearing, domains of the SR and they are often disposed in longitudinal linear arrangements, like the DHPR hot spots. We conclude that DHPRs are located in special domains of the surface membrane of cardiac muscle cells, but do not form tetrads and may not have a specific spatial relationship to the feet. Supported by AHA and NIH HL 4809.

W-Pos362

DENSITY OF RYANODINE RECEPTORS IS INCREASED IN CARDIOMYOPATHIC HAMSTER HEART PRIOR TO THE ONSET OF CELL NECROSIS.

((H.F. Chan and S.E. Howlett)) Department of Pharmacology, Dalhousie University, Halifax, Nova Scotia, Canada B3H 4H7

The objective of this study was to determine whether the density of [^{3}H]-ryanodine receptors, and thus of putative sarcoplasmic reticulum (SR) Ca^{2+} release channels, changes in cardiomyopathic (CM) hamster heart prior to the onset of cell necrosis. We compared density and affinity of [^{3}H]-ryanodine binding sites in crude homogenates and in purified heavy SR fractions from 30 day-old CM (CHF 146) and genetically-matched normal hamsters (CHF 148). Homogenate binding showed that B_{max} values were increased by a factor of 1.33 in 30 day-old CM hamsters compared to normal (values were 831 $\pm$ 95 vs. 626 $\pm$ 51 fmol/mg protein in CM and normal preparations, respectively; n=7 per group; mean $\pm$ SEM). In SR membranes, B_{max} values also were increased (by a factor of 1.37) in the 30 day-old CM group compared to normal (values were 2001 $\pm$ 212 vs 1458 $\pm$ 173 fmol/mg protein in CM and normal preparations, respectively; n=8 per group, $p<0.002$). K_d values were significantly lower in CM hearts when compared to normal in both homogenates and SR membranes, suggesting receptor properties may change in disease. These results demonstrate that ryanodine receptor density increases early in the development of disease, prior to the onset of cardiac necrosis. Thus, fundamental changes in the SR Ca^{2+} release mechanism may occur prior to the onset of disease.

W-Pos363

DISTINCTIVE REGULATION OF SARCOPLASMIC RETICULUM CALCIUM RELEASE CHANNEL ACTIVITY BY PROTEIN KINASES.

((Andrew J. Lokuta, Oscar Fuentes, W. J. Lederer, Terry B. Rogers and Hector H. Valdivia.)) Departments of Biochemistry and Physiology, University of Maryland Medical School, Baltimore, Md 21201.

The Ca^{2+} release channel/ryanodine receptor of cardiac and skeletal muscle constitutes the major pathway for calcium release from sarcoplasmic reticulum (SR) during excitation-contraction coupling. Gating of this channel in both muscle types is regulated by a variety of physiologically relevant cytosolic substances such as Ca^{2+}, Mg^{2+}, adenine nucleotides and calmodulin. Recently, evidence has been accumulating that indicates phosphorylation also regulates release channel activity. We tested the effect of the catalytic subunit of protein kinase A (*PKA*), the α-isozyme of protein kinase C (*PKC*), and purified Ca^{2+}, calmodulin-dependent protein kinase II (*CaMK*) on ryanodine receptors from cardiac and skeletal muscle. We examined the time-course of [^{3}H]ryanodine binding to determine the onset of effect and the cofactors required for phosphorylation while the functional impact of the phosphorylation reaction was directly assessed in planar bilayer recordings of calcium release channels. The level of channel phosphorylation by endogenous protein kinases was also evaluated with a dephosphorylating cocktail containing acid phosphatase. In native SR, PKA inhibited binding and channel activity of cardiac ryanodine receptors but identical phosphorylation conditions had no effect on skeletal receptors. PKC had a distinctive effect on channel activity that was Ca^{2+}- and ryanodine receptor isoform-dependent, while CaMK potentiated the effect of an endogenous CaMK of cardiac SR. The results show that ryanodine receptors are potential substrates for different protein kinases that can have different effects on channel behaviour. Supported by grants from NIH and AHA.

W-Pos364

ION CONDUCTION IN THE RYANODINE-MODIFIED SR Ca^{2+}-RELEASE CHANNEL.

((A.R.G.Lindsay, A.Tinker & A.J.Williams)) Natl.Heart & Lung Inst., Univ. of London, London SW3 6LY, U.K.

We have investigated the mechanisms underlying the modification of ion conduction in the sheep cardiac SR Ca^{2+}-release channel by ryanodine. The fractional conductance (FC) seen in symmetrical 210 mM solutions varies with the permeant species. The monovalent cations (K^+,Na^+,Cs^+,Li^+) have values of FC in the range 0.60-0.66. With divalent cations FC is considerably lower (Ba^{2+},0.22 and Sr^{2+},0.28) whilst modification in organic permeant cations can result in an increased FC (e.g. diethylamine 1.2). The conductance of the ryanodine-modified channel saturates with increasing permeant ion activity. With K^+, saturation follows a single-ite model with a G_{max} of 492pS and a K_D of 11.6mM. Permeability relative to K^+ is 1.14 for Na^+, 0.66 for Cs^+, 0.86 for Li^+, 3.48 for Ba^{2+} and 0.33 for diethylamine. Comparison of these data with equivalent parameters obtained in unmodified channels[1] indicates that ryanodine binding results in profound alterations in ion handling. On modification, single-channel K^+ conductance is reduced whilst affinity is increased; relative permeability of inorganic monovalent cations is unchanged whilst that of Ba^{2+} decreases and that of diethylamine increases. It is possible to account for these variations using a single-occupancy, four barrier, three binding site rate theory model[1] and interpret them in terms of altered structure of the conduction pathway. 1.*Tinker et al. 1992,J.Gen.Physiol.,100 495-517.* *Supported by the BHF & Wellcome Trust.*

W-Pos365

EFFECT OF R56865 AND ITS ANALOGUES ON SHEEP CARDIAC SARCOPLASMIC RETICULUM FUNCTION

((S.J.McGarry, E.Scheufler[1] and A.J. Williams)) Natl. Heart & Lung Inst., Univ. of London, London SW3 6LY and [1]Janssen Research Foundation, 4040 Neuss 21, Germany.

We have investigated the effects of the anti-arrhythmic flunarizine analogue R56865 on cardiac sarcoplasmic reticulum (SR) function. R56865 (0.5-50μM) failed to affect single SR Ca^{2+}-release channel open probability (Po) at 10μM Ca^{2+}. The Po was 0.035 $\pm$ 0.014 (n=4) before and 0.043 $\pm$ 0.018 (n=4) after addition of 50μM R56865. Rapid efflux of $^{45}Ca^{2+}$ from SR vesicles induced by 0.1μM Ca^{2+} yielded initial efflux rates of 176 $\pm$ 33 and 171 $\pm$ 17 nmoles $^{45}Ca^{2+}$ mg protein^{-1} sec^{-1} (n=5). Binding of ^{3}H-ryanodine to SR membranes was similarly unaffected by up to 50μM R56865. However, R56865 inhibited the ATP-stimulated uptake of $^{45}Ca^{2+}$ into SR vesicles by 26-37% at 0.5-50μM. R56865 also inhibited the binding of ^{3}H-digoxin to SR membranes with apparent IC_{50}s of 497nM and 16.6μM. Inhibition was non-competitive and there was also an increase in the K_d for ^{3}H-digoxin from 1.52nM to 15.1nM. Inhibition was due to R56865 increasing the dissociation rate of bound ^{3}H-digoxin without affecting the association rate. R56865 also decreased the Po of channels activated by 1nM digoxin at 10μM Ca^{2+}. The related compound R80122 was also a non-competitive antagonist of ^{3}H-digoxin binding, however flunarizine was ineffective at up to 100μM.

W-Pos366

ACTIVATION OF CARDIAC SARCOPLASMIC RETICULUM Ca^{2+} RELEASE CHANNELS BY VOLATILE ANESTHETICS.

((T.J. Connelly and R. Coronado)) Departments of Anesthesiology and Physiology, University of Wisconsin, Madison, WI 53792.

Halothane, enflurane and isoflurane are volatile anesthetics that cause an alteration in intracellular Ca^{2+} homeostasis which results in depression of myocardial contractility. We employed single channel recordings in planar bilayers to characterize the interaction of these agents with the cardiac Ca^{2+} release channel of porcine sarcoplasmic reticulum (SR). Halothane and enflurane activated the channel, while isoflurane did not. Mean channel open probability increased threefold (0.026 to 0.076, n=6) in the presence of halothane (1.2 vol%, 0.5 mM) and twofold (0.024 to 0.048, n=5) in the presence of enflurane (1.4 vol%, 0.6 mM). Activating anesthetics did not increase the frequency of open events but increased the duration of openings, as represented by a shift of the open distributions to longer times. No anesthetic altered channel closed-time distributions, access to a long-lived closed state or channel conductance. These results suggest an anesthetic interaction with an open state of the channel and demonstrate that the SR Ca^{2+} release channel is a crucial target for volatile anesthetics. This mechanism provides an explanation for the greater potency of halothane and enflurane as negative inotropic agents relative to isoflurane.

(Supported by NIH, MDA, AHA, IARS, ASA and PMAF)

W-Pos367

DITHIOTHREITOL MODIFIES THE GATING OF THE SHEEP CARDIAC SR Ca^{2+}-RELEASE CHANNEL. ((A. Boraso and A. J. Williams)) Natl. Heart & Lung Inst., Univ. of London, London SW3 6LY, U. K.

Oxidants of sulphydryl groups have been reported to increase Ca^{2+} release from the SR (*Abramson & Salama, J. Bioenerg. Biomembr. 21: 283-394, 1989*). We have now investigated the effects of the reducing agent dithiothreitol (DTT) on the gating of sheep cardiac SR Ca^{2+}-release channels. Vesicles of HSR were incorporated into planar phospholipid bilayers and current fluctuations through single Ca^{2+}-release channels were recorded. Cytosolic and luminal free Ca^{2+} were 10 μM and 50 mM respectively. Millimolar DTT at the cytosolic channel face reduced open probability (P_o) in a dose-dependent manner. The P_o of Ca^{2+}-release channels in the absence of DTT was 0.102 ± 0.024 (SEM, n=15). At 1 mM and 3 mM DTT the P_o was 0.055 ± 0.024 (SEM, n=7) and 0.063 ± 0.034 (SEM, n=5) respectively. 5 mM DTT reduced single-channel P_o to 0.002 ± 0.001 (SEM, n=4) and 10 mM DTT closed the channels (P_o=0, n=3). Mean open time was 2.22 ± 0.51 (ms$\pm$SD, n=6) and 1.97 ± 0.47 (ms$\pm$SD, n=3) in the absence and presence of 3 mM DTT. Mean closed times increased from 50.0 ± 69.5 (ms$\pm$SD, n=6) with 10 μM Ca^{2+} to 83.0 ± 58.6 (ms$\pm$SD, n=3) with 3 mM DTT. Following the reduction of P_o by DTT, channels could be activated by millimolar ATP and caffeine. Millimolar DTT also reduced [^{3}H]-ryanodine binding in the presence of 100 μM Ca^{2+} by 19.6 ± 10.2 (%$\pm$SD, n=3) with 1 mM DTT and 34.0 ± 19.1 (%$\pm$SD, n=3) with 10 mM DTT.

W-Pos368

THE ELECTROPHYSIOLOGICAL EFFECTS OF RYANODINE DERIVATIVES ON THE SHEEP CARDIAC CA^{2+}-RELEASE CHANNEL. ((A.Tinker, J.L.Sutko, LRuest, W.Welch, J.A.Airey, K.Gerzon, K.Bidasee, H.R.Besch Jr. & A.J. Williams.)) Natl.Heart & Lung Inst., Univ. of London, London SW3 6LY, U.K.

We have examined the effects of derivatives of ryanodine on K^+ conduction in the Ca^{2+}-release channel purified from sheep cardiac SR. As with ryanodine addtition of nM to μM quantities to the cytoplasmic face causes the channel to enter a state of reduced conductance which has a high open probability. However the amplitude of that reduced conductance state varies between the derivatives. In symmetrical 210 mM K^+ ryanodine leads to a conductance state approximately 60% of control, ryanodol leads to a level of 69.2 ± 0.7%(n=9), Ester A ryanodine modifies to one of 61.5 ± 1.4%(n=8), CBZ glcyl dehydroryanodine to one of 29.4 ± 1.0%(n=6), 21-p-nitrobenzoyl-amino-9-hydroxyryanodine to one of 26.1 ± 0.5%(n=11), β-alanyl ryanodine to one of 14.3 ± 0.5%(n=5), guanidino-propionyl ryanodine to one of 5.8 ± 0.1%(n=9) (chord conductance at 60 mV, $\pm$ S.E.M.). For all derivatives, except ryanodol, the effect is irreversible. In contrast, modification by ryanodol is reversible with dwell times in the substate lasting tens of seconds to minutes. The effect by ryanodol is voltage dependent with modification more likely to occur and lasting longer at +60 than -60 mV holding potential. At concentrations $\geq$ 1mM, ryanodine after initial rapid modification leads to irreversible closure within a minute. In contrast, comparable concentrations of β-alanyl ryanodine do not cause such a phenomenon following modification even after prolonged periods of recording (> 5 minutes). The modification of ryanodine structure leads to profound differences in the resultant electrophysiological effect on the Ca^{2+}-release channel.

W-Pos369

A PHOSPHORYLATED MEMBRANE COMPONENT MODULATES THE VOLTAGE DEPENDENT KINETIC OF THE SR Cl^- CHANNEL. ((Decrouy, A., M. Juteau and E. Rousseau)) Dept. of Physiology and Biophysics, University of Sherbrooke, Sherbrooke (Quebec) Canada.

Single Cl^- channels were studied upon isolation of cardiac SR vesicles and reconstitution into lipid bilayers. The channels display large conductances (90 to 135 pS for trans [Cl^-] ranging from 25 to 350 mM). The Cl^- selectivity was confirmed after plotting the theoretical E_{Cl} values and the reversal potentials. 70% of the channels display steady state kinetics despite a voltage-dependency of the Po. However, 30% of the recordings also show long silent episodes (30 s up to several min). Kawano et al., (1992, Circ. Research 71) ascribed this behaviour to a dephophorylation of the channel. Now, we report that voltage steps re-activate the inactivated channels in the absence of Mg-ATP and/or α subunit of PKA. However, upon voltage dependent reactivation, the Cl^- channels display changes in gating mode which are characterized by a bursting behavior and a decrease of the mean open times. Upon addition of a phosphorylation cocktail on the cytoplasmic side the channel reactivates in its standard gating mode. Conversely a protein phosphatase completely inactivates the Cl^- channel. So, we postulate that the changes in gating mode were due to either a voltage sensitive or a rapid association / dissociation mechanism with a phosphorylated component. A putative candidate would be the phospholamban molecules.

Supported by an HSFC grant. ER is a FRSQ Scholar.

W-Pos370

PURIFICATION AND BIOCHEMICAL CHARACTERIZATION OF THE 26-KDA CALSEQUESTRIN BINDING PROTEIN FROM CANINE CARDIAC SARCOPLASMIC RETICULUM (SR) VESICLES. ((L.R. Jones, J.S. Kelley, and K.L. Sanborn)) Indiana University School of Medicine, Indianapolis, IN 46202

Using the nitrocellulose blotting method, we previously identified a 26-kDa protein in cardiac and skeletal muscle junctional SR vesicles that binds ^{125}I-calsequestrin (Mitchell *et al.* (1988) *J. Biol. Chem.* 263,1376-1381). In the work described here, we purified this major calsequestrin binding protein (CBP) from junctional SR vesicles to homogeneity and obtained the partial amino acid sequence. The CBP was not extracted from junctional SR vesicles by pH 11.4 treatment, but instead required 2% Triton X-100 and 0.5 M NaCl for solubilization, demonstrating that it is an integral membrane protein. Substantial purification of the protein was achieved by loading the Triton X-100 extract from canine cardiac SR vesicles onto cellulose phosphate and eluting the protein with 0.6 M NaCl. The 26-kDa protein that bound ^{125}I-calsequestrin in the peak fraction was then purified to homogeneity in one additional step by preparative SDS-PAGE. The purified CBP ran as a closely spaced doublet of Mr=26,000. Approximately 50 µg of protein were purified 265-fold from 100 mg of cardiac SR vesicles. 90 amino acid residues were sequenced from proteolytic fragments generated from the CBP. A canine cardiac cDNA library is being screened with several different reverse translated oligonucleotide probes complementary to these regions of protein sequence. Knowledge of the complete primary structure of the CBP should provide more information on its possible role in anchoring calsequestrin to the junctional face membrane at the site where calsequestrin apposes the ryanodine receptor.

W-Pos371

PROBING THE FUNCTIONAL SIGNIFICANCE OF THE N-TERMINAL HYDROPHOBIC POCKET OF CARDIAC TROPONIN C. ((Darrell G. Dotson, Wen Liu and John A.Putkey)) University of Texas Medical School, Houston, TX 77030.(Spon. by E. N. Spudich)

It has been proposed that Ca^{2+}-binding to cardiac troponin C (cTnC) causes the exposure of a hydrophobic "pocket" which is important for the Ca^{2+}-dependent regulation of muscle contraction. Studies of the hydrophobicity of calmodulin (CaM) and cTnC indicate that they both exhibit Ca^{2+}-dependent increases in hydrophobicity. However, unlike cTnC, CaM can only be dissociated from a hydrophobic interactions column in the absence of Ca^{2+}. In addition, CaM appears to interact with the hydrophobic fluorescent probe 9-AC in a Ca^{2+}-dependent manner, whereas cTnC does not. Moreover, hydrophobic drugs either in solution or covalently attached to CaM in the vicinity of the N-terminal hydrophobic pocket inhibit the ability of CaM to activate some of its target enzymes but the same drugs actually stimulate the regulation of muscle contraction by cTnC in that, they sensitize cardiac myofibrils to activation by Ca^{2+}. To evaluate the functional significance of the N-terminal hydrophobic pocket in cTnC, we have employed the strategy of positioning blocking groups near this domain using cysteine-specific covalent attachment probes. Preliminary studies indicate that the ability of cTnC to regulate skeletal myofibril ATPase activity is not inhibited by either the attachment of a biotin probe at Cys 84 of cTnC or the subsequent association of the biotinylated protein with avidin. We are currently assessing the changes in hydrophobicity induced by these modifications, as indicated by Ca^{2+}-dependent elution patterns using hydrophobic interactions chromatography and Ca^{2+}-induced fluorescence responses in the presence of hydrophobic drugs.

W-Pos372

EFFECT OF R56865 ON THE RATE OF RIGOR DEVELOPMENT DURING METABOLIC INHIBITION IN RAT CARDIAC TRABECULAE.

((Yingming Zhang, Wei Dong Gao, Henk E.D.J. ter Keurs)) University of Calgary, Calgary, AB, Canada. (Spon. by Henk E.D.J. ter Keurs)

The compound R56865 (R) is considered to be a novel Na^+ and Ca^{++} overload inhibitor without effect on L-type sarcolemmal Ca^{++} channels. To test whether R decreases ATP consumption during excitation-contraction coupling (ECC) during ischemia, we investigated the effect of R on rate of ATP depletion during metabolic inhibition. Trabeculae from rat right ventricle, mounted between a force transducer and motor arm, superfused with Krebs-Henseleit solution (KH) at 30°C, were first depleted of glycogen by exposure to CN, glucose-free KH (CN-KH). After full recovery, trabeculae were exposed to CN-KH at varied $[Ca^{++}]_o$, while load was kept zero. The inverse of the time to maximal rigor force (1/TFumax) was used to indicate the overall rate of ATP depletion. R (0.1 μM) decreased twitch force by 20-30%, but did neither affect the duration of contraction nor the fraction of Ca^{++} that recirculates via the SR from beat to beat. R reduced 1/TFumax at all $[Ca^{++}]_o$, but had no effect on ATP depletion in unstimulated trabeculae. These results are consistent with the hypothesis that R decreases ATP demand of ECC due to decreased Ca^{++} cycling for each contraction probably by an increase of the threshold for Ca^{++} induced Ca^{++} release from the SR.

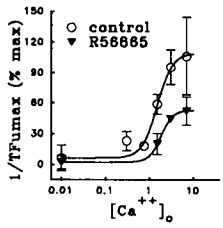

W-Pos373

CARDIAC MUSCLE REGULATION BY TROPONIN I PHOSPHORYLATION.

((R. Zhang, J. Zhao and J.D. Potter)) Department of Molecular & Cellular Pharmacology, University of Miami School of Medicine, Miami, Fl 33101.

Compared to skeletal muscle Troponin I, cardiac TnI (CTnI) contains an additional 32-33 NH_2-terminal amino acids as well as two serines (SER22 AND SER23) which can be phosphorylated by protein kinase A (PKA) *in vitro*, or as the result of β-adrenergic stimulation of the heart *in vivo*. It is thought that since this phosphorylation lowers the Ca^{2+} affinity of CTnC in the CTn complex *in vitro*, that this may contribute to the faster relaxation seen with catecholamine stimulation. To study this we have expressed mouse CTnI as well as several mutants of it in *E. Coli*. Using porcine cardiac muscle fibers, we have found that when they are phosphorylated by PKA the pCa_{50} decreases by ~ 0.3 pCa units, indicating a decrease in Ca^{2+}-sensitivity. Diazo-2, a photolabile Ca^{2+}-chelator was used to study the kinetics of muscle relaxation. The $t_{1/2}$ for force relaxation dropped two fold when comparing PKA treated to control fibers, suggesting that the decrease in Ca^{2+}-sensitivity seen with PKA treatment is probably due to a faster dissociation of Ca^{2+} from CTnC which in turn leads to the observed faster rate of relaxation. Treatment of cardiac fibers with orthovanadate (Strauss, JD, *et al.*, FEBS 310:229-234, 1992) removes CTnI and CTnC, and makes them insenitive to Ca^{2+}. When force was restored to these fibers with a complex of CTnC and a CTnI mutant where both SER22 and 23 were converted to ALA, the fibers no longer responded to PKA treatment, indicating that CTnI phosphorylation is responsible for the change in the observed Ca^{2+}-sensitivity. Further studies indicated that both SER22 and SER23 are required for the phosphorylation induced shift in Ca^{2+}-sensitivity. (Supported by NIH HL42325, AR37701 and AR40727)

W-Pos374

EFFECTS OF THIN FILAMENT REGULATION ON THE RATE OF TENSION DEVELOPMENT FOLLOWING PHOTOLYTIC RELEASE OF ATP IN SKINNED CARDIAC MUSCLE

((A. Arner, J.D. Strauss*, C. Svensson, J.C. Rüegg**)) Dept Physiology and Biophysics, Lund University, Sweden, *Dept Molecular Physiology and Biological Physics, University of Virginia, VA and **Dept Physiology II, Heidelberg, Germany. (Spon by A. Ehrenberg)

The rate of tension development following release of ATP from caged-ATP at different levels of activation was studied in skinned cardiac fibres from swine. A low-force rigor state was obtained by using butanedione monoxime (BDM) during the induction of rigor. BDM was washed out and following release of ATP in the presence of Ca^{2+} (pCa 4.5), the muscles contracted with a half-time for tension development ($t_{1/2}$) of ~0.4s. The rate of tension development was slower at low $[Ca^{2+}]$ suggesting a modulation of kinetics of force generation by $[Ca^{2+}]$. After treatment with vanadate to extract troponins I and C (Strauss et al., 1992; FEBS Lett 3, 229), the rate of contraction upon release of ATP was slower ($t_{1/2}$ ~0.7s) than prior to extraction and was independent of $[Ca^{2+}]$. The positive inotropic agent EMD 53998 increased rates of contraction, suggesting that EMD increases force by increasing the cross-bridge attachment rates. The results are consistent with the concept that cardiac contraction may be partially regulated by directly increasing attachment rate rather than by relieving a steric inhibition of attachment imposed by troponin/tropomyosin.

W-Pos375

Interaction of Genetically Engineered Human Cardiac Troponin C and Troponin I.

Ronglih Liao and Judith K. Gwathmey. Cardiovascular Disease & Muscle Research Laboratories, Harvard Medical School, Boston, MA 02115

In this study to obtain the desired amount of troponin C (TnC) and troponin I (TnI) from human myocardium we utilized contemporary recombinant DNA technology to synthesize the two proteins. The purified active structures of recombinant TnC and TnI were characterized and compared with their native counterparts using chemically skinned fibers. Addition of recombinant TnC or its complex with recombinant TnI to the TnC-depleted or TnC•TnI-depleted skinned fibers resulted in a recovery of tension development and Ca^{2+} sensitivity. Acrylamide quenching of the tyrosine fluorescence indicates that quenching profiles of recombinant human cardiac TnC was identical to that of bovine cardiac TnC whose amino acid sequence is identical to its human counterpart. The tyrosine residues in the recombinant cardiac TnC were sensitive to Ca^{2+}-induced conformational change. Using fluorescent derivative of recombinant TnC, the affinity of TnC for TnI reduced as the ionic strength was increased by increasing salt concentrations in the reaction mixture. These results suggest that the dominant forces stabilizing the complex formation between human cardiac TnC and TnI have a considerable ionic character, supporting the hypothesis that the charged side chains in the two proteins may have functional significance in the stabilization of the complex formation.

W-Pos376

Ca^{2+} HOMEOSTASIS IN CULTURED RAT NEONATAL MYOCYTES WITH α-ADRENERGIC STIMULATION-INDUCED HYPERTROPHY.

((Beth A. Bailey, Colleen A. Hefner, and Steven R. Houser.)) Dept. of Physiology, Temple University School of Medicine, Philadelphia, PA 19140.

Exposure of cultured rat neonatal ventricular myocytes (NVM) to α-adrenergic agonists such as phenylephrine (PHY) induces hypertrophy. The purpose of this study was to examine intracellular Ca^{2+} homeostasis in control and hypertrophied NVM. Hypertrophy was induced by exposure to 24 and 48 hours of 20μM PHY or its vehicle (CON). Intracellular Ca^{2+} was measured using the Ca^{2+} sensitive fluorescent dye, indo-1. Cells were perfused with normal Tyrode solution containing 2mM Ca^{2+} at room temp. Indo-1 transients were measured at 0.5, 1, 1.5, and 2 Hz. Indo-1 transients were significantly prolonged at 0.5, 1, and 1.5 Hz in cells treated with PHY (vs CON) for 24 hours (.82±.10 vs .54±.06, .53±.02 vs .41±.04, and .40±.02 vs .32±.02, respectively), and in cells treated with PHY (vs CON) for 48 hours (.83±.05 vs .56±.02, .50±.04 vs .41±.02, and .41±.02 vs .33±.02, respectively). These data show that NVM with hypertrophy induced by PHY have changes in Ca^{2+} transients like those seen in in vivo models of hypertrophy suggesting that similar signaling pathways are involved.

W-Pos377

CHANGES IN SARCOPLASMIC RETICULUM FUNCTION IN SINGLE CARDIOMYOCYTES FROM FAILING HUMAN VENTRICLE

((K. Davia, C. H. Davies and S. E. Harding)) Dept Cardiac Medicine, National Heart and Lung Institute, Dovehouse St., London SW3 6LY, UK.

We have shown that single cardiomyocytes enzymatically isolated from failing human ventricle relax more slowly than those from normal hearts. The time-to-half relaxation (R50) for myocytes contracting in Krebs-Henseleit solution at 32°C and field stimulated at 0.2Hz was increased from 0.16 ± 0.01s in cells from 8 non-failing hearts (mean ± sem) to 0.25 ± 0.02s in cells from 34 patients with moderate or end-stage heart failure ($p<0.001$). To investigate the function of the sarcoplasmic reticulum (SR), a subset of these cell was allowed increasing periods of rest. The size of the first post-rest contraction as a percentage of the preceding steady state (B1) is an indication of the amount of Ca^{2+} remaining in the SR. The rate of decay of B1 was faster in cells from normal than from failing hearts: after 3 min rest B1 was 19 ± 7% of steady state in 4 normal myocytes compared with 74 ± 14% in 15 myocytes from failing ventricle ($P<0.01$). This could mean either that the SR contributes less to Ca^{2+} removal in the failing heart or that SR Ca^{2+} loss during rest is slower. Comparing post-rest decay (PRD) with R50, it was found that myocytes which contracted more slowly also had a less pronounced PRD. The correlation between B1 and R50 was significant for both failing plus non-failing ($r=0.66$, $n=17$, $P<0.001$), or within the failing group alone ($r=0.62$, $n=13$, $P<0.05$). The actiologies in the failing group in this case included mitral and aortic stenosis as well as end-stage failure due to ischaemic or congenital heart disease. The results are consistent with a reduced contribution of the SR to Ca^{2+} removal leading to a decreased rate of relaxation in the failing human heart.

W-Pos378

FORCE FREQUENCY RELATIONSHIP IN NORMAL AND FAILING SHHF/MCC-*CP* RAT HEARTS. ((Prakash Narayan, Sylvia A. McCune, and Ruth A. Altschuld)) Department of Medical Biochemistry, The Ohio State University, Columbus Ohio 43210-1218

Effects of pacing frequency on left ventricular developed pressure (LVDP) were examined in Langendorff perfused normal rat hearts and in failing hearts from SHHF/Mcc-*cp* rats. (SHHF-Mcc/*cp* rats are a genetic model of dilated cardiomyopathy caused by hypertension and obesity). Atria were removed and the AV nodes crushed to decrease intrinsic heart rates. Ventricles were perfused with Krebs-Henseleit buffer (37°C, pH 7.4) containing 10 mM pyruvate and 11 mM glucose. In normal hearts, the response to a switch in pacing frequency from 3 to 5 Hz or 5 to 7 Hz was comparable to that described by P.D. Henry in 1975 (Am. J. Phys. 228:360-364). First beat LVDP was greatly reduced. This was followed by a steady increase in LVDP that plateaued 30% above the previous steady state. LVDP then declined slowly reaching a new steady state where LVDP was lower but rate pressure product was comparable to that in the previous steady state. Failing hearts did not exhibit this initial positive staircase but instead exhibited mechanical alternans when pacing frequency was suddenly increased. Left ventricular end diastolic pressures also increased substantially. These results confirm that normal rat myocardium provided with adequate oxygen and metabolic substrate exhibits a positive force frequency relationship between 3 and 7 Hz. This relationship is altered by end stage failure in the SHHF/Mcc-*cp* rat heart. *(Supported by HL48835.)*

W-Pos379

ATP AND ADENOSINE EFFECTS ON ADULT GUINEA-PIG VENTRICULAR MYOCYTES COCULTURED WITH CARDIAC NEURONS. ((M. Horackova, M.H. Huang, J.A. Armour)) Dept. of Physiology & Biophysics, Faculty of Medicine, Dalhousie University, Halifax, N.S. Canada.

To determine the capacity of ATP and adenosine to modify cardiomyocytes directly and/or indirectly via peripheral autonomic neurons, we studied their effects on long-term cultures of adult guinea-pig ventricular myocytes and their cocultures with extracardiac (stellate ganglion) or intrinsic cardiac neurons. Ventricular myocytes and cardiac neurons were enzymatically dissociated and plated together or alone. The beating frequency of ventricular myocytes cocultured with stellate ganglion neurons increased by 140% following superfusion with 10^{-5} M ATP. This effect was not modified significantly by $4x10^{-7}$ M TTX, or β-adrenoceptor blockade (10^{-5} M timolol), but were eliminated following application of the P_2 antagonist suramin (10^{-5} M). Basal spontaneous contractile rate was reduced by 86% in presence of suramin, indicating the existence of tonically active purinergic synaptic mechanisms in stellate-myocyte cocultures. Suramin did not affect significantly noninnervated myocyte cultures. ATP increased myocyte contractile rate in intrinsic cardiac neuron-myocyte cocultures by 40%, but when β-adrenergic receptors and TTX-sensitive neural responses were blocked, ATP induced similar augmentation in both types of cocultures (>100%). In contrast, in noninnervated myocyte cultures ATP induced much smaller effects (26%), which lasted only a few minutes. Adenosine (10^{-4} M) attenuated the beating frequency of myocytes in both types of cocultures, while not significantly affecting noninnervated myocyte cultures. Thus, the experimental model used in this study permitted the demonstration that extrinsic and intrinsic cardiac neurons activated by ATP via P_2 receptors, can greatly enhance cardiac myocyte contractile rate. On the other hand, since adenosine reduced contractile rate in both types of cocultures while not affecting noninnervated myocytes, it is concluded that some of these neurons possess P_1 receptors. (Supported by MRC of Canada grant T-4128).

W-Pos380

ANOXIA-INDUCED IONIC CURRENTS IN ISOLATED GUINEA PIG HEART CELLS RECONSTRUCT K^+ ACCUMULATION KINETICS DURING ISCHAEMIA

((S. Thierfelder, B. Doepner, C. Gebhardt, H. Hirche and K. Benndorf*)) Zentrum für Physiologie und Pathophysiologie, Universität zu Köln, 50924 Köln, Germany. *Heisenberg-fellow of the Deutsche Forschungsgemeinschaft.

Early myocardial ischaemia is accompanied by the extracellular accumulation of K^+ ions with a rapid increase during the first five minutes, a slow increase during the following 20 minutes and an intermediate speed thereafter. To investigate the mechanisms underlying the time course of ischaemia-induced K^+ accumulation, transmembrane ionic currents were measured during anoxia in enzymatically isolated guinea pig cells with a patch clamp technique in the whole cell and cell-attached patch configuration. Anoxia (PO_2 <$3.8x10^{-8}$ mm Hg) induced in guinea pig heart cells a large time independent K^+ current through K_{ATP} channels of 24.5±5.0 nA (mean±SEM). This current disappeared after reoxygenation within ten seconds. During maintained anoxia, the K_{ATP} channel current also disappeared, but slower (time constant 34±6 s). Either during or at the latest several minutes after the end of the transient K_{ATP} channel current, a nonspecific current developed gradually which was insensitive to reoxygenation. In cell-attached patches, maintained anoxia caused opening and closing of K_{ATP} channels. Either during the phase of channel closing or thereafter, noise-like current events with non-specific conductance appeared in a gradual manner. The integrated mean time course of the total current at +40 mV, calculated from the whole cell experiments in guinea pig cells, showed a similar time course to that in the respective first 20 min of K^+ accumulation in the ischaemic myocardium. Therefore, the underlying mechanisms in the ischaemic K^+ accumulation are most likely the initial transient opening of K_{ATP} channels followed/accompanied by a nonspecific current through the perturbed membrane.

W-Pos381

ARE STRETCH ACTIVATED CHANNELS INVOLVED IN TRIGGERED PROPAGATED CONTRACTIONS IN RAT CARDIAC TRABECULAE ?

((Yingming Zhang, Henk E.D.J. ter Keurs)) University of Calgary, Calgary, AB, Canada.

Previous studies have shown that triggered propagated contractions (TPCs) in rat cardiac trabeculae are triggered in damaged ends of trabeculae by a preceding twitch; the local contraction propagates along trabeculae with a constant velocity (Vp). We tested: 1) whether stretch of damaged regions by the twitch initiates TPCs; 2) whether stretch of tissue adjacent to a local contraction during propagation of TPCs increases Vp. Gadolinium(Gd) has been shown to block stretch activated channels (SAC). We studied the effects of Gd (100 nM~100 μM) on twitch force (Ft), TPCs force (Fpc), time to peak Fpc (Latency) and Vp. TPCs were elicited by trains of 15 stimuli (2Hz, 15-s intervals) at 20°C; using HEPES solution, $[Ca^{++}]_o$ of 0.5~0.75 mM. Laser diffraction techniques were used to measure sarcomere shortening at two sites of trabeculae; Ft was measured with a silicon strain gauge. Gd (1~30 μM) decreased Ft, Fpc, Vp and increased latency in a concentration-dependent manner. EC_{50} was 7.05±1.17 μM (mean±sem) for Ft, Fpc, latency, or Vp. High concentrations of Gd (>30 μM) almost abolished Ft and Fpc. The decrease of Vp and increase of latency, for the same decrease in Ft, were not significantly larger than those by decreasing $[Ca^{++}]_o$, indicating that Gd did not show an additional effect on TPCs above decreasing intracellular $[Ca^{++}]$. These observations suggest that it is not necessary to assume that SAC are involved in initiation or propagation of TPCs.

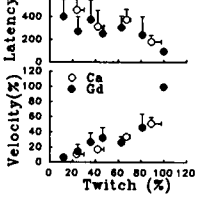

W-Pos382

POSITIVE INOTROPIC EFFECT OF 5-HYDROXYTRYPTAMINE AND SELECTIVE SEROTONERGIC AGONISTS ON ADULT RAT VENTRICULAR MYOCYTES ((E. Béjar, M. Majidy, G. Tatsukawa and P. Paolini)) Rees-Stealy Research Foundation and Department of Biology, San Diego State University, San Diego, CA 92182.

5-Hydroxytryptamine (5-HT) exhibits positive chronotropic and inotropic effects on the mammalian heart. These effects are related to presence of specific 5-HT receptor types (including 5-HT_1, 5-HT_2 and 5-HT_4) and depend on the animal species, age and region of myocardium. An unidentified 5-HT receptor is responsible for chronotropic effect on neonatal rat ventricular myocytes, while rat atrial cells are refractory to stimulation. Our results indicate that 5-HT also elicits a positive inotropic effect from adult ventricular myocytes. We have evaluated the effects of 5-HT and serotonergic agonists and are now attempting to characterize the responsible 5-HT receptor and its transduction mechanism. Cumulative concentration-response curves to 5-HT, nonselective and selective 5-HT_1, 5-HT_2, 5-HT_3 and 5-HT_4 serotonergic agonists were carried out on electrically paced (0.2 Hz, 5 msec, supramaximal stimulus) adult rat calcium-tolerant ventricular myocytes incubated in Krebs-Henseleit solution containing 50 mM of the MAOI pargyline. Myocytes were isolated as reported by Fischer *et al.* (*Life Sci.* 49: 1679, 1991). Serotonergic agonist effects on contractility were monitored by video image analysis: contracting cell images were digitized and records containing cell displacement coordinates were analyzed to yield values for initial cell length, shortening velocity, relaxation velocity, time to onset of contraction and time to maximum shortening. Data obtained from shortening records allowed calculation of affinity constants (pD_2) and intrinsic activity (I.A.) of serotonergics. The selective 5-HT antagonists methysergide, ketanserin, MDL 72222, among others, were used to block 5-HT myocyte responses. (Supported by grants from the Rees-Stealy and the California Metabolic Research Foundations.)

W-Pos383

INOSITOL (1,4,5) TRISPHOSPHATE INCREASES IN HYPOXIC VENTRICULAR CELLS ((1,2J.R. Lopez, 3B. Rojas)) 1Centro de Biofisica, IVIC Caracas, Venezuela. 2Department of Anesthesia, Brigham and Women Hospital, Boston, MA. 3Departamento de Medicina Interna, Hospital, Militar, Caracas, Venezuela.

In hearts as well as other tissues hypoxia has been associated with increased $[Ca^{2+}]_i$. Inositol 1,4,5 (InsP3) has been reported as a mediator in releasing Ca^{2+} from the sarcoplasmic reticulum in cardiac cells (Nosek et al. 1986). Sprague-Dawley rats were killed by decapitation and the hearts were removed, rinsed clear of blood, and then perfused via the dorsal aorta according to the methods of Langendorf. Hypoxia was induced by gassing the perfusion solutions with 95% N_2 and 5% CO_2 instead of 95% O_2 and 5% CO_2. Inositol phospholipid turnover was determined according with the method described by Woodcok et al. (1987). In normoxic ventricular cell the $[InsP3]_i$ was 62±8 cpm (n=8). However, after a short interval of hypoxia (5 minutes) the $[InsP3]_i$ was 102±12 (n=6). Increments in $[InsP3]_i$ were time dependent 118±10 (n=6) after 10 minutes, 129±16 (n=5) after 15 minutes, and 152±13 (n=6) after 20 minutes of hypoxia. Reoxygenation of the heart cells reverted the $[InsP3]_i$ to control levels when the hypoxic episode was not greater than 15 minutes. We conclude that hypoxia which represents an important element of myocardial ischemia is associated with an increase in $[InsP3]_i$. This increment in $[InsP3]_i$ might be in part related to increased $[Ca^{2+}]_i$ since calcium channel blockers do not completely block the changes in $[Ca^{2+}]_i$ during hypoxia. (Partially supported by Laboratorios Elmor de Venezuela.)

W-Pos384

INVOLVEMENT OF PHOSPHOINOSITIDE HYDROLYSIS IN THE CARBACHOL-INDUCED POSITIVE CHRONOTROPIC EFFECT IN CULTURED NEONATAL RAT VENTRICULAR MYOCYTES (NRVMs). ((H.M. Colecraft and S-S. Sheu)). Department of Pharmacology, University of Rochester, Rochester, NY 14642. (Sponsored by Jean M. Bidlack, Ph.D.)

We have previously reported that high concentrations (EC_{50} ≈ 40μM) of carbachol (CCh) produce an atropine-sensitive positive chronotropic effect in spontaneously beating cultured NRVMs pretreated with 1μg/ml pertussis toxin [Colecraft et.al.(1993) Biophys. J. 2(2):A209]. Speculation abounds that phospholipase C-catalyzed phosphoinositide (PI) hydrolysis is directly involved in the muscarinic receptor-mediated stimulation of the heartbeat. However, no causal relationship has been established nor has there been a determination of the relative contributions of IP_3 and PKC to the observed response. In this work we have investigated the involvement of PI hydrolysis in the CCh-induced positive chronotropic response in cultured NRVMs. Heart rate was monitored by measuring the frequency of fura 2-reported Ca^{2+} transients in spontaneously beating NRVMs. In pertussis toxin-treated cells, 300μM CCh resulted in a marked increase in beating rate. Pretreatment of the cells with 500μM neomycin, which inhibits phospholipase C-dependent events, completely prevented the CCh-induced increase in heart rate. The response to CCh was recovered upon washout of neomycin. Addition of 100nM TPA (phorbol 12-myristate 13-acetate), a PKC activator, also resulted in an increase in the heart rate. Down regulation of PKC induced by a prolonged (24-48hrs) treatment with 1μM TPA inhibited the TPA-induced increase in heart rate. However, this treatment appeared to have no effect on the CCh-induced increase in heart rate. These results suggest that while a product of PI turnover may be responsible for the CCh-induced positive chronotropic effect, PKC is not involved in mediating the response.

W-Pos385

INACTIVATION OF NOVEL CARDIAC INOTROPES BY FLASH PHOTOLYSIS IN ISOLATED RAT VENTRICULAR TRABECULAE. ((John A. Lee*, Sue Palmer & Jonathan C. Kentish)) Dept. Pharmacology, U.M.D.S., St. Thomas' Hospital, London SE1 7EH; *Dept. Pathology, The Medical School, University of Sheffield, Sheffield S10 2RX, U.K.

EMD 53998 was initially identified as a "Ca sensitising" drug in intact muscle [*Circ. Res.* (1991) **69**, 927], but it was later found that this activity resided mainly in one optical isomer (EMD 57033), while the other isomer (EMD 57439) was chiefly a PDE inhibitor [e.g. *Circ. Res.* (1993) **73**, 61-70]. We have found that these substances can be rapidly inactivated by flash photolysis in intact cardiac muscle. Addition of 57033 (5-20 μM) to isolated rat ventricular trabeculae increased twitch and diastolic force and prolonged relaxation. A flash of light (100 mJ, 310-400 nm) given during the twitch caused immediate acceleration of relaxation and a decrease of twitch and diastolic tension. A similar rapid decrease in Ca-activated tension was seen in Triton-skinned muscles. In intact muscle, the other isomer, 57439 (1-10 μM), reduced twitch tension with little effect on the twitch timecourse or diastolic tension. A flash reduced the inhibition of tension by 57439, i.e. tension increased towards control. The actions of the racemic mixture (53998, 10 μM), and the flash effects, were similar to those for 57033. These results indicate rapid breakdown of these compounds by flash photolysis and support a myofilament-based mechanism of action for 57033. Flash inactivation may help elucidate the mode of action of these compounds.

W-Pos386

Calcium Responsiveness of Myocytes Isolated from Turkey Hearts with Furazolidone-Induced Dilated Cardiomyopathy.
Chandana Saha & Judith K. Gwathmey. Cardiovascular Disease & Muscle Research Laboratories, Harvard Medical School, Boston, MA 02115

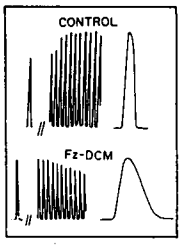

We investigated the calcium transient of cardiac myocytes using a fluorescent dye, fura-2. Cardiac myocytes were prepared from turkey poults with dilated cardiomyopathy (Fz-DCM) and from normal control turkey hearts (CON). Calcium transients obtained from fluorescent dye-loaded myocytes showed similar time duration to contraction. Compared to the controls, a markedly prolonged calcium transient and duration of contraction were observed in the myocytes from Fz-DCM hearts. Increasing contraction rate in Fz-DCM resulted in a blunted or negative force-interval relationship. Myocytes from CON demonstrated a normal positive force-interval relationship. It is known that intracellular Ca^{2+} release and uptake are closely associated with contraction and relaxation in cardiac myocytes. Thus, it is likely that a slow relaxation in a myocyte is associated with prolonged Ca^{2+} transients in the myocytes from Fz-DCM. These results suggest that abnormality in the molecular mechanisms of Ca^{2+} kinetics may lead to diastolic and systolic dysfunction in the Fz-DCM myocytes.

W-Pos387

SENSITIZING AGENT EMD 53 998 CAUSES LEFTWARD SHIFT OF STEADY-STATE TENSION-$[Ca^{2+}]_i$ RELATIONSHIP IN INTACT TWITCHING CARDIAC MUSCLE *((L.E. Dobrunz, P.H. Backx, and D.T. Yue)), Johns Hopkins School of Medicine, Baltimore MD 21205.*

EMD 53 998, a thiadiazinone which has positive inotropic effects, has been shown to produce a leftward shift of the tension-pCa relationship in skinned cardiac muscle. The proposed mechanism for this is an increase in myofilament calcium sensitivity. In order to test this mechanism in membrane intact cardiac muscle, we used our strategy for deriving steady-state $[Ca^{2+}]_i$-tension relationship in twitching muscle (Biophys J 64:A119, 1993). In rat trabeculae iontophoretically loaded with Fura-2, 50 μM cyclopiazoic acid and 1 μM ryanodine were added to eliminate phasic Ca^{2+} release from the SR. This allowed measurements of tension and $[Ca^{2+}]_i$ at high $[Ca^{2+}]_o$ (up to 6 mM) and greatly slowed twitch time course. Superposition of tension-$[Ca^{2+}]_i$ curves at different $[Ca^{2+}]_o$ revealed that during late relaxation tension and $[Ca^{2+}]_i$ were defined by a unique relationship independent of contraction history, indicating they were in steady state. We tested the effects of 2 μM EMD 53 998, which increased twitch tension with no change in $[Ca^{2+}]_i$ (A). It also produced a consistent leftward shift of the tension-$[Ca^{2+}]_i$ curve (B), decreasing the $[Ca^{2+}]_i$ required for half-maximal activation to 67% of control (as assessed by Hill equation fits, n=3). This was accompanied by a 5% increase in the maximal developed force. This provides direct evidence that EMD 53 998 increases myofilament $[Ca^{2+}]_i$ sensitivity in intact twitching cardiac muscle.

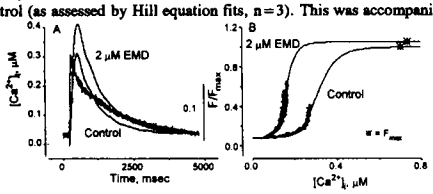

W-Pos388

REPERFUSION-INDUCED POSITIVE INOTROPY IS A PROPERTY OF A RYANODINE AND Ni^+-SENSITIVE Ca^{2+} RELEASE MECHANISM AND IS UNAFFECTED BY Ca^{2+} CURRENT BLOCKADE. ((Jonathan M. Cordeiro, Susan E. Howlett, Gregory R. Ferrier)) Dept. of Pharmacology, Dalhousie University, Halifax, Nova Scotia, Canada B3H 4H7.

To determine whether L-current (I_{Ca}) plays a role in potentiation of contraction during reperfusion, membrane currents and cell shortening were measured in a model of simulated ischemia and reperfusion with discontinuous single electrode voltage clamp and a video edge detector. Guinea pig myocytes were equilibrated in Tyrode's solution, exposed to simulated ischemia (hypoxia, acidosis, lactate, hyperkalemia, zero glucose) for 20 min, and then reperfused with oxygenated Tyrode's solution. Steps to -40mV from a potential of -55mV (to inactivate I_{Na}) initiated a ryanodine and Ni^+-sensitive contraction; an additional step to 0mV activated I_{Ca} (-0.93±0.12 nA) and an additional contraction. During ischemia, all contractions were abolished. Nifedipine (2μM) abolished I_{Ca} and contraction accompanying I_{Ca} during control and reperfusion. However, contractions at -40mV were insensitive to nifedipine. During early reperfusion (2-3 min), contractions observed at -40mV reappeared and increased beyond control even in the presence of nifedipine. These contractions gradually declined to control values over the next 30 min. Thus, rebound inotropy is due to a ryanodine and Ni^+-sensitive release mechanism which is independent of I_{Ca}.

W-Pos389

VARIANCE ANALYSIS OF CLONED CALCIUM CHANNELS IN GIANT MACRO PATCHES OF *XENOPUS* OOCYTES. ((P. Baldelli, A. Neely, T. Schneider, X. Wei, L. Birnbaumer and E. Stefani)). Dep. of Molec. Physiol. & Biophys. Baylor Col. Med. Houston, TX 77030.

The probability of being open (Po) for Ca^{2+} channels is below the level in which reasonable estimates can be obtained from "single" channel recording. Here we apply variance analysis of ionic-current recorded on giant macro patches (20-30 μm) of *Xenopus* oocytes co-expressing the α_1 and β subunit of the Ca^{2+} channel. We compare α_{1E} (Schneider et al, this meeting) and a deletion mutant of α_{1C} (ΔN60 Wei *et al.*, this meeting). In the on-cell configuration, using 79 mM Ba^{2+}, peak current can reach up to 6 nA for α_{1E} or 1 nA for ΔN60 during +20 mV depolarizing pulse. The number of channels active (N) in a patch can be obtained from variance analysis using $\sigma^2 = iI - I^2/N$ in which i is the single channel current and I is the mean current and σ^2 the variance. For a meaningful estimate of N the probability of the channel to be open (Po = I/iN) should be at least 0.5 while maintaining a large driving force for i. This was partially achieved at 30 °C, by depolarizing the patch to +150 mV from a holding potential of -60 mV and variance analysis was done on tail currents at -30 mV. In this condition, Po's of up to 0.7 were measured in $\alpha_{1E}\beta_2$. In contrast, for ΔN60 β_2, even in the presence of two Ca^{2+} channel agonist ((-)BK 8644 6 μM and FPL 5 μM), the mean current versus variance plot did no reach a maximum suggesting Po's < 0.5. However, gating currents were prominent in $\Delta N60\alpha_{1C}\beta_2$ even with 0.25 nA peak currents at +20 mV. This discrepancy suggests a large difference in maximum Po between α_{1E} and α_{1C} calcium channels and is consistent with the diferences in coupling between charge movement and pore opening (Olcese et al. this meeting). (Supported by an NRSA fellowship to A.N. and grants HL37044 to L.B. and AR38970 to E.S. from NIH).

W-Pos390

EXPRESSION AND PHOSPHORYLATION OF THE FULL LENGTH α_1 SUBUNIT OF SKELETAL MUSCLE L-TYPE Ca CHANNELS

((X-L Zhao, D.D. Sun, and M.M. Hosey)) Department of Pharmacology, Northwestern University, Med. School, Chicago, IL 60611

Voltage-dependent L-type Ca channels play an important role in excitation-contraction and excitation-secretion coupling. Previous studies showed that the L-type Ca channels expressed in skeletal muscle are regulated by phosphorylation by protein kinase A (PKA) and protein kinase C (PKC). In the present study, a baculovirus directing the expression of the α_1 subunit of skeletal muscle L-type Ca channels (CaCh1) was used to infect *Spodoptera frugiperda* (Sf9) insect cells. A full-length α_1 subunit was expressed in the insect cells and detected by both immunoblotting and immunofluorescence microscopy using three anti-peptide polyclonal antibodies against different regions of the α_1 subunit. Phosphorylation studies showed that PKA phosphorylated the expressed full-length α_1 subunit to a higher stoichiometry than the truncated α_1 subunit present in the native T-tubule membranes. Although PKC phosphorylated the truncated α_1 subunit in the native T-tubule membranes to a similar extent as PKA, there was little or no phosphorylation of the expressed full-length α_1 subunit with PKC. The results suggest that the conformation of the α_1 subunit plays a critical role in determining its availability as a substrate for PKC.

W-Pos391

ALTERNATIVE SPLICING OF mRNA FOR THE SKELETAL CALCIUM CHANNEL: A DIRECT TEST. ((N. Chaudhari)) Dept. of Physiology, Colorado State Univ., Fort Collins, CO 80523. (Spon.S.C.Kinnamon)

The extracellular loop linking the S3 and S4 transmembrane helices of Repeat I has been shown to play a critical role in determining activation kinetics of L-type Ca^{++} channels (Nakai et al., 1994). In a cDNA clone derived from fetal skeletal muscle, the S3-S4 linker of Repeat IV contained a 57 bp (19aa) deletion as compared to the adult form. Using RNase protection assays, I have determined that mRNA from fetal skeletal muscle contains mostly the shorter loop. As muscle matures, the relative fraction of the "short loop" form decreases until it represents 5% or less in the adult. It is possible that alternative splicing at this site may be responsible for the faster activation kinetics of L-type Ca^{++} current as skeletal muscle matures.

RNase protection has also been used directly to test whether the skeletal Ca^{++} channel transcript exists in a "two-domain" configuration as earlier postulated (Malouf et al., 1992). This postulate was based on PCR. PCR will amplify RNAs that are present even in trace quantities. The RNase protection assay is a direct test for the presence and relative concentration of variant forms of mRNAs. Using RNase protection, I find no evidence for a "two-domain" mRNA in muscle from fetal, neonatal or adult mice. The normal "four-domain" mRNA is readily detected.
Supported by RO1 GM42652

W-Pos392

PK AND SELECTIVITY OF ACIDIC SIDE CHAINS IN THE VOLTAGE GATED CALCIUM AND SODIUM CHANNELS. ((S. Bogusz and D. Busath)) Box G, Brown U., Providence RI 02912

A simple model of the selectivity sites of the voltage-gated Ca^{++} and Na^+ channels based on the proposed beta-barrel model of the K^+ channels (Bogusz *et al.*, Prot. Eng. 4:285, 1992) was computer generated. These models consist of an 8 stranded anti-parallel beta barrel with a ring of charged residues in the center: 4 Glu residues for the Ca^{++} channel and Asp, Glu, Lys, and Ala in the Na^+ channel model. These residues have been shown to control selectivity (Heinemann *et al.*, Nature 356:441) and we attempt to calculate selectivity properties to test the validity of the beta-barrel and charged ring structural models. Calculation of the selectivity of the sites to different cations first required estimation of the protonization state of the sites. In initial calculations of the pK shift the local electric field at each oxygen and the expected proton concentration was calculated for 30 conformations of the ion, waters, and side chains of interest (in the charged state) for each of the three channel types and for each of several ion occupancy conditions. The average carboxylate pK shift was +2.2 for Na^+ and -0.7 for Ca^{++} in the Ca^{++} channel. These conformations also give the expected selectivity order for the minimized average potential energies - the Ca^{++} channel binds Ca^{++} over Na^+ while the Na^+ channel binds Na^+ over Ca^{++}. Computations are currently underway using perturbation dynamics to calculate the difference in the free energy of binding of the Na^+ and Ca^{++} ions and the free energy of protonization to estimate the pK's of the sites.

W-Pos393

CHARACTERISATION AND DIFFERENTIAL PHOSPHORYLATION OF TWO SIZE FORMS OF THE CARDIAC L-TYPE CALCIUM CHANNEL ALPHA 1 SUBUNIT.

((Karen S. De Jongh, Anita A. Colvin, Brian M. Murphy, Masami Takahashi* and William A. Catterall)) Department of Pharmacology, SJ-30, University of Washington, Seattle, WA, 98195 and *Mitsubishi Kasei Institute of Life Sciences, Machida, Tokyo, 194, Japan.

The dihydropyridine-sensitive or L-type calcium channel mediates entry of calcium into cells in response to membrane depolarisation. It is modulated by cAMP-dependent phosphorylation events and the calcium entering the cell initiates cardiac contraction. The channel is a multi-subunit complex and the largest subunit, termed α1, forms the receptor for dihydropyridine binding. Two size forms of the calcium channel α1 subunit have been identified in cardiac microsomes using an antibody against a fusion protein corresponding to the C-terminal 550 residues of this subunit (Yoshida et al, 1992, FEBS Lett., 309:343-349). Only the longer of these forms was phosphorylated by cAMP-dependent protein kinase(cA-PK). In the present study we have used anti-peptide antibodies to demonstrate that the smaller of the two α1 subunit forms is truncated at its C-terminus. Only the full-length form containing an intact C-terminus was phosphorylated by cA-PK. Antibodies recognising both forms are able to immunoprecipitate specifically bound PN200-110. The C-terminal sites at which the full-length α1 subunit is phosphorylated by cA-PK have been identified by peptide mapping and protein microsequencing. Since cardiac contraction is regulated by phosphorylation of the L-type calcium channel, the full-length form of the α1 subunit may play a pivotal role in the stimulation of calcium flux into the cell and could be critical in controlling the beat rate and contractility of the heart in response to cAMP-mediated events.

W-Pos394

EXPRESSION OF SUBUNITS OF AN L-TYPE VOLTAGE DEPENDENT CALCIUM CHANNEL IN Sf9 INSECT CELLS.

((T. S. Puri[1], X.-L. Zhao[1], M. B. Ladner[2] and M. M. Hosey[1])) [1]Department of Pharmacology, Northwestern University Medical School, Chicago, IL 60611 and [2]Chiron Corporation, Emeryville, CA 94608.

Previously we reported expression of an L-type Ca^{+2} channel α_1 subunit isoform ("cardiac/brain", CaCh2) using the baculovirus/insect cell system. We now have expressed isoforms of the β ("cardiac/brain", CaB2a) and α_2/δ ("skeletal muscle", CaA2) subunits of these channels in insect cells. Both the CaA2 and CaB2a baculovirus constructs carry a sequence encoding the KT3 epitope from large T antigen. Insect cells infected with CaA2 or CaB2a viruses express α_2/δ or β_{2a} subunits of molecular weight and immunoreactivity (using monoclonal KT3 or subunit specific antibodies) consistent with the native proteins. Coexpression of channel subunits has been characterized using biochemical approaches and immunofluorescence microscopy. The α_1 subunit expressed alone fails to bind dihydropyridines with high affinity, however coexpression with accessory subunits confers high affinity binding. When expressed together, both the α_2/δ and β_{2a} subunits can be immunoprecipitated using monoclonal antibodies specific for the α_2/δ subunit suggesting a direct interaction between these two subunits. Interestingly, the β_{2a} subunit can be solubilized from insect cell membranes by 0.5 M salt when expressed alone or by digitonin when expressed with other Ca^{+2} channel subunits. Thus, coexpression of Ca^{+2} channel subunits in insect cells appears to be a useful system in which to characterize subunit interactions and their roles in channel function and regulation.

W-Pos395

ION-DEPENDENT INACTIVATION OF RECOMBINANT CARDIAC Ca CHANNELS IN HEK 293 CELLS.

((R. Shirokov[1], D.D. Sun[2], F.C. Chang[2], M.M. Hosey[2], E. Ríos[1])) Rush Univ.[1], Northwestern Univ[2]., Chicago,IL,60612.

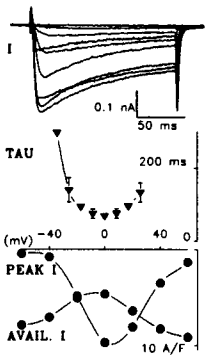

Ca currents (*I*) were recorded by the whole-cell patch-clamp technique in human embryonic kidney (HEK 293) cells cotransfected with the $\alpha 1$ and $\beta 2A$ subunits of the cardiac Ca channel. In most cases (Fig.) the kinetics of current decay were much slower than those of the native channels. The time constant of the current decay (*TAU*) was greater than 70 ms at 25 °C, while it is about 10 ms in native channels. Both the time constant and the availability of the current (*AVAIL. I*, measured in a double pulse experiment) showed a minimum at voltages corresponding to the peak of the current *vs.* voltage relationship (*PEAK I*). This shows that the observed inactivation has a current-dependent mechanism. In cases where the current density was especially high (up to 80 A/F), a much faster inactivation was observed ($\tau \approx 15$ ms at -10 mV). Supported by NIH and AHA.

W-Pos396

EXPRESSION OF FUNCTIONAL CARDIAC L-TYPE Ca^{++} CHANNELS IN TRANSIENTLY TRANSFECTED HEK (293) CELLS

((D.D. Sun[1], F.C. Chang[1], A. Chien[1], X-L. Zhao[1], R. Shirokov[2], E. Rios[2], and M.M. Hosey[1])) Northwestern Univ. [1], Rush Univ.[2], Chicago, IL 60611

The precise roles of the subunits of L-type Ca^{++} channels in the regulation of channel function are unknown. In this study, HEK293 cells were transiently transfected with pRBG4 vectors containing cDNAs encoding either the full-length CaCh2 α_1 or β_{2a} subunit. The latter was epitope-taged at its C-terminus with the KT_3 sequence from large T antigen. The expression of the α_1 and β_{2a} subunits was detected in Western blots of membranes from transfected cells with antibodies against the C-terminus of the α_1 subunit or the KT_3 epitope. Transfected cells expressed reactive proteins of ~ 210 and ~68 kDa, respectively, within 48-72 hrs post-transfection. Moreover, the expression of the α_1 subunit was enhanced by cotransfection with β_{2a}. Immunofluoresence staining of transfected cells with the specific antibodies showed similar results. Whole-cell patch-clamp recording of non-transfected cells and cells transfected with the α_1 cDNA revealed endogenous DHP-insensitive Ca^{++} currents, that exhibited a maximal peak current density of less than 1 A/F and fast inactivation. In cells transfected with both α_1 and β_{2a} subunits, we observed maximal Ca^{++}current density of 18±8 A/F. The expressed Ca^{++} currents were completely blocked by 10 μM nitrendipine. Our results indicate that the β subunit is an important component in the regulation of cardiac Ca^{++} channel formation and function.

W-Pos397

TRANSIENT EXPRESSION OF CARDIAC Ca^{++} CHANNEL α_1 SUBUNIT IN HEK293 CELLS.

((T. Perez-Garcia, T. J. Kamp, M. Appel, and E. Marban)) Division of Cardiology, Dept. of Medicine, Johns Hopkins University, Baltimore, MD 21205.

HEK293 cells are derived from human embryonic kidney and do not possess functional Ca^{++} channels when examined using the whole-cell patch clamp technique. HEK293 cells were transfected using the calcium phosphate method with a plasmid encoding the α_1 subunit of the rabbit cardiac Ca^{++} channel and a plasmid encoding ß-galactosidase. ß-galactosidase activity was observed in 40-70% of the transfected cells. Specific binding of the Ca^{++} channel blocker ^{3}H-PN200-100 was detected in the transfected cells (K_d = 0.8 nM and B_{max} = 0.4 fmoles/10^5 cells), but not in the control HEK293 cells. Screening of the transfected cells using the whole-cell patch clamp technique demonstrated currents carried by Ca^{++} or Ba^{++}, although robust currents could be elicited in less than 5% of the cells examined. The observed currents were typical for L-type Ca^{++} channels as demonstrated by: the high voltage threshold for activation; the presence of voltage- and Ca^{++}-dependent inactivation; the complete block in the presence of 1 μM nitrendipine; and the ~10-fold enhancement in the presence of 1μM Bay K8644. Thus, expression of the α_1 subunit of the rabbit cardiac Ca^{++} channel in HEK293 cells results in the expression of functional L-type Ca^{++} channels as well as ^{3}H-PN200-110 binding sites which appear to be present in greater number than functional channels.

W-Pos398

EFFECTS OF OXIDATION AND REDUCTION OF SULFHYDRYL GROUPS OF EXPRESSED L-TYPE CALCIUM CHANNELS

((N. Chiamvimonvat, B. O'Rourke, V. Flockerzi, F. Hofmann and E. Marban)) Johns Hopkins University, Baltimore, MD 21205

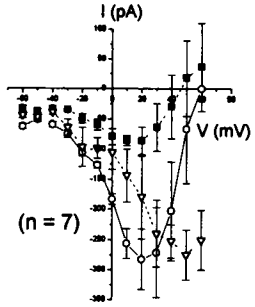

We studied the effects of oxidation and reduction of sulfhydryl groups on cysteine residues of rabbit airway smooth muscle L-type calcium channel, α_1 subunit, stably transfected in Chinese Hamster Ovarian cells. The known sequence suggests the presence of at least 2 cysteine residues within the putative pore of the channel. Ca^{2+} current (10 mM Ca^{2+}, 22 °C) was measured using the whole-cell patch-clamp technique. Within 10 min of exposure to 50 μM dithiodipyridine (DTDP, a specific oxidizer of the sulfhydryl groups, ■), Ca^{2+} current was reduced as compared to control (○) with no significant change in the kinetics or shift in the current-voltage relation. There was a consistent production of outward leak current. This reduction in the Ca^{2+} current can be reversed by 5 mM dithiothreitol (DTT, a specific reducer of the sulfhydryl groups, ▽). However, DTT induced a significant rightward shift of the current-voltage relation. Application of DTT alone produced a similar shift with no significant change in the peak magnitude of the current. The data suggest that accessible cysteine residues within the pore of the channel exist in the reduced state. In contrast, disulfide bonds in other parts of the channel may be important in the voltage-dependent gating of the channel.

W-Pos399

DOUBLE PULSE FACILITATION OF CURRENTS THROUGH THE α_1-SUBUNIT FROM SMOOTH MUSCLE L-TYPE Ca^{2+} CHANNELS.

((T. Kleppisch[1], K. Pedersen[2], E. Bosse[3], V. Flockerzi[3], F. Hofmann[3], J. Hescheler[4]))
[1] University of Vermont, Department of Pharmacology, Burlington, Vermont ; [2] Institut für Physiologie, Humboldt-Universität zu Berlin, Berlin, Germany; [3] Institut für Toxikologie und Pharmakologie, Technische Universität, München, Germany; [4] Institut für Pharmakologie, Freie Universität Berlin, Berlin, Germany (Sponsored by Blair E. Robertson)

Short depolarizing prepulses induce potentiation of Ca^{2+} channel currents in various cell types due to a drift of the Ca^{2+} channel gating towards mode 2. Studies on native Ca^{2+} channels showed a depolarization-induced phosphorylation as the underlying mechanism. Using the cell-attached and the whole-cell configuration of the patch clamp technique and Ba^{2+} as the charge carrier, we studied the voltage-dependent facilitation on the pore forming α_1-subunit of the smooth muscle dihydropyridine-sensitive Ca^{2+} channel stably expressed in Chinese hamster ovary cells. In cell attached patches, conditioning prepulses positive to +50mV induced the characteristic mode 2-like gating behavior which was reflected in a 2-5 fold increase of the single Ca^{2+} channel opening probability. This corresponded to a prepulse-induced potentiation of the whole-cell Ba^{2+} current by about 50%. Under facilitation, the mean open time of single Ca^{2+} channels was markedly prolonged from 0.38 ms to 3.9 ms, whereas in the closed time distribution there was an additional short-lived component. Further, we examined whether a voltage-dependent direct phosphorylation of the pore forming α_1-subunit is involved in facilitation. Unexpectedly, the catalytic subunit of the protein kinase A as well as the specific inhibitor of protein kinase A, PKI(6-22)amide, had no effect. Inhibition of G-proteins by GDPβS was also without effect. The data demonstrate that the L-type Ca^{2+} channel α_1-subunit solely expressed in Chinese hamster ovary cells is subject to a voltage-dependent facilitation. This type of modulation is apparently independent of cAMP-dependent phosphorylation and G-proteins.

W-Pos400

PREVENTION OF L-TYPE Ca^{2+} CHANNEL RUN-DOWN BY CALPASTATIN IS NOT CORRELATED WITH INHIBITION OF CALPAINS.

((K. Seydl, J.-O. Karlsson, A. Dominik and C. Romanin)) Inst. f. Biophysics, Univ. of Linz, Austria. (Spon. by A. Hermann)

Activity of L-type Ca^{2+} channels on a membrane patch disappears rapidly when the patch is excised from the cell into an artificial solution. Recently, we [Romanin, C., Grösswagen, P. and Schindler, H. (1991) Pflügers Arch. **418**, 86-92] have succeeded in preventing this channel run-down in isolated membrane patches upon application of calpastatin, an endogenous protease inhibitor, and of nucleotides. The high specificity of calpastatin to the protease calpain would clearly point to a participation of calpain activity in the run-down of Ca^{2+} channels. In an attempt to examine for an involvement of calpain three synthetic and rather specific calpain inhibitors were substituted for calpastatin. The potency of these compounds to inhibit calpain was first determined in a biochemical assay and then compared with their efficacy to prevent Ca^{2+} channel run-down. Surprisingly, calpastatin was least effective in calpain inhibition but by far the most potent in prevention of Ca^{2+} channel run-down. Furthermore, Ca^{2+} channel activity markedly recovered after run-down by application of calpastatin. These results indicate that proteolysis might only be partially responsible for channel run-down and suggest an as yet unidentified function for calpastatin in the regulation of Ca^{2+} channel activity beyond to its inhibitory action on calpain. (Supported by Austrian Research Funds S-6606)

W-Pos401

VOLTAGE-DEPENDENT REGULATION OF CLASS C L-TYPE CA CHANNELS.

((P. Charnet, E. Bourinet, W.J. Tomlinson, T.P. Snutch, and J. Nargeot)) CNRS CRBM, MONTPELLIER 34033 FRANCE and U.B.C. VANCOUVER, V6T 1W5 BC CANADA

L-type calcium channels (LTCC) are multimeric proteins (composed of α1, α2–δ, β, and possibly γ subunits, SU) that mediate a voltage-dependent Ca influx in many cell types. Various evidences suggest multiple types of LTCC on the body or at the base of the major dendrites of many neurons where a Ca influx could play a role in intracellular regulatory events. It has been proposed that the firing pattern of these neurons can influence the level of Ca entry during each individual action potential by a switch between gating modes at high frequency of stimulation. The α1 class C LTCC is highly expressed in diverse neuronal tissues and can potentialy be the major type responsible for these effects. We show that injection of expression plasmid for classs C α1, α2–δ and β SU in Xenopus oocytes induced the expression of Ca channels characterized by a slow inactivation in Ba that is strongly accelerated in Ca. This current either in Ba or in Ca can be potentiated by short depolarizing pulses to positive voltage. The turning ON of the potentiation is fast (around 2 to 20 s-1) and voltage dependent. Neither GTPγS, nor GDPβS altered the time course or the amplitude of this potentiation, suggesting that G-protein activation is not involved. Possible structural implications are discussed regarding of the mechanism by which this potentiation can take place.

W-Pos402

TIGHT COUPLING BETWEEN CHARGE MOVEMENT AND PORE OPENING IN TYPE E CALCIUM CHANNEL. ((R. Olcese, T. Schneider, A. Neely, X. Wei, J. Costantin, L. Birnbaumer and E. Stefani)). Dep. of Molec. Physiol. & Biophys. Baylor Col. Med. Houston, TX 77030.

The human Ca^{2+} channel α_{1E} subunit was expressed in *Xenopus* oocytes (Schneider et al, this meeting). The steady state properties of ionic and gating currents were characterized using the cut-open oocyte voltage clamp technique (Taglialatela et al, *Biophys.J. 61, 78-82,*1992). The voltage dependence of channel opening was measured from tail currents recorded in 10 mM Ba^{2+}at -50 mVafter subtraction of gating currents in oocytes pre-injected with BAPTA. Gating currents were recorded in 2 mM Co^{2+}. The half activation potential ($V_{1/2}$) for charge movement (Q-V) was about 20 mV more negative than for pore opening. This difference virtually disappeared with coexpression of the β_2 subunit which shifted the voltage dependence of channel opening to the left while the Q-V remained unchanged. The voltage dependence of channel opening was described by the sum of two Boltzmann distributions, indicating the presence of two modes of activation: the early component ($V_{1/2}$=1±6 mV) contribute to 47± 4% of the maximal conductance. For the second component $V_{1/2}$=43±8 mV. The presence of two modes of opening was also confirmed at the single channel level. Coexpression of β_2 increases the contribution of the early component to 72±4% while maintaining the effective valence and $V_{1/2}$ for each component. The slope for the early component was near 3-fold that of the Q-V and this relation was the same with or without the β_2 subunit. In contrast, for cardiac channel (α_{1C}) the slope for the conductance is twice the slope of the Q-V and $V_{1/2}$ of the Q-V (-18 mV) remain more than 30 mV negative to pore opening even in the presence of β_2. (Supported by an NRSA fellowship to A. N. and grants HL37044 to L. B. and AR38970 to E. S. from NIH).

W-Pos403

DEVELOPMENTAL CHANGES IN ß-ADRENERGIC AND MUSCARINIC MODULATION ON CONTRACTILITY, CALCIUM CURRENTS AND ADENYLYL CYCLASE ACTIVITY OF RABBIT HEART. ((Holly Clements, Toshiaki Akita, Rajiv Kumar and Ronald W. Joyner)) Department of Pediatrics, Emory University, Atlanta, GA 30322

We measured left ventricular developed pressure (LVDP) and its first derivatives (±dP/dt) by using an intraventricular balloon in isolated Langendorff perfused adult (AD) and newborn (NB, 1-3 day-old) rabbit hearts as well as L-type I_{Ca} and adenylyl cyclase (AC) activity in isolated rabbit ventricular cells. Isoproterenol (ISO, 0.1 μM) increased LVDP and max.+dP/dt 54.2% and 140.7%, respectively, in AD and 33.9% and 95.9%, respectively, in NB hearts over the basal levels. Subsequent addition of 1 μM carbachol reduced LVDP and max.+dP/dt to 37.7% and 84.9%, respectively, in AD and 13.5% and 30.4%, respectively, in NB hearts over the basal levels, with the carbachol effects being significantly greater in NB hearts. 10 μM Carbachol slightly shifted the dose-dependent effect of ISO on I_{Ca} to the right without affecting E_{max} in AD isolated cells, while completely abolishing the stimulatory effect of ISO on I_{Ca} in NB cells. 10 μM ISO increased AC activity in membranes by 250% in AD and 86% in NB, respectively. Subsequent addition of 10 μM carbachol then decreased AC activity to 180% above basal levels in AD and only 35% in NB, respectively. These results suggest that a weaker ß-adrenergic and stronger muscarinic effect on contractility in NB heart are explained by a weaker ß-adrenergic and stronger muscarinic effect on I_{Ca} and adenylyl cyclase activity in NB heart.

W-Pos404

TONICALLY ACTIVE (BACKGROUND) CALCIUM CHANNELS UNMASKED BY PHENOTHIAZINES IN RAT VENTRICULAR MYOCYTES. ((T. Lefèvre, A. Coulombe and E. Coraboeuf)) Lab. de Physiologie Cellulaire, URA CNRS 1121, Bât. 443, Université Paris-Sud, F-91405 Orsay and Hôpital M. Lannelongue, URA CNRS 1159, F-92350 Le Plessis Robinson, FRANCE

Although voltaged-activated calcium channels represent the main source of calcium entry in active cardiac cells, the existence in quiescent cells of a small calcium influx has been known for a long time. The mechanism by which this resting calcium influx occurs is still poorly understood. The background calcium channels described by Coulombe et al. (*J Membr Biol.* 111:57-67, 1989) might be one of the mechanisms involved in this phenomenon. Recent reports have shown that calcium efflux from SR vesicles was greatly increased by phenothiazines such as trifluoperazine (TFP) or chlorpromazine. Here we demonstrate that in membranes of cardiac myocytes, phenothiazines markedly activate divalent-permeable channels (see below), similar to those previously described. Such channels capable of tonic activity in quiescent cells may help to maintain homeostatic $[Ca]_i$ by operating *via* still unknown regulation mechanisms a balance between tonic calcium influx and calcium extrusion. Internal calcium store depletion might be one of these mechanisms.

Pipette medium (mM) : 96 $BaCl_2$, 10 HEPES, pH : 7.4 (BaOH). Bath medium (mM) : 100 K-aspartate, 25 Cs-aspartate, 1 EGTA, 1 EDTA, 10 HEPES, pH : 7.4 (CsOH).

W-Pos405

STIMULATION AND IRREVERSIBLE BLOCK OF CARDIAC CALCIUM CURRENTS BY A TYROSINE KINASE INHIBITOR. (X. Yi and A.S. Otero) Dept. Molecular Physiology and Biological Physics, University of Virginia, Charlottesville VA 22908.

Methyl-2,5-dihydroxycinnamate (MDC), an erbstatin analog that inhibits tyrosine kinases, was found to block cardiac muscarinic receptor function irreversibly through its quinone moiety (Otero & Sweitzer, Mol. Pharmacol. 44, 595, 1993). We report here that MDC also affects the whole cell calcium currents (I_{Ca}) of atrial myocytes: namely, extracellular application of MDC leads to a 2- to 5-fold increase in basal I_{Ca}. At low concentrations (0.1-0.3 μM) this increase is sustained; in contrast, 1- 10 μM MDC stimulates I_{Ca} to a maximal value which is reached in 1-3 minutes, and the currents then return to a level that is typically lower than that measured under control conditions. This pattern of stimulation followed by block is observed even in the presence of Bay K 8644 or during intracellular perfusion of the catalytic subunit of protein kinase A (cPKA). After the decay of MDC-induced currents, I_{Ca} no longer responds to stimulation by Bay K 8644, isoproterenol or forskolin, or to internal perfusion with cAMP or cPKA. The effects of MDC on calcium currents are mimicked by simple quinones such as benzoquinone, but not by 2,5-Di-*tert*-butyl hydroquinone or duroquinone. These results suggest that the quinone portion of MDC affects I_{Ca} through a direct action on cardiac calcium channels, as observed with muscarinic receptors. *Supported by HL48276.*

W-Pos406

FATTY ACID MODIFIED DIET ALTERS SARCOLEMMAL FATTY ACIDS, CA++ CURRENTS AND FLUIDITY OF RAT VENTRICULAR MYOCYTES. ((Xin Gong, PK. Ram, Gregory L. Florant and RL. White)) Temple University School of Medicine, Philadelphia, PA 19140 (Spon. by Lyle W. Horn)

We find that the phospholipid composition of ventricular myocytes isolated from rats kept on a diet deficient in essential fatty acids (EFADR) is altered. There is a decrease ($p<0.05$, n=5) in 18:2 fatty acids and others (*e.g.* 20:4) that depend on 18:2 as a precursor. Ca++ currents recorded from EFADR show increased temperature sensitivity of activation and inactivation. We also find, using indo-1, a 5-fold increase in resting cytosolic free Ca^{2+} ($[Ca^{2+}]_i$) in myocytes from EFADR when temperature was lowered from 30°C to 5°C, comparing with a 2-fold increase in $[Ca^{2+}]_i$ for myocytes from control rat subjected to the same temperature drop. We measured membrane fluidity using the lipophilic fluorescent dye Laurdan in the temperature ranges where we saw effects on $[Ca^{2+}]_i$ and inward currents.

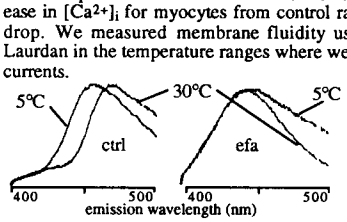

The peak Laurdan emission from ventricular myocytes from EFADR was blue-shifted even at 30°C compared with that recorded at 5°C from control rats.

We conclude that dietary manipulation alters sarcolemmal membrane phospholipid profile and fluidity in rat. Dietary manipulation also alters the temperature sensitivity of calcium homeostasis. Whether the latter effect is a direct result of altered membrane lipids or other effects of an EFAD diet is not known.

W-Pos407

REGULATION OF Ca CURRENT IN VENTRICULAR MYOCYTES BY FORSKOLIN AND THE PROTEIN KINASE INHIBITOR H-89.
((W. Yuan and D.M. Bers)) Loyola University Chicago, Maywood, IL 60153

Calcium current (I_{Ca}) was measured in freshly isolated single rabbit and ferret ventricular myocytes using the whole-cell patch clamp technique with Na and K currents blocked by TEA_o and Cs_i (i.e. net inward current elicited by depolarizations from -110 to 0 mV for 150 ms). Activation and steady-state inactivation curves were determined at various test potentials (-40 to +60 mV) and fit with a Boltzmann relation where $V_{0.5}$ is the E_m at half maximal conductance. Forskolin (at 1 μM, like isoproterenol at maximal concentration) increased I_{Ca} amplitude by 2-3-fold and shifted $V_{0.5}$ for both activation and inactivation to more negative potentials by ~8 mV (see figs). The effect of forskolin on the amplitude of I_{Ca} could be reversed by an inhibitor of cAMP-dependent protein kinase (H-89, 5-10 μM). However, H-89 did not reverse the shift of $V_{0.5}$ induced by forskolin. H-89 application by itself does not decrease basal I_{Ca}, but does shift the $V_{0.5}$ of both activation and inactivation to more negative values of E_m (possibly unrelated to the *regulatory* phosphorylation of Ca channel). It is possible that H-89 reverses the shift induced by regulatory phosphorylation (due to forskolin), but induces a coincidental negative shift itself.

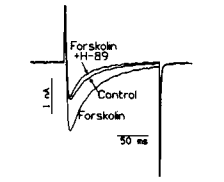

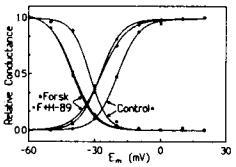

W-Pos408

SIMULATION STUDIES OF THE MECHANISM OF ARRHYTHMOGENIC EARLY AFTERDEPOLARIZATIONS IN CARDIAC MYOCYTES
((J.Zeng, Y.Rudy)) Department of Biomedical Engineering, Case Western Reserve University, Cleveland, OH 44106.
(Spon. by grant HL-49054 from NIH)

Early afterdepolarizations (EADs), defined as membrane depolarizations that occur during the repolarization phase of a cardiac action potential, play an important role in the genesis of ventricular arrhythmias. To investigate the mechanism of EADs, a theoretical model of the cardiac ventricular action potential that accounts for dynamic changes in ionic concentrations and simulates calcium handling by the cell was used. Results demonstrate that the L-type calcium current is the only carrier of depolarizing charge during an EAD and that EAD results from reactivation of this current during the action potential. Other currents can modulate EAD formation by affecting the balance of currents during a "conditional phase" prior to EAD take-off. Spontaneous calcium release from the sarcoplasmic reticulum is not required for EAD formation. Simulated drug interventions that affect $[Ca^{2+}]_i$ (e.g. ryanodine, Bay K 8644, isoproterenol) can modulate currents that depend on $[Ca^{2+}]_i$ such as Na^+-Ca^{2+} exchange to affect EAD formation.

W-Pos409

DIHYDROPYRIDINE (DHP) BINDING SITE LOCALIZATION IN THE CARDIAC L TYPE CALCIUM CHANNEL BY CUSTOM-SYNTHESIZED PROBES.
((R. Bangalore[1], N. Baindur[2], A. Rutledge[2], D. J. Triggle[2] and R.S. Kass[1])), [1]University of Rochester School of Medicine, Rochester, NY 14642, [2]Dept. of Biochemical Pharmacology, SUNY at Buffalo, Buffalo, NY 14260.

A series of neutral and permanently charged dihydropyridine (DHP) antagonists in which the head group (CH_2CH_3 or $(CH_3)_3N^+$) was linked to the active DHP moiety by alkyl spacer chains of varying lengths (n = 2, 10 and 16 carbons) were used in whole cell patch clamp experiments to probe the location of the DHP binding site relative to the membrane surface. Extracellular access of the drugs to the DHP binding site was measured by applying the drugs in the bath solution and intracellular access of the drugs to the binding site was measured by including the maximum extracellular concentrations of charged DHPs in the patch pipette. Extracellular application of neutral DHPs showed that the relative block was similar with both spacer chain lengths used (n=2, 10), with 500 nM of either compound blocking about 70% of the whole cell current. On the other hand, the relative block with 500 nM of the charged DHPs was <1%, 50% and 28% for spacer chain lengths of 2, 10 and 16 carbons respectively. Depolarized holding potentials, but not channel openings, enhance block, suggesting that access to the binding site is not via an intra-pore pathway. Intracellular application of the charged DHPs had no effect on the L type calcium current, providing evidence that the DHP binding site is not accessible from the inner surface of the membrane, confirming previous results with the compound SDZ 207-180. A 10 carbon spacer chain appears to be optimal for extracellular access to the DHP binding site while a spacer chain of up to 16 carbons is inadequate for intracellular access to the binding site. In conclusion, the binding site for DHP antagonists in guinea pig cardiac L type calcium channels appears to be located closer to the outer surface of the membrane. Our data further suggest that the binding site is located within the lipid bilayer.

Na CHANNELS III: TOXINS AND BLOCKERS

W-Pos410

FUNCTIONAL EFFECTS OF PENTOBARBITAL ON VOLTAGE-GATED SODIUM CHANNELS
((E. Bennett, B. Rehberg, S.R. Levinson, and D.S. Duch)) Dept. of Physiology & Program in Neuroscience, UCHSC, Denver, CO 80262, and the Dept. of Anesthesiology, Cornell University Medical School, New York, NY, 10021.

The mechanism underlying the role of the intravenous anesthetic pentobarbital (PB) on voltage-gated sodium channels was investigated through whole cell recording of Chinese Hamster Ovary (CHO) cells exogenously expressing the tetrodotoxin-sensitive rat skeletal muscle sodium channel, RSkM1. The steady state inactivation of RSkM1 in the presence and absence of 1.36, 2.38, 3.4, and 6.8 mM PB was determined and data indicate that steady state inactivation of the channel is shifted by PB in a concentration dependent manner. The shift in the voltage of half inactivation (V_i) over the range of PB concentrations studied is nearly linear, showing little indication of saturation at 6.8 mM PB (V_i is 10, 15, 20, and 35 mV hyperpolarized following exposure to 1.36-6.8 mM PB, respectively). This implies that the concentration of PB required for half maximal shift (EC_{50}) is at least 6.8 mM (EC_{50} = 15.9 mM assuming reversible single-site binding characteristics). As reported previously, exposure of sodium channels to PB causes a reduction in current, which might be explained by the observed shift in V_i. However, the data indicate that this cannot solely account for the reduction in current. Peak current levels in the presence of PB are still inhibited following a prepulse to a membrane potential at which virtually all channels have recovered from inactivation. In addition, the "blocked" portion of the current (i.e., the portion of the reduced current that cannot be accounted for by the shift in inactivation of the channel) is approximately ten-fold more sensitive to PB (EC_{50} = 1.5 mM) than the inactivation shift, indicating that exposure of PB to RSkM1 affects channel function through at least two different pathways: through a shift in the voltage dependent characteristics of steady state inactivation, and possibly through direct block of the channel (although this is yet to be shown directly). Together, the two phenomena combine to reduce activity of the sodium channel such that sensitivity to PB is much greater at physiological membrane potentials than either effect separately (EC_{50} = 0.4 mM). Supported by NIH: NS09327 (EB), NS15879 (SRL), and GM41102 (DSD).

W-Pos411

POTENT USE-DEPENDENT SODIUM CHANNEL BLOCK BY THE NOVEL WATER-SOLUBLE ANTICONVULSANT FPL 14937AA
((D.Y. Sanchez, R.J. Schmiesing, M.L.Stagnitto, G. E. Garske, G.C.Palmer, N.A. Mahmood, H. Cheung, D.Kamp and E.W. Harris)) Departments of Biology, Chemistry and Preclinical Research Support, Fisons Pharmaceuticals, Rochester, NY 14603

FPL 14937AA, the hydrochloride salt of a diphenyl lactam, is a new anticonvulsant with a unique efficacy and safety profile. It is selective for maximal electroshock seizures (MES) seizures in mice and rats with a wide therapeutic index (orally, >20 in mice and >40 in rats), and has no effect on convulsions elicited by PTZ, bicuculline, NMDA, kainic acid or BAY K8644. FPL 14937AA delays the time to first twitch in the PTZ seizure threshold test in which phenytoin is proconvulsant. Since sodium channels appear to be a primary target of many compounds effective against MES seizures, the effects of FPL 14937AA on voltage-gated sodium channels were studied.

In rats showing protection in the MES test after oral administration of FPL 14937AA, serum free concentrations were 1-2 μM. At up to 30μM, FPL 14937AA had no effect on synaptic transmission or antidromic population spikes in hippocampal slices. FPL 14937AA reduced ^{3}H-batrachotoxin binding to rat brain synaptosomes (K_i=66μM for phenytoin, 28μM for FPL 14937AA). FPL 14937AA limited sustained repetitive firing (SRF) of TTX-sensitive action potentials in cultured mouse spinal cord neurons. As is observed with phenytoin and carbamazepine, the block is use- and voltage dependent, but FPL 14937 is 4-10 fold more potent (EC_{50}=0.8μM). FPL 14937AA also appears to act differently from phenytoin and carbamazepine in the SRF test: the latter have steep concentration/effect curves (~1 log unit), whereas FPL 14937AA has a shallow curve extending over 4-5 log units.

Whole cell patch-clamp of acutely dissociated neonatal rat cortical neurons was used to study the concentration and voltage-dependence of tonic (0.1Hz) and use-dependent (2-15Hz) block of sodium currents, as well inactivation and recovery from inactivation rates.

W-Pos412

HALOTHANE REDUCES IONIC CURRENTS THROUGH VOLTAGE-GATED SODIUM CHANNELS IN PLANAR BILAYERS. ((R.J. Silver, B. Rehberg, Y.-H. Xiao and D.S. Duch)) Depts. Anesth. and Phys., Cornell Univ. Med. Coll., New York, N.Y. 10021. (Spon. by B.W. Urban).

The mechanisms by which anesthetic agents induce anesthesia are still poorly understood, with the relevant site(s) of action being the lipid membrane and/or ligand operated and voltage-gated ionic channels. To examine the interactions of volatile anesthetics with relevant membrane protein targets, we examined the effects of halothane on highly purified preparations of eel electroplax sodium channels incorporated into planar lipid bilayers in the presence of either 5μM veratridine (VTD) or 250nM batrachotoxin (BTX). In the absence of channels, halothane significantly increased the background conductance of the bilayer in a dose-dependent manner (165% increase at 1.5mM halothane). Halothane had no effect on the single channel current-voltage relationships of channels modified by either toxin (11.67±0.83 pS [±SD] for VTD-control vs. 11.72±1.04 pS for 1.5mM halothane and 21.95±2.35 pS vs. 20.65±1.66 pS, respectively, for BTX). However, it reduced the steady-state open probability of VTD-modified channels in a dose-dependent manner, having an EC_{50} of about 0.6mM (~1.3 MAC) when the data were fitted with a rectangular hyperbola. No effects on BTX-modified channels were observed up to 1.5mM halothane.

W-Pos413

BREVETOXIN-3 (PbTx-3) AND ITS DERIVATIVES MODULATE SINGLE SODIUM CHANNELS IN RAT SENSORY NEURONS. (G. Jeglitsch*, K. Rein, D.G. Baden & D.J. Adams*) NIEHS Marine & Freshwater Biomedical Sciences Center, RSMAS and *Dept. of Mol. & Cell. Pharmacology, Univ. of Miami Sch. of Med., Miami, FL

The dinoflagellate, *Ptychodiscus brevis*, produces 10 different brevetoxins, responsible for toxic "red tides" occuring periodically off the coasts of Florida and Mexico. PbTx-3 is a heat stable, lipophilic 11-ring polyether molecule, which binds with high affinity to site 5 of the voltage-sensitive Na channel. PbTx-3, a sodium channel activator, causes a shift in activation to more negative potentials and inhibits the inactivation (Baden, 1989, *FASEB J.* 3:1807-1817). Single channel studies demonstrate that, unlike other Na channel modifiers, PbTx-3 is able to stabilize more than one conductance state (Schreibmayer & Jeglitsch, 1992, *BBA* 1104:233-242). The effects of PbTx-3 and its derivatives were studied in cell-attached membrane patches on neurons dissociated from rat nodose ganglia using the patch clamp technique. PbTx-3 (30 nM - 500 nM) produced a shift in activation to more hyperpolarized membrane potentials whereby steady-state recordings were obtained at -70 mV. The unitary current-voltage relationship is linear exhibiting a reversal potential of +60 mV. Two "sublevels" could be observed with slope conductances of approximately 10 pS and 20 pS. The inactivation of modified Na channels is inhibited and the mean channel open time (τ_o) is increased. The Na currents could be blocked by 1 μM tetrodotoxin added to the pipette solution indicating that the single channel currents are due to the opening of TTX-sensitive sodium channels. The PbTx-3 molecule is proposed to have multiple active centers (A-ring lactone, C-42 of R side chain) interacting with the Na channel binding-site. Modification of the molecular structure of PbTx-3 at these centers produced derivatives which differ in their potency. The derivatives KRI31 (A-lactone ring is opened) and KRI57 (double bonds of the A-lactone ring and R side chain are reduced) were less potent requiring higher doses (KRI31: 1 μM - 10 μM; KRI57: 500 nM - 1 μM) to produce similar effects to PbTx-3. Furthermore, at least 5 subconductance states could be observed by using KRI31. PbTx-3 and its derivatives may provide insight to the mechanics of Na channel gating.

W-Pos414

LIGHT-DEPENDENT IRREVERSIBLE INHIBITION OF THE SODIUM CURRENT AND ^{3}[H]-BTX-B BINDING BY A MODEL LOCAL ANESTHETIC ((J.McHugh, W.Mok, G.K.Wang, and G.Strichartz)) Anes. Res. Labs, BWH, Boston MA 02115 (Spon. by M.Holman)

N-(2-di-N-butylaminoethyl)-4-azidobenzamide (DNB-AB) is a model local anesthetic (LA) containing the photoactivatable aryl azido moiety which is known to form a covalent bond to adjacent molecules when exposed to UV light. We studied the effects of DNB-AB on the sodium current (I_{Na}) under whole cell voltage clamp in clonal mammalian GH_3 cells and on ^{3}[H]-BTX-B binding to sheep brain synaptoneurosomes. In the absence of UV illumination, DNB-AB behaved similarly to known LAs, producing both reversible block of I_{Na} (IC_{50}=30μM, 20°C) and reversible inhibition of ^{3}[H]-BTX-B (50nM) binding (IC_{50}=3μM, 37°C), implying a non-covalent association between DNB-AB and its receptor(s). After exposure to UV light, both block of I_{Na} and inhibition of ^{3}[H]-BTX-B binding were only partially reversible (reversibility of I_{Na} block to 27% of control; ^{3}[H]-BTX-B binding = 60% of control) implying a covalent association between DNB-AB and its receptor(s). UV light in the absence of drug had little effect on I_{Na} (post exposure I_{Na} = 96% of control), or on ^{3}[H]-BTX-B binding (post exposure binding = 85% of control). The irreversible block of I_{Na} was prevented by co-incubation of DNB-AB with 1mM bupivacaine (IC_{50} = 45μM, 20°C) during illumination, indicating that the site of irreversible inhibition of I_{Na} is shared with the clinical local anesthetic bupivacaine.

W-Pos415

DIFFERENTIAL EFFECTS OF TETRAMETHRIN ON TETRODOTOXIN-SENSITIVE AND TETRODOTOXIN-RESISTANT SODIUM CHANNELS. ((H. Tatebayashi and T. Narahashi)) Dept. of Pharmacology, Northwestern University Medical School, Chicago, IL 60611. (Spon. by C. H. Wu)

The dorsal root ganglion (DRG) neurons of rat express two types of sodium channels, tetrodotoxin-sensitive (TTX-S) and tetrodotoxin-resistant (TTX-R) channels. The effects of (+)-trans tetramethrin, a pyrethroid insecticide, on both channels were studied with new born rat DRG neurons in primary culture using the whole-cell patch-clamp technique. In TTX-S sodium channels, the slow sodium current during step depolarization was increased somewhat by tetramethrin, and a tail sodium current with a slowly rising and falling phase appeared upon repolarization. In TTX-R sodium channels, the decay phase during step depolarization was markedly slowed by tetramethrin, and upon repolarization a large instantaneous tail current was generated and decayed slowly. The minimum concentration of tetramethrin to induce a slowly decaying tail current was 100 nM and 10 nM for TTX-S and TTX-R channels, respectively. At a concentration of 10 μM, tetramethrin modified only 10-20 % of the TTX-S channels, whereas the modification was as high as 80 % in the TTX-R channels. Activation curves for sodium channels were shifted by 10 μM tetramethrin in the hyperpolarizing direction by 6.5 mV and 22.4 mV for TTX-S and TTX-R channels, respectively. Steady-state inactivation curves were also shifted by 10 μM tetramethrin in the hyperpolarizing direction by 13 mV for both TTX-S and TTX-R channels. In conclusion, although both TTX-S and TTX-R channels are modified by tetramethrin, the detailed kinetic mechanisms are different and TTX-R channels are much more sensitive to tetramethrin.

W-Pos416

MODULATION OF SQUID AXON SODIUM CHANNELS BY GRAYANOTOXIN

((I. Seyama[1], M, Yakehiro[1] and T. Narahashi[2])) [1]Dept. Physiol., Sch. of Med., Hiroshima Univ., Hiroshima 734 Japan and [2]Dept. Pharmacol., Northwestern Univ. Med. Sch., Chicago, IL 60611.

α-Dihydro-grayanotoxin II (GTX) has been shown to alter the physiological property of Na channels in squid axons. The gating mechanism of activation is shifted in the hyperpolarizing direction by about 50 mV and inactivation is abolished. We now report the mechanism of GTX modulation of Na channels as studied by voltage clamp and internal perfusion methods. When preceded by a conditioning depolarizing pulse, a step depolarization to -70 mV from a holding potential of -150 mV generated a GTX-modified channel current. The amplitude of this current increased during the conditioning pulse with a dual exponential time course. The time constants became shorter with the increase in the conditioning depolarization and GTX concentration. The recovery from GTX modulation followed a single exponential time course, and the time constant became shorter with the depolarization during recovery. This modulation occurred even after the removal of inactivation by pronase. The dose-response analysis for the GTX-modified current showed a one-to-one stoichiometry with an EC_{50} of 11.6 μM. These results are compatible with the idea that GTX binds to and unbinds from the channel site in a voltage-dependent manner.

W-Pos417

CONUS VENOM ACTIVATES CATION CONDUCTANCES IN SQUID NEURONS. ((M.T. Lucero)) Department of Physiology, University of Utah School of Medicine, Salt Lake City, Utah 84108.

Marine snails from the genus *Conus*, produce venoms that rapidly paralyze their prey. The venom from these snails contains 40-200 small peptides that are highly potent agonists and antagonists of membrane receptors and ion channels. The peptides are unique in that they contain only 10-30 amino acids that fold into relatively stable conformations. Venom from the mollusk hunting cone snail, *Conus marmoreus*, was tested on two types of neurons from the squid *Lolliguncula brevis*: the olfactory receptor neurons (ORN's) and giant fiber lobe (GFL) neurons. Application of crude venom to voltage-clamped ORN's resulted in the activation of a non-selective cation current that inactivated in the presence of venom. The inactivation or desensitization of the venom response in ORN's lasted for several minutes following washout of the venom. In contrast, when applied to GFL cells, the venom activated a conductance that was selective for Na^+. In the absence of Na^+, a K^+ current was activated by the venom. The venom-dependent cation conductance in GFL cells remained active as long as venom was present, and reversed rapidly after removing the venom. The conductance activated by *C. marmoreus* venom was remarkably similar to the conductance activated by glutamate. However, the venom was capable of activating the cation conductance even in GFL cells that had not yet developed a response to glutamate, suggesting that the toxin(s) is not acting through a glutamate receptor.

W-Pos418

MODIFICATION OF NaIIA NA^+ CHANNELS BY BATRACHOTOXIN. ((G.K. Wang* and S-Y Wang)) *Department of Anesthesia Research Laboratories, Harvard Medical School and Brigham and Women's Hospital, Boston, MA 02115 and Department of Biology, State University of New York at Albany, Albany NY 12222.

The effects of batrachotoxin (BTX) on cloned α-subunit Na^+ channels were examined in CHO-K1 cells transfected with rat brain NaIIA cDNA. Under whole-cell patch clamp conditions, BTX shifted the voltage dependence of the activation process by about 45 mV toward the hyperpolarizing direction and eliminated the inactivating phase of Na^+ currents. Repetitive depolarizations greatly facilitated the binding of BTX with NaIIA channels while the membrane was held at -100 mV. The estimated association rate constant for BTX binding with the open form of NaIIA channel was $1.11 \times 10^6\ M^{-1}s^{-1}$ at 22°C. BTX-modified NaIIA channels were blocked by TTX in a complicated manner. First, the TTX binding toward the closed state of BTX-modified NaIIA channels was not voltage dependent. The K_D value of TTX was measured at 8.9 nM, which was similar to that of unmodified channels (K_D=14.2 nM). Second, the block of the open state of BTX-modified NaIIA channels by TTX was voltage dependent; depolarization reduced the potency of TTX block between -20 mV to +50 mV. Below -30 mV, the TTX affinity began to level off, probably because of the increased presence of the closed state. Steady-state inactivation of BTX-modified NaIIA channels was minimal as measured by the two-pulse protocol, a phenomenon distinctly different from that found in GH_3 cells. Neutral local anesthetic benzocaine, however, drastically enhanced the steady-state inactivation of BTX-modified NaIIA channels, with its maximal effect around -60 mV.

W-Pos419

AROMATIC SODIUM CHANNEL PORE BLOCKERS. WHAT CAN THEY TELL US ABOUT INACTIVATION? ((Gerald W. Zamponi and Robert J. French)) Department of Medical Physiology, University of Calgary, Alberta, Canada T2N 4N1.

Lidocaine causes two modes of block of batrachotoxin-activated, cardiac sodium channels in planar lipid bilayers (Zamponi et al., 1993, Biophys. J. 65:80; 65:91): a fast open channel blockade, and a slow blocking mode that results from stabilization of a long closed state. The 'fast' blocking mode is seen as a decrease in aparent single channel current and an increase in open channel noise, and probably results from a rapid, voltage-dependent occlusion of the conducting pathway (t_{block}<1 ms). Diethylamide (pKa ≈ 10.5) represents the isolated, protonated amine group of the lidocaine molecule. Diethylamide, and 12 other tertiary and quaternary amines (including aromatic and non-aromatic compounds), when applied to the intracellular side, mimicked lidocaine's rapid blocking mode, suggesting that a charged amino group, which binds at an effective electrical distance of 30-50% from the cytoplasmic solution, is the fundamental requirement for this mode of block. Phenylmethylamine is as potent a fast blocker as lidocaine, indicating that neither the carbonyl group in the aryl-amide link of lidocaine, nor the alkyl groups on the amine nitrogen and the aromatic ring, are absolutely required for fast, open-channel block. However, aromatic compounds were more potent fast blockers, by greater than one order of magnitude, than structurally similar compounds lacking a ring. Probably, the charged amine group binds at the cytoplasmic end of the narrow, ion-selective region of the pore, while the aromatic moiety interacts with another binding domain on the channel. Binding to this domain is not required for fast block, but enhances its potency. Another recent study implies that the receptor for the inactivation gate may interact with an aromatic residue on the gate (West et al., 1992, PNAS 89: 10910). Furthermore, the aromatic drugs could bind to the same receptor. If so, the smallest aromatic fast blocker, phenyl-trimethyl-ammonium, would serve as a molecular ruler, suggesting that the receptor for the inactivation gate and the selectivity filter must be spaced less than 5 angstroms apart.

W-Pos420

LIDOCAINE BINDING TO INTERNAL SITE OF CARDIAC MYOCYTES BLOCKS PROTON ACCESS TO SODIUM CHANNEL

Takafumi Anno, Eiichi Watanabe, Itsuo Kodama, and Junji Toyama. Department of Circulation, Research Institute of Environmental Medicine, Nagoya University, Nagoya 464, Japan.

It has been suggested that the cardiac sodium channel has the external binding site as well as the cytoplasmic site for a sodium channel blocker (Alpert et al.). We examined such site-dependent effects of lidocaine (Lid), which were characterized by the concentration clamp and proton binding. The concentration was clamped within 50 msec positioning perfusion tubes so that their tips were close to the cell (< 50 μm). Sodium current was recorded at 19-21°C and 20 mM $[Na]_O$ in the whole cell clamp mode and its peak (I_{Na}) was used as an indicator of available sodium channels. The block during the concentration clamp of Lid (1 mM) was time-dependent, with the fast block (FB: < 0.5 sec) being followed by the slow block (SB: > 2 sec). The time constant of development of FB was 0.19 ± 0.1 sec (mean ± SD) which was determined by using various Lid clamp times. SB was independent of the frequency of the pulse train between 0.5 and 0.2 Hz. The voltage-dependence of availability was unaffected by FB (0.5-sec clamp) but shifted to the negative direction by SB (2-sec clamp). The additional 2-sec clamp of proton (pH = 6.3) to FB showed a further decrease of I_{Na} but not its clamping to SB. The present results suggested that FB and SB were due to the binding of Lid to the external and the internal sites of the cardiac cell membrane, respectively and that the latter interaction may limit proton access to sodium channels.

W-Pos421

EFFECTS OF TOCAINIDE ENANTIOMERS ON EXCITABILITY OF MYOTONIC GOAT SKELETAL MUSCLE FIBERS. ((D. Conte-Camerino and S.H. Bryant)) Dept. Farmacobiology, Faculty of Pharmacy, Univ. of Bari, Bari, Italy 70125 and Dept. Pharmacology and Cell Biophysics, Univ. Cincinnati, Cincinnati, OH 45267

Racemic Tocainide is effective in the treatment of human myotonia (Rüdel et al.,J.Neurol. 222:275, 1980). The R(-) and S(+) enantiomers of Tocainide were used in experiments reported here to test for stereospecificity in antagonizing the increased excitability of myotonic skeletal muscle fibers. Six external intercostal muscle preparations, removed under anesthesia from 4 congenitally myotonic goats, were studied in vitro at 32°C in a normal goat physiological solution. Excitability of individual fibers was measured by two micro-electrodes, one to inject current pulses, and the other to monitor action potentials. The current intensity at rheobase, the latency, the fraction of fibers responding spontaneously, the number of repetitive action potentials, during or following the pulse, were used to estimate the myotonic excitability of the fibers. Using these quantitative criteria, the R(-) enantiomer at 10 and 30 μM was very effective in restoring normal excitability to the myotonic fibers whereas, S(+) at 50 and 100 μM was essentially ineffective. For example, the maximum number of action potentials during a pulse was reduced by 75% in 10 μM R(-), but by only 19% in 50 μM S(+). We conclude that myotonia can be controlled by modulation of a highly stereospecific site on the SkM-1 Na+ channel (Trimmer et al.,Neuron 3:33, 1989), and this may prove important in the design of specific myotonia antagonists for therapy. (Grants: CNR 93-227, Telethon-Italy and USPHS NS-03178)

W-Pos422

DIFFERENCES IN STATE-DEPENDENT BINDING BETWEEN TWO SITE-3 NA CHANNEL TOXINS ((D.A. Hanck*, K.M. Blumenthal†, M.J. Gallagher†, and M.F. Sheets‡)) Univ. of Chicago, Chicago, IL*; Univ. of Cincinnati Col. of Med., Cincinnati, OH†; Northwestern Univ. Med. School, Chicago, IL‡

The sea anemone, *Anthopleura xanthogrammica*, produces two major Na channel peptide toxins, ApA and ApB, which bind extracellularly to voltage-dependent Na channels and produce slowing of inactivation. ApA toxin has greater than 10-fold higher affinity for cardiac Na channels than for neuronal Na channels when assayed by either binding, ^{22}Na flux, or by electrophysiology. The ApB isoform has nanomolar affinity for both isoforms of the channel when assayed by ^{22}Na flux. We report here on electrophysiological studies comparing the action of native ApA and recombinant ApB toxin on cardiac Na channels in canine Purkinje cells. For ApA toxin ED_{50} was 49 ± 12 nM, which was similar to the value of 14 ± 3 nM measured with veratridine-dependent uptake of ^{22}Na for cardiac Na channels in RT4-B cells. Modification, i.e. prolongation of the decay of the current, was prompt, e.g. at 85 nM modification occurred over 5-8 min. ED_{50} for ApB toxin was estimated to be 10 nM, similar to the value of 9 ± 3 nM measured by ^{22}Na flux. Despite the higher affinity, modification by ApB toxin occurred much more slowly than for ApA toxin, with full modification at the ED_{50} requiring >100 minutes. These data suggest that the on rate of ApB toxin to the closed conformation of the channel is at least three orders of magnitude slower than for ApA toxin. Work supported by HL-P01-20592 (DH), HL-R01-41543 (KB), and HL-R29-44630 (MS).

W-Pos423

TEMPERATURE DEPENDENCE OF NA CHANNEL BLOCK BY BIDISOMIDE. ((K. CHINN)) Searle, 4901 Searle Parkway, Skokie, IL 60077.

Bidisomide is a class 1 antiarrhythmic agent currently in phase III clinical trials. In the present studies, whole cell Na currents were examined from guinea pig ventricular myocytes. Current was evoked using stimulus pulses from -80 mV to -20 mV or -10 mV for 145 ms. Block by bidisomide was temperature dependent. 2.5 min. of exposure to an external solution containing bidisomide (100 μM) reduced Na current 6 ± 7% SEM (n=3) at 23°C and 30 ± 7% (n=3) at 34°C. Block at 34°C was 61% to 81% after 8.5 - 15.5 min. (n=3). Because Na channel block occurred over a period of minutes and was slower at 23°C than at 34°C, an internal site of drug action was explored. Unlike control experiments without bidisomide, in the presence of bidisomide (100 μM, 23°C) contained in the internal solution, Na current was observed to progressively decrease from maximal levels during the recording period. Current reduction from the maximum was 60 ± 12% (n=3) after 8.5 min. The results show that bidisomide block of Na channels occurs over several minutes and is temperature dependent. These effects may be due to slow access to an internal blocking site.

W-Pos424

POTASSIUM AND CALCIUM CHANNELS IN CULTURED HUMAN OSTEOBLAST-LIKE CELLS..

((C.E. Yellowley, A.J. Levi, *T.M. Skerry and J.C. Hancox)) Departments of Physiology and *Anatomy, School of Medical Sciences,Bristol University. U.K. (Spon. by J.F. Ashmore)

Little is known about the ion channels present in osteoblasts or about their role in bone cell physiology. We have investigated the electrophysiological characteristics of cultured human osteoblasts from the MG63 cell line using the whole cell configuration of the patch clamp technique. Until recently these cells proved extremely difficult to record from, but using a novel scraping method to prepare them for experiments, we have increased our success rate of patch clamp enormously. Cells were held at -40mV (zero current potential) and steps to more negative potentials elicited an inward current. This current was sensitive to block by external barium and enhanced by increased external K, features characteristic of an inward rectifier K current. On stepping from -40 to positive potentials (0, +30mV), the cells displayed a delayed rectifier K current. Stepping to more positive potentials (+60, +100mV) elicited a transient outward current. Both these outward currents were sensitive to potassium channel blockers and are greatly inactivated by setting the holding potential at 0mV. We also have preliminary evidence suggesting that these cells possess a low density of L-type calcium channels.

W-Pos425

COMPARATIVE EFFECTS OF NISOLDIPINE AND CADMIUM ON THE DELAYED RECTIFIER K^+ CURRENT (I_K) OF GUINEA PIG VENTRICULAR MYOCYTES.

((P. Daleau & J. Turgeon)) Quebec Heart Institute, Ste-Foy, PQ, Canada.

Inorganic compound (cadmium; Cd^{2+}) or dihydropyridine derivatives (such as nisoldipine; NIS) are used to block the slow inward Ca^{+2} current (I_{si}) during assessment of I_K of cardiac ventricular myocytes. Effects of these two I_{si}-blockers on I_K characteristics of guinea pig ventricular myocytes were compared in this study. Cells held at -40mV were superfused at 30°C either with Cd^{2+} 10^{-4}M (n=30) or NIS 2.10^{-7}M (n=10) containing solutions and currents measured in the whole cell configuration of the patch-clamp technique. I_K tail amplitude of voltage- and time-dependent currents were measured at -30mV after depolarization to test potentials (V_{test}, -20 to +50mV) for either 250 msec (I_{K250}) or 5 sec (I_{K5000}). Normalized I_{K250} tail currents plotted *vs* V_{test} showed that Cd^{2+} decreases relative tail amplitude at low V_{test} (-10mV and 0mV; $P < .05$) compared to NIS and experiments performed without Ca^{+2}-channel blockers. In contrast, normalized I/V curve of I_{K5000} were similar with either agents. Decay of tail current was slower in the presence of NIS (τ_i increased by 85±47% vs Cd^{2+} at 0mV V_{test}). This suggests that concentrations of NIS used to study I_K modify the gating properties of I_{K_r}. These results establish that block of I_{si} by both Cd^{2+} or NIS influences properties of I_K.

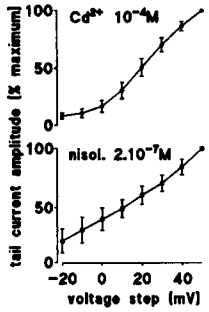

W-Pos426

TRANSIENT OUTWARD CURRENT IS MARKEDLY REDUCED IN SUBENDOCARDIAL PURKINJE CELLS FROM INFARCTED HEARTS.

Cynthia D. Jeck, Judith M.B. Pinto, Penelope A. Boyden, Department of Pharmacology, Columbia University, New York NY 10032

Altered electrical activity of subendocardial Purkinje (P) fibers contributes to arrhythmias in the 48 hour infarcted canine heart. We used whole cell voltage clamp techniques to study 4-aminopyridine (4-AP) sensitive transient outward currents (I_{to}) in control P cells isolated from subendocardial (n=12) and free running bundles (n=15). I_{to} in these two groups of control cells (NPC) did not differ. NPC I_{to} was compared to I_{to} of P myocytes from subendocardium of hearts 48 hrs post total coronary artery occlusion (IPC, n=12). I_{to} amplitude and current density were significantly reduced ($p<.01$) in IPC (1765±447pA, 9.7±2.6 pA/pF; x±SE) compared to NPC (2904±279pA, 20.2±1.8 pA/pF) at V_t=+55mV, V_h=-60mV. Decay of I_{to} was biexponential in all NPC, but monoexponential in 50% of IPC. Both NPC and IPC have a sustained 4-AP sensitive component (at 250 ms, V_t=+55mV: 4.2±.5pA/pF, 3.7±.7pA/pF, respectively). I_{to} voltage dependence of inactivation did not differ. In IPC, recovery of I_{to} was slowed. Significantly ($p<.05$) more I_{to} was seen with rapid pacing in NPC (CL 5000ms=100%, CL 1300ms=73%, CL 300ms=46%) than in IPC (CL 5000ms=100%, CL 1300ms=58%, CL 300ms=31%). In 3 IPC cells no I_{to} was seen at CL=300ms. Thus, I_{to} plays a major role in NPC electrophysiology, contributing both a large transient and sustained component. In Purkinje cells that survive in the infarcted heart (IPC), I_{to} is markedly reduced thus contributing less outward current to repolarization, especially at rapid pacing rates.

W-Pos427

VOLTAGE-ACTIVATED POTASSIUM CURRENTS OF RABBIT OSTEOCLASTS: EFFECTS OF EXTRACELLULAR CALCIUM.

((L.G. Hammerland, A.S. Parihar, E.F. Nemeth and M.C. Sanguinetti)) NPS Pharmaceuticals, Salt Lake City, UT 84108.

During bone resorption, osteoclasts are probably exposed to high concentrations of extracellular calcium ($[Ca^{2+}]_e$) resulting from dissolution of mineralized matrix. In vitro studies show that increasing $[Ca^{2+}]_e$ can inhibit osteoclastic bone resorption, although how $[Ca^{2+}]_e$ acts is unknown. We examined the effects of increased $[Ca^{2+}]_e$ on a delayed outward rectifier K^+ current (I_K) and an inward rectifier K^+ current (I_{K1}) in rabbit osteoclasts to determine whether increased $[Ca^{2+}]_e$ affects these currents in manner suggesting a role for these channels in the control of bone resorption. Under whole cell voltage clamp a majority of rounded osteoclasts showed a large I_K that averaged 65.5±12.7 pA/pF at a test potential of -10 mV. The current was blocked by 4-aminopyridine (10 mM) and charybdotoxin (IC_{50} = 2.2 nM). The elevation of $[Ca^{2+}]_e$ from 1.8 mM to 18 mM caused a shift in the half-point for I_K activation by +11.5 mV, and in the voltage-dependence of deactivation by +13 mV. Resting membrane potential was also shifted by an average of +10 mV. Elevation of $[Mg^{2+}]_e$ from 1.8 mM to 18 mM or the lowering of extracellular pH from 7.3 to 6.5 also caused a positive shift in the voltage dependence of I_K activation. Osteoclasts expressing I_{K1} had an average current magnitude of 21.2±3.0 pA/pF at -130 mV that was reduced by 39% when $[Ca^{2+}]e$ was elevated from 1.8 to 18 mM. These effects on I_K and I_{K1} can be explained by a simple screening of cell surface negative charges by the various cations. Thus, the effects of $[Ca^{2+}]_e$ on bone resorption do not appear to involve these prominent K^+ channels.

W-Pos428

KETANSERIN INHIBITS DEPOLARIZATION-ACTIVATED OUTWARD K^+ CURRENT IN RAT VENTRICULAR MYOCYTES.

((Z.H. Zhang, M. Boutjdir, and N. El Sherif)) SUNY/ Health Science and V.A Medical Centers, Brooklyn, NY 11209. (Spon. by M. Boutjdir)

Ketanserin (KT), an antihypertensive agent, has been shown to prolong action potential duration (APD) and Q-T interval and to induce *torsade de pointes* in some patients. We previously suggested that the prolongation of APD could be due to KT inhibition of the fast component of delayed rectifier, I_{K_r}, in guinea-pig myocytes. However, in other tissues including human atrial and rat ventricular cells, the transient outward current (I_{to}) is one of the major repolarizing currents. We investigated the possibility that KT could also increase APD by blocking I_{to} in rat ventricular myocytes using whole cell patch clamp techniques. KT (50 μM) significantly prolonged APD_{50} by 55.4%, and APD_{90} by 78.8%. Time-dependent I_{to} was measured in the presence of 400 nM nisoldipine during depolarizing pulses to 40 mV from a holding potential of -100 mV every 10 sec. KT resulted in a concentration-dependent inhibition of I_{to} with EC_{50}=5.2 μM. The inhibitory effect of KT (10 μM) was seen at voltages from 0 to 80 mV without any shift of the I-V relationship of peak I_{to}. KT did not significantly change neither inactivation nor reactivation curves of I_{to}. Kinetic analysis of I_{to} showed a biexponential fit of inactivation in 80.5 % of total traces studied at voltages between -30 to 80 mV (n=149, R=0.99±0.01). The charge areas of fast (Q_f) and slow (Q_s) components of I_{to} were evaluated by integration. The inhibitory effect of KT was more prominent on Q_s than Q_f (Q_f=33.2±6.2 and Q_s=235.5±7.4 Sec·pA for control, and 12.4±4.3 and 59.6±17 for KT at 40 mV, n=4). KT had no significant effect on both I_{K1} and I_{Ca}. We conclude that: 1) KT exerted an open channel block on I_{to} and accelerated the inactivation of I_{to} as a result of its potent block of Q_S; 2) KT prolongation of APD is not only mediated primarily through I_K block but also through inhibition of I_{to} especially in cells where I_{to} is prominent. KT block of K outward currents in the heart could participate in the Q-T prolongation reported in patients treated with KT.

W-Pos429

SIMULTANEOUS $[Ca^{2+}]_i$ AND K^+ CHANNEL MEASUREMENTS IN HUMAN T LYMPHOCYTES.

((Jos A.H. Verheugen[a], Marga Oortgiesen[a], Michael D. Cahalan[b])) [a]Research Institute for Toxicology, Utrecht University, Utrecht, The Netherlands and [b]Department of Physiology and Biophysics, University of California, Irvine, CA

Currents from Ca^{2+}-activated K^+ (K(Ca)) channels of activated human T lymphocytes were recorded using the cell-attached configuration of the patch clamp technique, with a high K^+ solution in the pipette. Simultaneous measurements of the intracellular $[Ca^{2+}]$ of the same cell were obtained using Fura-2. The K(Ca) channels displayed a single channel conductance of 46 pS. By manipulating the $[Ca^{2+}]_i$ with ionomycine (1-5 μM) we determined the Ca^{2+}-sensitivity of these channels: EC50 of 450 nM. In response to acute stimulation of the T cell receptor/CD3 complex by PHA (10 μM), a rise in $[Ca^{2+}]_i$ was observed concomitant with an increase in K(Ca) channel activity. In addition, the single channel amplitude increased in parallel with the K(Ca) channel activity, indicating a membrane hyperpolarization. The data indicate that stimulation of the T-cell receptor raises $[Ca^{2+}]_i$ which in turn activates K(Ca) channels, resulting in membrane hyperpolarization.

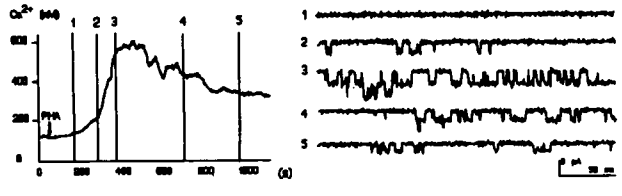

W-Pos430

SMALL CONDUCTANCE K+ CHANNEL IN DEVELOPING RAT SKELETAL MUSCLE FIBERS

((D. Tricarico & D. Conte-Camerino)) Unit of Pharmacology, Department of Pharmacobiology, Faculty of Pharmacy, University of Bari, Via Orabona 4, 70125 Bari, ITALY.

The population of K+ channels present on the surface membrane of skeletal muscle fibers from developing (59-82 days old) and young adult (5-7 months old) male Wistar rats, was surveyed by using patch clamp technique. In particular, our studies were focused on K+ channels responsible for the resting macroscopic conductance (Conte-Camerino et al., Pflügers Archiv, 413: 568, 1989). Single fibers were isolated enzymatically at 30° C from Flexor Digitorum Longus toe muscle of the rat. Continuous recording of the channel activity was performed in Cell-attached (C-A) and Inside-out patch (I-O) configuration at steady state at 20 °C in symmetrical KCl (150 mM). Six out of six and two out of two C-A patches performed, respectively, on 59 and 82 day old rat muscle fibers, showed a K^+ channel with a slope conductance of 37±2 pS. A minimum of 3-4 channels per patch area were observed. The estimated open probability (P_{open}) of the channel was 0.19 at -20 mV ΔVm. The channel showed a slow gating process (see trace below), and did not show voltage dependency. When the bath solution was enriched with 5 mM EGTA, the excision of the patch from the fiber led to the loss of channel activity.

C-A recording; HP:-40 mV ΔVm; acquisition rate 20kHz; filter 2 kHz (-3dB).

This small conductance K+ channel was never observed in the 5-7 month old rat muscle fibers, suggesting that its expression in the sarcolemma is correlated with the developing process. Small conductance K+ channels have been characterized in cultured rat skeletal muscle (Blatz & Magleby, Nature, 323: 718, 1986). In our experiments, the high frequency of occurrance of this type of channel, led us to believe that it may substantially contribute to the macroscopic resting K+ conductance in developing rat skeletal muscle. (CNR 93-227)

W-Pos431

TEMPERATURE EFFECTS ON K CHANNELS IN GUARD CELL PROTOPLASTS FROM THE BROAD BEAN

((Nitza Ilan*, Amnon Schwartz* and Nava Moran#)) *Faculty of Agriculture, Hebrew University, Jerusalem and #Dept. Neurobiology, Weizmann Inst. Rehovot 76100 Israel.

High temperature (>32°C) promotes the opening of stomata which control the exchange of gases in plant leaves. Since the changes in stomatal aperture reflect the balance of K^+ fluxes via K channels into and out of stomatal guard cells, we examined the effects of temperature changes (13-36°C) on the activity of K channels in the guard cell plasma membrane using patch-clamp. In a whole cell configuration, elevation of the temperature shortened 2- 10-fold the time constants of channel activation and deactivation of both Depolarization-activated K channels (K_D channels) and Hyperpolarization-activated channels (K_H channels) in a monotonic fashion. The temperature dependence of the K_H channels steady-state conductance, $G_{K\text{-}H}$, was monotonic and saturated at ~28°C (at ~8 nS). In contrast, that of the K_D channels, $G_{K\text{-}D}$, had an optimum (~4 nS) at ~20°C. The $G_{K\text{-}H}$ (at -217 mV) increased by ~60% and the $G_{K\text{-}D}$ (at 63 mV) increased by ~70% with temperature change from 13°C to 20°C. However, further heating from 20 to 36°C, increased $G_{K\text{-}H}$ additionally by ~30%, but dramatically decreased $G_{K\text{-}D}$ to 20% of maximum. Thus, at the higher temperatures two processes prevent the closure of stomata: the inhibition of the K_D channel which normally serves as the pathway for K^+ efflux, and the promotion of activity of the K_H channel, which normally serves as the pathway for K^+ uptake. In outside-out patches we did not observe changes in the single channel conductance sufficient to explain the observed changes in GK. We suggest that changes in the gating kinetics are the underlying mechanism of temperature effects.

W-Pos432

DEVELOPMENTAL CHANGES IN POTASSIUM CURRENTS RECORDED FROM HUMAN ATRIAL MYOCYTES

((C.W. Clarkson, W.J. Crumb Jr., J.D. Pigott, and A.M. Brown)) Tulane School of Medicine, New Orleans, LA and Baylor College of Medicine, Houston, TX; supported by HL 37044 (A.M.B.) and HL 36096 (C.W.C.)

There is evidence in humans for developmental changes in the morphology of the atrial action potential. The reasons for such changes are not clear. We therefore characterized the potassium currents recorded at room temperature from isolated atrial myocytes obtained from neonatal (3-7 days old) and adult (28-72 yrs old) human hearts. In 10 of 10 adult myocytes (C_m = 132.25 ± 11.88 pF) (mean ± SEM), depolarizing pulses to +40 mV (V_{hold} = -40 mV, 320 ms) elicited a rapidly activating current which decayed to an apparent steady-state. The peak of this current reflects a combination of I_{to} (current density = 6.49 ± 0.63 pA/pF) and a rapidly activating, slowly inactivating potassium current, I_{Kur}. In contrast to adult, neonatal atrial myocytes (C_m = 58.76 ± 2.69 pF, n = 9) displayed only a rapidly activating, slowly inactivating current (0.69 ± 0.16 pA/pF, n = 8). Activation time constants ranged from 3.87 ± 0.38 ms at +20 mV to 1.69 ± 0.18 ms at +60 mV (n = 5-10), very similar to values reported for I_{Kur} recorded from adult human atrial myocytes. A current similar to I_{to} was absent in 10 of 10 neonatal cells. In addition to developmental differences in I_{to}, there were also differences in the inwardly rectifying potassium current, I_{K1}. Current density measured at -100 mV (V_{hold} = -40 mV) in neonatal atrial myocytes was 0.89 ± 0.09 pA/pF (n = 4) whereas in adults it was twofold greater, 1.76 ± 0.38 pA/pF (n = 7). In summary, neonatal atrial myocytes display:1) a current similar to I_{Kur} observed in adult cells, 2) a significantly lower density of I_{K1} vs. adult cells, and 3) an absence, or extremely low expression of I_{to} compared to adult myocytes. These developmental differences in the presence of potassium currents provides an explaination for the reported changes in action potential morphology which occur with age.

W-Pos433

EFFECTS OF NE-10064 ON K^+ CURRENTS IN CARDIAC CELLS.

((Mary Lee Conder, Mark A. Smith, Karnail S. Atwal and John R. McCullough)), Bristol-Myers Squibb Pharmaceutical Research Institute, Princeton, NJ 08543-4000. (Spon. N.J. Lodge)

The effects of NE-10064, (E)-1-[((5-(4-chlorophenyl)-2-furanyl] methylene]amino]-3-[4-(4-methyl-1-piperazinyl)-butyl-2,4-imidazoldinedione di-HCl, a new Class III antiarryhthmic, were studied on inward rectifier (IK1), transient outward current (Ito) and the rapid component of the delayed rectifier (IKr) in guinea pig (GPVM) and canine (CVM) ventricular myocytes by using whole cell patch-clamp techniques. Experimental conditions were selected to study each current in isolation of other ionic currents and electrogenic processes. NE-10064 significantly inhibited IK1 (measured at -110 mV) in GPVM at a threshold concentration of 1 μM (-2.8 ± 0.3 nA vs. -2.3 ± 0.2 nA, $p<0.05$, n=5). Higher concentrations (3-10 μM) significantly inhibited both inward and outward current through IK1. In CVM, IK1 at -110 mV was significantly inhibited by 10 μM NE-10064 (-2.1 ± 0.1 nA vs. -1.5 ± 0.2 nA, $p<0.05$, n=5). In CVM, little or no inhibition of Ito was observed at concentrations ≤ 100 μM (n=5). In GPVM, NE-10064 inhibited IKr with an IC_{50} ≈0.2 μM (n = 6-8). NE-10064 also inhibits the slow component of the delayed rectifier (IKs) with an IC_{50} ≈2 μM (Smith, Conder and McCullough, this meeting; Busch et al., Circulation 88:I-231, 1993). These results indicated that NE-10064 inhibits a number of cardiac K^+ channels which may account for its Class III activity.

W-Pos434

MODULATION OF K^+ CHANNELS OF CANINE CORONARY ARTERY SMOOTH MUSCLE CELLS BY NS-004 AND FENAMATES

X. Xu, T.D. Tsai, J. Wang, E.W. Lee and K.S. Lee. Cardiovascular Diseases Research, Upjohn Laboratories, Kalamazoo, MI 49007

K^+ channels of dog coronary artery smooth muscle cells were studied using suction pipette method. Step depolarizations positive to -30 mV from -60 mV holding potential elicited a low threshold, slowly inactivating, Ca^{2+}-insensitive K^+ current (I_K) and a high threshold (20 mV), non-inactivating, Ca^{2+} activated K^+ current (I_{KCa}). I_{KCa} was studied at 0 mV holding potential that selectively inactivated I_K, while I_K was recorded at depolarizations below 20 mV from -60 mV holding potential to minimize the contamination from I_{KCa}. Both I_K and I_{KCa} were modulated by NS-004, a Ca^{2+} activated K^+ channel opener, and structurally related anti-inflammatory agents of the fenamate group (flufenamic, niflumic and mefenamic acids). External NS-004 and all three fenamates activated I_{KCa} which was reversed upon washout or by 1 mM TEA. I_{KCa} at 80 mV was increased from 0.34 ± 0.02 nA to 4.5 ± 1.4 nA and 8.2 ± 0.4 nA (n=4) in 25 μM and 50 μM NS-004, respectively. The fenamates, though less potent, also increased I_{KCa} at 80 mV from 0.30 ± 0.07 nA to 3.1 ± 1.0 nA (n=4) by flufenamic, from 0.20 ± 0.03 nA to 1.7 ± 0.5 nA (n=5) by niflumic, and from 0.24 ± 0.03 nA to 1.2 ± 0.5 nA (n=5) by mefenamic at 100 μM. Therefore, NS-004 is a much more potent Ca^{2+} activated K^+ channel opener than the three fenamates. In contrast to the activating effect on I_{KCa}, NS-004 inhibited I_K as well, starting at 2 μM and reached 50% inhibition at 22 μM. While niflumic acid, at 100 μM, shifted I_K activation threshold by about 5 mV negative and accelerated its inactivation time course. These compounds may represent a new class of vasodilators that target the I_{KCa} channels instead of the ATP-inhibited K^+ channels.

W-Pos435

KINETIC ANALYSIS OF VOLTAGE-DEPENDENT POTASSIUM CURRENTS IN MOUSE NEUROBLASTOMA CELLS.

((J.K.W. Blandino and D.W. Johns)) Cardiovascular Division, University of Virginia School of Medicine, Charlottesville, VA 22908.

The voltage-dependent potassium current (I_k) of differentiated mouse neuroblastoma (Neuro-2A) cells were studied using the whole-cell patch-clamp recording technique. I_{Ca} was not seen in bath solutions containing 10mM calcium nor up to 50mM barium after suppressing I_{Na} and I_k simultaneously. I_k was examined in the presence of 5μM tetrodotoxin. From a holding potential of -80mV, I_k activated at test potential greater than -30 mV and exhibited no inactivation with a 40ms pulse. Internal application of TEA (20mM) and CsCl (120mM) eliminated I_k as did external application of TEA (15mM). Using tail current analysis, the reversal potential was between -100 and -90 mV, which approximated the Nernst potential (103mV) for K^+ ions, with $[K^+]_i$=155.7mM and $[K^+]_o$ =2.8 mM.

For a step potential to +90mV, I_k reached 278±30pA and cell membrane capacitance was 15±1pF (mean±sem, n= 24). The activation of I_k followed n^4 kinetics of the Hodgkin-Huxley activation model. Activation time constants decreased with increasing depolarization. With 200ms depolarizing current, I_k inactivated with a single exponential decay and a time constant of 918±173ms (n=7). Thus, Neuro-2A cells exhibit voltage-dependent potassium currents with characteristics of a delayed outward rectifier.

W-Pos436

Zn^{2+} IONS DIFFERENTIALLY AFFECT INWARD RECTIFIERS IN HIPPOCAMPAL NEURONS AND RBL-1 CELLS.

((Simon J. Gibbons and Neil L. Harrison.)) Depts. of Anes. and Crit. Care & Pharm. and Phys. Sci., U. of Chicago, Chicago Il 60637. (Spon. by M. Villereal)

We have observed that application of Zn^{2+} ions to cultured rat hippocampal neurons during whole cell recordings causes an increase in input resistance. We have studied two hyperpolarization-activated currents in neurons, a fast inward rectifier (FIR) which conducts K^+ and a more slowly activating mixed cation conductance (I_Q). We have also studied a rapidly activating inward rectifier in the rat basophilic leukemia cell line (RBL-1). Whole cell recordings were made at 25°C using intracellular solutions based on K gluconate (2mM Mg^{2+}, 20nM Ca^{2+}) and continuous extracellular perfusion with HEPES-buffered saline. For recording FIR currents we used an extracellular solution containing 50mM K^+, 0.2mM Ca^{2+}, 2.3 Mg^{2+}, 20 TEA^+, 10μM DNQX and 0.5μM TTX. Neurons were held at -20mV. 200μM Zn^{2+} caused a reduction in slope conductance (measured at -70mV) by 34.4 ± 5.8% (mean ± SEM, n=5). 10mM Cs^+ caused a qualitatively similar but larger effect on the same cells (71.1 ± 10.6%). The slowly activating I_Q and the inward rectifier current in RBL-1 cells were unaffected by 200μM Zn^{2+} but blocked by 10mM Cs^+. We suggest that the effect of Zn^{2+} on hippocampal neuronal input resistance is mediated by inhibition of FIR current. The effect of Zn^{2+} is not observed on all inward rectifiers suggesting that there is a specific Zn^{2+} binding site on the FIR channel.

SJG is supported by DHHS training grant # DA 07255-02

W-Pos437

SLOW Ca^{2+}-DEPENDENT K^+ CURRENT IN CULTURED BULLFROG SYMPATHETIC GANGLION NEURONS.

((S.D. Hochertman and P.R. Adams)) HHMI and Dept. of Neurobiology and Behavior, SUNY at Stony Brook, NY 11794-5230.

A slow Ca^{2+}-dependent K current (I_{AHP}) of the order of 1nA is responsible for the afterhyperpolarization of sympathetic neurons of intact bullfrog ganglia (Pennefather et al., 1985, PNAS 82:3040). This current has not been reported in neurons dissociated according to Kuffler and Sejnowski (1983), kept in culture in the presence of serum at 8°C. We have attempted to record this current in a variety of conditions to try to account for the apparent loss of this current. Currents elicited by trains of action potentials of varying durations were recorded in hybrid clamp mode.

In the standard culture conditions outlined above, perforated patch recordings reveal an I_{AHP} with a time course similar to neurons in the intact ganglion but with amplitude reduced to roughly 0.1nA at a holding potential of -55mV. Whole cell recordings with internal solutions containing 0.1 mM EGTA show currents of the same magnitude but faster time course. These currents can be blocked reversibly by removal of Ca^{2+} from the external medium or by application of d-tubocurarine (0.2 mM). The reduction in current may be due partly to the removal of the axon during the dissociation procedure. This loss can be reversed by changing culture conditions. Cells kept at room temperature without serum, either in the presence or in the absence of NGF, tend to grow processes. In cells with processes, I_{AHP}s of up to 0.7nA can be measured. These currents decay with time constants comparable to intact ganglion neurons even in whole cell recordings. In collaboration with D. O'Malley, Ca transients under these various conditions are being studied using Fluo-3 and confocal microscopy. In these experiments calcium signals were recorded in the processes as well as the soma. These findings indicate that the growth of the cell in culture is accompanied by expression of new channels and suggest that the geometry of the cell may play a role in the time course of I_{AHP}.

W-Pos438

NOISE ANALYSIS OF THE SLOW I_{AHP} MEASURED DURING WHOLE-CELL RECORDINGS FROM DENTATE GRANULE CELLS OF THE HIPPOCAMPUS.

(Valiante T.A., Abdul-Ghani M.A., Pennefather P.S., and Carlen P.L.) MRC Group Nerve Cell and Synapse, University of Toronto. (Spon. by M.A. Abdul-Ghani).

The slow afterhyperpolarization current (I_{AHP}) is important in controlling neuronal excitability. Many neurotransmitters and neuromodulators can alter neuronal behaviour through modulation of I_{AHP}. To understand the mechanism by which I_{AHP} is altered, it is important to be able to examine single channel properties. We have performed noise analysis on I_{AHP} recorded in dentate granule cells in slices of the rat hippocampus at -45 mV using the whole-cell configuration of the patch clamp technique. I_{AHP} was evoked by 200 ms voltage-clamp commands to 0 mV in 4.5 mM K^+_{out}/140 K^+_{in}. Background variance was around 60 pA^2. The extra noise during I_{AHP} was linear with current amplitude suggesting a low open probability even at the peak of I_{AHP}. The current variance to mean amplitude ratio suggests that I_{AHP} is generated by a 0.2 pA channel under these conditions. Power spectra of the current fluctuations yielded an estimated mean channel open time of 6 msec.

Acknowledgements: T.A.V. is an MRC student and M.A.G. is an MRC fellow. Research was supported by an MRC Group Grant to P.L.C.

W-Pos439

ROLE OF TRANSIENT OUTWARD K^+ CURRENT IN OPOSSUM ESOPHAGEAL CIRCULAR MUSCLE.

((H.I. Akbarali, N. Hatakeyama, Q. Wang, J. Saha and R..K. Goyal)). G.I. Division, Harvard Medical School & Beth Israel Hospital. Boston.

In the esophageal circular muscle, Ca^{2+} spikes superimposed on EJP's, provide Ca^{2+} entry for esophageal contraction. In the present study, a fast-inactivating K^+ current (I_{TO}) was studied with respect to its properties and modulation of action potentials in esophageal circular muscle cells. I_{TO} was resolved from -80 mV holding potential in the presence of TEA (30 mM). The transient current activated around -40 mV and were identified as K^+ currents from tail current analysis. 4-AP (3 mM) completely abolished I_{TO}. The availaibility curve showed a $V_{0.5}$ of -66mV with a slope factor of 8.3. Inactivation was monoexponential between -20 and 0 mV and showed little voltage dependence. In the current clamp mode, 4AP (3 mM) depolarized by 6 mV and reduced the time to peak of the action potential (Fig). These results suggest that I_{TO} modulates the rate of action potential discharge in this smooth muscle and may be involved in the latency and amplitude of peristaltic contraction.

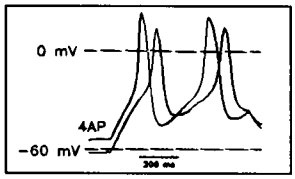

W-Pos440

INWARD-RECTIFIER K^+ CURRENTS FROM RAT CORONARY ARTERY SMOOTH MUSCLE CELLS.

((Adrian Bonev, Blair E. Robertson, and Mark T. Nelson)). Univ. of Vermont, Dept. of Pharmacology, Medical Research Facility, Colchester, VT 05446

Currents showing inward rectification were identified using the whole-cell patch-clamp technique on cells isolated from rat septal coronary artery smooth muscle. At potentials negative to the potassium equilibrium potential (E_K) large inward currents were observed, with only small outward currents positive to E_K. Changing external K^+ (mM; 6, 60, 140) with a constant internal K^+ concentration (140mM) shifted $E_{reversal}$ from -78.3 to -19.7 and -1.2mV respectively, suggesting the current observed was indeed a potassium current. The current was inhibited by μM concentrations of external Ba^{2+} (Fig. 1.) with a half-block constant (K_d) at -100mV of 0.5μM, increasing *e*-fold every 25mV, confirming Ba^{2+} as a potent blocker of this channel at these concentrations. The currents were inhibited less effectively by Cs^+ (K_d at -100mV, 43.4μM), and were not affected by 1mM TEA, 1mM 4-AP, or 10μM glibenclamide. Both Ba^{2+} and Cs^+ block increased at more negative potentials. The time-constant for the development of block at -100mV and 10μM Ba^{2+} was 55ms, decreasing at more positive potentials and lower $[Ba^{2+}]$.

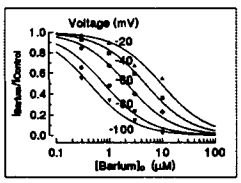

Fig.1. Fractional inhibition of Ba^{2+} current.

These results, along with whole vessel experiments (see Knot, Zimmermann & Nelson this meeting), suggest that these channels may be involved in the regulation of vascular smooth muscle cell membrane potential, and hence vessel diameter. Indeed increasing external potassium (1-20mM) dilates cerebral and coronary vessels which may result from activation of inward rectifier K^+ channels.

BER is an International Research Fellow of the AHA. Supported by the NSF.

W-Pos441

EFFECTS OF EXTRACELLULAR CATIONS ON Kv1.3 IN MAMMALIAN OSTEOCLASTS

((Stuart A. Arkett, S. Jeffrey Dixon and Stephen M. Sims)) Dept of Physiology, Univ. Western Ontario, London, Canada. N6A 5C1

Bone resorption by osteoclasts involves the transport of H^+ into the resorption lacuna, leading to the dissolution of bone mineral and liberation of free Ca^{2+}. Changes in the ionic milieu of cells are known to affect properties of voltage-gated ion channels. Furthermore, elevation of $[Ca^{2+}]_o$ and changes in extracellular pH have been shown to influence osteoclastic bone resorption *in vitro*. Therefore, we examined effects of extracellular Ca^{2+} and H^+ on K^+ currents in isolated rat osteoclasts using patch-clamp techniques. In control saline (1 mM Ca^{2+}, pH 7.4), a transient K^+ current with properties of Kv1.3 activates at -45 mV with half-activation ($V_{0.5}$) at -29 mV. Increasing $[Ca^{2+}]_o$ rapidly and reversibly shifted the current-voltage (I-V) relation to more positive potentials, due to a positive shift of the K^+ current activation range. Current at $V_{0.5}$ decreased to 28% and 9% of control current at 5 and 10 mM $[Ca^{2+}]_o$, respectively. Reducing $[Ca^{2+}]_o$ to 0.2 mM shifted the I-V relation to more negative potentials. Increase of pH_o (from 7.4 to 8) shifted the I-V negatively, whereas decrease of pH_o (from 7.4 to 6.8 or 5.3) shifted the I-V to more positive potentials. Changes in surface charge can account for the effects of Ca^{2+} and H^+ on the voltage activation of the outwardly rectifying K^+ channel. Such surface charge effects are common to most voltage-gated ion channels. Changes in K^+ channel activity and membrane potential may be one mechanism by which extracellular cations influence osteoclastic bone resorption.

Supported by The Arthritis Society and Medical Research Council (Canada).

W-Pos442

ACETYLCHOLINE RECEPTOR AND INWARD RECTIFIER CHANNELS IN EMBRYONIC SKELETAL MUSCLE CELLS. ((P. Moody-Corbett and S. Hancock)) Basic Med. Sci., Memorial University, St. John's NF A1B 3V6

Acetylcholine receptors (AChRs) and K+ channels are very early membrane components of embryonic skeletal muscle, however the distribution of these channels relative to each other has not been examined. In the present study single channel recordings were used to examine the distribution of AChR channels with respect to K+ inward rectifier (IR) channels in embryonic muscle cells. The cells were isolated from 1 day old *Xenopus* embryos and grown on collagen-coated coverslips in culture for up to 1 day. Single channel currents were recorded in cell-attached patches using a List patch clamp. The electrode contained (in mM) 140 KCl, 1 BAPTA, 5 $MgCl_2$, 10 HEPES (pH 7.4) and the external recording solution contained (in mM) 140 NaCl, 5 KCl, 1.2 $MgCl_2$, $CaCl_2$, 10 HEPES (pH 7.4). In the absence of ACh in the electrode membrane patches showed 1 or 2 classes of IR channels. In 50% of these patches (n=77) 2 other classes of channels were apparent which by kinetics and conductance resembled the 2 classes of AChR channels. In 20 patches of membrane examined with 0.1 μM ACh in the electrode every patch contained both IR and AChR channels. These results indicate that AChR channels and IR channels are in close spatial association.

W-Pos443

KINETIC ANALYSIS OF THE CARDIAC TRANSIENT OUTWARD POTASSIUM CURRENTS IN RODENT MODELS OF DIABETES ((J. Magyar, Z. Cseresnyés, I. Sipos, G Szücs, L. Kovács)) Department of Physiology, University Medical School of Debrecen, Debrecen, Hungary

The transient outward potassium current (I_{to}) in ventricular cells of spontaneously diabetic rats (BB/Wor) and mice (ob/ob) was measured in whole-cell configuration. There was no significant difference between the non-diabetic and diabetic BB rats (Type I diabetes, IDDM) in the amplitude, the rate of recovery from inactivation and the voltage dependence of activation of I_{to}. Steady-state inactivation in the non-diabetic animals was shifted towards more positive voltages. The inactivation of I_{to} and the transition rate from open to inactivated states of the channel were accelerated in diabetic BB rats, while the inactive to open transitions did not change. The amplitudes and the steady-state inactivation of I_{to} of the lean and obese mice (Type II diabetes, NIDDM) were the same. The voltage dependence of the activation and the transition rate from closed to opened state of the channel were significantly faster in obese mice, while the inactivation and the transition rate from opened to closed states of their I_{to} are significantly slower. The recovery from inactivation of I_{to} was also slower in obese mice. The results indicate that some cardiac electrophysiological changes described for streptozotocin-induced diabetes are also present in genetically diabetic rodents.

Supported by grants from the Hungarian Science Foundation (OTKA 1453) and from the Ministry of Welfare (ETT T-473/90).

W-Pos444

HYPOXIC INHIBITION OF A Ca^{2+}_i - SENSITIVE DELAYED RECTIFIER K^+ CHANNEL IN CANINE PULMONARY ARTERY CELLS. ((J.M. Post, C.H. Gelband and J.R. Hume)) Department of Physiology, University of Nevada, Reno NV 89557-0046.

A possible mechanism responsible for hypoxic pulmonary vasoconstriction (HPV) involves inhibition of K^+ currents causing membrane depolarization, Ca^{2+} influx and contraction. Our previous study (AJP 262:C882, 1992) implicated a Ca^{2+}_i-sensitive K^+ channel in HPV, since hypoxic inhibition of whole-cell K^+ currents was reduced when Ca^{2+}_i was buffered with $BAPTA_i$. Although the exact type of K^+ channel involved in HPV has not yet been identified, a recent report (AJP 264:L323, 1993) suggests that an important initial event in HPV is release of Ca^{2+} from intracellular stores. We performed experiments on isolated pulmonary arterial cells to assess the effects of hypoxia on the two predominent types of Ca^{2+}_i-sensitive K^+ channels present: large conductance, Ca^{2+}_i-activated K^+ channels and smaller conductance, delayed rectifier K^+ channels, which are inhibited by intracellular divalent cations (Circ. Res. 73:24, 1993). Whole-cell K^+ currents could be divided into a 4-AP-sensitive (1mM), low noise, low threshold current and a TEA (1 mM)- and charybdotoxin-sensitive, high noise, high threshold current. Na-dithionite induced hypoxia (pO_2 ≈ 5 mmHg) inhibited the low threshold, low noise K^+ current, which was prevented by pretreatment with 4-AP (1mM); pretreatment of cells with TEA (1mM) failed to prevent hypoxic inhibition of K^+ currents. The effects of hypoxia on K^+ currents were mimicked by acute exposure of cells to caffeine, and both effects were prevented by buffering $[Ca^{2+}]_i$ with BAPTA (10 mM). In inside-out membrane patches, switching from normoxia to hypoxia failed to consistently alter N*p(open) of the large conductance Ca^{2+}-activated K^+ channel. A 4-AP-sensitive 25 pS K^+ channel (physiological K^+ gradient) was identified and N*p(open) of this channel was reduced from 0.72 to 0.28 by Mg^{2+} (1 mM, 0 mV, n=3) applied to the cytoplasmic surface. We conclude that hypoxic-induced mobilization of $[Ca^{2+}]_i$ and subsequent inhibition of 4-AP-sensitive delayed rectifier K^+ channels may play a key initial role in HPV. (Supported by AHA Nevada Affiliate and NIH HL49254).

W-Pos445

AGONIST-INDUCED DEPOLARIZATION OF RENAL ARTERY: Ca^{2+}_i INHIBITION OF $I_{K(dr)}$. ((Craig H. Gelband and Joseph R. Hume)) Department of Physiology, University of Nevada School of Medicine, Reno, NV 89557.

We have previously demonstrated that increasing intracellular divalent cations in vascular smooth muscle cells causes depolarization via an inhibition of delayed rectifier K^+ channels ($I_{K(dr)}$, *Circ. Res.* 1993;73:24). In tissue bath experiments with canine renal artery, KCl (80 mM), angiotensin II (Ang II, 100 nM), caffeine (10 mM), and 4-aminopyridine (4-AP, 1-10 mM) caused contraction in Ca^{2+} containing PSS. However, in Ca^{2+}-free (2 mM EGTA) PSS, Ang II and caffeine caused a transient contraction, while KCl and 4-AP had no effect. These data suggest that intracellular Ca^{2+} is released by Ang II and caffeine. During voltage clamp experiments, Ang II or caffeine caused a biphasic effect: reduction of $I_{K(dr)}$ and an increase in $I_{K(Ca)}$. The two effects could be pharmacologically separated. With 4-AP (10 mM) present to inhibit $I_{K(dr)}$, Ang II and caffeine increased $I_{K(Ca)}$ by shifting the activation curve -13 ± 5 mV (n=3). Conversely, with charybdotoxin (ChTX, 100 nM) present to inhibit $I_{K(Ca)}$, Ang II and caffeine only caused inhibition of $I_{K(dr)}$. Block was achieved within 15 seconds of drug application and was reversible upon washout (n=3). Intracellular BAPTA (10 mM) abolished the effects of Ang II and caffeine. In current clamp experiments, the application of ChTX (100 nM) and niflumic acid (100 μM, an inhibitor of Ca^{2+}-activated Cl^- current) caused little change in resting membrane potential, however, subsequent application of caffeine (10 mM) caused a 26 ± 2.9 mV depolarization from -54 ± 3.1 to -28 ± 1.7 mV (n=3). 4-AP (10 mM) blocked the caffeine-induced depolarization. These results suggest that an increase in intracellular Ca^{2+} can alter membrane potential via regulation of $I_{K(dr)}$. (Supported by NIH grants HL-08531 and HL-49254).

W-Pos446

EFFECT OF TEMPERATURE ON SINGLE IONIC CHANNEL ACTIVITY IN MUSCLE FIBERS FROM A TROPICAL AMPHIBIAN. ((Betsy Navarro and Carlo Caputo)) CBB,IVIC, Caracas,Venezuela

We have studied the effects of temperature (T) on single channel activity of skeletal muscle fibers of the tropical toad Leptodactylus insularis, using the patch clamp technique in the cell-attached and inside-out configuration. For K channels the solutions were (mM), bath:95 K-glutamate, 5 KCl, 3 $MgCl_2$, 1 EGTA-K, 10 HEPES-K (pH 7.2); pipette: 80 NaCl, 20 NaF, 3 KCl, 0.2 $CaCl_2$, 1 $MgCl_2$, 10 HEPES, 5 glucose and 300 nM TTX (pH 7.4). I_K was identified as delayed rectifier by its I-V and TEA sensitivity. Cooling the fibers from 18°C to 11°C diminished by about 16% the channel conductance; a much larger decrease, >45%, occurred between 11°C and 7°C. As shown in the figure, the mean open probability was similarly diminished. I_{Na} in these fibers was even more affected, decreasing by about 80%, when T was lowered from 16 to 10°C. These results may be interpreted assuming that in these fibers, increasing the membrane microviscosity puts constraints on the channel protein capacity to undergo conformational changes. Supported by CONICIT S1-2148 and CEE I1-CT92-0020.

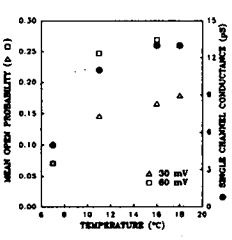

W-Pos447

ION CHANNELS IN THE HUMAN MACROPHAGE CELL LINE THP-1. ((S.Y. Kim, T.E. DeCoursey and M.R. Silver)) Departments of Physiology and Medicine, Rush-Presbyterian-St. Luke's Medical Center, Chicago, IL 60612.

The ionic conductances in the human monocytic cell line THP-1 were studied using whole-cell and single-channel patch clamp techniques. Ionic conductances were characterized as follows: 1) Unstimulated cells expressed predominantly delayed rectifier K^+ current which activated upon depolarization, inactivated with a time constant of several hundred msec, and was blocked by TEA or charybdotoxin. 2) Cells stimulated with 10 ng/ml PMA for 72 hrs expressed predominantly inward rectifier K^+ current which activated upon hyperpolarization beyond E_K, was blocked in a voltage-dependent manner by Ba^{2+} and Cs^+, and had a $[K^+]_o$-dependent voltage-dependence. 3) A voltage-independent Ca^{2+}-activated K^+ current was observed in unstimulated cells when using a pipette solution containing 10 μM Ca^{2+} during whole-cell recordings. This current was not blocked by charybdotoxin, but was blocked by external Ba^{2+} and Cs^+ in a voltage-dependent manner that is similar to the block of inward rectifier currents but with order of magnitude less sensitivity. The single channel conductance was much smaller than that of the voltage- and Ca^{2+}-activated "maxi-K^+" channels. 4) A H^+ selective conductance (g_H) was observed in unstimulated and stimulated cells. The g_H was activated by depolarization with a very slow time course, the outward currents rising throughout pulses of 8-10 sec duration. The H^+ selectivity was confirmed by determining the reversal potential over a range of external *pH*. The g_H was blocked by divalent cations such as Cd^{2+} and Zn^{2+}.

W-Pos448

MEMBRANE CURRENTS IN HUMAN AND RAT MEGAKARYOCYTES
((L.Kapural, A. Fein)) University of Connecticut Health Center, Farmington, CT, 06030 (Sponsored by L. A. Jaffe)

Using the whole-cell patch-clamp technique we have observed a voltage activated outward current in human and rat megakaryocytes that resembles the outward rectifier of other cells. For human megakaryocytes at 20° C an 80 mV voltage step from a holding potential of -60 mV elicited a peak outward current of about 3 nA, with a time to peak of 35 ms, which partially inactivated and was blocked by 100 μM 4AP and 20 mM TEA.

Using the on-cell patch-clamp technique we have found spontaneous oscillations of membrane current in human and rat megakaryocytes. In rat megakaryocytes at 37°C in standard extracellular solution (NaCl 140 mM, KCl 4.7 mM, $MgCl_2$ 1.13 mM, $CaCl_2$ 1.2 mM, HEPES 5 mM, glucose 8mM, pH 7.35) with no applied voltage, these inward fluctuations of membrane current typically have a 10-60 pA amplitude and maximum frequency of 3-6 sec^{-1}. At 20°C oscillatory currents were present in 6 out of 9 cells but typically with much smaller amplitude (2-5 pA) and frequency (0.2-0.4 sec^{-1}).

We applied hyperpolarising and depolarizing voltage steps to the patch pipette in increments of 20 mV from +80 to -100 mV. With extracellular solution in the pipette we found the reversal potential of these oscillations to be -60 ± 10 mV applied to the pipette.

When a PAF agonist [DL-α-phosphatidylcholine,β-acetyl-γ-o-hexadecyl] or arachnidonic acid were added in concentrations of 10 μM and 100 μM respectively, they significantly increased the amplitude of the oscillations.

W-Pos449

COMPARISON OF K+ CURRENTS FROM HUMAN EPICARDIAL AND ENDOCARDIAL MYOCYTES. ((H. Konarzewska, G. Peeters, K. Karwande and M. Sanguinetti)) Univ of Utah, Cardiology, Salt Lake City, UT 84132.

Regional differences in the types and magnitudes of repolarizing K^+ currents may be important in normal dispersion of refractoriness, arrhythmogenesis and responsiveness to drugs. For example, in cats and dogs (1,2), but not in rabbits (3) the magnitude of a voltage-dependent transient outward K^+ current (I_{to1}) is much greater in epicardium compared to endocardium. In this study we compare the characteristics of 3 types of human ventricular repolarizing K^+ currents: I_{to1}, inward rectifier K^+ current (I_{K1}), and the steady-state current remaining after complete inactivation of I_{to1} (I_{ss}) in myocytes isolated from biopsy specimens of relatively normal tissue. Endocardial (endo) tissues were obtained during RV biopsy of the heart transplant recipient (n=5). Epicardial (epi) tissues were obtained from patients with normal LV function during open heart surgery (n=5). Myocytes were bathed in a nominally Ca^{2+}-free saline containing 1 mM $CoCl_2$. I_{to1} and I_{ss} were only slightly larger in epi *vs* endo cells. At 0 and +60 mV, I_{to1} was 1.82+.0.12 pA/pF and 6.01±0.41 pA/pF in epi cells (n=33) vs 1.32±0.13 and 6.18±0.5 pA/pF in endo cells (n=33). The voltage dependence of I_{to1} activation and inactivation was similar in myocytes isolated from both regions. The $V_{1/2}$ for I_{to1} activation was -8.9±0.2 mV (epi, n=15) and -7.5±0.2 mV (endo, n=19); the slope factor (k) was 6.3±0.2 mV (epi) and 5.7±0.2 mV (endo). The $V_{1/2}$ and k for I_{to1} inactivation was -36.5±0.3 mV and 5.7±0.3 mV (epi, n=23), and -33.5±0.3 mV and 5.1±0.3 mV (endo, n=24). The rate of I_{to1} inactivation was also similar for both epi and endo cells (60-80 ms, depending upon voltage). I_{ss} at 0 and +60 mV were 0.22±.03 and 1.50±.13 pA/pF (epi, n=30); 0.12±.02 and 1.38±.13 pA/pF (endo, n=26). I_{K1} at -140 mV averaged -18.2±1.4 pA/pF for epi cells (n=32), and -18.8±1.1 pA/pF for endo cells (n=32). Thus, under the conditions of our study, the magnitude of I_{to1} and I_{ss} in human ventricular myocytes were only slightly greater in endo *vs* epi cells.

(1) Circ Res 1990;*67*:1287; (2)Circ Res 1993;*72*:671; (3)J Physiol 1991;*442*:191.

W-Pos450

CALCIUM REGULATION OF INWARD-RECTIFYING K^+ CHANNELS IN GUARD CELLS

((W.B. Kelly and J.I. Schroeder)) Dept. of Biology and Center for Molecular Genetics, Univ. of California San Diego, La Jolla, CA 92093-0116.

Accumulating evidence indicates that stomatal movements are controlled by the level of cytosolic calcium ($[Ca^{2+}]_{cyt}$) in guard cells. A direct correlation between elevation of $[Ca^{2+}]_{cyt}$ and stomatal closure has been shown (1). We have shown previously that the inward-rectifying K^+ channels in guard cells which are necessary to effect stomatal opening are inhibited by elevated $[Ca^{2+}]_{cyt}$ (2). To elucidate the mechanism by which calcium acts as a second messenger to regulate these K^+ channels, we have performed patch clamp studies in *Vicia faba* guard cells. When $[Ca^{2+}]_{cyt}$ is buffered at an elevated level of 1.5μM using dibromoBAPTA, inhibition of inward K^+ currents is consistent and virtually complete. There is a lesser degree of inhibition when $[Ca^{2+}]_{cyt}$ is buffered at 1.0μM. G proteins have been reported to regulate these channels as well (3), but preliminary experiments in which 200μM GTPγS was added to the above cytosolic solutions have yielded highly variable results. Further experiments are underway to determine the nature of the interaction between these second messengers. It has been suggested that Ca^{2+} may regulate K^+ channels by modulation of the phosphorylation state of the channel or an intermediate protein. Results of experiments which alter the phosphorylation state of K^+ channels in guard cells and of K^+ channel clones expressed in oocytes will be presented.

1. S. Gilroy *et al.* (1990) Nature 346, 769.
2. Schroeder, J. and Hagiwara, S. (1989) Nature 338,427.
3. Fairley-Grenot, K. and Assmann, S. (1991) Plant Cell 3,1037.

W-Pos451

REGULATION OF THE DELAYED RECTIFIER K^+ CURRENT IN RAT PULMONARY ARTERIAL CELLS. ((S.V.Smirnov and P.I.Aaronson)) UMDS, St Thomas's Hospital, London SE1 7EH, UK. (Spon. by W. Coetzee)

Effects of substances affecting three main protein phosphorylation systems have been studied on the delayed rectifier K^+ current (I_{DR}) in single pulmonary arterial (PA) smooth muscle cells using the whole cell patch clamp technique. Bath application of 25 and 100 μM forskolin, an activator of adenylyl cyclase, decreased I_{DR} by an average of 20% and 43% in two cells. This effect was potentiated by the phosphodiesterase inhibitor IBMX (200 μM). The tyrosine kinase inhibitor ST 638 (10 μM), suppressed I_{DR} by 90±3% (n=3, mean ± S.D.). 4-β-PDBu, an activator of protein kinase C (PKC) blocked I_{DR} in a dose-dependent manner with IC_{50}=25 μM, however this effect was not blocked by the PKC inhibitor RO 31-8220 (10 μM), nor mimicked by 5-10 μM PMA, a more potent activator of PKC. 4-α-PDBu (10 μM), which does not stimulate PKC, also suppressed I_{DR}, but to a smaller extent (13±3%, n=5). At high concentrations, all substances tested promoted the decay of I_{DR}, which under control conditions showed minimal inactivation over 100-300 ms. These results suggest that both tyrosine kinase and cAMP-dependent phosphorylation are involved in the regulation of the I_{DR} channels in these cells, possibly inducing N-type inactivation. Although phorbol esters can reduce the amplitude of I_{DR}, this action does not appear to involve an activation of PKC.

W-Pos452

ACTIVATION OF ATP-SENSITIVE K^+ CHANNEL IN CARDIAC MYOCYTES UNDER OXIDATIVE STRESS: ROLE OF THE DNA REPAIR ENZYME POLY(ADP-RIBOSE) POLYMERASE.
((Jeffrey J. Almrud and Aruni Bhatnagar)). Department of Physiology and Biophysics, University of Texas Medical Branch, Galveston, TX (SPON: Burgess N. Christensen).

To understand the mechanism of free radical damage, implicated in the genesis of reperfusion injury, ageing and drug toxicity, electrophysiological and biochemical effects of hydrogen peroxide on isolated rat cardiac myocytes were studied. Exposure to hydrogen peroxide led to rigor-shortening and hypercontracture of myocytes. Rigor shortening was accompanied by an abrupt decrease in the input resistance of the myocytes and loss of excitability. Whole-cell voltage clamp experiments revealed that the decrease in input resistance was due to an increase in time-independent currents. These currents displayed an ohmic dependence on the membrane voltage, a reversal potential of -85 mV; and were sensitive to glibenclamide - indicating that they represent K^+ conductance through the ATP sensitive K^+ channels. HPLC analysis of peroxide-treated myocytes showed an 89% decrease in the intracellular concentration of ATP and a decrease in the energy charge of the cell from 0.9 to 0.5. The presence of 5 mM 3-aminobenzamide (an analog of NAD and a competitive inhibitor of poly(ADP-ribose) polymerase) delayed peroxide-induced rigor and attenuated the loss of intracellular ATP. On the basis of these results it is hypothesized that hydrogen peroxide-initiated DNA strand breaks activate poly(ADP-ribose) polymerase. The activated polymerase utilizes NAD for auto-ADP-ribosylation, thereby depleting intracellular ATP. ATP depletion leads to activation of the ATP sensitive K^+ channel, a decrease in the input resistance and loss of electrical excitability of the myocyte (supported by NIH grant 44675)

W-Pos453

FLICKERING Ba^{2+}-BLOCK OF MAXI-K^+ CHANNELS ON HUMAN FETAL VAS DEFERENS CELLS ((Y.Sohma, *A.Harris, *C.Wardle, B.E.Argent, M.A.Gray)) Dept. of Physiological Sciences, University Medical School, Newcastle upon Tyne NE2 4HH, and *Institute of Molecular Medicine, John Radcliffe Hospital, Headington, Oxford OX3 9DU, U.K.

We recently reported that extracellular Ba^{2+} blockade of maxi-K^+ channels, situated on the apical membrane of cultured human fetal vas deferens epithelial cells, produced both long closings events (seconds duration) as well as fast, flickering (milliseconds duration) closures (Sohma. Y. *et al.* J.Physiol. (1993) 459 423P). Here we have studied in more detail the kinetics of extracellular Ba^{2+}-block. The plot of P_0block/P_0control against $[Ba^{2+}]$ could not be fitted to a single-site inhibition scheme. The flickering Ba^{2+} blockade was concentration and voltage-dependent, with an apparent zero-voltage dissociation constant, $K_D(0)$, of 8.5mM and effective valence, $z\delta$, of 1.3. The slow Ba^{2+} block showed little voltage-dependence over the potential range -20 to 60 mV, but was sensitive to the local K^+ concentration. Lowering external K^+ increased the amount of block. These data suggest that the maxi-K^+ channel has two different Ba^{2+} binding sites accessible from the extracellular face. Site 1 is situated ≈ 65 % into the voltage-drop and causes a rapid flickering block; site 2 senses little of the electric field across the membrane and causes a slow block of the channel, which can be antagonised by increasing K^+ concentration.

Supported by the MRC and the CFT (UK).

W-Pos454

INWARD, RECTIFYING AND CA^{2+}-ACTIVATED K^+ CHANNELS IN EMBRYONIC HEPATOCYTES. ((C.E. Hill)) Dept. Physiol. & Gastrointestinal Disease Research Unit, Queen's Univ., Kingston K7L 3N6, Canada.

Analysis of the steady-state currents of cultured embryonic chick hepatocytes indicates the presence of at least two types of K^+ channels in addition to the transient outward rectifier already identified in our laboratory. These are an outward component that is stimulated by increased intracellular Ca^{2+} or ATP, and an inward component. At the single channel level these are clearly identified as inward, rectifying ($I_{K(ir)}$) and Ca^{2+}-activated ($I_{K(Ca)}$) K^+ conductances. 90% of cell-attached (CA) patches had $I_{K(ir)}$-like channels that open with bursting kinetics upon membrane hyperpolarization and have a slope conductance of about 80 pS with 145 mM external K^+ ($[K^+]_o$). From reversal potential measurements and relative permeability calculations the channel is moderately K^+ selective. As with other $I_{K(ir)}$'s, conductance is dependent on $[K^+]_i$ and can be fit to a Michaelis-Menten model, and the open probability (P_o) decreases with increased membrane hyperpolarization. Under the same recording conditions less than 10% of CA patches had an outward, K^+-selective current that opens at potentials positive to +70 mV and whose P_o increases with further depolarization. Exposure of the inside-out patch to increased $[Ca^{2+}]$ causes the channel P_o x V relationship to shift to successively more negative potentials and increases the slope conductance to 250 pS. The contribution of the single channel events to the observed whole-cell currents are being assessed. Supported by the Natural Sciences & Engineering Research Council.

W-Pos455

EFFECTS OF OXIDATIVE PHOSPHORYLATION INHIBITION ON Ca^{2+}-ACTIVATED AND VOLTAGE-GATED K^+ CHANNELS IN PULMONARY ARTERY CELLS. ((X.-J. Yuan, W.F. Goldman, L.J. Rubin and M.P. Blaustein)) Depts. of Med. & Physiol., Univ. of Maryland Sch. of Med., Baltimore, MD 21201.

Hypoxia decreases voltage-gated K^+ (K_v) current ($I_{K(V)}$) and Ca^{2+}-activated K^+ (K_{Ca}) current ($I_{K(Ca)}$) in pulmonary (PA), but not systemic, artery cells. This inhibition may be due to i) a localized decrease of ATP production and/or ii) a cellular redox status change. Inhibition of oxidative phosphorylation decreases ATP production and increases NADH levels. Thus, FCCP (carbonyl cyanide-*p*-trifluoromethoxyphenyl-hydrazone), a mitochondrial uncoupler, was used to test whether ATP and NADH production regulate $I_{K(V)}$ and $I_{K(Ca)}$ in primary cultured PA and mesenteric artery (MA) cells with the whole-cell patch clamp. The external solution (PSS) included (mM): 141 Na^+, 1.8 Ca^{2+}, 4.7 K^+; the internal solution included (mM): 125 K^+, 5 ATP, 10 EGTA. $I_{K(V)}$ was isolated from $I_{K(Ca)}$ by i) using Ca^{2+}-free PSS (with 0.5 mM EGTA) and ii) pre-incubating the cells in medium with BAPTA-AM, a permeable Ca^{2+} chelator. FCCP increases $[Ca^{2+}]_i$ within 1 min, whereas the FCCP-induced decrease in ATP level is reported to occur after 4 min. Brief application of 5 μM FCCP (<3 min) reversibly activated $I_{K(Ca)}$ in both PA and MA cells. This $I_{K(Ca)}$ augmentation is abolished if the cells are pre-treated with BAPTA and bathed in Ca^{2+}-free PSS. In PA cells, FCCP-induced $I_{K(Ca)}$ enhancement is maintained for at least 14 min, whereas, in MA cells, the $I_{K(Ca)}$ augmentation is transient (<3 min). Further, in PA cells, long exposure (~14 min), but not short exposure (<3 min), to FCCP reversibly reduces $I_{K(V)}$. These results indicate that, in PA cells, the $I_{K(V)}$ that contributes to the hypoxia-induced depolarization is also regulated by oxidative phosphorylation, whereas this is not the case for $I_{K(Ca)}$. The difference in the time-course of FCCP-induced effects on $I_{K(Ca)}$ between PA and MA cells suggests that $I_{K(Ca)}$ in systemic artery cells is more sensitive to inhibition of oxidative phosphorylation. The data may indicate that either a decreased ATP production or an increased NADH production due to the FCCP-induced reduction of oxidative phosphorylation contributes to inhibition of K_v channels but not of K_{Ca} channels in PA myocytes.

Na/Ca EXCHANGE

W-Pos456

MUTUALLY EXCLUSIVE AND CASSETTE EXONS UNDERLIE ALTERNATIVELY SPLICED ISOFORMS OF THE NA/CA EXCHANGER. ((P.Kofuji, W.J.Lederer and D.H. Schulze)) University of Maryland School of Medicine, Baltimore, MD 21201.

We have analyzed the gene structure that gives rise to tissue-specific isoforms of the Na/Ca exchanger. Five distinct isoforms of the Na/Ca exchanger from rabbit brain, kidney and heart have been identified previously to which we now add a new brain isoform. RT-PCR, library screening and sequence analysis of cDNA coding regions indicate that the only changes in the Na/Ca exchanger cDNA in these tissues are located in the carboxyl end of the putative intracellular loop of the protein, a region linked to ionic and metabolic regulation of the exchanger. The gene structure of the Na/Ca exchanger in rabbit indicates a single gene that encodes the exchanger is alternatively spliced to give rise to the six rabbit isoforms. Sequence analysis of the intron-exon boundaries reveals the presence of two mutually exclusive exons and four cassette exons in the region of the Na/Ca exchanger gene that codes for a limited region of the predicted intracellular loop region. This arrangement of exons in the Na/Ca exchanger gene could allow for the generation of up to 32 different mRNAs and account for all isoforms identified.

W-Pos457

TISSUE-SPECIFIC EXPRESSION OF Na, Ca EXCHANGER ISOFORMS. ((S.L. Lee, A.S.L. Yu and J. Lytton)) Renal Div., Dept. Medicine, Brigham & Women's Hospital and Harvard Medical School, Boston, MA 02115.

The renal tubular sodium-calcium exchanger (NCE) is thought to play an important role in calcium reabsorption and body calcium homeostasis. We have isolated a full-length cDNA encoding the rat renal NCE, denoted F1, that is highly homologous to previously reported NCEs except for two regions: one in the 5'-untranslated region (5'-UTR) and the other in a region of the coding sequence (nt 1800-1989) previously shown to be alternatively spliced. RT-PCR was used to investigate the region of alternative splicing, resulting in the identification of five major species that are expressed in a tissue-specific fashion with unique products present in striated muscle, brain and other tissues. In order to compare the 5'-end of our F1 clone with the 5'-ends of NCE transcripts in different tissues, we employed "rapid amplification of 5'-cDNA ends" using RNA from heart, brain and kidney. Restriction enzyme analysis of the products amplified from these tissues and sequencing of multiple clones revealed the existence of three species each with a unique 5'-end, spliced at nucleotide –34 in the 5'-UTR to a common NCE core. To determine the tissue distribution of NCE transcripts containing these 5'-ends, probes from both the unique and common regions were used in Northern blot analysis. The result shows that one 5'-end isoform, corresponding to our F1 clone, is unique to and abundantly expressed in kidney; a second is expressed abundantly in heart and only weakly elsewhere; while the third corresponds to a ubiquitous NCE transcript which is most abundant in brain. The differential expression of NCE transcripts with unique 5' ends indicates that the NCE gene is controlled and regulated under the influence of different promoters in a tissue-specific fashion.

W-Pos458

MUTATIONS IN THE PUTATIVE TRANSMEMBRANE SEGMENTS OF THE CANINE CARDIAC SARCOLEMMAL Na/Ca EXCHANGER. ((D.A. Nicoll, L.V. Hryshko, S. Matsuoka, R.-Y. Wu, D.W. Hilgemann, and K.D. Philipson)) Cardiovascular Research Laboratories, UCLA, Los Angeles, CA 90024.

Single site mutations in the putative transmembrane segments of the Na/Ca exchanger have been generated and mutant exchangers expressed in *Xenopus* oocytes. The ion transport properties of the mutant exchangers have been studied by ion flux or giant excised patch measurements. Three groups of amino acids have been targeted for mutation: 1) Acidic residues, 2) Residues in the regions which show similarity to the photoreceptor Na/Ca,K exchanger (amino acids 106-145, 807-844) and 3) Residues in the region which shows similarity to the Na/K pump (amino acids 180-203). Of the mutations to the acidic residues, four (E120Q, E196Q, D740N, and D748N) display wild-type activity, and three (E113Q or D, E199Q or D, and D785N) express inactive exchangers. For mutations in the regions similar to the photoreceptor exchanger, four (G108A, P112A, S117A, and E120Q) display wild-type activity while seven (S110A, T, or C, S109A or T, E113Q or D, T810V, S818A, S838A, and N842V) are inactive. For mutations in the region which is similar to the Na/K pump, two have wild-type activity (E196Q, and G200A) and two have no activity (E199Q or D and T203V). These results suggest that residues which are mutated to produce inactive exchangers are involved in ion translocation in the exchanger.

W-Pos459

LOCALIZATION OF A HIGH-AFFINITY CALCIUM BINDING SITE IN THE Na/Ca EXCHANGER. ((D.O. Levitsky, E.A. Burke, D.A. Nicoll, and K.D. Philipson)) Cardiovascular Research Laboratories, UCLA School of Medicine, Los Angeles, CA 90024.

In addition to transporting Ca, the Na/Ca exchanger of cardiac sarcolemma has a high affinity Ca-regulatory site. Ca regulation disappears after deletion of the hydrophilic intracellular domain of the exchanger (PNAS 90:3870-3874, 1993). To localize the regulatory Ca-binding site (CBS), we expressed different fragments of the hydrophilic loop as fusion proteins in E. coli. Ca binding was analyzed by ^{45}Ca-overlay after PAGE and protein transfer onto nitrocellulose. A region of the loop responsible for strong Ca binding is narrowed to amino acids 371-508. It contains two acidic segments (446-DDDIFEEDE and 498-DDDHAGIFTFEE) separated by 50 amino acids. The Ca affinity of fusion proteins overlapping this region is about 0.5 μM. Mutation of D447 or D498 in the putative CBS or deletion of either acidic segment results in a decrease in Ca binding. For example, high affinity Ca binding was not present in constructs expressing 371-445, 371-470, or in deletion mutant Δ450-456. Thus, both acidic portions are essential for high affinity binding. Ca binding progressively decreases upon shortening the polypeptide from the N-terminus (first residues of the constructs being 371, 384, 394, 445) and is not affected by similar manipulations at the C-terminus (until position 508). Interestingly, fusion proteins with high affinity site(s) display three bands on Ca overlays. The two lower bands decrease and the upper band increases in intensity if the samples are preincubated with EGTA before electrophoresis. The data suggest that both acidic regions are required, and may interact cooperatively, for high affinity Ca binding.

W-Pos460

Ca_i REGULATION OF THE CARDIAC Na-Ca EXCHANGER. ((L.V. Hryshko, S. Matsuoka, D.A. Nicoll, D. Levitsky, *D. H. Hilgemann, J.N. Weiss, and K.D. Philipson)) Cardiovasc. Res. Lab., UCLA Sch. Med., Los Angeles, CA 90024 and *Univ. Texas Southwestern Med. Cent., Dallas TX 75235.

Na-Ca exchange is the primary mechanism for transsarcolemmal Ca removal in cardiac muscle. However, in addition to transporting Ca, the cardiac Na-Ca exchanger is also regulated by intracellular Ca (Ca_i). We have investigated the Ca_i regulatory properties of the cardiac Na-Ca exchanger using electophysiological and molecular biological techniques. Wild type and mutant Na-Ca exchangers expressed in *Xenopus* oocytes were examined using the giant excised patch technique. Outward Na-Ca exchange current was examined as this permits transported and regulatory Ca to be on opposite membrane surfaces. Ca_i regulation is evident as a concentration dependent activation of outward exchange current by Ca_i. To define the region(s) responsible for Ca_i regulation, several deletion and point mutations have been examined. These fall into 3 general categories, as follows:
1) Mutants with wild-type regulation. These mutants allow us to exclude several portions of the cytoplasmic loop from being important in Ca_i regulation.
2) Mutants without Ca_i regulation. These exhibit similar currents in the presence or absence of regulatory Ca_i. This group include G503P, G558P, Δ562-569, Δ672-679, and Δ680-685.
3) Mutants with altered regulatory Ca_i affinities. Activation of exchange current in these mutants (e.g. D447V, Δ450-456, D498I, D498K) requires up to 10-fold higher Ca_i concentrations compared to the wild type exchanger. These mutations are targeted at two highly acidic portions of the cytoplasmic loop which have been shown to be important for Ca binding (Levitsky et al., adjacent poster).
The effects of mutations on Ca binding and function are consistent and localize the functionally important Ca regulatory site on the cytoplasmic loop of the exchanger. Physiologically, this gating of the exchanger by Ca_i may serve to prevent excessive depletion of cytoplasmic Ca.

W-Pos461

EXPRESSION OF THE CANINE Na/Ca EXCHANGER IN TRANSGENIC MOUSE HEARTS ((Z. Li, R.-Y. Wu, D.A. Nicoll, and K.D. Philipson)). Cardiovascular Research Laboratories, UCLA, Los Angeles, CA 90024. (Spon. by J. Frank).

Myocardial cells have multiple Ca transport mechanisms. That the sarcolemmal Na/Ca exchanger is an important regulator of myocardial contractility has been inferred from many investigations of excitation-contraction coupling. To further define the role of the Na/Ca exchanger, we are developing a transgenic mouse line with cardiospecific overexpression of the Na/Ca exchanger. A construct was made containing the coding region of the canine cardiac Na/Ca exchanger cDNA between the α-myosin heavy chain promoter and the SV40 large T transcriptional terminator (courtesy of L. Field and J. Robbins). This DNA construct was injected into the pronuclei of fertilized oocytes. From ten litters, eight transgenic founder mice were identified by Southern blot analysis of EcoRI-digested genomic DNA. The founder mice are being bred and transgenic F1 offspring are being identified. On an initial immunoblot of heart homogenate, a distinct Na/Ca exchanger protein band could be obtained from a transgenic mouse but not from a nontransgenic littermate. Thus, initial indications are that the Na/Ca exchanger is being overexpressed in transgenic mouse hearts.

W-Pos462

MODIFICATION OF THE POSITIVE CHARGES OF THE EXCHANGE INHIBITORY PEPTIDE (XIP) DECREASES ITS INHIBITION OF NA-CA EXCHANGE ACTIVITY. ((H. A. Denison, B.J. Wilson, C.C. Hale, and M.A. Milanick)) Dept. of Physiology, School of Medicine and Dept. of Veterinary Biomed. Sci., Dalton Research Center, Univ. of Missouri-Columbia, Columbia, MO 65212

Synthetic XIP (RRLLF YKYVY KRYRA GKQRG) corresponds to 20 residues of the Na-Ca exchanger (JBC 266:1014, 1991). We sought to determine 1) if the 8 positive charges on XIP were important, 2) if the type of positive side chain on XIP, arginine (a guanidino) or lysine (an amino) was significant, and 3) which positive charges within XIP inhibit activity. Na/Ca exchange was measured as 45Ca uptake (12 uM Ca) at 3 sec, into Na-loaded cardiac sarcolemmal vesicles. Two analogues of XIP were synthesized in which all 8 positive charges were arginine (ArgXIP) or lysine (LysXIP). Each peptide maximally inhibited 40 to 50% of the exchange activity with similar IC50 values (0.4 to 1 uM) Apparently whether the positive charge is from a lysine or arginine is not important. To enhance the peptides' inhibition properties exchange was measured in 10mM KCl and 300mM mannitol(JBC 267:17836, 1992). The maximal inhibition was 100%. The peptides were reacted with sulfosuccinimidyl acetate (SNA) (at pH 9) to neutralize covalently the amino positive charge. This essentially eliminated inhibition by LysXIP (IC50 > 50 uM for SNA-LysXIP). This suggests that the positive charges are necessary for inhibition. SNA modification of XIP increased the IC50 from 1 to 4 uM. Two models are consistent with this small increase in IC50: 1) One or more of the remaining positive side chains of XIP-SNA (1, 2, 12, 14, and 19) are most significant to the inhibitory strength or 2) each of the positive charges contributes approximately equally to the potency. Supported by NIH DK37512 (MAM), NIH RCDA (MAM), AHA (CCH) and AHA, MO Affl. (HD)

W-Pos463

EOSIN, A POTENT INHIBITOR OF THE PLASMA MEMBRANE CA PUMP, DOES NOT INHIBIT THE CARDIAC NA-CA EXCHANGER. ((C. Gatto, C.C. Hale, and M.A. Milanick)) Department of Physiology, School of Medicine and Veterinary Biomedical Sciences, Dalton Cardiovascular Research Center, University of Missouri, Columbia, MO 65212.

The Na-Ca exchanger and the plasma membrane (PM) Ca pump are the two major pathways for Ca transport to the extracellular space in many cells. In cardiac myocytes, the Na-Ca exchanger appears to be qualitatively responsible for a greater portion of this Ca flux. However, the respective roles of these two transporters are not defined in all tissues (e.g. smooth muscle). We propose that eosin (tetrabromofluorescein) may be a useful tool for quantitatively determining the proportion of Ca transported by the Na-Ca exchanger vs. the PM Ca pump in various cells. Eosin is the most potent inhibitor known for the PM Ca pump (IC_{50} < 0.2 μM in red blood cell inside-out vesicles); unlike the Na/K and H/K pumps, eosin does not compete with ATP for the PM Ca pump (AJP:Cell 264: C1577, 1993). In the present study, we demonstrate that eosin (≤ 20 μM) does not inhibit the Na-Ca exchanger. Na-Ca exchange activity was measured as ^{45}Ca uptake into Na-loaded (160 mM) bovine cardiac sarcolemmal (CSL) vesicles (flux media contained: 160 mM KCl, 2 μM valinomycin, 20 μM $MgCl_2$, 0 mM ATP); background was ^{45}Ca uptake with 160 mM NaCl replacing KCl. In addition, we have shown that eosin is a potent inhibitor of the CSL Ca pump (IC_{50} ≈ 0.25 μM). Ca pump activity was measured as ^{45}Ca uptake into CSL vesicles (flux media contained: 160 mM NaCl, 0.52 mM $MgCl_2$, 0.5 mM ATP); background was ^{45}Ca uptake in the absence of ATP. Supported by NIH DK-37512 (MAM) NIH RCDA (MAM) AHA (CCH).

W-Pos464

MOLECULAR CLONING OF THE SARCOLEMMAL SODIUM-CALCIUM (Na / Ca) EXCHANGER OF VASCULAR SMOOTH MUSCLE (S. Ahmed, K. Combs, M.F. Rabbi, and M.A. Matlib) Dept. of Pharmacology & Cell Biophysics, University of Cincinnati, College of Medicine, Cincinnati, OH 45267-0575

The existence of a sarcolemmal Na/Ca exchanger in vascular smooth muscle (VSM) is well established. However, its molecular nature remains unknown. The purpose of this study is to clone the VSM Na/Ca exchanger gene. Northern blot analysis of the mRNA from rat aorta indicates that the VSM exchanger transcript is about 7kb similar to that of rat cardiac mRNA. Using a 1.5kb cDNA fragment of the guinea-pig cardiac Na/Ca exchanger as a probe a rat aortic cDNA library was screened, and a 2.3kb fragment was isolated. Sequence analysis of this 2.3kb cDNA fragment indicated a close homology to the 3' end of the coding region of the rat cardiac Na/Ca exchanger. An additional 733 nucleotides of rat aorta were isolated using an oligonucleotide probe corresponding to the 5' end of the 2.3kb cDNA fragment. A total of 3033 nucleotide bases of the rat VSM exchanger have been sequenced. This nucleotide sequence was found to be 91% identical to that of the rat cardiac exchanger. However, distinct variations between the sequences in certain regions were observed. Specifically, segments of 87, 12, and 10 nucleotide bases in length were deleted. Based upon the corresponding amino acid sequence and Kyte and Doolittle hydropathy plot of the Na/Ca exchanger, the deletions and the variations lie in the cytoplasmic loop observed in the cardiac exchanger. Comparison of the partial amino acid sequence of the VSM Na/Ca exchanger to the corresponding regions of Na/Ca exchanger of rat brain and rabbit kidney indicates that the exchanger of VSM is a new isoform.

W-Pos465

INCREASED SODIUM-CALCIUM EXCHANGER EXPRESSION IN SPONTANEOUSLY HYPERTENSIVE RAT HEARTS ((Malcolm M. Bersohn and Kenneth D. Philipson)) V.A. Medical Center and University of California, Los Angeles, CA 90073

Sodium-calcium exchange Vmax is increased by 50% in left ventricular sarcolemmal vesicles of 4 month old spontaneously hypertensive rats (SHR) compared to age-matched Wistar-Kyoto (WKY) controls. We investigated levels of sodium-calcium exchanger mRNA in the left ventricles of a similar group of animals to determine whether altered expression of the sodium-calcium exchanger might be a regulatory mechanism in this hypertensive model. Total RNA was purified, and Northern blots were performed using a 1300 bp cDNA probe from the 3' end of the hamster cardiac sodium-calcium exchanger. The blots were rehybridized with a 500 bp human β-actin cDNA probe to normalize for variability in RNA extraction and blotting efficiency. Autoradiograms were analyzed by densitometry. Results (means ± SE in arbitrary units, n=5) were:

	Exchanger	β-actin
SHR	64 ± 20	58 ± 11
WKY	19 ± 8	54 ± 16

Although the variability is high, the β-actin data indicate that an equal amount of mRNA was present on the blots for SHR and WKY. Exchanger mRNA concentration was three times higher for SHR than WKY, possibly due to altered transcriptional regulation.

W-Pos466

XIP AND FMRFa PEPTIDES, INHIBITORS OF CARDIAC SARCOLEMMAL Na/Ca EXCHANGE, ALSO INHIBIT Na/Ca EXCHANGE IN SQUID GIANT AXONS. Reinaldo DiPolo and Luis Beaugé. CBB, IVIC, Caracas, Venezuela and M.y M. Ferreyra, Argentina.

The aim of the present work was to indirectly determine the presence of conserved structures in the cardiac sarcolemma and squid axon Na/Ca exchangers. The strategy was to study the effects on squid axons of two peptides of known inhibiting action of the cardiac sarcolemma Na/Ca exchange system: the 20 amino acids XIP peptide and the molluscan cardioexcitatory tetrapeptide Phe-Met-Arg-Phe-NH_2 (FMRF-a). The results showed that XIP had no effect on the Na_o-dependent Ca efflux when dialyzed at a final concentration of 100μM. However, when injected into the axon at approximately the same final concentration, it caused a 49±7% (n=4) inhibition of the forward Na/Ca exchange. The inhibitory effect was the same in axons dialyzed with saturating $[Ca^{2+}]_i$ (100μM) and no MgATP, or in axons containing submicromolar $[Ca^{2+}]_i$ (0.7μM) and 2 mM MgATP. The FMRFa a peptide which shows no obvious homology with XIP also caused a marked inhibition in the Na_o-dependent Ca efflux. As it is the case in cardiac sarcolemmal vesicles, the FMRFa inhibited with low apparent affinity (K_i=1.88±0.32) (n=3). Similar to the inhibition by XIP, FMRFa inhibition was the same effect whether the axons were dialyzed with or without MgATP. In the cardiac exchanger, XIP was originally designed to interact with a calmodulin like binding site while FMRFa appears to bind to a putative opiate site. Our data suggest that these two sites are present (conserved) also in the invertebrate squid exchanger, and do not participate in the nucleotide (MgATP) regulation mechanism of the system. (CONICIT, Proyecto S1-2651. CONICET-PID-BIB 1053) and NSF-BNS-9120177).

W-Pos467

REGULATION OF SODIUM-CALCIUM EXCHANGE BY CYTOSOLIC CALCIUM IN CHO CELLS TRANSFECTED WITH THE BOVINE CARDIAC SODIUM-CALCIUM EXCHANGER (CK1.4 CELLS). ((M. Condrescu, G. Chernaya, J. F. Aceto, J. P. Gardner, & J. P. Reeves)) Department of Physiology and Hypertension Research Center, UMD-NJ Medical School, Newark, NJ 07103.

Numerous studies with squid axons, barnacle muscles and cardiac myocytes have shown that Na_i-dependent Ca influx via Na/Ca exchange is activated by cytosolic Ca. $[Ca]_i$ in CK1.4 cells rapidly declined to less than 50 nM when Ca_o was removed. This treatment had two different effects on subsequent ^{45}Ca uptake by Na/Ca exchange, depending upon whether intracellular Ca chelators were present or not. Ouabain-treated CK1.4 cells preincubated with 10 μM BAPTA-AM during the Ca-free preincubation period showed a 40% reduction in the initial rate of ^{45}Ca uptake; the degree of inhibition increased to 60% when 10 μM $LaCl_3$ was included in the assay medium. Inhibition by BAPTA-loading was not observed with CK138 cells, which express a deleted form of the exchanger that does not exhibit activation by Ca_i. In the absence of BAPTA-loading, a 50% *increase* in ^{45}Ca influx and a reduced rate of ^{45}Ca efflux were observed compared to cells preincubated in the presence of Ca_o. The CK138 cells exhibited similar behavior. The increased rate of Ca influx was attained within 15 sec of removing Ca_o. This was not due to an increase in $[Na]_i$ because a comparable increase in activity was noted when Ca_o was removed in a Na-free medium. The results suggest that reduction of $[Ca]_i$ promotes Ca entry from the exterior by a La-sensitive pathway, and that the incoming Ca activates Ca influx via the exchanger. Intracellular BAPTA retards the increase in $[Ca]_i$ and reduces the initial rate of Na/Ca exchange.

W-Pos468

ATP-DEPENDENT REGULATION OF SODIUM-CALCIUM EXCHANGE ACTIVITY IN CHO CELLS TRANSFECTED WITH THE BOVINE CARDIAC SODIUM-CALCIUM EXCHANGER (CK1.4 CELLS). ((M. Condrescu, J. F. Aceto, C. Kroupis, J.P. Gardner & J. P. Reeves)) Department of Physiology & Hypertension Research Center, UMD-NJ Medical School, Newark, NJ 07103

Cellular ATP levels were reduced by 95% within 10 min when CK1.4 cells were treated in the absence of glucose with 2.5 μg/ml oligomycin plus 2 μM rotenone (OR). Na/Ca exchange activity was assayed as ^{45}Ca uptake by ouabain-treated CK1.4 cells. After 10 min OR-treatment, ^{45}Ca uptake declined by 50% when assayed in a Na-free medium, and by >80% when assayed in 140 mM NaCl. This suggested that ATP-depletion increased the effectiveness of Na_o as an inhibitor of Ca uptake by Na/Ca exchange. This was verified by examining the initial rate of ^{45}Ca uptake at various $[Na]_o$: OR treatment reduced the IC_{50} of Na_o from 90 mM to 57 mM. $[Ca]_i$ was monitored in ouabain-treated CK1.4 cells loaded with fura-2. OR-treatement (30 min) produced a 50% decline in the rate of increase in $[Ca]_i$ when $[Na]_o$ was reduced by 100 mM and profoundly inhibited recovery of $[Ca]_i$ when 140 mM Na_o was restored. The effects of ATP depletion were also examined in CHO cells expressing a mutated form of the Na/Ca exchanger, in which 440 out of 520 amino acids were deleted from the central hydrophilic domain (CK138 cells). In CK138 cells, OR-treatment had no effect on the inhibition of ^{45}Ca uptake by Na_o and produced much smaller effects on Na_o-dependent Ca efflux than in CK1.4 cells. The results indicate that ATP depletion sharply reduces both Ca influx and Ca efflux by the exchanger in a Na-containing medium, and that these effects are mediated by the central hydrophilic domain. The increased sensitivity to inhibition by Na_o may represent a protective mechanism to prevent Ca overload during periods of ATP depletion.

W-Pos469

VOLTAGE-DEPENDENCE OF THE Na/Ca EXCHANGER IN BARNACLE MUSCLE CELLS. ((R. Espinosa-Tanguma & H. Rasgado-Flores)) Dept. Physiol & Biophys. UHS/Chicago Medical School. N. Chicago, IL 60064.

Our aim was to study the voltage dependence of the partial reactions of the Na/Ca exchanger in barnacle muscle cells. For this purpose we assessed the effect of membrane potential (V_M) on the extracellular Na^+ (Na_o)-dependent $^{22}Na^+$ efflux (Na/Na exchange) and extracellular Ca^{2+} (Ca_o)-dependent $^{45}Ca^{2+}$ efflux (Ca/Ca exchange) in internally perfused, voltage-clamped cells. To circumvent activation of the exchanger by increasing the intracellular concentration of Ca^{2+} (which also activates non-selective cation channels), the cells were transiently perfused with α-chymotrypsin (which renders a highly activated Na/Ca exchanger). In the presence of 46 mM intracellular Na^+ (Na_i) and high Na_o (456 mM), Na/Na exchange was not significantly ($p>0.05$) affected by changes in V_M from 0 mV (204 ± 27 pmoles cm^{-2} s^{-1}, n=13) to -40 mV (178 ± 43 pmoles cm^{-2} s^{-1}, n=7). Na/Na exchange was also unaffected by V_M changes in the presence of low (30 mM) Na_o (35.5 ± 2.14 pmol cm^{-2} s^{-1}, at 0 mV, n=6, and 35.33 ± 3.54 pmol cm^{-2} s^{-1}, at -40 mV, n=6). On the other hand, in the presence of extracellular Li^+ and 6 mM Na_i, there is a linear relationship between the normalized (%) Ca_o-dependent Ca^{2+} efflux and V_M (from -60 to +20 mV). Ca/Ca exchange increases linearly with depolarization and decreases with hyperpolarization (slope= -22 ± 1.75 % per 25 mV of membrane depolarization).

W-Pos470

POTENCY OF EXCHANGE INHIBITORY PEPTIDE (XIP) INHIBITION OF THE NA-CA EXCHANGER IN ALTERNATE TRANSPORT MODES ((Thomas R. Shannon, Calvin C. Hale, and Mark A. Milanick)) Dalton Cardiovascular Research Cntr., Vet. Biomed. Sci. and Physiology Depts., University of Missouri, Columbia, MO 65211

We tested the hypothesis that XIP inhibits the cardiac Na^+-Ca^{2+} exchanger with less potency when it operates in the Ca^{2+}-Ca^{2+} exchange mode than when it operates in the Na^+-Ca^{2+} exchange mode. Na^+_i-dependent $^{45}Ca^{2+}$ uptake and Ca^{2+}_i-dependent $^{45}Ca^{2+}$ uptake were measured in cardiac sarcolemmal (SL) vesicles. K_m's of 37.8 and 107.4 μM Ca^{2+} and V_{max}'s of 3.6 and 0.72 nmol Ca^{2+}/mg protein/s were found, respectively. XIP inhibited Na^+-Ca^{2+} exchange in an uncompetitive manner for Ca^{2+}. The peptide was not competitive for Ca^{2+} when the Na^+-Ca^{2+} exchanger was tested in Ca^{2+}-Ca^{2+} exchange mode. The inhibitory constant for uncompetitive inhibition (K_i) of Na^+-Ca^{2+} exchange was 1.6 μM XIP whereas the K_i for Ca^{2+}-Ca^{2+} exchange was 20.0 μM. To further test the hypothesis, XIP inhibition of equilibrium Ca^{2+}_i-dependent $^{45}Ca^{2+}$ uptake was measured. The equilibrium K_m and V_{max} for this mode of exchange were 205.3 μM and 0.59 nmol/mg/s, respectively. XIP inhibited equilibrium Ca^{2+}-Ca^{2+} exchange in an uncompetitive manner which with a K_i of 11.4 μM XIP. The uncompetitive inhibition suggests that XIP binds to ion loaded conformations of the exchanger. These data suggest that XIP inhibition of Ca^{2+}-Ca^{2+} exchange is less potent than Na^+-Ca^{2+} exchange and that inhibition may be more effective at Na^+ bound conformations over Ca^{2+} bound conformations of the exchanger.
Supported by the AHA (CCH), AHA-MO Affl. (TRS), NIH DK37512 (MAM) and NIH RCDA (MAM).

W-Pos471

A SINGLE MUTATION IN THE UNCOUPLING PROTEIN OF RAT BROWN ADIPOSE TISSUE MITOCHONDRIA ABOLISHES GDP SENSITIVITY OF H^+ TRANSPORT. ((K.D. Garlid[a], K.B. Freeman[b], D.L. Murdza-Inglis[b], M. Modriansky[a], H.V. Patel[b], and G. Woldegiorgis[a])) [a]Dept. of Chemistry, Biochemistry, & Molecular Biology, Oregon Graduate Institute, P.O. Box 91000, Portland, OR 97291-1000; [b]Dept. of Biochemistry, McMaster University, Hamilton, Ontario L8N 3Z5 Canada.

The uncoupling protein, one of a family of mitochondrial transport proteins involved in energy metabolism, dissipates oxidative energy to generate heat. It does so by catalyzing fatty acid anion uniport, enabling fatty acids to act as cycling protonophores. This transport process is tightly regulated by purine nucleotides. We have expressed uncoupling protein in yeast and examined its proton transport activity following its reconstitution into proteoliposomes. A directed change of Arg276 to Leu or Gln abolished nucleotide inhibition of protonophoretic action of the reconstituted mutant uncoupling proteins without affecting the transport process itself. Arg276 is the first functionally important residue identified in uncoupling protein. Mutation of the homologus residue in the yeast ADP/ATP translocator prevented growth of yeast on a non-fermentable carbon source, presumably by interfering with nucleotide exchange. Demonstration of the essential role of a single homologous residue in protein-nucleotide interaction within these two transporters is the first direct evidence that uncoupling protein and the ADP/ATP translocator belong to the same gene family. (Supported by NIH grant GM 31086 and MRC grant MT 1940.)

W-Pos472

THE UNCOUPLING PROTEIN IS AN ANION CHANNEL WHOSE PHYSIOLOGICAL ROLE IS TO ENABLE FATTY ACIDS TO ACT AS PROTONOPHORES IN BROWN ADIPOSE TISSUE MITOCHONDRIA. ((Martin Modriansky, David E. Orosz, Petr Jezek, and Keith D. Garlid)) Chemistry, Biochemistry, and Molecular Biology, Oregon Graduate Institute of Science & Technol., P.O. Box 91000, Portland, OR 97291-1000.

The uncoupling protein (UCP) catalyzes regulated futile cycling of protons in order to generate heat. To elucidate the mechanism of uncoupling by UCP, we applied the fluorescent probe technique to assay H^+ and anion transport in proteoliposomes reconstituted with purified UCP. As expected, laurate induced H^+ flux in liposomes containing UCP. Evidence that this protonophoretic action of UCP is mediated by laurate/lauric acid cycling includes the following: Undecanesulfonate, a laurate analogue, was transported by UCP but did not induce H^+ flux. Furthermore, undecanesulfonate inhibited laurate-activated H^+ flux with competitive kinetics. Finally, lauric acid exhibited rapid nonionic diffusion in liposomes, whereas undecanesulfonic acid was not permeable. We infer that UCP catalyzes electrophoretic transport of anions, including anions of fatty acids, probably by a channel mechanism. Nonionic diffusion of the fatty acid completes the protonophoretic cycle. Thus, proton transport by UCP is not required to explain its uncoupling mechanism. (Supported by NIH grant GM31086).

W-Pos473

cAMP binding to Adenine Nucleotide Translocase (AdNT). ((C. Marfella, A. Romani and A. Scarpa)) Dept. Physiology and Biophysics, Case Western Reserve University, Cleveland, OH 44106, USA. (Spon. by A. Scarpa).

A large and time dependent efflux of Mg^{2+} from rat liver or heart mitochondria is observed upon the addition of 50 nM cAMP. This effect is not due to the phosphorylation of a mitochondrial kinase but to a binding of cAMP to the AdNT. The binding of cAMP has an apparent Km of 40 nM and it is selective since it is not prevented by the presence of larger concentrations of cGMP, AMP, ADP or ATP. Atractyloside, a specific inhibitor of the AdNT, completely inhibits mitochondrial Mg^{2+} efflux but not cAMP binding to the AdNT. Photoaffinity labelling experiments using ^{32}P-8azido-cAMP show the binding of cAMP to AdNT in the whole mitochondrial protein pattern and also to the purified translocase. ^{32}P-8azido-cAMP binding follows a Michaelis-Menten kinetic with saturation at 40 nM cAMP. The partially purified AdNT from beef heart mitochondria is retained on an Agarose-cAMP affinity chromatography column, while contaminant proteins in the purification procedure are rapidly eluted. The single protein that can be specifically eluted from the column using 2 μM cAMP has been sequenced and possesses 99% homology with isoform 1 of beef heart mitochondrial AdNT. The analysis of ADP/ATP carrier primary structure shows a cAMP binding consensus sequence. (Supported by Grant N.I.H. HL 18708).

W-Pos474

HOW IS THE ADP/ATP CARRIER REGULATED? COMPETITION BETWEEN PRODUCTIVE AND UNPRODUCTIVE TRANSPORT MODES AS SHOWN BY MUTANT AAC. ((M. Klingenberg and D.R. Nelson)) Institute for Physical Biochemistry, University of Munich, Goethestrasse 33, 80336 Munich, Germany; Dept. of Biochemistry and Biophysics, University of North Carolina, Chapel Hill, NC 27599-7260, U.S.A.

Regulation of transport activity of mitochondrial carriers is (with one exception) only governed by external factors not affecting the carrier protein, such as $\Delta\psi$, ΔpH and the solute gradients. Since mitochondrial carriers are mostly exchange systems the double ratio $(S_1/S_2)_{ext}/(S_1/S_2)_{int}$ controls the transport effectivity. In addition, the exchange rate is dependent on the individual rate constant of the carrier with S_1 and with S_2, $k_1^{\rightarrow}$, $k_1^{\leftarrow}$, $k_2^{\rightarrow}$, $k_2^{\leftarrow}$. The interplay of these factors has been elucidated for the bovine-heart AAC in mitochondria and in the reconstituted system. More recently in yeast-AAC mutants striking examples for the importance of this control were found. In the AAC intrahelical α2 mutation R96H in domain I and R294A in domain III yielded gly-minus cells indicating that the mutant AAC was ineffective. However, reconstitution of isolated mutant-AAC yielded moderate or good activity in the basic ADP-ADP (D/D) exchange. This paradoxon was solved by finding that the ATP containing modes of exchange (D/T, T/T) are reduced to 1/5 or 1/10 of the D/D exchange, whereas in wild type the T-modes could be even faster than the D/D mode. It is concluded that in the mutant cells the D/T exchange, required for ATP export into cytosol, is suppressed by the competition with the much higher unproductive D/D exchange. Most strikingly, in the revertant (gly-positive) R294A + E45Q the D/D exchange rate is decreased by 80% reaching the same level as the slow D/T rate. As a result, in the revertant cells the inhibition of the D/T exchange due to the competition by D/D exchange is suppressed and allows ATP efflux although at a tenfold reduced rate as in wild type. Thus, in the cell not the absolute rates but the ratio of the unproductive to the productive modes control the effectivity of the AAC and are vital for aerobic cell growth.

W-Pos475

SYNTHESIS OF A PHOTOAFFINITY PROBE AND IDENTIFICATION OF THE ADENOSINE TRANSPORTER IN CARDIAC SARCOLEMMAL VESICLES. ((M.J. Rovetto, J.A. Zimmerschied, S. Bliler, and C.C. Hale)) Dalton Cardiovascular Res. Center, Vet. Biomed. Sci. and Physiology Depts., University of Missouri, Columbia, MO 65211.

We have developed and utilized a photoaffinity probe to identify the adenosine transporter in cardiac sarcolemmal (SL) vesicles. Adenosine or ^{14}C-adenosine was reacted with N-hydroxsuccinimidyl azidosalicylic acid (NHS-ASA) in 4:1 (v:v) dimethylsulfoxide: 10 mM sodium phosphate, pH 8.4. The mixture containing nonradiolabeled adenosine was radiolabeled with Na^{125}I. Both reaction mixtures were fractionated by HPLC which yielded several radioactive peaks. ^{125}I-labeled material from the first synthesis and ^{14}C-labeled material from the second synthesis eluted at comparable times. Both reaction mixtures were subjected to a second HPLC fractionation protocol which again gave common eluting fractions. The ^{14}C peaks collected from each HPLC protocol were subjected to the other protocol to confirm peak identity. The common peak was judged to be ASA-adenosine. ^{125}I-ASA-adenosine, upon radiation with uv light, covalently labeled a 70 kD protein in bovine cardiac SL vesicles. Labeling of this protein was greatly diminished in the presence of nonradiolabeled adenosine, 5'-amino adenosine, or guanosine but not glucose. We conclude that the cardiac adenosine transporter is a protein with an apparent Mr of 70 kD. (supported by NIH HL-27336)

W-Pos476

CONCENTRATION AND VOLTAGE DEPENDENT PROPERTIES OF BASOLATERAL ORGANIC-CATION TRANSPORT IN THE KIDNEY PROXIMAL TUBULE ((M. R. Weber and E. L. Boulpaep)) Dept. of Cellular & Molecular Physiology, Yale University, New Haven, CT 06510

This study examined mechanisms of tetramethylammonium (TMA) cation transport in the basolateral membrane of isolated perfused proximal tubules from *Ambystoma tigrinum*. Apical and basolateral membrane voltages were recorded with intracellular Ling-Gerard electrodes. Simultaneously, cellular TMA activities ($[TMA]_{cell}$) were obtained with intracellular TMA-selective electrodes. The resulting measurements had high spatial and temporal resolutions.

Adding TMA to the bath caused an immediate uptake of TMA into the cell and a simultaneous transient positive depolarization of the basolateral membrane (ΔV_{TMA}). The magnitude of ΔV_{TMA} was directly proportional to the basolateral TMA influx (J_{TMA}). The peak initial ΔV_{TMA} hyperbolically increased as bath TMA activity ($[TMA]_{bath}$) was increased with a Hill coefficient of 1.3±0.3 (n=29), a 6.4±1.8 mM K_m, and a ΔV_{TMA}^{max} of 16.4±4.3 mV. Both J_{TMA} and ΔV_{TMA} were immediately abolished upon addition of either 1 mM amiloride or 1 mM cimetidine to the bath.

Basolateral membrane voltage (V_{bl}) was varied by changing bath potassium and barium activities. J_{TMA} decreased by 85% with a +60 mV change in V_{bl}. Extrapolated J_{TMA} reversal potentials (36.0±10.0 or 9.1±0.3 mV) were close to the calculated reversal potentials expected for a rheogenic uniporter (35.0 or 17.5 mV) when $[TMA]_{bath}$ is 4 mM and $[TMA]_{cell}$ is either 1 or 2 mM respectively. Steady-state $\log([TMA]_{cell}/[TMA]_{bath})$ measurements linearly followed V_{bl} and never exceeded the ratio that is predicted by electrochemical equilibrium.

Complete removal of either bath Na or Cl, or changing the bath K from 2.5 to 82.5 mM did not significantly change either J_{TMA} or the steady-state $[TMA]_{cell}$. Use of HEPES-buffered/HCO_3-free solutions precluded any coupling with HCO_3.

Thus, the basolateral organic-cation transporter is a rheogenic uniporter that moves one positive charge into the cell for each monovalent organic-cation that is taken up by the cell. *(Supported by NIH grants and a Dorothy Danforth Compton Graduate Fellowship)*

W-Pos477

ELECTROGENIC PROPERTIES OF SODIUM/SULFATE COTRANSPORT MEDIATED BY THE EXPRESSION OF A CLONED Na^+/SO_4^{2-} TRANSPORT PROTEIN (NaSi) IN *XENOPUS* OOCYTES

((A.E. Busch[1], S. Waldegger[2], T. Herzer[1], J. Biber[2], D. Markovich[2], H. Murer[2] and F. Lang[1])) Dept. Physiology, [1]University of Tübingen, D-72076 Tübingen and [2]University of Zürich, CH-8057 Zürich (Spon. by C. Jahr)

The Na^+/sulphate cotransporter cloned from rat kidney cortex (NaSi) has been expressed in oocytes of *Xenopus laevis* and subjected to electrophysiological analysis by voltage clamp methods. At -50 mV holding potential and pH 7.5, addition of 1 mmol/l sulphate induced an inward directed current of 2.4 ± 0.3 nA in oocytes expressing the transporter but not in oocytes injected with water. The current was dependent on both, sulphate and Na^+ concentration. Halfmaximal current was observed at about 0.1 mmol/l sulphate concentration and beyond 30 mmol/l Na^+ concentration. Thiosulphate created similar currents as sulphate with a similar K_M. At saturating concentrations of thiosulfate addition of sulfate could not induce an additional current, while phosphate did not inhibit sulfate induced currents. The sulfate induced currents were not affected by the addition of bicarbonate. A linear relation was observed between sulphate induced current with a reversal potential at approximately 0 mV. Conclusion: From previous studies on sulfate transport a cotransport of 2 Na^+ ions and one SO_4^{2-} was concluded. As such cotransport would be electroneutral, the results presented here can only be explained if there is 1) a different stoichiometry for the sodium/sulfate cotransport (i.e. 3:1) or 2) additional cotransport and/or exchange with other ions.

W-Pos478

SUBSTRATE DEPENDENT CURRENTS CARRIED BY A RENAL AND INTESTINAL TRANSPORTER FOR DIBASIC AND NEUTRAL AMINO ACIDS.

((A.E. Busch[1], T. Herzer[1], J. Biber[2], D. Markovich[2], H. Murer[2] and F. Lang[1])) Dept. Physiology, [1]University of Tübingen, D-72076 Tübingen and [2]University of Zürich, CH-8057 Zürich (Spon. by K. Thornburg)

Voltage clamp studies have been performed on a putative renal and intestinal transporter for neutral and dibasic amino acids (rBAT) expressed in *Xenopus* oocytes. In voltage-clamped oocytes the dibasic amino acids L-arginine, L-lysine and L-histidine induced a net inward current; transport of L-arginine was favoured over D-arginine. The neutral amino acids L-leucine, L-cysteine, L-alanine, L-glutamine and L-homoserine induced an outward current; L-leucine was transported better than D-leucine. The currents induced by L-arginine and L-leucine were voltage-dependent, being larger at more negative potentials for L-arginine and at more positive potentials for L-leucine. The relation between current and substrate concentration could be fitted by simple Michaelis Menten kinetics yielding a K_M of about 40 µM and 11 µM for L-leucine and L-arginine, respectively. Within the range of 6.25 and 10.0, pH had little effect on current induced by L-arginine, L-lysine and no effect on the current induced by L-leucine. In contrast, L-histidine induced an inward current at acidic and neutral pH (6.25 - 7.5) and an outward current at alkaline pH (8.75). In conclusion, rBAT-mediated transport displays unique properties accepting both, neutral and dibasic amino acids and carrying charge; transport of positively charged amino acids is associated with a net inward current and transport of neutral amino acids with a net outward current.

W-Pos479

pH REGULATION IN A CANCER CELL LINE IN AN ACIDIC ENVIRONMENT

((Owen, C.S.*, Wahl, M.L., Bobyock, S.B., and D.B. Leeper)) Thomas Jefferson U., Philadelphia, PA 19107

Mammalian intracellular pH (pH_i) is tightly regulated by active extrusion of metabolic protons. Otherwise, when cells are in an acidic environment, their pH_i would decrease, inhibiting normal cellular functions. Many tumor cells exist in an environment which is acidic enough to inhibit normal cells. They must adapt in order to raise pH_i to a level permissive for cell growth. A model for this process is the prolonged growth of cell lines in medium of pH 6.7. A malignant rodent ovarian tumor (OvCa) has been used and pH_i has been measured by analyzing whole spectra for intracellular BCECF on cells in suspension (Owen, C.S., Anal.Biochem 204:65-71,1992). The adapted cell phenotype was detectable hours after cells were removed from growth medium and loaded with indicator dye. It was apparent as an elevated pH_i at all values of extracellular pH_e over the range of 6.50-7.70. The effect was bicarbonate independent, which implicates the Na^+/H^+ antiporter rather than bicarbonate-chloride exchange. The magnitude of the enhanced pumping was a function of the length of time cells were kept at pH 6.7, in order to adapt. Inhibition of this upregulation of pH_i may thus be a mechanism to increase tumor cell killing during hyperthermia.

W-Pos480

Ca^{2+}/H^+ COUNTERTRANSPORT AND ELECTROGENICITY IN PROTEOLIPOSOMES CONTAINING ERYTHROCYTE PLASMA MEMBRANE Ca-ATPase AND EXOGENOUS LIPIDS

((L. Hao, J-L. Rigaud* and G. Inesi)) Biological Chemistry, University of Maryland School of Medicine, Baltimore MD 21201; *CEA Saclay, 91191 Gif-Sur-Yvette Cedex, France

A reconstituted proteoliposomal system was obtained with Ca-ATPase purified from human erythrocyte membrane, and liposomes prepared by reverse-phase evaporation. ATP dependent Ca^{2+} uptake and development of transmembrane electrical potential were followed by measuring light absorption changes undergone by Arsenazo III and Oxonol VI in the reaction medium. H^+ ejection was followed by measuring the fluorescence intensity of pyranine trapped in the lumen of the vesicles. ATP dependent Ca^{2+} uptake into the vesicles was stimulated by calmodulin, and was accompanied by H^+ ejection from the vesicles with a stoichiometric ratio of 1 H^+ per 1 Ca^{2+} soon after addition of ATP. The H^+/Ca^{2+} ratio and the rate of Ca^{2+} uptake became lower as the reaction proceeded toward the asymptote (i.e., several minutes). Ca^{2+} uptake was markedly stimulated by collapsing the H^+ gradient with the H^+ ionophore FCCP, indicating that lumenal alkalinization by H^+ contertransport inhibits Ca^{2+} uptake. Under optimal conditions (calmodulin, FCCP, 30°C) the reconstituted system sustained transport rates of 0.98±0.03 µmol Ca^{2+} per mg protein min^{-1}, and reached asymptotic levels of 5.20±0.39 µmol Ca^{2+} per mg protein. Under these conditions, net charge transfer by the transport ATPase produced initial rates of 22.1±1.61 mV min^{-1} and a steady state electrical gradient of 40.5±1.8 mV. (Supported by the N.I.H. and the Am. Heart Ass.)

W-Pos481

MITOCHONDRIAL UPTAKE FROM RAPID PULSES OF CALCIUM

((G.C. Sparagna, K.K. Gunter, T.E. Gunter, and S-S. Sheu))
Univ. of Rochester Dept. of Biophysics, Rochester, NY 14642

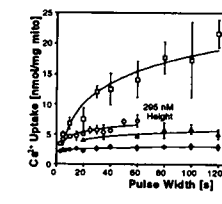

We have exposed isolated rat liver mitochondria to *in vitro* pulses of Ca^{2+} similar to those observed in the cytosol of many types of cells *in vivo*. These Ca^{2+} pulses are produced in a cylindrical fluorescence cuvette using a computer-controlled automatic pipettor system in conjunction with a fluorescence spectrometer. Ca^{2+} and Ca^{2+}-buffer are injected independently into the medium within the cuvette so that the intensity, duration, shape, and periodicity of the pulses can be controlled.

We have studied the uptake of square pulses of $^{45}Ca^{2+}$ by isolated liver mitochondria (see figure) by producing pulses of variable width ranging from 3 to 120 s and heights ranging from 176 to 456 nM free Ca^{2+} ($[Ca^{2+}]$). The most surprising feature of the data shown above is the apparent extremely rapid uptake of Ca^{2+} even at very low $[Ca^{2+}]$. For example, in the data for pulse heights of 176 nM $[Ca^{2+}]$, it appears that almost all of the Ca^{2+} sequestered was taken up during the first 3 s. We performed control experiments which determined that this rapid uptake was not caused by binding of $^{45}Ca^{2+}$ to the outside of the mitochondria or exchange of cold Ca^{2+} inside for $^{45}Ca^{2+}$ in the pulses. These control experiments verify that this mitochondrial Ca^{2+} uptake is actual net uptake.

(Supported by NIGMS Grant GM-35550 and NIDA Grant 27334)

W-Pos482

POTASSIUM EFFECT ON AMINO ACID TRANSPORT IN YEAST.

((Rosas, G. and Peña, A.)) Departamento de Microbiología. Instituto de Fisiología Celular. Universidad Nacional Autónoma de Mexico. Apartado 70-242; México D.F. 04510.

Starved yeast cells accumulate potassium when the cation plus glucose is present in the incubation medium. Under these conditions, an increased aminoacid transport capacity was developed within 30 to 60 minutes in comparison with cells incubated only with glucose. There seems to be a correlation between K^+ accumulation and the amino acid transport increase; K^+ added to the medium in fact inhibits amino acid uptake, and other monovalent cations do not produce the effect. The effects of K^+ preincubation with the cation were blocked by cycloheximide, indicating that the cation produced an increased protein synthesis. Transport systems are inactivated to practically zero by ammonium (Grenson, M. Eur. J. Biochem. 133:135-139,1983) and this effect is partially reverted by K^+ preincubation. Our results also showed that K^+ could "protect" the amino acid transport systems from the inactivation produced by ammonium, since in the absence of K^+, amino acid carriers were inactivated. It appears that K^+ accumulation during the first minutes of preincubation, may have some effect on the rate of synthesis of the amino acid carriers, but effects of K^+ appear to exist also on the degradation or inactivation of the carriers.

W-Pos483

REGULATION OF K-Cl COTRANSPORT IN SHEEP RED CELLS. ((I. Bize and P.B. Dunham)). Dept. of Biology, Syracuse University, Syracuse, NY 13244.

K-Cl cotransport is involved in restoration of cell volume after swelling. In sheep red cells, activation of cotransport by swelling proceeds by a two step process, a slow step inhibited by Mg, followed by a fast step. The mechanisms responsible for activation of K-Cl cotransport are poorly understood. Calyculin A, an inhibitor of some ser/thr phosphatases, inhibits the swelling-induced activation of K-Cl cotransport, indicating that dephosphorylation promotes activation of cotransport. Using kinase inhibitors, we attempted in this study to identify the kinase that reverses the calyculin-sensitive reaction. We also studied the effects of H_2O_2 on the signal transduction pathway leading to activation of the cotransporter. K-Cl cotransport is stimulated by staurosporine, a potent, nonspecific kinase inhibitor. No other kinase inhibitor tested stimulated K-Cl cotransport. Cells treated with staurosporine display further activation by swelling and this occurs without a measurable delay, indicating that the drug stimulates the slow step. Stimulation by staurosporine in normal-volume cells, also occurs without delay, showing that, contrary to our expectation, this kinase inhibitor is stimulating the calyculin-sensitive dephosphorylation, rather than inhibiting the kinase that reverses the calyculin-sensitive step. Stimulation by staurosporine is prevented by calyculin. Therefore the activation of cotransport by staurosporine demonstrates that there is regulation of the phosphatase by an inhibitory kinase. In cells with cotransport activated by staurosporine, H_2O_2 further stimulates K-Cl cotransport. The stimulation by H_2O_2 is also prevented by calyculin, suggesting that the phosphatase that activates cotransport may be regulated by oxidation as well as phosphorylation.

W-Pos484

K^+/H^+ EXCHANGE IN THE SF-9 INSECT CELL LINE. ((V. Vachon, M.-J. Paradis, M. Marsolais, J.-L. Schwartz* and R. Laprade)) GRTM, Univ. de Montréal, Montreal, Que., H3C 3J7, and *Biotechnol. Res. Inst., NRC, Montreal, Que., H4P 2R2.

The fluorescent pH indicator BCECF was used to investigate changes in the intracellular pH of Sf-9 cells from the lepidopteran species *Spodoptera frugiperda* (Fall armyworm) in response to changes in the composition of the external medium. The experiments were carried out in a K^+-rich (50 mM) medium similar to insect hemolymph in terms of its ionic composition. Under standard conditions, the intracellular pH (6.3) was about 0.2 units lower than the extracellular pH. Removal of K^+ from the medium resulted in a rapid acidification of the cells and the intracellular pH reached a constant level (5.3) within about 1 min. This acidification was reversible upon reintroduction of the K^+ in the bathing solution. The cells also acidified when Na^+ was removed from the medium, but at a much slower rate. K^+ was about 30 times more effective in promoting the realkalinization of the cells than Li^+, Na^+, Rb^+ and Cs^+. The initial rate (dpH_i/dt) and final level (ΔpH_i) of changes in the intracellular pH induced by a decrease in extracellular K^+ were linearly related to the logarithm of the ratio of final to initial extracellular K^+ concentrations. For ΔpH_i, the slope was close to unity. In the presence of K^+, changes in external pH caused rapid changes in the intracellular pH which reached a constant level within 1-2 min. In contrast, in the absence of K^+, changes in the external pH had little effect on the pH of the cells. These results suggest that, in Sf-9 cells, a K^+/H^+ antiporter with a stoichiometry close to 1:1 plays a key role in the movement of protons across the cell membrane.

W-Pos485

CLONING AND PARTIAL SEQUENCE REVEALS NUCLEOTIDE REGULATION OF BOVINE HEART MITOCHONDRIAL K^+/H^+ ANTIPORTER PROTEIN. ((X. Sun, H. Zhu, N. Xu, V.P. Zinchenko, and K.D. Garlid)) Dept. of Chemistry, Biochemistry, and Molecular Biology, Oregon Graduate Institute of Science and Technology, P.O. Box 91000, Portland, OR 97291-1000.

Affinity-purified polyclonal antibodies to the beef heart K^+/H^+ antiporter protein recognized 82-kD bands in rat liver, heart and kidney, but they reacted with two proteins, 74 kD and 88 kD, from beef heart mitochondria. It is likely that beef heart contains two isoforms of K^+/H^+ antiporter: Antibodies purified with one protein recognized the other, both affinity-purified antibodies inhibited K^+/H^+ antiport, and northern blot analysis revealed two bands at 3.4 and 4.6 kb. Antibody screening of a $\lambda gt11$ expression library yielded one positive clone of 1.6 kb missing both the 5' and 3' ends. The deduced sequence shows multiple trans-membrane domains with no significant homology to any known sequence. Analysis of the partial sequence of this clone revealed a nucleotide binding site, suggesting a hitherto unknown regulation of this antiporter. Assay of reconstituted K^+ flux revealed inhibition of K^+/H^+ antiport activity by ADP, but not by ATP. (Supported by NIH grant HL43814).

W-Pos486

CLONING, EXPRESSION, AND CHROMOSOMAL LOCALIZATION OF THE BUMETANIDE-SENSITIVE Na-K-Cl COTRANSPORTER IN HUMAN COLON ((J.A. Payne, J.-C. Xu, C.Y. Lytle, Melanie Haas, D.C. Ward, and B. Forbush III)) Depts. of Cellular and Molecular Physiology and Genetics, Yale University School of Medicine, 333 Cedar Street, New Haven, CT 06510

A human colonic (T84 cell) library was screened under low stringency conditions using cDNA probes from the shark rectal gland Na-K-Cl cotransporter (Xu et al., PNAS, submitted). A full-length cDNA was constructed from 2 overlapping clones. The predicted protein is 1212 amino acids in length, and the hydropathy profile indicates 12 putative transmembrane segments. The primary structure displays 77% identity to the rectal gland Na-K-Cl cotransporter, 51% identity to the thiazide-sensitive Na-Cl cotransporter, and significant homology to cyanobaterial and *C. elegans* genes. Similar to the rectal gland cotransporter cDNA, the 5'-end of the human colonic cotransporter is rich in GC content. Interestingly, a triple repeat $(GCG)_7$ occurs within the 5'-coding region and contributes to a large alanine repeat (Ala_{15}). Human embryonic kidney cells (HEK-293) stably transfected with the full-length cDNA expressed a ~175kDa protein recognized by anti-cotransporter antibodies. Following treatment with N-glycanase, the molecular mass of the expressed protein was identical to that of deglycosylated T84 cotransporter (~135kDa). The stably transfected cells exhibited a ~15-fold greater bumetanide-sensitive ^{86}Rb influx than control cells, and this flux absolutely required external Na and Cl. Preincubation in Cl-free media was necessary to activate the cotransporter, suggesting a [Cl]-dependent regulatory mechanism. Northern blot analysis revealed a ~7.2kb message in T84 cells and shark rectal gland and a ~7.0kb message in rabbit colon, kidney, lung, and stomach. Metaphase spreads from lymphocytes were probed with biotin-labeled cDNA and avidin fluorescein— the cotransporter gene was localized to position 5q2.23 on the human chromosome. (Supported by DK-17433)

W-Pos487

DIFFERENTIAL DISTRIBUTION OF ALTERNATIVELY SPLICED ISOFORMS OF THE PUTATIVE Na-K-Cl COTRANSPORTER IN RABBIT KIDNEY ((J.A. Payne and B. Forbush III)) Dept. of Cellular and Molecular Physiology, Yale University School of Medicine, 333 Cedar Street, New Haven, CT 06510

We screened under low stringency conditions both cortical and medullary rabbit kidney libraries using cDNA probes from the human colonic Na-K-Cl cotransporter (Payne et al., this volume). Forty-two cDNAs were isolated and characterized. The cDNA encoding the putative kidney Na-K-Cl cotransporter possesses a total sequence length of 4752bp, and the deduced primary structure is 1099 amino acids. From the hydropathy profile, we predict 12 transmembrane segments with large N- and C-terminal hydrophilic regions. The kidney protein displays an overall 63% identity to the shark rectal gland bumetanide-sensitive Na-K-Cl cotransporter and 52% identity to the flounder urinary bladder thiazide-sensitive Na-Cl cotransporter. Most of the kidney cDNAs were identical over all regions of overlap; however, there was a region of ~100bp for which there were three different but homologous variants (A, B, and F). This region of divergence was identified as an alternatively spliced 96bp cassette exon since clones possessing consensus intron-exon splice sites were found on either side. In addition to A, B, and F cDNAs, a single cDNA clone contained the A and F cassettes in tandem. Interestingly, the cassette exons code for most of putative transmembrane segment 2. Tissue northern blot analysis revealed a broad band at ~5.1kb that was unique to the kidney. When mRNA from cortex or medulla alone were probed, sharper bands were observed at 5.2 and 5.0kb, respectively. Northern blot analysis of cortical and medullary mRNA using high stringency conditions and antisense cDNA probes synthesized over each of the 3 cassette exons revealed that the isoforms are differentially distributed within the kidney— B mainly in cortex, F mainly in medulla, and A equally distributed. (Supported by DK-17433)

W-Pos488

LABELLING OF KIDNEY NA^+/D-GLUCOSE TRANSPORTER WITH A FLUORESCENT SULFHYDRYL GROUP SPECIFIC REAGENT. ((Bryan Lo, and M. Silverman)) MRC Group in Membrane Biology, Department of Medicine, University of Toronto, Toronto, Ontario, Canada, M5S 1A8.

The Na^+/d-glucose cotransporter (SGLT1) in intestinal brush border membrane vesicles (BBMV) can be labelled with fluorescent amino group specific reagents (B. Peerce, AJP 1993). This has not been done using kidney BBMV where Na^+-dependent glucose transport is believed to be mediated by a protein identical to SGLT1 as well as a low affinity Na^+/d-glucose cotransport system (M. Silverman, BBA 1993). In this study we have attempted to label the Na^+/d-glucose cotransporters in kidney BBMV using fluorescent sulfhydryl group specific reagents. To reduce non-specific labelling, BBMV prepared from dog kidney cortex were first pretreated with N-ethyl-maleimide (NEM) in the presence of 100 mM NaCl and 5 uM of the Na^+/glucose cotransporter inhibitor phlorizin. These vesicles were then treated with 7-diethylamino-3(4'-maleimidylphenyl)-4-methylcoumarin (CPM), a fluorescent sulfhydryl group specific reagent, in the presence of 100 mM NaCl. This labelling reaction was monitored by the increase in fluorescence at 475 nm. We observed that a component of the CPM labelling was inhibited by addition of 5 uM phlorizin. Using ^3H-phlorizin, both CPM and NEM were shown to inhibit high affinity Na^+-dependent phlorizin binding in an irreversible but phlorizin protectable manner. These results suggest that the Na^+/d-glucose cotransporters in kidney BBMV can be specifically labelled with CPM. Thus, CPM may prove to be a useful probe in studying the conformational dynamics of the Na^+/d-glucose transporter and the differences in Na^+-dependent glucose transport in the kidney and intestine.

W-Pos489

REGULATION OF THYROIDAL SODIUM/IODIDE SYMPORT ACTIVITY.((Orlie Levy, Jingwei Xiong, Ge Dai, Nishi Sharma, Stephen Kaminsky and Nancy Carrasco)). Department of Molecular Pharmacology, Albert Einstein College of Medicine, Bronx, NY, 10461.

The Na^+-dependent active uptake of I^- in the thyroid is mediated by the Na^+/I^- symporter. In addition to promoting protein biosynthesis, TSH increases I^- uptake by activating Na^+/I^- symporter molecules that reside in the plasma membrane. We report a ~2 fold enhancement in Na^+/I^- symport activity in membrane vesicles (MV) from cultured rat-thyroid (FRTL-5) cells or from rat thyroid when the vesicles are prepared under conditions that favor proteolysis, raising the possibility that a proteolytic event may play a role in the activation of the symporter by TSH. While the TSH-cAMP-protein kinase A (PKA) pathway is central in the regulation of thyroidal I^- transport, other pathways are involved. Tetradecanoyl-phorbol acetate (TPA), a direct activator of protein kinase C (PKC), has been reported to inhibit cAMP-dependent I^- accumulation in FRTL-5 cells. We show that the inhibitory effect of TPA is blocked when FRTL-5 cells are incubated in the presence of TPA and specific inhibitors of PKC, suggesting that the effect of TPA is mediated by PKC. The effect of TPA is probably due to a decrease in the number of functional Na^+/I^- symporter molecules. TPA has no effect on I^- transport unless the cAMP-PKA pathway is activated first. Preliminary data suggest that activation of PKC leads to inhibition of PKA. Clearly, the regulation of I^- transport is more complex than previously thought.

W-Pos490

STRUCTURAL SPECIFICITY OF THE HUMAN ERYTHROCYTE AMINOPHOSPHOLIPID TRANSPORTER. ((D. L. Daleke and E. Nemergut)) Department of Chemistry, Indiana University, Bloomington, IN 47405.

Transmembrane phospholipid asymmetry is maintained in biological membranes, in part, by a phosphatidylserine (PS) and phosphatidyl-ethanolamine (PE) specific transporter, or flippase. The aminophospholipid flippase is a vanadate- and calcium-sensitive Mg^{2+}-ATPase that selectively transports PS and PE to the cytofacial monolayer of the membrane. In contrast to its headgroup specificity, flippase activity is not acyl chain length dependent. The headgroup structural specificity of aminophospholipid transport was studied further using short chain (dilauroyl), synthetic, structural and stereoisomeric analogs of PS. Transport activity was detected by measuring characteristic changes in erythrocyte morphology. The amine group, but not the carboxyl group, is essential for transport: previous studies have shown that PE is transported at a rate 10-fold slower than PS. Furthermore, esterification of the carboxyl group of PS also results in decreased transport. However, phosphatidylhyroxypropionate, a PS analog without the amine group, is not transported. Increasing the distance between the phosphate and the PS headgroup (phosphatidylhomoserine) also prevented normal transport. The role of the phosphate group was tested with a sulfonate analog of PS. Replacing the phosphate group with the isosteric, but uncharged, sulfonate abolished transport of the lipid. The stereospecificity of the flippase was tested using all four stereoisomers of PS. The flippase recognizes the configuration of the glycerol backbone, but not the serine headgroup: the naturally-occurring *sn*-1,2-PS analogs were transported, whereas the *sn*-2,3-analogs, containing either L-or D-serine, were not. Thus, the aminophospholipid flippase shows an extreme specificity for the structure of its lipid substrate that involves several recognition elements, including headgroup, phosphate, and glycerol backbone structures.

W-Pos491

MOUSE RETINAL TAURINE TRANSPORTER: CLONING, EXPRESSION AND *IN SITU* LOCALIZATION. ((H.K. Sarkar[1], V. Sarthy[2], X.J. Qian[1] and H. Egal[2])) [1]Baylor College of Medicine, Houston, TX 77030; [2]Northwestern University Medical School, Chicago, IL 60611.

Na^+-dependent taurine uptake activity is known to be present in various ocular tissues, such as, retinal cells, retinal pigment epithelial cells, ciliary body-iris preparations and lens. The present study describes cloning of a taurine transporter cDNA from mouse retina, examines the biochemical and pharmacological properties expressed by this clone in *Xenopus* oocytes and determines its cellular localization. We have isolated a cDNA clone (mrTauT-1) from a mouse retinal cDNA library that encodes a protein whose sequence is identical to that of the mouse brain taurine transporter. *In vitro* transcribed RNA (cRNA) from this clone induces a Na^+- and Cl^--dependent [^{3}H]-taurine uptake activity with an apparent K_m of ~4.0 μM in *Xenopus* oocytes microinjected with this cRNA. This induced uptake is inhibited by known taurine transporter inhibitors, such as, β-alanine, guanidinoethane sulfonic acid, guanidinopropionic acid and hypotaurine. Additionally, a Na^+- and Cl^--dependent [^{3}H]-GABA uptake activity is induced in *Xenopus* oocytes microinjected with mrTauT-1 cRNA. *In situ* hybridization studies indicate the presence of this transporter specific mRNA predominantly in the ciliary bodies of the mouse eye and, to a much lesser extent, in various retinal cells. Supported by: AHA Grant-in-Aid 9012730 and Fight for Sight Grant-in-Aid GA93013 (to HKS); and NIH EY-03523 (to VS).

W-Pos492

NOISE ANALYSIS OF GLUTAMATE ACTIVATED CURRENTS IN CONE PHOTORECEPTORS IN TIGER SALAMANDERS.
((H. Peter Larsson[1], Serge A. Picaud[2], Frank S. Werblin[2] and Harold Lecar[2])) Graduate Group in Biophysics[1] and Division of Neurobiology[2], UC Berkeley, Berkeley CA 94720

It is known that cones have a glutamate-activated current. This current has features of both a sodium/glutamate co-transporter, since it requires external sodium, and a glutamate-activated chloride current, since the reversal potential follows that of chloride. We have done noise analysis on whole cell currents. The power spectrum of the glutamate activated current is a single Lorentzian with a time constant equal 2 ms. We estimate, from the variance-to-mean plot, the single channel conductance to 0.7 pS. Currents activated by another agonist, beta-Hydroxy-Aspartate, also show a single lorentzian spectrum but with a time constant of 0.7 ms. The single channel conductance is the same as for glutamate. We have also examined the effect of sodium on the single channel conductance. We will present a model of a transporter/channel that could explain these results.

W-Pos493

VOLTAGE CLAMP ANALYSIS OF STEADY-STATE AND TRANSIENT CURRENTS MEDIATED BY HUMAN GLUTAMATE TRANSPORTERS
((J.I. Wadiche, J.L. Arriza, S.G. Amara, and M.P. Kavanaugh)) Vollum Institute, Oregon Health Sciences University, Portland, OR 97201

Three members of a human glutamate transporter gene family (EAAT1, EAAT2, and EAAT3) were cloned from a motor cortex cDNA library. These molecules were expressed in *Xenopus* oocytes, and steady-state and pre-steady state currents associated with the transporters were studied using two-microelectrode and vaseline-gap open-oocyte recording techniques. Most classical uptake "blockers" tested induced inward currents with properties similar to currents induced by application of L-glutamate: the concentration-dependence of the inward currents obeyed Michaelis-Menten kinetics, the currents were increased by hyperpolarization, and they were abolished in the absence of extracellular Na^+. In contrast, kainic acid blocked steady-state currents induced by L-glutamate without inducing a current by itself. This block was selective for EAAT2. Schild analysis suggested a competitive action of kainate at the glutamate binding site of the transporter, with a calculated equilibrium dissociation constant of 17 μM. In the absence of glutamate, voltage jumps induced non-linear capacitive currents which were blocked by kainate with the same concentration dependence as the block of the steady-state transport currents ($K_{0.5}$=15 ± 4 μM s.e., n=4) The time integrals of the transient currents for voltage jumps were equal for the reverse jumps and saturated at extreme hyperpolarized and depolarized potentials. The transient currents were not seen in the absence of extracellular Na^+. The current-time integrals obeyed a Boltzmann function of membrane potential ($z\delta$=0.58 ± .03; $V_{0.5}$=1 ± 4 mV; n=4). The quantity of kainate-sensitive capacitive charge movement in individual cells was proportional to the steady state current induced by glutamate in the same cells. By normalizing $Q_{max}/e_0 z\delta$ to the steady-state current in the presence of 1mM glutamate, values of 154 ± 9 sec^{-1} and 476 ± 29 sec^{-1} are obtained for steady-state charge transfer mediated by a single transporter at -80 mV and -160 mV, respectively.

W-Pos494

STEADY STATE L-GLUTAMATE (GLU) UPTAKE DRIVEN BY A SINUSOIDAL CELL MEMBRANE POTENTIAL ((Lyle W. Horn)) Dept.Physiol., Temple University School of Medicine, Philadelphia, PA 19140

Nonlinear kinetic relaxation theory predicts that a voltage-sensitive membrane transporter should have a net response to a pure sinusoidal (AC) membrane potential (Ψ_m) even if it is not electrogenic. The periodic average response of a transporter is frequency-dependent, characterizes the specific transporter, and can yield valuable dynamic information. The GLU transporter in barnacle muscle is Ψ_m-sensitive and may not be electrogenic. The frequency response of ^{14}C-GLU uptake by intact single barnacle muscle cells was measured in order to test the prediction. Each fiber was exposed to an external AC electric field at only one frequency during uptake. Field-exposed fibers were compared to unexposed control cells taken from the same muscle bundle and run in parallel. The AC field can affect protein kinases which act to inhibit GLU uptake, but the effect is blocked by H7. H7 has no effect on control uptake. In the presence of H7 there is no effect of an AC field on GLU uptake at frequencies up to 1 kHz. Above 1 kHz the field stimulates uptake, having a maximum effect at about 10 kHz, while uptake appears to approach a plateau at higher frequencies. This response can be reproduced qualitatively by a six-state ordered binding model for the transport reaction in which only the membrane translocation steps are voltage-sensitive. "Loaded" carrier translocation rate constants must be of order 2500 s^{-1}.

W-Pos495

Conducting States of a Mammalian Serotonin Transporter

(Sela Mager, Churl Min, Douglas J. Henry[1], Charles Chavkin[1], Beth J. Hoffman[3], Norman Davidson, Henry A. Lester). Division of Biology 156-29, California Institute of Technology, Pasadena CA 91125 [1]Department of Pharmacology SJ-30, University of Washington, Seattle WA 98125 [2]Laboratory of Cell Biology, National Institute of Mental Health, Bethesda MD 20892. (Sponsored by B. Cohen)

We used voltage-clamp analysis, [^{3}H]5-HT uptake, and [^{125}I]RTI-55 binding to study permeation at a cloned rat 5-HT transporter expressed in Xenopus oocytes. [^{3}H]5-HT uptake corresponded to a turnover rate of ~ 1/sec and did not depend on membrane potential. However, three distinct currents resulted from 5-HT transporter expression. In our experimental conditions all three currents were inward and were inhibited by 5-HT uptake inhibitors but depended differentially upon membrane potential, organic and inorganic ions and 5-HT itself.

(1) The ***transport-associated current*** was observed upon application of organic substrate (5-HT, amphetamine or dopamine). This inward current increased with hyperpolarization and at -80 mV was up to -40 nA. Like 5-HT uptake it was Na^+ and Cl^- dependent. By comparison with the [^{3}H]5-HT uptake data there were 5 to 15 charges transferred per 5-HT molecule transported.

(2) The ***transient current*** developed in response to voltage jumps to negative potentials. This current increased exponentially with the membrane potential, increased by depolarizing prepulses and inactivated with a time constant of ~100 ms. In response to a voltage jump to -180 mV after a prepulse to +60 mV, a transient current as large as 7 μA was evoked. The current was Na^+ dependent with a Hill coefficient of 1.7 but could also be carried by Li^+. It was not Cl^- dependent and was blocked by Cs^+, Ba^{2+}, amiloride or 5-HT.

(3) The ***leakage current*** was revealed in the absence of 5-HT by the application of 5-HT uptake inhibitors or amiloride. It increased at more negative potentials, and was ~3 fold lagrer in Li^+ Ringer then in normal Na^+ Ringer. Typically the amplitude of the leakage current was ~1/4 of the transport-associated current; and in some cases, it increased ~10-fold during recording.

We conclude that the conducting states of the 5-HT transporter may reflect the existence of a permeation pathway similar to that of ionic channels.

Supported by NIH, MDA and L. Deutsch Foundation.

W-Pos496

EVIDENCE THAT FACILITATIVE GLUCOSE TRANSPORTERS MAY FOLD AS BETA-BARRELS. ((1,2J. Fischbarg, [2]M. Cheung, [3]F. Czegledy, [2]J. Li, [2]P. Iserovich, [2]K. Kuang, [4]J. Hubbard, [5]M. Garner, [6]O. M. Rosen, [6]D. W. Golde, and [6]J. C. Vera)). Depts. of [1]Physiol., [2]Ophthalmol., [3]Med., and [4]Biochem., P&S, Columbia Univ., NYC 10032; [6]Progs. in Molec. Biol. and Molec. Pharmacol. and Therapeutics, Mem. Sloan Kettering Cancer Ctr., NYC 10021; [5]Dept. Ophthalmol., SWstrn. Med. Ctr, Univ. of Texas, Dallas, TX 75235.

According to a widely accepted model, facilitative glucose transporters (GLUTs) form 12 transmembrane α-helices and have the highly conserved sequence Ile386–Ala405 in GLUT1 as intracellular. Yet, we found that a polyclonal antibody against a peptide encompassing this conserved sequence increased 2–deoxy–D–glucose (2–DOG) uptake in oocytes expressing GLUT1, GLUT2 or GLUT4 only when applied to the extracellular side. This effect was dose–dependent, was specifically competed by the peptide Ile386–Ala405, and was due to a decrease in the Km for the transport of 2–DOG. Control antibodies against intracellular GLUT C-terminal sequences increased 2–DOG uptake only when injected into oocytes expressing their target GLUTs. This led us to note some sequence similarity between GLUTs and porins, two of which are known from crystallography to form 16–stranded transmembrane antiparallel ß–barrels. Further analysis of the hydrophobicity, amphiphilicity and turn propensity of GLUT1 leads us to propose that GLUTs fold as porin–like transmembrane ß–barrels. Such barrel would explain the previously observed high accessibility of solvent to the GLUT backbone, while its diameter (≈ 11 Å) would suffice for permeation of hydrated hexoses. This new model accounts for the present antibody studies, and for previously published experimental evidence on ATB-BMPA binding which appears also inconsistent with the 12-helix model.

W-Pos497

Three-dimensional Structure of the Membrane Domain of Human Band 3, the Anion Transporter of the Erythrocyte Membrane

D. N. Wang[1], W. Kühlbrandt[1], V.E. Sarabia[2] and R.A.F. Reithmeier[2]

[1] European Molecular Biology Laboratory, Meyerhofstrasse 1, 6900 Heidelberg, Germany; [2] MRC Group in Membrane Biology, Department of Medicine and Department of Biochemistry, University of Toronto, Toronto, Canada, M5S 1A8

The membrane domain of human erythrocyte Band 3 protein (Mr = 52,000) was reconstituted with lipids into two-dimensional crystals in the form of sheets or tubes. Crystalline sheets were monolayers with six-fold symmetry (layer group $p6$, $a = b = 170$ Å, $g = 60°$) whereas the symmetry of the tubular crystals was $p2$ ($a = 104$ Å, $b = 63$ Å, $g = 104°$). Electron image analysis of negatively stained specimens yielded three-dimensional map of the protein at 20 Å resolution. Maps derived from both crystal forms show that the membrane domain is a dimer. There is a central depression at the position of the two-fold axis, which may represent the channel for anion transport.

W-Pos498

^{35}CL NMR LINE-BROADENING (LB) SHOWS THAT EOSIN-5-MALEIMIDE (EM) DOES NOT BLOCK THE EXTERNAL ANION ACCESS CHANNEL OF BAND 3. ((D. Liu, S. Kennedy and P.A. Knauf)) Dept. of Biophysics, Univ. of Rochester, Rochester, NY 14642.

It has been suggested that Lys-430, with which EM reacts, is located in the external channel through which anions gain access to the external transport site, and that EM inhibits anion exchange by blocking this channel. To test this, we have used ^{35}Cl NMR to measure Cl^- binding to the external transport site in control and EM-treated human red blood cells (RBC). Intact cells were used, rather than ghosts, because in this case all LB results from binding to external sites. On a 400 MHz spectrometer, RBC at 50% concentration (v/v) in 150 mM Cl^- medium at 3°C caused 17.7±1.2 Hz LB. Of this, 7.9±0.7 Hz was due to band 3, because it was prevented by 4,4'-dinitrostilbene-2,2'-disulfonate (DNDS). The LB was not due to hemoglobin released from the cells, as little LB remained in the supernatant after cells were removed by centrifugation. Saturable Cl^- binding remained in EM-treated cells, although the binding was no longer DNDS-sensitive, because EM prevents binding of DNDS. The lower limit for the rate at which Cl^- goes from the binding site to the external medium is 4.3×10^5 s^{-1} for control cells and 1.86×10^5 s^{-1} for EM-treated cells, far higher than the Cl^- translocation rate at 3°C (about 500 s^{-1}). Thus, EM does not inhibit Cl^- exchange by blocking the external access channel. EM may be useful to fix band 3 in one conformation for studies of Cl^- binding to the external transport site. (Supp. by NIH grant DK27495).

W-Pos499

CONFORMATIONAL CHANGES IN THE LACTOSE PERMEASE OF *E. coli* INDUCED BY SUBSTRATE BINDING. ((K. Jung, H. Jung and H.R. Kaback)) Howard Hughes Medical Institute, University of California, Los Angeles, Los Angeles, CA 90024-1662.

The lactose (lac) permease of *E. coli* is a polytopic cytoplasmic membrane protein that catalyzes the coupled stoichiometric translocation of a β-galactoside with an H^+. Based on spectroscopic studies, hydropathy analysis and a series of lac permease-alkaline phosphatase (*lacY-phoA*) fusions, the protein has 12 hydrophobic domains in α-helical conformation that traverse the membrane in zigzag fashion. Site-directed fluorescence labeling with N-(1-pyrene)maleimide (PM) is being used to study proximity relationships in the permease, and excimer fluorescence measurements have led to a model describing the proximity of the helices in the C-terminal half of the permease [Jung, K. Jung, H. et al. (1993) *Biochemistry*, in press]. Recent studies reveal that excimer fluorescence observed with PM-labeled E269C (helix VIII)/H322C (helix X) permease is quenched by Tl^+ in a manner that is markedly inhibited by β,D-galactopyranosyl β,D-galactopyranoside (TDG), less so by lactose and not by glucosides. TDG also dramatically alters the rate of PM labeling of single Cys replacements in a number of transmembrane helices. The results suggest that lac permease undergoes a widespread conformational alteration upon ligand binding.

(K. Jung and H. Jung are Postdoctoral Fellows of the Deutscher Akademischer Austauschdienst and the European Molecular Biology Organization, respectively.)

W-Pos500

FUNCTIONAL EXPRESSION OF *ESCHERICHIA COLI* LACTOSE PERMEASE IN *BACILLUS SUBTILIS*. ((Kevin H. Zen and H. Ronald Kaback)) Howard Hughes Medical Institute, Departments of Physiology and Microbiology and Molecular Genetics, Molecular Biology Institute, University of California Los Angeles, Los Angeles, CA 90024-1662 (Spon. by T. Consler)

There are very few examples for the functional expression of Gram-negative membrane proteins in Gram-positive bacteria. The lactose permease of *Escherichia coli* is a well characterized membrane transport protein with 12 transmembrane domains that catalyzes the coupled translocation of a single β-galactoside with a single proton. In this study, we test the functional expression of *lac* permease in *Bacillus subtilis*. The coding sequence of the *lacY* gene has been cloned into a *B. subtilis* expression vector which is under the control of *ermC* promoter and inducible by erythromycin. *B. subtilis* harboring *lacY* gene not only actively transports lactose, but *lac* permease can be induced to levels comparable to these in *E. coli*. When the biotin acceptor domain from a *Klebsiella pneumoniae* oxaloacetate decarboxylase is inserted into the middle cytoplasmic loop or at the carboxyl tail of *lac* permease, the chimeric proteins are biotinylated and functional. Biotinylated *lac* permease is solubilized from the membrane and purified to a high state of purity by monomeric avidin affinity column. The results demonstrate that an integral membrane protein of a Gram-negative bacterium can be functionally expressed in a Gram-positive organism, *B. subtilis*.

W-Pos501

SHRINKAGE-INDUCED INTRACELLULAR ALKALINIZATION IN FIBROBLASTS CAUSED BY HUMAN CYTOMEGALOVIRUS INFECTION.

((A.A. Altamirano, W.E. Crowe and J.M. Russell)) Dept. of Physiology, Medical College of Pennsylvania, Philadelphia, PA 19129.

Infection of human fibroblasts (MRC-5) with human cytomegalovirus (HCMV) produces marked cellular enlargement. The mechanism(s) of development of this cytomegaly are not understood. It is possible that the virus may subvert cell volume regulatory mechanisms such as to result in cell enlargement. Enhanced activity of the Na^+/H^+ exchanger may provide at least some of the additional intracellular solute and obligatory water. This hypothesis was tested by measuring intracellular pH (pH_i), using the fluorescent pH probe BCECF. Seventy-two hours after exposure, the resting pH_i of mock-infected (MI) cells tested in a HEPES-buffered saline solution was 7.38 ± 0.04 (n=10) compared to 7.65 ± 0.03 (n=11) for HCMV-infected (HI) cells. Exposure of MI cells to a 20% hyperosmotic saline solution (57 mM sucrose added) caused a slight acidification ($\Delta pH_i=-0.054 \pm0.006$; n=5), whereas HI cells exposed to the hyperosmotic saline responded with a dramatic alkalinization ($\Delta pH_i=+0.15\pm0.02$;n=4). Five μM diethyl amiloride (DEA) caused an acidification of both HI and MI cells. Upon exposure to 20% hyperosmotic saline, the response of the MI, DEA-treated cells was little changed. However, DEA pretreatment abolished the alkalinization caused by exposure to hyperosmotic saline in HI cells. These results are consistent with HCMV activation of a shrinkage-sensitive acid extrusion mechanism, presumably Na^+/H^+ exchange. Supported by DHHS NS 11946.

STRUCTURE AND FUNCTION OF THE NUCLEAR PORE

Th-AM-SymI-1

CLUES TO NPC ASSEMBLY DERIVED FROM ATYPICAL NINE-FOLD AND 10-FOLD NPCS

J.E. Hinshaw and R.A. Milligan. The Scripps Research Institute, 10666 N. Torrey Pines Rd., La Jolla, CA 92037

Nuclear pore complexes (NPCs) are large supramolecular assemblies located in the nuclear envelope where they provide a channel of communication between the cytoplasm and nucleus. Structural analysis of the NPC to date has focused on NPCs with octagonal rotational symmetry, which have eight radial spokes extending out from the central pore. Occasionally NPCs are found, however, with 9 or 10 spokes. We have examined these unusual NPCs by negative stain electron microscopy and image analysis and compared the results to the data previously obtained from the octagonal NPCs. Comparisons of the two-dimensional projection maps show that the substructure of the spoke is the same in all three forms, 8-fold, 9-fold and 10-fold. Details from the 3 dimensional maps confirms this result, suggesting the spoke is a immutable constituent of the NPC and therefore may be an important building block for NPC assembly. The distance between the annular subunits is equivalent in all three forms which causes the distances between the spokes at higher radius to be smaller in the larger NPCs. For example, the distance between the lumenal subunits is 20Å closer in the 9-fold NPC compared to the 8-fold NPC. This data illustrates that the NPC is flexible to an extent that allows 9 and 10-fold NPCs to form and further suggests that the annular connections are important and may play a role in NPC assembly.

Th-AM-SymI-2

GENETIC ANALYSIS OF NUCLEAR PORE COMPLEX FUNCTION.

((L.I. Davis*◊†, K.D. Belanger†, M.A. Kenna*◊ and S. Wei†)) Howard Hughes Medical Institute*, Department of Genetics◊ and Cell Biology†, Duke University Medical Center, Durham, NC, 27710.

The nuclear pore complex (NPC) is a hetero-oligomeric structure that forms a large channel through the nuclear envelope. It is the only known conduit for export of RNA, and for import of nuclear proteins. A detailed understanding of the mechanism by which the NPC controls macromolecular traffic, and indeed whether it has other functions as well, has been hindered by the complexity of its structure. Among the small number of NPC proteins characterized to date is a family of related polypeptides conserved from vertebrates to yeast. We have used a genetic approach to study the functional and physical relationships between these proteins, and to identify novel proteins involved in NPC function. Temperature sensitive mutants of one of the yeast nucleoporins, *NUP1*, were used to assay the terminal phenotype resulting from loss of function. We found defects in protein import, mRNA export and nuclear envelope structure. To identify novel proteins that are functionally related, we performed a genetic screen for new mutants that are lethal in combination with *nup1* mutations (synthetic lethals). Sixteen mutants were identified, one of which was allelic to *SRP1*. We have now shown that Srp1 is an NPC protein that is physically associated with two of the nucleoporins, Nup1 and Nup2. *srp1* was originally identified by suppression of defective RNA polymerase I. Mutation causes loss of nucleolar integrity and defects in chromosome segregation. The primary structure of *SRP1*, and the phenotypes of *srp1* mutants, suggest that it is required for attachment of the NPC to the underlying nuclear skeleton.

Th-AM-SymI-3

TRANSPORT ACROSS THE NUCLEAR ENVELOPE.

((P.L. Paine, J. Rupesova, and I. Vancurova)) Department of Biological Sciences, St. John's University, Jamaica, NY 11439.

Eukaryotic form makes necessary mechanisms for specific and controlled transport of a variety of materials across the nuclear envelope. Transport of different materials through the nuclear pore complex (NPC) in each direction will be reviewed. Current understanding of mechanisms relies heavily upon the available data pertaining to selective transport of specific proteins from the cytoplasm and their accumulation to higher nuclear vis-a-vis cytoplasmic concentrations. This selective protein transport at the NPC must be viewed as one step of an overall multi-step transport process which also includes important interactions between the transported proteins and other cytoplasmic and intranuclear proteins. Quantitative studies have begun to resolve the transport mechanisms at the level of the NPC from those in the cytoplasm and nucleus and will be examined. Further focus will be on the biophysical nature of the NPC transport machinery and mechanisms, e.g., facilitated diffusion or active transport, as well as coupling of the NPC transport processes to cytoplasmic and intranuclear steps.

Th-AM-SymI-4

ELECTROPHYSIOLOGY OF THE NUCLEAR ENVELOPE.

((Roberta Assandri and Michele Mazzanti)) Dept. Physiology and Biochemistry, I-20133 Milano, Italy

What is the role of ion channels found on the outer nuclear membrane? Channels in the envelope are selective for potassium or chloride. They have conductances from 25 to 1000 pS. The current flowing from the nucleus to the cytoplasm has a time-variant component absent in the other direction. Chemicals interact with and modulate the ionic flux. ATP greatly increases the current and zinc reduces it. Ion channels must underlie the nuclear resting potential recorded in some cells. This could be a transient nucleo-cytoplasmic voltage difference utilized to initiate or to control some nuclear functions. The potential could trigger nuclear envelope breakdown by global constriction. An electrical barrier could regulate nucleo-cytoplasmic traffic. These hypotheses envisage the channel as a bridge across the envelope, but the channels may reside only in the outer membrane. In this case they could be involved in calcium discharge or protein release from the nuclear cisternae. The patch-clamp technique used on either isolated or in *in-situ* nuclei has allowed the observation of 2-3 μ^2 of the outer membrane. Nuclear envelopes from different tissues show a density of pores between 1 and 100 /μ^2. These data suggest that nuclear pores are closed in particular conditions, and that the ion channels may actually be part of the pore complex.